Role of gamma interferon in the pathogenesis of Murine gammaherpesvirus-68

Babunilayam Gangadharan

PhD
University of Edinburgh

2005

Declaration

I declare that this thesis has been composed by myself and has not been submitted for any other degree. The work described herein is my own except where otherwise indicated and all other authors are duly acknowledged.

Babunilayam Gangadharan

November, 2005

Laboratory for Clinical and Molecular Virology,
Department of Veterinary Biomedical Sciences,
Royal (Dick) School of Veterinary Studies,
University of Edinburgh,
Summerhall Square,
Edinburgh, EH9 1QH

Acknowledgements

I would like to thank my supervisors, Professor Tony Nash and Dr. Bernadette Dutia for their support and guidance throughout my studies. I am indebted to Tony for giving me the opportunity to carry out this work and for his ideas and vision which kept me enthused. The patience and commitment of Tony in going through the manuscript of this thesis is gratefully acknowledged. I wish to thank Bernadette for her excellent supervision during the design and conduct of experiments. The willingness of Bernadette to offer help and guidance at every stage of this project made a world of difference. Histopathological examination formed a major part of this study. Help was always available from Dr.Susan Rhind and Dr. David Brownstein in driving me in the right direction while interpreting those countless number of slides. Susan was kind enough to go through the manuscript. I would like to record my heartfelt gratitude to Susan.

Help and support from a number of people were always available at the time of need during the course of this project. I would like to thank Billy, Christine and other members of small animal unit for help with animal experiments and Neil MacIntyre and other members of Veterinary Pathology Unit at Easter Bush Veterinary Centre for help with histopathology and histochemical analysis. I am thankful to past and present members of MHV-68 group for their help and assistance. Help and assistance from Anna, Vicky and Kerra for carrying out *in situ* hybridisation and quantitative PCR studies is gratefully acknowledged. I am thankful to Maloo for help in carrying out CD4 and CD8 staining. I would like to record my gratitude to Dr.T.Gotoh, Kumomoto University, Japan for providing anti- arginase -1 antibody.

Thoughts of my late father and late grand father kept me focussed, encouraging me to persevere. I am thankful to my family and friends far and near for their kind words of support. Very special thanks to Leena and Anju for taking care of me and sharing all the ups and downs during the last few years.

Abstract

Intranasal infection of gamma interferon receptor knockout ($IFN\gamma R^{-/-}$) mice with murine gammaherpesvirus - 68 (MHV-68) causes unique pathological changes in the spleen characterised by development and resolution of fibrosis. Delineation of virological, cellular and molecular events taking place in the spleen during these pathological changes was the main objective of this study.

Sequential histopathological and cellular characterisation studies showed early invasion of lymphoid follicles (harbouring latently infected B-lymphocytes) with CD4+ and CD8+ T lymphocytes. Concomitantly, invasion of alternatively activated macrophages characterised by arginase -1 expression was observed. These events were followed by a reduction in the number of B-lymphocytes and development of a 'fibrotic cage' around the shrinking lymphoid follicles. In spite of the decrease in the number of B-lymphocytes, the number of latently infected cells showed a progressive increase until the development of fibrosis. During fibrosis, a dramatic reduction in the number of latently infected cells was observed followed by repopulation of lymphoid follicles with B-lymphocytes indicating a recovery phase of the fibrotic response. These observations suggest that: 1) the progressive reduction and repopulation of B-lymphocytes in the lymphoid follicles of the spleen constituted the primary events during the development and resolution of fibrosis respectively. 2) Fibrosis as a host response mechanism is able to contain the expansion of latently infected cells in the spleen. 3) Presence of latently infected cells might be the trigger for fibrosis development by preventing the repopulation of lymphoid follicles.

The role of IFNγ responsiveness of bone marrow derived cells in the pathogenesis of splenic fibrosis was investigated by generating radiation bone marrow chimera mice and subsequent infection with MHV-68. The study showed that, replacing the bone marrow derived cells in $IFN\gamma R^{-/-}$ mice with bone marrow derived cells from wild type mice prevented the development of splenic fibrosis following MHV-68 infection.

Other pathological changes occurred in the lung, liver, aorta and spleen of IFNγR$^{-/-}$ mice infected with MHV-68. 1) Focal areas of interstitial fibrosis were observed in the lung during day 12-16 post infection. At the same time, cuffing of pulmonary vessels with primarily mononuclear cells was observed. A few of the infiltrating cells were productively infected with MHV-68 which coincided with clearing of productive infection from alveolar epithelial cells. The change in the tropism of viral infection may be related to the development of fibrosis. 2) The pathological changes observed in the liver was characterised by proliferation of intrahepatic bile ducts and infiltration of mononuclear cells around them. Productively and latently infected mononuclear cells were present among the infiltrating cells. At later stages, some of the lesions progressed to degeneration and necrosis of intrahepatic bile ducts and encircling 'onion skin' type fibrosis. The pathological changes observed in the liver mimic the changes observed in primary sclerosing cholangitis. 3) The incidence of bony metaplasia in the spleen of IFNγR$^{-/-}$ mice infected with MHV-68 was higher in comparison to mock infected IFNγR$^{-/-}$ mice and MHV-68 infected wild type mice. Bony metaplasia was observed in the spleen of IFNγR$^{-/-}$ mice before the development of fibrosis. These observations suggest that development of bony metaplasia is independent of fibrosis. There was no direct correlation between the expression of bone morphogenic protein-4 and development of bony metaplasia in the spleen. 4) The incidence of chronic arteritis at the base of aorta was in the range of 6-11% and viral antigen was demonstrated in the tunica media of blood vessels.

Contents

List of figures

List of tables

Abbreviations

AlHV – 1	Alcelaphine herpesvirus –1
A	Antisense
Aa	Alternate activation
ACV	Acylcyclovir
ADAR	RNA specific adenosine deaminases
AE	Alkaline exonuclease
AIDS	Acquired immunodeficiency syndrome
AMAC	Alternate macrophage activation associated CC chemokine
AP	Activator Protein
ApoE	Apolipoprotein E
BAC	Bacterial artificial chromosome
BAL	Broncho alveolar lavage
BART	Bam H1A RNA transcript
BCA-1	B - cell attracting Chemokine -1
BCBL	Body cavity based lymphoma
BCIP	5-Bromo-4-Chloro-3-Indolyl phosphate
Bcl	B cell lymphoma
BCR	B-cell receptor
BCRF-1	Bam H1 C rightward open reading frame -1
BD	Bile duct
BFS	Buffered formal saline
BH	Bcl-2 homology
BHK	Baby Hamster Kidney
BHRF-1	Bam H1 H rightward open reading frame -1
BL	Burkitt's lymphoma
BLC	B-lymphocyte chemoattractant
BMDC	Bone marrow derived cells
BMP	Bone morphogenic protein
BoHV – 4	Bovine herpesvirus–4
bp	base pair

BRLF-1	Bam H1 R Leftword open reading frame -1
BV	Blood Vessel
BZLF-1	Bam H1 Z leftward oper reading frame -1
Ca	Classical activation
cAMP	cyclic Adenosine monophosphate
CBP	Chemokine binding protein
CBP	CREB - binding protein
CCN	CYR-61, CTGF, NOV
CD	Clusture of differentiation
CD40L	CD40 ligand
cDNA	Complimentary DNA
CPE	Cytopathic effect
CREB	cAMP response element binding protein
CTGF	Connective tissue growth factor
CTLs	Cytotoxic T lymphocytes
CYR61	cystein rich 61
DAB	3,3 diaminobenzidine
dATP	Deoxyadenosine triphosphate
DC-SIGN	Dendritic cell specific ICAM-3 gabbing non integrin
dCTP	Deoxycytidine triphosphate
DEPC	Diethyl pyrocarbonate
dGTP	Deoxyguanosine triphosphate
DHFR	dihydrofolate reductase
DNA	Deoxyribonucleic acid
dNTP	Deoxynucleoside triphosphate
dpol	DNA polymerase
dpp	decapentaplegic gene
dsDNA	double stranded deoxyribonucleic acid
dsRNA	double stranded ribonucleic acid
DTT	Dithiothreitol
dTTP	Deoxythymidine triphosphate
dut	dUTPase

dUTP	Deoxyuracil triphosphate
E	Early
EBER	EBV encoded RNA
EBNA	EBV nuclear associated antigen
EBV	Epstein - Barr virus
ECM	Extra cellular matrix
EDTA	Ethylene diamine tetra acetic acid
EGF	Epidermal Growth factor
EHV –2	Equine herpesvirus - 2
EMT	Epithelial mesenchymal transition
ENA-78	Epithelial cell derived neutrophil activating -78
ER	Endoplasmic reticulum
FADD	fas associated death domain
FCS	Foetal calf serum
FDC	Follicular dendritic cell
FGF	Fibroblast growth factor
FIZZ	First in inflammatory zone
FLICE	FADD - interleukin-1β converting enzyme
FLIP	FLICE inhibitory protein
FOP	Fibrodysplasia ossificans progressive
g/gp	Glycoprotein
GAF	Gamma interferon activation factor
GaHV	Gallid Herpesvirus
GAS	Gamma interferon activation sequence
GC	Germinal Centre
GDP	Guanosine Diphosphate
gfp	green fluorescent protein
GITC	Guanidine Isothiocynate
GM-CSF	Granulocyte macrophage colony stimulating factor
GMEM	Glasgow modified eagle's medium
GPCR	G protein coupled receptor
Gro-a	Growth related oncogene - a

GTP	Guanosine Triphosphate
GVHD	Graft versus host disease
HBV	Hepatitis B virus
HCMV	Human cytomegalovirus
HCV	Hepatitis C Virus
HD	Hodgkin's disease
HDNA	High GC DNA
HHV	Human herpesvirus
HIV	Human immunodeficiency virus
HLA	Human leukocyte antigen
HRS cells	Hodgkin's and Reed- Sternberg cells
HSC	Hepatic Stellate cells
HSV-1	Herpes simplex virus – 1
HVS	Herpes Virus Saimiri
ICAM	Intra cellular adhesion molecule
ICTV	International committee on taxonomy of viruses
IE	Immediate early
IF	Initiation factor
IFN	Interferon
IFNγ	Gamma interferon
Ig	Immunoglobulin
IHC	immunohistochemistry
IL	Interleukin
ILD	Interstitial lung disease
ILT	Infectious Laryngotracheitis
IM	Infectious mononucleosis
iNOS	Inducible nitric oxide synthase
IP-10	IFNγ -inducible protein -10
IPF	Interstitial pulmonary fibrosis
IR	Internal repeats
IRF	Interferon regulatory factor
ISH	in situ hybridisation

I-SMAD	Inhibitiry SMAD
JaK	Janus kinase
kb	kilo base
kDa	kilo Dalton
KS	Kaposi's sarcoma
KSHV	Kaposi's sarcoma associated herpesvirus
L	Late
L	Ladder
LANA	Latent Nuclear Antigen
LCL	Lymphoblastoid cell lines
LDNA	Low GC DNA
LF	Lymphoid follicle
LGL	large granular lymphocytes
LMP	Latent membrane proteins
LPS	Lipopolysacharide
LT	Leukotreines
LTA	Lymphotoxin -Alpha
MAD	mothers against dpp
MAPK	Mitogen activated protein kinase
MCD	Multicentric Castleman's disease
MCF	Malignant Catarrhal fever
MCMV –1	Murid Cytomegalovirus –1
MDSCs	muscle derived stem cells
MFG-E8	Milk fat globule EGF 8
MHC	Major histocompatability complex
MHV-68	Murine gammaherpesvirus -68
MIG	Monokine induced by IFNγ
MIP	Macrophage inflammatory protein
Ml	Millilitre
mM	milli mole
MM	Marginal metallophils
MMPs	Matrix metalloproteinase

MOI	multiplicity of infection
MOM	Mouse on mouse
mRNA	Messenger RNA
MSB	Martius- yellow- brilliant crystal scarlet soluble blue
MT	Masson's Trichrome
mta	M(immediate early) transcriptional transactivator
MuHV-4	Murid -Herpesvirus-4
Mx	Myxovirus resistance
MZ	Marginal Zone
MZB	Marginal Zone B cells
MZM	Marginal zone macrophages
NAP-2	Neutrophil activating peptide-2
NASH	non-alcoholic steato hepatitis
NBCS	New born calf serum
NBT	Nitro Blue Tetrasolium
NC	Negative control
NCAM	neural cell adhesion molecule
NF-kB	Nuclear factor - kB
NO	Nitric oxide
NOS	Nitrous oxide synthase
NOV	Nephroblastoma over expressed
NPC	nasopharyngeal carcinoma
OAS	2-5 oligoadenylate synthetases
OM	Oxidative macrophage
ORF	open reading frame
OvHv-2	Ovine herpesvirus – 2
p.i.	post infection
PALS	Peri arteriolar lymphoid sheath
PBC	Primary Biliary cirrhosis
PBL	Peripheral blood leukocytes
PBS	Phosphate buffered saline
PC	Positive control

PCR	Polymerase chain reaction
PDGF	Platelet derived Growth factor
PEC	Peritoneal exudate cells
PEL	Primary effusion Lymphoma
PFU	plaque forming unit
PI3	Phosphatidyl inositol
PIPES	Piperazine- N,N - bis (2-ethane sulfonic acid)
PKR	protein kinase
pM	Pico mole
PMN	Poly morpho nuclear
POD	Peroxidase
PSC	Pancreatic stellate cells
PSC	Primary Sclerosing cholangitis
PSR	Picrosirius red
PTLD	Post Transplantation Lymphoproliferative Disorder
Q-RTPCR	Quantitative RT-PCR
R	Red pulp
RCA	Regulator of compliment activation
rDNase	recombinant DNase
RM	Reductive macrophage
RNA	Ribo nucleic acid
Rnase L	ribonuclease -L
ROI	Reactive oxygen intermediates
RPM	Red pulp macrophages
RPMI	Roswell Park Memorial institute
rr1	large sub unit ribonuclease reductase
rr2	small sub unit ribonuclease reductase
R-SMAD	Receptor activated SMAD
Rta	Reactivation and Transcriptional activator
RT-PCR	Reverse transcriptase - PCR
S	Sense
SaHV-2	Saimiriine Herpesvirus –2

SA-MCF	Sheep associated - MCF
SAP	SLAM-associated protein
SARA	SMAD anchor for receptor activation
SCID	severe combined immunodeficiency
SD	Standard Deviation
SDF-1	Stromal cell derived factor-1
SDS	Sodium dodecyl sulphate
SH	Src homology
SLAM	Signalling lymphocyte activation molecule
SMA	Smooth muscle actin
SMAD	mothers – against decapentaplegic homologue
SPI-1	Serine protease inhibitor -1
SS DNA	Salmon sperm DNA
SS	Systemic Sclerosis
SSC	Standard Saline citrate
SSc	splenic stellate cells
ssDP	single stranded DNA binding protein
STAT	signal transducers and activators of transcription
TAM	Tumour associated macrophage
TAP	Transporter associated with antigen processing
TBM	Tingible body macrophage
TBS	Tris buffered saline
TCR	T cell receptor
TGF	Transforming growth factor
TIMP	Tissue inhibitors of MMP
TK	Thymidine kinase
TLR	Toll –like receptor
TNF	Tumour necrosis factor
TNFR	TNF receptor
TPA	12-O-tetradeconyl phorbol 13 - acetate
TPB	Tryptose phosphate broth
TR	Terminal Repeats

TRAF	TNFR associated factor
tRNA	transfer RNA
TUNEL	Terminal deoxynucleotide transferase - mediated dUTP nick end labelling
ug	Uracil DNA glycosylase
ug	microgram
µl	micro litre
v/v	volume/volume
VCA	Viral capsid antigen
VZV	Varicella -zoster virus
w/v	weight/volume
WA-MCF	Wildebeest associated - MCF
WP	white pulp
XLP	X-linked lymphoproliferative disease

CHAPTER ONE: INTRODUCTION

1.1. THE HERPESVIRUS

The Herpesviridae represent a large family of viruses, which cause life-threatening disease in man and animals throughout the world. More than 130 different herpesviruses have been identified to date which include viruses infecting vertebrates and at least one invertebrate (Arzul *et al.*, 2002). The size of herpes virions varies from 120 – 300 nm in diameter. The structure of a typical herpes virion consists of a linear double stranded deoxyribonucleic acid (dsDNA) genome encased in the central core. The size of the viral genome is characteristic of each virus, which varies from approximately 120 – 250 kilo base (kb). The core is surrounded by an icosadeltahedral capsid, which is approximately 100 – 110 nm in diameter containing 162 capsomeres. Tightly adherent to the outside of the capsid is a structure known as the tegument, which appears to consist of amorphous protein material. The tegument is encircled by a lipid bilayer of envelope derived from host cell membranes. The envelope contains cellular polyamines, lipids and viral glycoproteins (Roizman and Pellett, 2001).

In addition to sharing a common structure, the herpesviruses also share the following biological properties: 1) encoding of enzymes involved in nucleic acid synthesis and metabolism (e.g. DNA polymerase, helicase, thymidine kinase, and ribonucleotide reductase) 2) synthesis of viral DNA and assembly of capsids occurs in the nucleus of infected cell 3) production of infectious progeny is accompanied by death of the infected cell and 4) ability to establish latency in their natural host. Inspite of sharing a common structure and key biological properties, they differ substantially in their host range, tissue tropism and growth characteristics in tissue culture. Based on these features, the family of *herpesviridae* is classified into three subfamilies namely, *alphaherpesvirinae*, *betaherpesvirinae* and *gammaherpesvirinae* (Roizman and Pellett, 2001). Classification of *herpesviridae* and type species in each genus along with their associated diseases are presented in table 1.1. [http: // www. ncbi. nlm .nih .gov /ICTVdb/ Ictv/index.htm and (Knipe *et al.*, 2001;Percy and Bartholh, 2001)].

Table.1.1.Classification of Herpesviridae and disease associations

(The names in the square brackets represent the common name of the virus)

Name	Host	Disease
Sub family: Alphaherpesvirinae		
Genus: Simplexvirus		
Human herpesvirus –1 (HHV-1) [Herpes simplex virus – 1 (HSV-1)]	Human	Cold sores, keratitis
Genus: Varicellovirus		
Human herpesvirus – 3 (HHV-3) [Varicella -zoster virus (VZV)]	Human	Chicken pox and shingles
Genus: Mardivirus		
Gallid Herpesvirus – 2 (GaHV-2) [Marek's Disease Herpesvirus –1]	Chickens	Marek's Disease (T cell lymphoma)
Genus: Iltovirus		
Gallid Herpesvirus –1 (GaHV-1) [Infectious Laryngotracheitis virus]	Chickens	Infectious Laryngotracheitis (ILT)
Sub family: Betaherpesvirinae		
Genus: Cytomegalovirus		
Human Herpesvirus – 5 (HHV-5) [Human cytomegalovirus (HCMV)]	Human	Mononucleosis, multi-system disease in immunocompromised patients
Genus: Muromegalovirus		
Murid Cytomegalovirus –1 (MCMV –1)	Mouse	Cytomegalic inclusion disease
Genus: Roseolavirus		
Human herpesvirus- 6 (HHV-6)	Human	Fever and rash in children Mononucleosis in adults
Sub family: Gammaherpesvirinae		
Genus: Lymphocryptovirus		
Human herpesvirus – 4 (HHV-4) [Epstein - Barr virus (EBV)]	Human	Infectious mononucleosis (IM), Burkitt's lymphoma (BL), Post Transplantation Lymphoproliferative Disorder (PTLD), nasopharyngeal carcinoma (NPC), Hodgkin's Lymphoma (HD), X-linked lymphoproliferative disorder (XLP)
Genus: Rhadinovirus		
Saimiriine Herpesvirus –2 (SaHV-2) [Herpesvirus Saimiri (HVS)]	Squirrel monkey	Fatal lymphoproliferations in cottontail rabbits & new world monkeys e.g. marmosets

The distinguishing characteristics of alphaherpesviruses include their extremely short reproductive cycle (hours), ability to infect a wide variety of host tissues and rapid destruction of susceptible infected cells. Sensory ganglia are the preferred sites of latency, although this is not the exclusive site. Members of the betaherpesvirus subfamily have a restricted host range, a long reproductive cycle (days) and very slow growth in tissue culture system. Cytomegalia of infected cells is a common feature. Secretary glands, lymphoreticular cells and kidney are the known sites of viral latency. Gammaherpesviruses have the most restricted host range. All members are capable of replication in lymphoblastoid cells, but some produce lytic infection in epithelial and fibroblastic cells as well. Gammaherpesvirus establish latency mainly in lymphocytes.

1. 1. 1. REPLICATION OF HERPESVIRUSES

Replication of herpesviruses is a multistep process. Schematic representation of productive virus replication of herpesvirus is presented in figure 1.1. Attachment of virion envelope glycoprotein with receptors on the cell surface is the first step in the process of lytic replication [Reviewed in (Spear and Longnecker, 2003)]. Following the attachment phase, fusion of the virion envelope and plasma membrane takes place and the virion is internalised leading to release of capsid and tegument proteins into the cytoplasm. The information on tegument and capsid dissolution and transport of genome to the nucleus is limited. In the case of HSV, the tegument protein VP16 moves to the nucleus of the cell and it is involved in the stimulation of immediate early (IE) gene transcription. The cell cytoskeleton probably mediates the transport of nucleocapsids to the nucleus for the release of viral deoxyribonucleic acid (DNA) into the nucleus (Mabit *et al.*, 2002). Following the release of viral DNA into the nucleus, it undergoes circularisation (Lindahl *et al.*, 1978). The host ribonucleic acid (RNA) polymerase II mediates the transcription of viral DNA in a well co – ordinated cascade of events (Takada and Ono, 1989;Costanzo *et al.*, 1977). There are three kinetic groups of genes encoded by herpesviruses: the immediate early genes (IE), the early genes (E) and the late genes (L). They are also referred as α,β and γ genes respectively.

Figure 1.1. Schematic representation of lytic replication of herpesvirus.

(1) The entry of the virus is through the attachment of glycoprotein molecules and receptors on the cell surface (CD21 in the case of EBV)

(2) Attachment follows fusion of viral envelope with host cell membrane and internalisation of virion resulting in the release of viral capsid proteins and teguments into the cytoplasm.

(3) Cellular proteins (?) drive the trafficking of nucleocapsid into the nuclear pores and viral genome is released into the nucleus.

(4) Circularisation of linear genome occurs on entering the nucleus.

(5) Viral gene expression ensues in a temporal pattern of immediate early (IE orα), Early (E orβ) and Late (L orγ) genes.

(6) Viral DNA replication and it is packaged into the newly formed nucleocapsids. β gene products are mainly involved in viral DNA synthesis and the γ gene products are required for nucleocapsid synthesis.

(7) Some of the γ gene products are responsible for viral glycoprotein and are matured and processed in the Golgi complex

(8) Initial envelope and tegument layer is acquired during budding through the nuclear membrane.

(9) The egress of the enveloped virion particle takes place through lumenal pathway of rolling through the Golgi apparatus and transported to the surface by vesicular transport

(10) The reenvelopment pathway of egress suggests that, the de-enveloped nucleocapsids buds into the Golgi derived vesicles, forms an enveloped virion and it is transported to the surface by vesicular transport.

(11) Another theory of virion egress suggest that, the de –enveloped nucleocapsids bud through the plasma membrane by acquiring envelope with viral glycoproteins.

Adapted from (Roizman and Knipe, 2001 and Gong and Kieff, 1990)

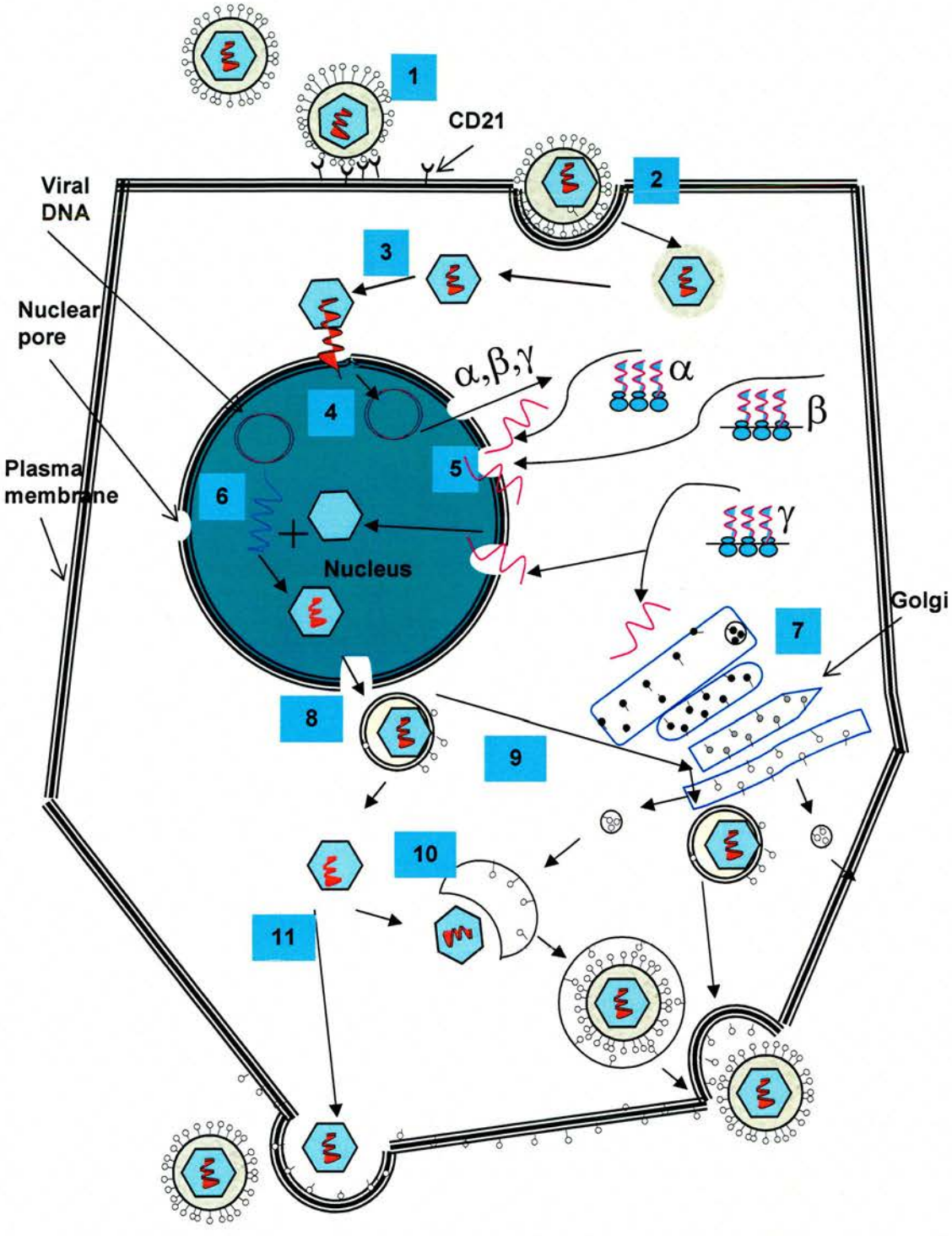

Figure 1.1. Please see the legend on the facing page

The IE genes regulate the sequential expression of E and L genes. The E genes encode the viral proteins necessary for nucleic acid metabolism, DNA replication and virus assembly (e.g. DNA polymerase, dUTPase and thymidine kinase). The L genes encode the virus structural proteins. Replication of the viral genome occurs by a rolling circle mechanism leading to the production of head to tail concatemers that are cleaved at specific points of DNA sequences into single genome units. Such single genome units are subsequently packaged into newly synthesised capsids (Jacob and Roizman, 1977;Deiss and Frenkel, 1986). The envelopment and egress of the virion particle from the infected cell is not clearly defined. The tegument is acquired during the budding of nucleocapsid through the inner nuclear membrane. The initial envelope is acquired during budding through the nuclear membrane. De–envelopment occurs in the cytoplasmic vesicles leading to the release of nucleocapsids into the cytoplasm. The nucleocapsids then bud through the Golgi network, forming an enveloped virion, acquire processed glycoproteins, and move to the surface of the cell in a Golgi-derived vesicle and are released from the cell by a process of reverse exocytosis. This pathway is usually referred to as the re-envelopment pathway. The second pathway, which is commonly referred to as the lumenal pathway of virion egress, follows the budding of enveloped virions through the outer nuclear membrane and it is transported through a vesicular movement through the Golgi apparatus to the exterior of the cell (Roizman and Knipe, 2001). Another argument in the case of EBV favours acquiring the envelope at the plasma membrane and release of virion (Gong and Kieff, 1990).

1.1.2. LATENT INFECTION OF HERPESVIRUS

Establishment of latency during infection is a characteristic biological feature of herpesviruses. During latent infection, the virus genome is maintained as a circular episome with restricted expression of viral genes. The latent virus uses the host cell machinery for its own genome replication. The latent virus retains the ability for productive replication, which occurs during reactivation of infection. The factors controlling this level of suppression of productive replication and events leading to the trigger of reactivation are poorly understood. Stress, tissue

damage and immunosuppression are implicated as factors responsible for reactivation from latent HSV infection (Wagner and Bloom, 1997). The cellular tropism, mechanism of establishment and gene expression profile during latency vary between viruses. The details of the latency programme will be discussed later with relevance to individual viruses.

1.2. GAMMAHERPESVIRUS

The *gammaherpesvirinae* consist of two genera: Lymphocryptovirus and Rhadinovirus. Lymphocryptovirus means virus hidden in lymphocytes ('Cryptos' originated from a Greek word 'Kryptos' meaning 'hidden'). EBV is the type species of this genus. Rhadinoviruses share a common genome structure. The linear dsDNA has a central segment of low GC DNA (LDNA) that is flanked by multirepetitive high GC DNA (HDNA) (Bornkamm *et al.*, 1976). This extreme intragenomic GC heterogeneity resulting in fragmentation during density centrifugation led to the coining of the term Rhadinovirus (Roizman *et al.*, 1981). Important members of this genera are: Kaposi's sarcoma associated herpesvirus (KSHV) or Human herpesvirus – 8 (HHV –8), Alcelaphine herpesvirus –1 (AlHV -1), Ovine herpesvirus–2 (OvHv-2), Herpesvirus saimiri (HVS), Bovine herpesvirus–4 (BoHV–4), Equine herpesvirus-2 (EHV–2), Herpes virus saimiri (HVS) and Murine gammaherpesvirus – 68 (MHV–68).

1.2.1. HUMAN GAMMAHERPESVIRUS

Two important viral pathogens causing major disease in humans are EBV and KSHV. These two important gammaherpesviruses are associated with a variety of fatal human diseases and hence the biology of the viruses and pathogenic mechanisms associated with these viruses has been the subject of intense study in recent years [Reviewed in (Young and Rickinson, 2004;Cathomas, 2003)].

1.2.1.1. EPSTEIN – BARR VIRUS (EBV)

EBV or HHV –4 was discovered as the aetiological agent of Burkitt's Lymphoma (BL), which is the first human tumour virus to be discovered (Epstein *et al.*, 1964). Recent estimates show that more than 95% of the world adult population

are seropositive for the virus [Reviewed in (Rickinson, 2002)]. Primary infection usually occurs early in childhood and persists in the host throughout their lifetime. If the exposure is delayed to early adult life, it leads to the development of disease condition called infectious mononucleosis (IM) or glandular fever. EBV is also the aetiological agent of X-linked lymphoproliferative disease (XLP), Hodgkin's disease, nasopharyngeal carcinoma (NPC) and post transplantation lymphoproliferative disorder (PTLD) (Wolf *et al.*, 1973;Tanner and Alfieri, 2001).

1.2.1.1.1 EBV GENOME

The EBV genome was the first herpesvirus genome to be sequenced in full (Baer *et al.*, 1984;Hatfull *et al.*, 1988). The EBV genome structure is characterised by terminal repeats and many unrelated internal repeats in the body of the genome. The genome size is around 172 kb and comprises long and short unique regions interspersed by internal repeats of 3kb in length. The terminal repeats are 500 base pair (bp) in size. The immediate early gene, Bam H1 Z leftward open reading frame -1 (BZLF1) is closely related to the *jun/fos* family of transcriptional activators (Farrell *et al.*, 1989). The Bam H1 C rightward open reading frame -1 (BCRF1) shares 90% amino acid homology to human interleukin -10 (IL-10) sequence (Moore *et al.*, 1990).

1.2.1.1.2. LYTIC REPLICATION

Lytic replication of EBV is usually studied by inducing lytic infection in latently infected cell lines such as BL cell lines. Treatment of cell lines with phorbol esters such as 12 – O – tetradeconyl phorbol 13 – acetate (TPA) is the common method for inducing reactivation (Baumann *et al.*, 1998). Entry of EBV into B-lymphocytes is mainly through the interaction of viral envelope glycoprotein 350/220 (gp350/220) with the complement receptor -2 (CD21) (Fingeroth *et al.*, 1984). It has also been shown that a complex of three glycoproteins namely; the gH, gL, and gp42 are also required for the entry of virus into host cells (Molesworth *et al.*, 2000) . The proteins encoded by BZLF-1 or Zta and Bam H1 R leftward open reading frame – 1 (BRLF-1) or Reactivation and transcriptional

activator (Rta) genes are key transactivators to induce the cascade of lytic EBV gene expression. Bam H1 H rightward open reading frame -1 (BHRF1) is thought to be important in preventing apoptotic cell death during lytic replication (Henderson *et al.*, 1993).

1.2.1.1.3. EBV LATENCY

EBV encodes nine latency-associated proteins. Six of them are nuclear associated and referred to as EBV nuclear associated antigens (EBNA). They include EBNA-1, EBNA -2, EBNA-3A, EBNA -3B, EBNA3C and EBNA-LP. The other three latency-associated genes are membrane associated and hence called as latent membrane proteins (LMP). The LMP genes are LMP-1, LMP2A and LMP2B. EBNA -1 tethers the viral episomal genome to the host chromosome (Yates *et al.*, 1985) EBNA-2 is a transcriptional activator and turns on all the other latency associated genes in the growth programme of latency. The proposed function of EBNA-3C is to inactivate the retinoblastoma (Rb) tumour suppressor gene similar to adenovirus E1A and papillomavirus E7 proteins (Parker *et al.*, 1996). EBV latency is complex and has been classified into three types. Table 1.2. shows the gene transcription pattern observed in different forms of EBV latency.

Table. 1.2. Gene transcription pattern and associated functions during different forms of EBV latency [Adapted from (Thorley-Lawson, 2001)]

Latency programme	Gene expression	Function
Growth programme (Latency III)	EBNA -1-6 LMP-1 LMP-2A-B	Stimulation of B lymphocytes
Default programme (Latency II)	EBNA-1 LMP-1 LMP-2A	Survival signals for infected lymphoblasts to differentiate into memory B-lymphocytes and its survival
Latency programme (Latency I)	EBNA -1, often LMP-2A	Persistence of the virus in memory B-lymphocytes and avoids immune recognition

During primary infection of B lymphocytes, EBV uses the growth programme with expression of full complement of latency associated genes and then switches

to the default programme to promote differentiation of infected B-lymphocytes into memory B-cell phenotype (Babcock *et al.*, 2000). How this shift takes place from growth programme to default programme is not known. Probably, turning off of EBNA-2 is involved in this shift. As shown in table 1.2, three viral proteins are expressed during the default programme. Tethering of viral genome through EBNA-1 to the host chromosome ensures the replication of viral genome during cell division. LMP -1 is the functional homologue of CD40 (Kilger *et al.*, 1998). LMP-1 signalling rescues B-lymphocytes from apoptosis and drives their proliferation. LMP-2A signalling shows similarity to the downstream signals following B–cell receptor (BCR) signalling that are essential for the survival of B – lymphocytes (Caldwell *et al.*, 1998). Activation of PI3K/AKT pathway by LMP2A favours blocking apoptotic signals and EBV infected cell survival (Fukuda and Longnecker, 2004). In addition to the latency-associated genes described above, non-polyadenylated (non – coding) RNA molecules such as EBV encoded RNA (EBER1 and EBER2) and BAM H1A RNA transcripts or BART are also expressed during latency.

1.2.1.1.4. BURKITT'S LYMPHOMA (BL)

BL was identified in endemic proportions among the children from equatorial Africa and Papua New Guinea in late 1950's and early 1960's (Burkitt, 1963). This B-lymphocyte specific tumour most often affects the jaw and abdominal organs of children. The endemic area of BL falls in the endemic area for malaria and the relationship between the two conditions is poorly understood. The adult population is resistant to the infection and the reason for the increased childhood susceptibility also is not well characterised. There are two other forms of BL reported from different geographical locations throughout the world. They are termed as sporadic and acquired immunodeficiency syndrome (AIDS) associated BL. Almost 97% of the endemic tumour tissue carry EBV genome whereas in sporadic BL tissues, virus is detected in only 12 – 25% of the samples (Ziegler *et al.*, 1976). 30 – 40 % of the AIDS associated BL are EBV related. Deregulation of *c-myc* gene is shown in the tumour cells derived from endemic and sporadic BL and it is believed to be the major molecular mechanism responsible for

oncogenesis. The vast majority of EBV positive BL cells show a highly restricted latency I type of gene expression (Rowe *et al.*, 1987).

1.2.1.1.5. POST - TRANSPLANT LYMPHOPROLIFERATIVE DISORDER (PTLD)

Lymphoid neoplasm is a serious problem in patients undergoing organ transplants along with the risk of rejection of the graft. EBV is considered as the major cause of such neoplastic diseases. PTLD arise in the first year of transplantation and almost all of them are EBV positive and express latency III type of gene expression. Adoptive immunotherapy with EBV specific cytotoxic T-lymphocytes from human leukocyte antigen (HLA) matched healthy blood donors has been successfully used to treat PTLD patients (Haque *et al.*, 2002). Terminal AIDS patients also develop PTLD like B-cell lymphomas and confirms the notion that immunosuppression is a primary trigger for the development of this type of neoplasm [Reviewed in (Gaidano *et al.*, 1998)].

1.2.1.1.6. HODGKIN'S DISEASE (HD)

Approximately 30 - 50% of the classic HD in the western world is associated with EBV [Reviewed in (Gandhi *et al.*, 2004)] . In EBV positive HD tumours, the EBV genome is present in every Hodgkin's and Reed-Sternberg cells (HRS cells) and expresses latency II type of gene expression. HRS cells show many characteristics of LMP1 - induced phenotypic changes including strong activation of nuclear factor -κB (NF -κB) (Pallesen *et al.*, 1991;Krappmann *et al.*, 1999).

1.2.1.1.7. NASOPHARYNGEAL CARCINOMA (NPC)

NPC is an epithelial undifferentiated tumour arising from nasopharyngeal epithelium [Reviewed in (Chan *et al.*, 2004)]. A small proportion of tumours show the phenotype of squamous cell carcinoma. The incidence of this neoplastic condition is unusually high in southeast China and in emigrant Chinese population elsewhere in the world (Ablashi *et al.*, 1983). The precise role of EBV in the tumourogenesis of NPC is not well established. EBV was detected in tumour tissues by *in situ* techniques (Brooks *et al.*, 1992). Circumstantial evidence

suggests the contribution from other chemical factors like nitroso – dimethyl amine in carcinogenesis. A variety of other co-factors are also suggested to contribute to tumourogenesis.

1.2.1.1.8. INFECTIOUS MONONUCLEOSIS (IM)

IM is the most common manifestation of EBV infection in the western world. As mentioned earlier, this condition is the result of delayed exposure of young adults to the virus. The productive replication of the virus occurs in the oropharyngeal epithelium and contact with saliva is the most common route of virus transmission (Yao *et al.*, 1989). General lymphadenopathy, especially at the pharyngeal region, splenomegaly and hepatomegaly are common manifestations of this condition. A key laboratory diagnostic feature of this condition is the presence of 'atypical mononuclear cells' in the peripheral circulation. There is expansion of a specific subset of CD8+ T-lymphocytes which are specific for lytic and latent viral antigen epitopes in peripheral circulation (Callan *et al.*, 1996). The specific reason for this disease manifestation in young adults is not clearly defined. However, exposure to a massive dose of virus through heavy kissing is considered as one of the reason for this selective susceptibility.

1.2.1.1.9. X –LINKED LYMPHOPROLIFERATIVE DISEASE (XLP)

An XLP affected individual dies rapidly. A simple mutation in the signalling lymphocyte activation molecule – (SLAM) – associated protein (SAP) is the basic defect which diverts EBV infection from benign persistence to a fatal disease (Coffey *et al.*, 1998). The disease is characterised by immune disregulation, lymphoproliferation and resulting massive infiltration of bone marrow and liver by CD8+ T lymphocytes, macrophages and EBV infected B-lymphocytes.

1.2.1.1.10. IMMUNE RESPONSE

Immune control of primary EBV infection is mediated by the induction of EBV specific CD8+T-lymphocytes. The huge expansion of CD8+ cytotoxic T-lymphocytes (CTLs) is directed against a wide variety of lytic and latent viral antigens and is capable of destroying the infected cells (Moss *et al.*, 1981). CD4+

T-cells also contribute to immune regulation against EBV infection (Leen *et al.*, 2001). Antibody response against EBV infection is well studied in IM patients. At the time of clinical onset of disease, the patients develop immunoglobulin M (IgM) antibodies against viral capsid antigen (VCA). Virus neutralising antibodies (IgM and IgG) develop relatively late in disease and are targeted against the glycoprotein antigen gp350. Antibodies against EBNA –1 develop late in disease and healthy carriers of the virus have antibodies (IgG) against VCA, gp350 and EBNA –1 (Rickinson and Kieff, 2001).

1.2.1.2. KAPOSI'S SARCOMA ASSOCIATED HERPESVIRUS (KSHV)

KSHV or HHV-8 is the most recently identified human gammaherpesvirus. Viral DNA fragments of KSHV were isolated from Kaposi's sarcoma (KS) lesions of immunosuppressed patients (Chang *et al.*, 1994). In addition to KS, KSHV is also etiologically associated with body cavity based lymphoma (BCBL) or primary effusion lymphoma (PEL) and some plasma cell forms of multicentric Castleman's disease (MCD).

1.2.1.2.1. KSHV GENOME

The KSHV genome is about 145 kb in size and contains about 87 genes, which are flanked by terminal repeats (Russo *et al.*, 1996;Moore and Chang, 2001). In common with rhadinoviruses, varying numbers of terminal repeats are present. The genomic arrangement of KSHV is similar to that of HVS, the prototype rhadinovirus. The genes that are not homologous to HVS genes are given the K prefix (K1 – K15). The cellular homologues encoded by KSHV are v-fas-associated death domain (FADD) interleukin (IL)-1β-converting enzyme (FLICE) inhibitory protein (FLIP) [open reading frame -71 (ORF71)] (Thome *et al.*, 1997), v cyclin (ORF72), v-G-protein-coupled receptor (ORF74), v-interferon regulatory factors (v-IRF) (e.g. K9 –IRF1), v- B-cell lymphoma (Bcl) –2 (Bcl-2) (ORF16) (Cheng *et al.*, 1997b), v – dihydrofolate reductase (DHFR) (Cinquina *et al.*, 2000) and v-IL-6 (Neipel *et al.*, 1997). ORF4 is a homologue of complement binding protein. K14 encodes a neural cell adhesion molecule (NCAM) like protein, which is homologous to human OX-2 membrane antigens (recently designated as

CD200). Homologues of the macrophage inflammatory protein (MIP)-I, II and III are encoded by K6, K4, and K4.I respectively [Reviewed in (Jenner and Boshoff, 2002)] .

1.2.1.2.2. LYTIC REPLICATION

The information on mode of cell entry or cellular receptor for KSHV is limited. KSHV has structural glycoproteins like gB used by other herpesviruses for cell entry (Pertel *et al.*, 1998). Direct transmission from KS lesions and PEL cell lines to 293 cells demonstrates that tumour-derived virus is fully permissive for productive infection (Foreman *et al.*, 1997;Renne *et al.*, 1998).

1.2.1.2.3. KSHV LATENCY

The primary reservoir for persistent asymptomatic KSHV infection appears to be B-lymphocytes. Other reported sites of natural infection include endothelium, CD68+ monocyte – macrophage cells, prostate epithelia and dorsal root sensory ganglion (Blasig *et al.*, 1997;Corbellino *et al.*, 1996;Diamond *et al.*, 1998). During latency, the viral genome is tethered to the host DNA molecule as closed circular episomal DNA (Renne *et al.*, 1996). Latent nuclear antigen (LANA) encoded by ORF 73 facilitates the tethering of viral genome to the host genome (Ballestas *et al.*, 1999). Along with LANA, v-FLIP and v-Cyclin are located adjacent in the genome and transcribed as polycystronic messages (Talbot *et al.*, 1999;Sarid *et al.*, 1999;Sarid *et al.*, 1998;Dittmer *et al.*, 1998).

1.2.1.2.4. KAPOSI'S SARCOMA (KS)

Moritz Kaposi described KS in 1872 as an 'idiopathic multiple pigmented sarcoma of the skin' [Reviewed in (Antman and Chang, 2000)]. There are four distinct clinical variants of KS. The classic KS predominantly affect elderly men of Mediterranean, eastern European and Jewish descent. The endemic KS is prevalent in equatorial, eastern and southern Africa. The classic KS lesion is more indolent in nature and less clinically aggressive than endemic KS. Iatrogenic or post-transplant KS is seen in organ transplant patients receiving immunosuppressive therapy. The most aggressive form of the disease is AIDS

associated [Reviewed in (Verma and Robertson, 2003)]. The pathogenesis of this vascular tumour is not clearly understood and the histogenesis of the tumour is from spindle shaped cells derived from endothelial origins.

1.2.1.2.5. PRIMARY EFFUSION LYMPHOMA (PEL)

PEL is a rare, rapidly fatal, non-Hodgkin's lymphoma found in pleural or pericardial effusions. Rarely such tumour mass was found in the lymph nodes, lungs or gastrointestinal tract. Presence of hyper-mutated immunoglubulin genes and surface expression of syndecan -1 along with lack of Bcl-6 expression in the tumour cells suggest that histogenesis of the tumour is from post-germinal centre B-lymphocytes (Carbone *et al.*, 1998).

1.2.1.2.6. MULTICENTRIC CASTLEMAN'S DISEASE (MCD)

MCD is a lymphoproliferative disorder characterised by expanded germinal centres and proliferating endothelial vessels in affected lymph node. Based on the histological feature there are two variants namely the plasmacytoid and hyaline vascular form. Most of the KSHV associated MCD are plasmacytoid type (Dupin *et al.*, 2000). KSHV encoded v-IL-6 is thought to be a key initiator of this proliferative disorder (Parravicini *et al.*, 2000).

1.2.2. ANIMAL GAMMAHERPESVIRUS

An important disease condition-affecting cattle caused by gammaherpesvirus is malignant catarrhal fever (MCF). There are two main viruses responsible for this condition namely AlHV – 1 and OvHV –2 [Reviewed in (Coulter *et al.*, 2001)]. Other members of the gammaherpesvirinae, which are associated with disease condition in animals, are EHV-2 and BoHV- 4. (Telford *et al.*, 1995;Lomonte *et al.*, 1996). EHV-2 is widespread in horses and has been associated with immunosuppression in foals and respiratory tract disease. BoHV-4 has been isolated from cattle with respiratory and ocular disease, abortion, metritis, pneumonia, diarrhoea and mammary pustular dermatitis.

AlHV –1 is a gammaherpesvirus isolated from wildebeest (*Connochaetes taurinus*) in Africa (Plowright *et al.*, 1960). The genome of the AlHV-1 has been sequenced (Ensser *et al.*, 1997). AlHV –1 does not cause disease in its natural host. Sheep carry OvHV –2 asymptomatically (Bridgen and Reid, 1991). Recent evidence suggest that experimental infection of sheep with ovHV-2 can result in MCF like disease (Li *et al.*, 2005;Taus *et al.*, 2005). Lymphoblastoid cell lines (LCL) propagated from naturally infected cattle and experimentally infected rabbits are being used for molecular characterisation of the virus. OvHV–2 genome is very similar to that of AlHV –1 (Rosbottom, 2003).

1.2.2.1. MALIGNANT CATARRHAL FEVER (MCF)

MCF affects cattle, deer and other ruminants throughout the world. The outbreak of the disease is generally sporadic. However, severe herd outbreaks affecting large numbers of animals have been reported. The disease caused by AlHV–1 and OvHV–2 are usually referred as Wildebeest associated MCF (WA – MCF) and Sheep associated MCF (SA – MCF) respectively. The clinical signs of both forms of disease are similar and indistinguishable. High fluctuating fever, nasal discharge, corneal ulceration and lymphadenopathy are consistent clinical signs. It is generally believed that MCF is a fatal disease. However, there are reports of domestic cattle showing mild clinical symptoms and remaining as chronically infected with occasional recrudescence (O'Toole *et al.*, 1997).

The most consistent histopathological lesion in almost all organs derived from infected animals is marked perivascular and intramural infiltration of mononuclear cells. The infiltrating cells are mainly lymphocytes with large nuclei and prominent nucleoli. Medial necrosis and endothelial swelling are also observed. These lesions may be segmental or involve the entire wall of the blood vessel (Liggitt and DeMartini, 1980). The infiltrating lymphocytes were characterised as CD8+ T lymphocytes (Ellis *et al.*, 1992;Nakajima *et al.*, 1992). Recently it has been shown that CD8+ T cells infiltrating the perivascular sites carry virus genome (Simon *et al.*, 2003).

Experimental transmission of AlHV-1 to hamsters, rats and guinea pigs (Jacoby *et al.*, 1988a) and OvHV–2 to rabbits and hamsters (Buxton *et al.*, 1988) has been reported. Laboratory mice are refractory to both viruses (Jacoby *et al.*, 1988b). The clinical symptoms and lesions shown by the experimentally infected rabbits are similar to those seen in natural disease (Buxton and Reid, 1980;Reid *et al.*, 1984). Lymphoblastoid cell lines have been derived from the tissues of naturally infected cattle and experimentally infected rabbits with both viruses (Cook and Splitter, 1988;Reid *et al.*, 1983). The cells were morphologically classified as large granular lymphocytes (LGL).

1.2.2.2. HERPESVIRUS SAIMIRI (HVS)

HVS or Saimiriine Herpesvirus –2 (SaHV-2) is the prototype rhadinovirus. Like AlHV-1, HVS does not cause any overt disease in its natural host, the squirrel monkey (*Saimiri sciureus*). However, infection of new world primates results in rapid development of T – cell lymphoma. A permissive tissue culture system is available for virus propagation. Consistent production of lymphomas in susceptible animal models has made it a popular system to study virus-mediated oncogenesis. The HVS genome is approximately 140kb in size and contains up to 77 ORFs (Albrecht *et al.*, 1992). In agreement with the general features of gammaherpesviruses, HVS also encode for several genes homologous to cellular genes (Fickenscher and Fleckenstein, 2001). The oncogenic viral proteins involved in transformation, proliferation, cell signalling and episome maintenance encoded by HVS are homologous to those found in KSHV and EBV [reviewed in (Damania, 2004)].

1.3. MURINE GAMMAHERPESVIRUS – 68 (MHV-68)

MHV–68 is a tractable small animal model for studying the pathogenesis of gammaherpesvirus infections [Reviewed in (Virgin and Speck, 1999;Stewart *et al.*, 1998a;Simas and Efstathiou, 1998;Doherty *et al.*, 2001;Nash *et al.*, 2001)]. MHV -68 is being used as a small animal model for studying the pathogenesis of gammaherpesviruses by virtue of its following features: 1) Ability to grow in a variety of tissue culture system. 2) Infectivity of different strains of laboratory

mice (close to natural host) and cause disease mirroring EBV infection. 3) Known structure and relative ease to manipulate the genome.

1.3.1. ISOLATION AND CHARACTERISATION OF THE VIRUS

MHV – 68 was originally isolated from a Bank Vole (*Clethrionomys glareolus*) in Slovakia (Blaskovic *et al.*, 1980). The electron microscopic studies of the rabbit embryo fibroblast infected by the virus revealed morphological changes resembling that induced by herpesviruses (Ciampor *et al.*, 1981). Different cell cultures of human and animal origin (birds, rodents, carnivore, pigs, monkeys and human) were found to support the growth of virus (Svobodova *et al.*, 1982). Recently, wood mice *(Apodemus sylvaticus)* captured from around Liverpool, UK was shown to carry MHV – 68 DNA, primarily in the lung (Blasdell *et al.*, 2003). The *International committee on Taxonomy of viruses (*ICTV) officially named MHV-68 as Murid herpesvirus – 4 (MuHV-4).

1.3.2. GENOME

The MHV-68 genome consists of a unique stretch of DNA of 118.2 kb, which is flanked, by a variable numbers of 1.23 kb repeat units (Efstathiou *et al.*, 1990a;Efstathiou *et al.*, 1990b). The unique stretch of the DNA has a G+C content of 45%. The complete DNA sequence of the MHV-68 genome has been determined by two independent groups and deposited in the gene bank (Gene bank data base accession number: AF105037 and U97553). The published genome sequence is derived from strain WUMS which was plaque purified from g2.4 strain (Virgin *et al.*, 1997). The sequences are very similar except for few differences (Nash *et al.*, 2001) . The majority of the genes encoded by MHV-68 are collinear and homologous with those of other gammaherpesviruses such as HVS and KSHV. The organisation of MHV–68 genome is presented in figure.1.2. The details of individual viral genes are discussed later in relation to their role in pathogenesis.

1.3.3. PATHOLOGY

Pathogenesis of MHV-68 infection was studied by infecting one-day-old baby mice via the oral route (with suggested inhalation of the virus). Virus titres were observed in the lung on day 1, in the liver in traces on day 2, in blood on day 3, in brain and heart on day 4 and in kidney and spleen on day 5 post infections (p.i.). In all the above organs, virus titres peaked between day 7 and 9 p.i. Characteristic pathological lesion in the lung was small foci of inflammation with desquamation of epithelial cells and exudates rich in macrophages. Some epithelial cells of alveolar ducts and bronchioles revealed typical inclusion bodies. Focal necrosis of alveolar septa was prominent and was associated with mononuclear infiltration. In the liver, necrosis of hepatocytes with occasional intranuclear inclusion bodies was reported. The hepatic sinusoids were widened and contained macrophages, lymphocytes and the nests of extramedullary haematopoiesis (Blaskovic *et al.*, 1984).

Pathogenesis in outbred laboratory mice aged 5, 10, and 21 days and infected by oral and/or intra nasal route was investigated (Rajcani *et al.*, 1985). The lung showed severe exudative pneumonia. The alveoli were filled with oedema fluid, fibrin, macrophages and necrotic alveolar cells. Lymphocytic infiltration was abundant in the peribronchial connective tissue and the septal walls. Ventricular musculature showed focal necrotic changes associated with mononuclear infiltration at the edge of the lesion. Minimal lymphocytic infiltration was noticed in the portal areas of the liver. The meninges around the brain stem showed round cell infiltration. The anterior horn of the spinal cord revealed small nodular infiltrates and few neurons were showing necrotic changes.

Primary infection of three to four weeks old BALB/c mice with MHV-68 showed that pathological features are in common with that of EBV infection of man and that lung and lymphoid tissue are the major sites of pathology and persistence (Sunil-Chandra *et al.*, 1992a). In mice infected intranasally, a peak virus titre was observed in lung, spleen and thymus on third day p.i. The virus presence in heart and kidney showed a sudden peak on day 10 p.i. Whole blood showed traces of

Figure 1.2. Diagrammatic representation of the MHV-68 Genome. The unique portion of the genome is represented by a single black line, with co-ordinates marked at 10 kb intervals. The terminal repeats (TR) and internal repeats (IR) are marked as dark blue blocks. The open reading frames (ORFs) are indicated in arrows and direction of arrow represent its initiation of transcription. The unique ORFs of MHV-68 are shaded in yellow except the one with known functions. The ORFs whose function is unknown is shaded in blue and the genes with known function are shaded in different colors and their function is given in an abbreviated form on top of the arrows. CBP, Chemokine binding protein; RCA , regulator of complement activation; ssDP, single stranded DNA binding protein; gB, Glycoprotein B; dpol, DNA polymerase; K3, homologue of HHV-8 gene; TK , Thymidine Kinase; gH, glycoprotein H; AE, alkaline exonuclease; gM, glycoprotein M; ug, Uracil DNA glycosylase; gL, glycoprotein L; Rta, reactivation and transcriptional activator; gp150, glycoprotein 150 (homologue of EBV gp340/220); dut, dUTPase; mta, M(immediate early) transcriptional transactivator; rr2, small sub unit ribonuclease reductase; rr1, large subunit ribonucleotide reductase; cyc D, homologue of mammalian cyclin D; Bcl-2, homologue of mammalian Bcl-2, LANA, homologue of latent nuclear antigen of HHV-8, GPCR, homologue of mammalian g protein coupled receptor.

Adapted from Stewart *et al.,* (1998a) accordance with published sequence of MHV –68 (Virgin *et al.*, 1997).

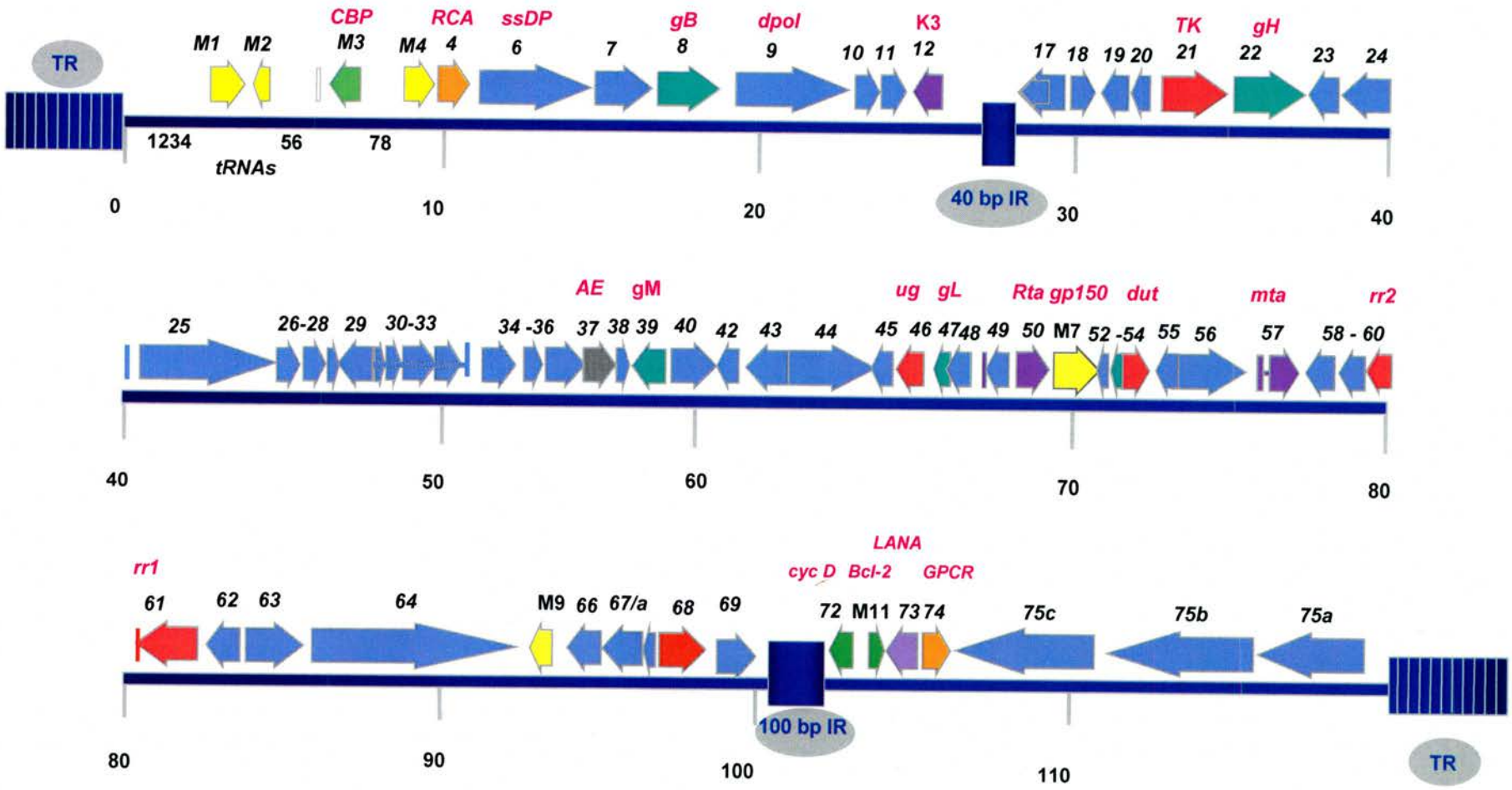

Figure 1.2: Please see the legend on the facing page

virus on day 10 p.i, whereas the adrenal gland showed traces of virus on day 3 and 5 p.i. The presence of virus in the mesenteric lymph node was insignificant. Liver, serum, brain or trigeminal ganglia did not show any presence of virus. When the virus was administered through the intravenous route, virus was observed on day 3 p.i. in lung, spleen, thymus, liver and mesenteric lymph node, on day 5 p.i. in the adrenal and on day 10 p.i. in heart and kidney. The presence of virus in the whole blood, trigeminal ganglia and brain was insignificant. This study established the intranasal route of infection as the best route for studying the pathogenesis of MHV-68. Probably, this may be the natural route of infection.

1.3.4. LATENT INFECTION

In an attempt to determine the site of viral latency, a variety of tissues from infected mice were co-cultivated with permissive cells to isolate latent virus (Infective centre assay). Latent virus was readily isolated by this method from spleen of mice killed at day 3, 5, 10, 36 and 90 days p.i. Infectious virus could not be detected from spleen of mice at 90 days p.i by conventional plaque assay. This data implied that, spleen is a major site of latency for MHV-68. Infectious or latent virus could not be recovered from non - lymphoid organs at later time points (Day 90 p.i.). However, improvement in the sensitivity of the assay could recover infectious virus from lung of two out of five mice after 90 days p.i. This suggests that the lung in addition to spleen also is a site of latent/persistent infection (Sunil-Chandra *et al.*, 1992a).

The consistent recovery and enrichment of latent virus in the B-cell fraction of splenocytes recovered from MHV–68 infected mice clearly demonstrated that B-cells are the major site of virus latency (Sunil-Chandra *et al.*, 1992b). Further evidence to confirm the B-cell tropism of the virus during latent infection was obtained from a study of *in vitro* infection of different cell lines (Sunil-Chandra *et al.*, 1993). Persistent infection could be established in mouse myeloma cells (B-cell – NSO cell line) but not in mouse thymoma cells (T cell – BW 5247 cell line). The virus persists indefinitely in myeloma cells, without any apparent cytopathic effect, but with production of infectious virus. Acylcyclovir (ACV) abolished the

productive infection, but large number of cells continued to harbor virus in a latent form.

This observation was further confirmed by demonstrating the absence of splenic latency in B-cell deficient mice (Usherwood *et al.*, 1996c). Transgenic μMT mice, which lacked mature B-cells, were used in this study. No infective centres or viral DNA was detected in the spleen of μMT mice following intranasal infection. In addition, the infected μMT mice failed to develop splenomegaly suggesting that latently infected B-cells are required for the establishment of splenomegaly. Viral DNA could be detected in both control mice and μMT mice at late time intervals from lung, which, confirmed the earlier observation that lung, is a site of viral persistence/latency. However, in a separate study, it was reported that μMT mice infected via intraperitoneal route developed latently infected cells in the spleen at a level about 100 fold higher than that in wild type mice (Weck *et al.*, 1996). Combined *In situ* hybridisation studies with viral tRNA probe and immunohistochemistry with monoclonal antibodies for cytokeratin proved that the cell type in the lung harbouring MHV-68 genome was epithelial in nature. By adoptive transfer experiments, it was also shown that virus resident in splenic B-cells is able to spread infection to the lung. In the presence of B-cells, virus present in lungs can establish infection in spleen. This two-way movement of the virus between lymphoid and non-lymphoid tissue during latent infection may be a part of the survival strategy of the virus (Stewart *et al.*, 1998b).

Latent infection of macrophages occurs in the peritoneum of normal and B-cell deficient C57BL/6 mice (Weck *et al.*, 1999a). This indicates that MHV-68 has broader cellular tropism for the establishment of latency. The F4/80 positive macrophage harboured most of the viral genome and efficiently reactivated from latency. Whereas, CD19 positive, B-cell enriched peritoneal exudate cells (PEC) harboured about 10 fold lower frequencies of virus. It has been shown that latent infection in the spleen after intranasal infection with MHV–68 is harboured in B-cells, macrophages and dendritic cells (Flano *et al.*, 2000). Among B-cells, latency was preferentially associated with activated B-cells expressing the

phenotype of germinal centre B-cells. Long-term latency is preferentially maintained in two different subsets of isotype switched B-cells, germinal centre and memory B-cells. Cell cycle analysis indicated that MHV-68 is located in both cycling and resting isotype switched B-cells (Flano *et al.*, 2002a) . In a separate study, it was also shown that long term latency is maintained in immunoglobulin D negative B-cells which exhibit features of memory B-cells (Willer and Speck, 2003). The requirement of CD40 on the surface of B-cells for establishment of latency was tested by developing bone marrow chimera mice containing CD40+ve or CD40-ve B-cells and monitoring latent infection. CD40-ve B-cells progressively lost MHV – 68 latency whereas isotype- switched CD40+ve B-cells maintained latent infection (Kim *et al.*, 2003).

1.3.5. INFECTIOUS MONONUCLEOSIS LIKE SYNDROME

Another characteristic feature of MHV – 68 infection is the massive expansion of CD8+ T-lymphocyte population expressing Vβ4 T-cell receptor (TCR) in conjunction with variety of other TCR α chains (Tripp *et al.*, 1997;Hardy *et al.*, 2000;Flano *et al.*, 2004). The timing of this T- cell response also is significant as it appears subsequent to the resolution of acute phase of infection and persists for more than a month. It is suggested that this expansion of the T- cell population may be comparable to the IM syndrome shown by young adults exposed to EBV [Reviewed in (Doherty *et al.*, 1997;Flano *et al.*, 2002b)]. However, there is a major difference between this T- cell response and T -cell response shown by IM patients. Tetramer studies of the T-cell response from IM patients have shown that CD8+ T- cell population largely consist of EBV specific major histocompatability complex (MHC) class I restricted T-cells, whereas in MHV-68 induced T-cell responses are not completely viral antigen specific (Callan *et al.*, 1998;Callan *et al.*, 2000). It was suggested that the non-viral antigen specific T-cell response shown by mice infected with MHV –68 might be in response to a 'super antigen' encoded by the virus (Tripp *et al.*, 1997). However, there are classical differences between a 'super antigen' driven response and the Vβ4 restricted CD8+ T-cell response shown in response to MHV-68 infection: The MHV–68 driven response is oligoclonal in nature and this response is not

mediated by binding to MHC glycoproteins which distinguishes it from other 'super antigen' driven responses (Hardy *et al.*, 2000;Coppola *et al.*, 1999).

1.3.6. *IN VIVO* REACTIVATION

As discussed above, spleen is a major organ harbouring latently infected cells following intranasal infection of mice with MHV–68 (Sunil-Chandra *et al.*, 1992b;Sunil-Chandra *et al.*, 1992a). It has been shown that the latently infected cell load in the spleen reaches a concentration of $1/10^4$-spleen cells at two weeks p.i. and then drops to $1/10^6$ spleen cells and is maintained at this level throughout the life of mice (Cardin *et al.*, 1996). Recently, limiting dilution assays coupled with polymerase chain reaction (PCR) for viral DNA have shown that, the actual number of latently infected cells in the spleen is much higher than that detected by the conventional assays depending on *ex vivo* reactivation (Weck *et al.*, 1999b;Flano *et al.*, 2000).

Establishment of latency and periodic reactivation are the key events in the persistence of gammaherpesvirus infection (Tibbetts *et al.*, 2002). It has been very difficult to detect and quantify this low level of reactivating virus in the lymphoid compartment with the conventional plaque assay (Weck *et al.*, 1999b;Flano *et al.*, 2000). Modifications to the conventional assay were successful in detecting low levels of infectious MHV–68 in the range of less than 100 PFU / whole spleen or lung (Flano *et al.*, 1999). Other evidence for the low level of productive replication/reactivation of virus is the detection of activated CD8+ T-cells specific for epitopes in lytic cycle viral proteins long after the clearance of acute infection (Liu *et al.*, 1999;Stevenson *et al.*, 1999).

Recently, it has been shown that gamma interferon (IFNγ) regulates the reactivation from latency: there was 30 fold increase in reactivation from latency in PEC from IFNγ knock out animals compared with control animals infected with MHV–68 (Tibbetts *et al.*, 2002). Interestingly, the reactivation from latency in splenocytes in this system was slightly decreased in comparison to control mice. This discrepancy may be due to the type of cells harbouring latent virus

between PEC and splenocytes. It has been shown recently that there are differences in viral gene transcription and reactivation efficiency among latently infected dendritic cells, macrophages and different subsets of B- lymphocytes at early stages of latent infection (Marques *et al.*, 2003) . The viral genes transcribed during latency in spleen included M2, M3, M8, M9, M11, ORF 73 and K3 (Simas *et al.*, 1999;Virgin *et al.*, 1999;de Lima *et al.*, 2005;Husain *et al.*, 1999;Rochford *et al.*, 2001). Whereas, it is shown that ORF50 (which is associated with lytic infection) transcription was detected in macrophages and dendritic cells of latently infected mice at day 14 p.i. In addition to ORF50, transcription of ORF6 in macrophages and ORF6 and M7 in dendritic cells is consistent with a pattern of lytic replication (Marques *et al.*, 2003). Along with the transcription of lytic replication associated genes, the latently infected macrophages did not show transcription of ORF73, which is a latency-associated gene (Fowler *et al.*, 2003). These observations suggest that viral gene transcription during latency is dependent on the type of cell harbouring latent virus.

1.3.7. THE ROLE OF VIRAL GENES IN PATHOGENESIS

The knock out strategy employing homologous recombination technique is widely employed to knock out specific gene expression in order to study their role in pathogenesis. The cloning of MHV-68 genome into a bacterial artificial chromosome (BAC) has greatly enhanced the ability to manipulate the viral genome (Adler *et al.*, 2000;Adler *et al.*, 2001). More recently, a natural deletion mutant of MHV-68 called MHV–76 was utilised to successfully create 'knock in' mutants with specific genes to study their role in pathogenesis (Townsley *et al.*, 2004). MHV–76 is a natural deletion mutant of MHV–68 lacking left hand end of the genome encoding M1 - M4 genes and vtRNA sequences (Macrae *et al.*, 2001).

The viral genes expressed during latency are intimately associated with the pathogenesis of disease caused by gammaherpesvirus such as EBV and KSHV. The putative latency associated genes of MHV–68 include tRNA like molecules, M1, M2, M3, M4, v-Bcl-2 (M11), K3 (ORF12), v-Cyclin (ORF72), LANA (ORF73) and v G- protein coupled receptor (GPCR) (ORF74) (Fowler *et al.*,

2003;Gangappa *et al.*, 2002;Jacoby *et al.*, 2002;Macrae *et al.*, 2003;Moorman *et al.*, 2003a;Simas *et al.*, 1998;Townsley *et al.*, 2004;van Dyk *et al.*, 2000;Virgin *et al.*, 1999;Wakeling *et al.*, 2001;Hoge *et al.*, 2000;Moorman *et al.*, 2003b;Bridgeman *et al.*, 2001;Clambey *et al.*, 2000;Lee *et al.*, 2003;Marques *et al.*, 2003;Stevenson *et al.*, 2002;Van Berkel *et al.*, 2000) .

1.3.7.1. tRNA LIKE MOLECULES

There are eight tRNA like molecules encoded in the left hand end of the genome. The tRNA molecules are not aminoacylated and their function is currently unknown. Deletion of four of the tRNA like sequences along with M1 from the virus genome does not affect the ability of the virus to replicate *in vitro* or to establish and reactivate from latency *in vivo* (Simas *et al.*, 1998). The recombinant virus was also able to establish a persistent/latent infection in NS0 cells (Murine B-cell myeloma cell line) in a manner indistinguishable from the parental virus.

1.3.7.2. M1

M1 gene exhibits sequence homology to poxvirus serine protease inhibitor -1 (SPI –1)(Bowden *et al.*, 1997;Virgin *et al.*, 1997). Disruption of MHV-68 M1 (M1.LacZ) leads to enhanced reactivation from latency (Clambey *et al.*, 2000). Although M1.LacZ replicated normally in tissue culture, it exhibited decreased splenic titres at days 4 and 9 p.i in both immunocompetent and immunodeficient mice on a B6 background. Despite the decreased level of acute virus replication, the recombinant virus established latent infection comparable to the normal wild type virus and it exhibited approximately five-fold increase in efficiency of reactivation from latency.

1.3.7.3. M2

Study of the transcription profile of latent genes in S11 cell line [a B-lymphocyte cell line latently infected with MHV–68 (Usherwood *et al.*, 1996b) and spleen of latently infected mice identified M2 as a latency associated gene (Husain *et al.*, 1999). The M2 protein is found to have an epitope recognised by CD8+ T-lymphocytes. Disruption of M2 gene of MHV-68 resulted in altered splenic

latency following intranasal but not intraperitoneal inoculation in mice (Jacoby *et al.*, 2002). In another study, introduction of a frame shift mutation in the M2 ORF did not show any defect in productive replication in tissue culture system or lungs after intranasal inoculation of mice (Macrae *et al.*, 2003). This mutant virus also showed no difference in transient increase in spleen cell number, IM like syndrome and establishment of latency in the spleen in comparison to the normal virus following intranasal infection in mice. However, this mutant virus showed a defect in its ability to produce transient increase in the latent viral load in the spleen. This study also demonstrated restricted expression of M2 to B-cells in the spleen. The localisation of protein was found to be predominantly in the plasma membrane and cytoplasm of B-cells. A recent study showed that M2 gene product might be required for efficient latent infection of splenic follicles (Simas *et al.*, 2004).

Another study suggested that M2 might be involved in inhibiting the interferon response elicited by infected cells (Liang *et al.*, 2004). The mechanism through which inhibition of interferon response is carried out is through the downregulation of signal transducers and activators of transcription (STAT) expression. Interestingly, in addition to downregulation of STAT-1 and STAT-2 in a cell type dependent manner, M2 protein could downregulate the expression of STAT–6 as well, which is involved in the Th2 mediated immune response. The property of M2 protein to downregulate interferon response is homologues to the property of BZLF1, the immediate early gene product of EBV. BZLF1 downregulates the interferon response through a variety of mechanisms including the downregulation of expression of IFNγ receptor (Morrison *et al.*, 2001).

1.3.7.4. M3

M3 is a secreted protein of 44-kDa size encoded by MHV-68 which is a high affinity broad-spectrum chemokine binding protein. The M3 protein lacks homology to known chemokines, chemokine receptors or chemokine binding proteins suggesting the involvement of this protein in a novel herpesvirus mechanism of immune evasion (Van Berkel *et al.*, 1999;Parry *et al.*, 2000).

Encoding homologues of cytokines, chemokines, their receptors and binding proteins by viruses represent a molecular 'cat and mouse' game designed to upset immune regulation of infection. The importance of this 'molecular mimicry' operated by viruses are recognised as a major strategy utilised by viruses for immune evasion [Reviewed in (Alcami, 2003)]. Considering the co – evolution theory of herpesviruses, it is reasonable to conclude that herpesviruses would have acquired these genes from their host during the process of evolution to circumvent the host immune response.

Targeted disruption of M3 gene had little effect on the lytic cycle replication of virus in the respiratory tract or the initial spread of virus to lymphoid tissues. However, there was a marked reduction in latent virus recoverable by *in vitro* reactivation. *In vivo* CD8+ T- cell depletion largely reversed this deficiency. Thus, it is suggested that, chemokine neutralisation afforded by M3 may function to block effective CD8+ T-cell recruitment into lymphoid tissue during the expansion of latently infected B-lymphocytes (Bridgeman *et al.*, 2001) . M3 gene is essential for the efficient induction of lethal meningitis by MHV- 68. An M3 mutant MHV- 68 virus was 100 fold less virulent than wild type or rescue virus after intracerebral inoculation (Van Berkel *et al.*, 2002). M3 protein blocks chemotaxis induced by CCL19 and CCL21, the chemokines constitutively expressed by lymphoid tissue and peripheral lymphatic vessels in an *in vitro* system. A very significant observation with regard to the *in vivo* role of this protein was also provided by studies using double transgenic mice expressing CCL21 and M3 in the pancreatic islets of mice. This system showed that M3 protein prevented the chemotaxis induced by the expression of CCL21 into the islets of pancreas (Jensen *et al.*, 2003). It appears that selective disruption of leukocyte trafficking in tissues may be a strategy employed by MHV–68 to evade the immune response.

Transgenic mice with conditional expression of M3 protein was generated (Pyo *et al.*, 2004). Conditional induction of M3 resulted in 67% reduction in intimal area and a 68% reduction in intimal/medial ratio in femoral artery injury model in

these transgenic mice. It suggests that chemokines regulate intimal hyperplasia and M3 has a role in controlling this.

1.3.7.5. M4

The role of M4 gene in the biology of MHV-68 infection was studied by a novel strategy of 'knocking in' the gene along with its putative promoter at the 5' end of MHV–76 genome (Townsley *et al.*, 2004). Studies with this recombinant virus showed that the M4 gene has a role in regulating establishment of acute infection in the lung, as the 'knock in' virus showed higher titer in the lung compared to MHV–76 at early time points after infection. More significantly, there was elevated level of latent viral load in the spleen at days 17 and 21 p.i. in mice infected with 'knock in' virus compared to the wild type MHV–76 viruses suggesting a role for this protein in modulation of latency .

1.3.7.6. M11

M11 protein is predicted to encode a 171 amino acid protein with homology to Bcl-2. It has a well-conserved Bcl-2 homology (BH)-1 domain and the BH2 domain is apparently absent. This is a major difference with the Bcl-2 homologue proteins encoded by other known gammaherpesviruses. M11 protein of MHV –68 could protect cells from apoptosis (Wang *et al.*, 1999). M11 gene expression was noticed during lytic and persistent infection in mice infected with MHV-68. This suggests that MHV-68 Bcl–2 homologue promotes virus survival by protecting not only the productively infected but also the persistently infected cells from apoptotic death (Roy *et al.*, 2000). Caspases are a family of apoptosis inducing proteases and are capable of converting Bcl-2 and Bcl – x (L) proteins of mammals into potent pro-apoptotic factors (Cheng *et al.*, 1997a). The viral Bcl-2 protein encoded by MHV–68 is susceptible to caspase digestion. However, the cleavage product lacked pro -apoptotic activity (Bellows *et al.*, 2000).

The *in vivo* role of M11 gene product during infection was studied by constructing a mutant virus with insertion of stop codons in the coding region of the gene. Intraperitoneal infection of immunocompetent mice showed the mutant virus

established normal levels of latency in the PEC in comparison to wild type MHV–68. However, the *ex vivo* reactivation of latently infected cells was 4-5 fold less efficient in comparison to the wild type virus (Gangappa *et al.*, 2002). It was also shown that, the mutant virus failed to establish persistent replication in PEC of IFNγ knock out ($IFN\gamma^{-/-}$) mice. It demonstrated that the viral genes required for acute and persistent replication of the virus in $IFN\gamma^{-/-}$ mice are different. Another mutant virus with disruption of BH-1 domain or C–terminal domain of M11 protein was created and phenotype of the virus in immunocompetent mice via intranasal route was assessed. The study showed the role of M11 protein in establishment of peak latent viral load. However, the long term latent levels were unaffected (de Lima *et al.*, 2005).

1.3.7.7. K3

The K3 gene product of MHV-68 is a KSHV K3 / K5 homologue (Virgin *et al.*, 1997). K3 transcription occurs in the lung during lytic infection and lymphoid tissue during latent infection following intranasal infection of mice. K3 protein of MHV-68 downregulates the expression of MHC class I molecule (Stevenson *et al.*, 2000;Stevenson *et al.*, 2002). The downregulation of MHC class I expression by K3 gene product is through binding of nascent MHC class I heavy chains that associate with transporter associated with antigen processing (TAP) in the endoplasmic reticulum and catalysing their ubiquitination leading to proteosome dependent degradation (Boname and Stevenson, 2001). K3 protein is predominantly detected in association with incompletely assembled class I molecules implying that K3 may block interaction of class I heavy chains with molecular chaperones to prevent their assembly. It is also possible that K3 may be using molecular chaperones to target incompletely assembled class I molecules for their destruction (Yu *et al.*, 2002). K3 deletion mutant virus is deficient in amplification of latency and this phenotype can be reversed by supplementing with CD8+T-lymphocytes (Stevenson *et al.*, 2002). This data along with observations made with M3 deletion mutants argue for an important role for CD8+ T- lymphocyte during the establishment of latency.

1.3.7.8. ORF 72

MHV-68 v–Cyclin gene (ORF 72) is an oncogene that promotes cell cycle progression in primary lymphocytes (van Dyk *et al.*, 1999) . A transgenic line of mice was generated by using lck proximal promoter to express the MHV-68 v–cyclin in early T-lymphocytes. Expression of MHV-68 v-cyclin gene significantly increased the number of thymocytes in cell culture and it interfered with thymocyte maturation, as shown by increased numbers of CD4+ and CD8+ double positive thymocytes. There was a striking difference in the architecture of thymus in transgenic mice. The thymus of transgenic mice showed an increase in the percentage of the cortex and a greatly reduced medullary area. There was an increased rate of apoptosis in the thymus of transgenic mice. About 50% of transgenic mice developed lymphoid neoplasm within 3 to 12 months of age. Based on these observations, it was concluded that MHV68 v- cyclin gene is an oncogene (van Dyk *et al.*, 1999).

A recombinant virus that lacks the cyclin homologue and expresses β-galactosidase as a marker (MHV-68^{cy}) was generated to study its effect on pathogenesis. Infection of BALB/c mice and severe combined immunodeficiency (SCID) mice indicated that cyclin D homologue mediates important functions during acute infection and it is required for efficient reactivation from latency (Hoge *et al.*, 2000) . Another mutant virus with insertion of lacz cassette within the gene also showed defect in reactivation from latency (van Dyk *et al.*, 2000). It was also shown that ORF72 is required for maintenance of latency in B-lymphocyte deficient mice (van Dyk *et al.*, 2003).

1.3.7.9. ORF 73

ORF73 is well conserved among gammaherpesviruses and they encode latency associated nuclear antigen (LANA) in KSHV and HVS (Smith *et al.*, 2001;Ballestas *et al.*, 1999). EBNA –1 is the homologue of LANA in EBV (Lee *et al.*, 1999). Two independent mutant viruses involving deletion of the gene and frame shift showed no difference in *in vitro* and *in vivo* productive replication. Whereas, consistent with its expected function, the mutant virus showed severe

defect in establishment of latency (Fowler *et al.*, 2003). In a separate study, another mutant MHV-68 virus with insertion of stop codon in the ORF73 was created and showed similar defect in establishment of latency (Moorman *et al.*, 2003b).

1.3.7.10. ORF 74

ORF74 of gammaherpesviruses has significant sequence homology with mammalian GPCR. MHV–68 ORF74 is encoded on multiple early transcripts and expressed during acute and persistent infection of the lung as well as latent infection of the spleen. Expression of MHV-68 ORF74 also resulted in transformation of NIH 3T3 cells (Wakeling *et al.*, 2001). Chemokines like KC and MIP-2 acts as agonists of MHV-68 ORF74; whereas, IFNγ inducible protein–10 (IP-10)/CXCL10 bind to MHV–68 ORF74 and behaves as an antagonist (Verzijl *et al.*, 2004).

A mutant virus with deletion in ORF74 region of MHV–68 genome was generated. The growth of the mutant viruses in NIH 3T3 cells was similar to that of wild type virus. The mutant viruses showed significantly reduced reactivation from latently infected mouse splenocytes. Chemokines such as KC and MIP-2 significantly contributed to the replication of the wild type virus but not the mutant viruses. This property was not observed with IP–10. Utilisation of a GPCR homologue to enhance replication and reactivation from latency by MHV–68 represent a novel mechanism utilised by gammaherpesviruses to subvert the immune response (Lee *et al.*, 2003). Another mutant with deletion of 440 bp of ORF74 was also created. This mutant virus did not show any defect during *in vitro* and *in vivo* acute replication, establishment of latency or reactivation from latency at day 16 p.i. However, there was significant decrease in the efficiency of virus reactivation by day 42 p.i. (Moorman *et al.*, 2003a).

1.3.8. IMMUNE RESPONSE

Transgenic mice defective in specific arms of immune response have been used extensively to delineate the immune response against MHV-68. Conclusions from

such studies showed that, there is considerable redundancy in their capacity to prevent exacerbated disease. Surprisingly, even organised secondary lymphoid tissue is not essential to successfully clear MHV–68 infections. Lymphotoxin α knock out ($LTA^{-/-}$) mice lack lymph nodes and have disrupted splenic architecture (Banks *et al.*, 1995). $LTA^{-/-}$ mice could clear productive MHV-68 infection with delayed kinetics compared to wild type mice. $LTA^{-/-}$ mice failed to develop splenomegaly or lymphocytosis following MHV-68 infection (Lee *et al.*, 2000).

1.3.8.1. B - LYMPHOCYTE

MHV–68 specific IgM antibodies are evident within first week of infection, which is followed by class switched antibodies dominated by IgG2a and IgG2b isotypes during the second week of infection (Sangster *et al.*, 2000;Stevenson and Doherty, 1998). Transgenic μMT mice lack B-lymphocytes and hence the capacity to produce antibody (Kitamura *et al.*, 1991). Little difference was observed in the acute lung infection in comparison with wild type mice following MHV-68 infection implying that antibody has little role to play in controlling acute infection in the lung (Usherwood *et al.*, 1996c).

1.3.8.2. CD4+ T- LYMPHOCYTES

CD4+ T-lymphocytes play a key role in the immune response by providing support for protective antibody response and driving the Th1 – mediated immune responses. MHV-68 specific CD4+ T-lymphocytes remain activated and a stable frequency during persistent infection (Christensen and Doherty, 1999). Control of MHV-68 infections in B-lymphocyte deficient mice mediated by CD4+ T-lymphocytes were shown to be through the action of IFNγ (Christensen *et al.*, 1999). Infection of CD4+ T-cell deficient mice with MHV-68 follows the same kinetics of virus clearance from the lung and spleen by 12-day p.i as that of normal mice. It was also shown that, CD4+ T-cells contribute to the lymphoproliferation seen in the spleen (Ehtisham *et al.*, 1993). Depletion of CD4+ T-lymphocytes prevented the splenomegaly and greatly reduced the peak infective centre level, while having no effect on the long-term level of latently infected cells (Usherwood *et al.*, 1996a).

MHC class II deficient mice are another *in vivo* system available to study the role of CD4+ T-lymphocytes in the pathogenesis of virus infections. Following MHV-68 infection of MHC class II deficient mice, the clearance of infection from the lung is comparable to that of normal mice. However, these knock out mice fail to produce antiviral antibodies and induce splenomegaly. As a consequence, the latent viral load also was low in these mice. A significant feature of MHV–68 infections in MHC class II deficient mice is the reactivation of virus infection in the lung and development of a chronic unresolving lung disorder. This progression of disease occurs inspite of an active CD8+ T cell response (Cardin *et al.*, 1996). The progression of chronic lung disorder in MHV–68 infected MHC class II deficient mice is not preventable by vaccination with protective T cell epitope p56 and p79 (Belz *et al.*, 2000). However, stimulation of CD40 molecule with an agonistic antibody substituted the CD4+ T-cell function in MHC class II deficient infected mice in preventing the reactivation of infection in the lung (Sarawar *et al.*, 2001). The virus specific CD8+ T-lymphocytes from MHV-68 infected MHC class II deficient mice showed no sign of functional exhaustion, even though these cells probably encounter viral antigens at fairly frequent intervals (Belz *et al.*, 2003).

1.3.8.3. CD8+ T- LYMPHOCYTES

CD8+T- lymphocytes recognising p56 and p79 were identified in high numbers in the lung of MHV–68 infected mice up to 22 days post infection. p56 (AGPHNDMEI) is an epitope from ORF6, which encodes a single stranded DNA binding protein, which is H-2D^b restricted. p79 (TSINFVKI) from ORF61, which encode the large ribonuclease reductase subunit is H-2K^b restricted epitope (Stevenson *et al.*, 1999). CD8+T-lymphocytes specific for these epitopes were also observed in MHC class II deficient mice indicating that, these response are induced and maintained in the absence of help from CD4+ T-lymphocytes (Stevenson *et al.*, 1998).

Pathogenesis of MHV-68 infection in mice depleted of CD8+ T-cells prior to infection resulted in great exacerbation of infection of the lung and spleen. It also

resulted in dissemination of infection to the liver and adrenal gland. This finding indicates that, CD8+ T-lymphocytes have a major role in recovery of acute MHV-68 infection (Ehtisham *et al.*, 1993). The β_2–microglobulin knock out ($\beta_2^{-/-}$) mice, which are naturally deficient in CD8+ T-lymphocytes showed a defect in clearing infectious virus from the spleen up to six weeks p.i., when mice were infected with MHV-68 via intraperitoneal route (Weck *et al.*, 1996). Release of perforin and granzymes are the known mechanisms by which the CD8+ T- cells exert their cytotoxic effect. Surprisingly, absence of perforin did not significantly affect the kinetics of either the lytic lung infection or latent spleen infection (Usherwood *et al.*, 1997). The mechanism by which the CD8+ T-cells achieve the control of acute infection remains to be elucidated.

1.3.8.4. CO-STIMULATORY MOLECULES

CD28 is a molecule expressed on resting T-lymphocytes and its expression increases following activation. CD40 ligation on an antigen presenting cell up-regulates surface expression of B7.1 (CD80) and B7.2 (CD86), which interact with CD28 molecule on T-cells (Allison, 1994;Cella *et al.*, 1996). The interaction of CD28 with B7.1 or B7.2 leads to up-regulation of additional molecules and thus initiates "cross talk" between CD8+ T-cells and antigen presenting cells resulting in further activation of both cell types. The role of CD28 dependent co-stimulatory interactions in the development and maintenance of antiviral immune responses during MHV-68 infection was studied using CD28 knock out ($CD28^{-/-}$) mice (Lee *et al.*, 2002). $CD28^{-/-}$ mice could clear a productive infection, although the lung virus titre was significantly increased. Splenomegaly developed normally in $CD28^{-/-}$mice, whereas virus specific antibody responses were significantly reduced and aberrant class switching was observed. It was concluded that co-stimulatory interactions involving CD28 are not an absolute requirement for the control of infection with MHV-68.

CD40 is constitutively expressed on macrophages, B Lymphocytes and dendritic cells [Reviewed in (Mackey *et al.*, 1998)]. $CD40^{-/-}$ mice infected with MHV–68 showed defective long term control of infection (Lee *et al.*, 2002). A recent study

showed that $CD40^{-/-}$ mice efficiently established long term latency (three months) in memory B cells of spleen. The mutant mice also showed significantly higher levels of virus replication in the lungs at late times post infection (Willer and Speck, 2005). CD40 ligand (CD40L/CD154) is expressed in high quantities on the surface of activated CD4+T-lymphocytes. $CD40L^{-/-}$ mice infected with MHV–68 do not show expansion of Vβ4 T-lymphocytes indicative of its role in developing IM like syndrome (Brooks *et al.*, 1999).

1.4. INTERFERON (IFN)

IFNs are best known for their ability to induce cellular resistance to viral infection and they were identified for the first time based on this property [Reviewed in (Schroder *et al.*, 2004). The known types of IFNs were grouped as either type I IFN comprising IFNα, IFNβ and IFNω or type II IFN with a single member namely IFNγ. Recently, a novel family of cytokines that are structurally related to the type I IFNs and to the IL-10 family was reported (Kotenko *et al.*, 2003;Sheppard *et al.*, 2003). Like other IFNs, the newly described cytokines protect cells from virus infection and induce MHC class I antigen expression suggesting that, these previously unknown mediators contribute to the antiviral defences and perhaps carry out other functions similar to those of the type I and type II IFNs. The three member of this newly identified cytokine family termed IFN-λ1, IFN-λ2, and IFN- λ3 bind to a heterodimeric receptor, in which one subunit is a novel member of class II cytokine receptor family and the other is identical to the IL-10 receptor (Vilcek, 2003).

1.4.1. TYPE I INTERFERON

The genes encoding type I IFNs form a cluster and the genes and proteins of this family are structurally related to each other. IFNβ was earlier known as fibroblast IFN as it is principally produced by fibroblasts. IFNβ is the most divergent member of this family and shows about 29% homology with members of IFN α family at the amino acid level and about 45% homology in the coding sequence level (Taniguchi *et al.*, 1980). IFNβ has a potential N-glycosylation site at position 80 and the mature protein is known to be glycosylated, whereas the IFNα

is not glycosylated (Knight E Jr, 1976a;Knight E Jr, 1976b). Both IFNα and IFNβ appear to be active in the monomeric form (Chelbi-Alix and Thang, 1986;Utsumi *et al.*, 1989). All type I IFNs bind with the same receptor and in most experimental systems examined they generally exert similar biological activities [Reviewed in (Smith *et al.*, 2005)].

One of the mechanisms by which type I IFNs exert their action is by early induction of inducible nitric oxide synthase (iNOS) (Diefenbach *et al.*, 1998). One study showed that infection with MHV-68 was lethal in iNOS deficient mice when infected with 10^6 PFU of MHV-68 (Kulkarni *et al.*, 1997). In contrast, iNOS deficient mice were resistant to infection with $4x10^5$ PFU of MHV-68 administered via intranasal route (Dutia *et al.*, 1999). Thus it appears that mortality observed in iNOS deficient mice following MHV-68 infection is dependent on dose of administration. MHV-68 infection in mice with a targeted disruption in an essential chain of the type I IFN receptor gene (IFNα/βR$^{-/-}$) at high dose of infection ($4x10^6$ PFU) was lethal in 80 – 90 % of IFNα/βR$^{-/-}$ mice and at low dose of infection ($4X\ 10^3$ PFU) mortality rate was 50%. Both high and low doses of virus lead to 100 to 1000 fold higher lung virus titres in IFNα/βR$^{-/-}$ mice in comparison to wild type mice. Latently infected cells were detectable in the spleens of IFNα/βR$^{-/-}$ mice earlier than in wild type mice, and the numbers of latently infected cells were 10 fold higher in the IFNα/βR$^{-/-}$ mice during the acute phase of infection (Dutia *et al.*, 1999). Interferon regulatory factor-1 knock out mice (IRF1$^{-/-}$) mice were also highly susceptible to MHV-68 infection and behaved similar to IFNα/βR$^{-/-}$ mice (70% of mice died in response to $4x10^5$ PFU of virus) (Dutia *et al.*, 1999).

1.4.2. TYPE II INTERFERON / GAMMA INTERFERON (IFNγ)

Type II IFNs are structurally different from type I IFNs, but they share functional similarity. A single IFNγ gene has been found in all mammalian species examined so far. Human IFNγ gene is located in the chromosome 12 (Naylor *et al.*, 1983) whereas in murine species, the gene is located at chromosome 10 (Naylor *et al.*, 1984). The human and murine genes are 6 kb in size and contain four exons and

three introns. The coding part of the murine gene displays an overall nucleotide homology with the human gene of about 40% and the protein homology is 65%. As a result of this relative lack of conservation, IFNγ tends to be strictly species specific in its actions. The activation of human gene leads to generation of a 1.2 kb mRNA that encodes a 166 amino acid polypeptide (Gray *et al.*, 1982;Derynck *et al.*, 1982;Gray and Goeddel, 1982). The amino terminal 23 residues of the human protein constitute a typical hydrophobic signal sequence which when proteolytically removed, gives rise to a mature 143 amino acid residue positively charged polypeptide with a predicted molecular mass of 17 kilo Dalton (kDa). The carboxy terminus of the molecule is susceptible to post – translational enzymatic degradation. At least six different carboxy termini have been detected on natural and recombinant forms of human IFNγ. Two polypeptides self associate to form a homodimer with an apparent molecular mass of 34 kDa. Only the dimer can exert its biological activity. The murine gene gives rise to 1.2 kb mRNA that encodes a mature 134 amino acid polypeptide with a predicted molecular mass of 15.4 kDa (Gray and Goeddel, 1983).

1.4.2.1. BIOSYNTHESIS

In the normal host, the T-lymphocytes represent the major cellular source of IFNγ. All CD8+ T-cell population and certain subsets of CD4+ T-cells [Th1 helper subset, Th0 (less differentiated CD4+ T-cell)] and NK cells can produce IFNγ (Vilcek *et al.*, 1985). The primary physiologic stimulus is antigen in the context of either MHC class II (for CD4+ T-cells) or MHC class I antigen (for CD8+ T-cells). The T-cell dependent production of IFNγ is enhanced by products of activated T-cells and macrophages such as IL-2, hydrogen peroxide, and leukotrienes (LT) such as LTB4, LTC4 and LTD4 (Kasahara *et al.*, 1983;Vilcek *et al.*, 1985;Farrar *et al.*, 1986;Munakata *et al.*, 1985;Johnson and Torres, 1984;Johnson *et al.*, 1986). NK cells require support from tumour necrosis factor (TNF)α and macrophages for generation of IFNγ. IL –12, which was formerly called NK stimulatory factor is a product of B-cells and macrophages and induce IFNγ synthesis from T-cells and NK cells. IL-10 inhibits IFNγ production by T-cells (Fiorentino *et al.*, 1989).

1.4.2.2. RECEPTOR

The IFNγ receptor contains two subunits namely α or R1 and β or R2. The intracellular domain of this group of cytokine receptors is devoid of intrinsic kinase or phosphatase activity. The human and murine IFNγ receptors display strict species specificity in their ability to interact with IFNγ. The characterisation of the structure of IFNγ receptor was facilitated by the cloning of human cDNA and murine homologue(Aguet *et al.*, 1988;Gray *et al.*, 1989;Kumar *et al.*, 1989;Munro and Maniatis, 1989). The human IFNγ receptor α chain is encoded by a 30 kb gene located on the long arm of chromosome 6 (Pfizenmaier *et al.*, 1988). The murine homologue is a 22 kb gene present in the chromosome 10. Both murine and human genes consist of seven exons. Exons 1- 5 encode the extra cellular domain; exon 6 encodes a small portion of membrane proximal region of the extra cellular domain and the transmembrane domain. The exon 7 encodes the entire intracellular domain. Transcription of both human and murine genes give rise to 2.3 kb mRNA. The α receptor chain polypeptide is posttranslationally modified as it moves from endoplasmic reticulum (ER) to the Golgi by the addition of N-linked carbohydrates (Hershey and Schreiber, 1989;Mao *et al.*, 1989). The human IFNγ receptor β chain gene is located in chromosome 21q22.1 (Soh *et al.*, 1994;Cook *et al.*, 1994) and the murine homologue resides in chromosome 16 (Hibino *et al.*, 1991). Transcriptional activation of the IFNγ receptor β chain results in the generation of an mRNA transcript of 1.8 kb in human cells or 2 kb in mouse cells (Soh *et al.*, 1994;Hemmi *et al.*, 1994). The murine IFNγ receptor β gene consists of 7 exons.

1.4.2.3. THE SIGNAL TRANSDUCTION

The proposed model of signal transduction leading to the activation of IFNγ responsive genes is presented in figure.1.3. [Reviewed in (Platanias, 2005;Schroder *et al.*, 2004)]. In unstimulated cells, the IFN receptor α and β sub unit are not pre-associated with each other but rather associate through their intracellular domains with the inactive form of specific Janus kinases (JaK). JaK1 and JaK2 constitutively associate with the receptor α and β chains respectively

(Sakatsume *et al.*, 1995). JaK1 binds to α subunit of the receptor through a four-residue sequence ($_{266}$ LPKS $_{269}$) in the membrane proximal region of the intracellular domain. JaK2 binds to a 12 residue proline rich Box 1 – like sequence ($_{263}$ PPSIPLQIEEYL $_{274}$) in the membrane proximal region of the β subunit of the receptor intracellular domain. Addition of IFNγ induces the rapid dimerisation of the α receptor chain. This dimerisation of the α receptor chain leads to formation of a site recognised by the β receptor chain. The ligand induced assembly of the complete receptor complex containing two α receptor chains and two β receptor chains brings into close juxtaposition, the intracellular domains of these proteins together with the inactive JaKs that they carry. In this complex, JaK2 undergoes autophosphorylation, which in turn allows JaK1 transphosphorylation and then phosphorylate the functionally critical tyrosine on 440 residues in the α receptor chain, thereby forming a paired set of docking sites for STAT-1. Two STAT-1 molecules then associate with the paired docking site. The activated STAT-1 complex is phosphorylated near the C terminus at Y701. Phosphorylation on a single serine (residue 727) is also required for maximal transcriptional activity (Wen *et al.*, 1995). This phosphorylation induces dissociation of STAT -1 homodimer from receptor.

The active STAT-1 homodimers also known as IFNγ activation factor (GAF) translocate to the nucleus and bind to specific IFNγ activated sequence (GAS) elements of IFNγ inducible genes and stimulates or suppresses their transcription (Decker *et al.*, 1997).

1.4.2.4. ANTIVIRAL EFFECTS

Inhibition of viral growth by IFNs has been described at various levels of virus multiplication. At the same time viruses have also evolved different mechanisms to circumvent the antiviral effects of interferons [Reviewed in (Katze *et al.*, 2002;Schroder *et al.*, 2004)]. The best-characterised IFN inducible components of the antiviral response mechanisms are double stranded RNA (dsRNA) dependent protein kinase (PKR), the 2' – 5' oligoadenylate synthetases (OAS) and the Mx

Figure 1.3. Diagrammatic representation of signal transduction pathway of IFNγ.

(1) Ligand binding of IFNγ receptor causes rapid dimerisation of α chains and in formation of receptor complex comprising two α chains and two β chains. The JaK2 associated with β chain undergoes autophosphorylation and which in turn causes transphosphorylation of JaK1

(2) The activated JaK1 phosphorylates functionally critical tyrosines (Y) on residue 440 of each α chains of the receptor.

(3) The phophorylated α chains forms a docking site for Src Homology (SH)2 domains of latent STAT1

(4) The STAT1 undergoes phosphorylation near C terminus at Y701. The phosphorylation induces dissociation of STAT1 homodimer from receptor.

(5) The STAT1 homodimers translocate to the nucleus and bind to promoter elements (IFNγ activation site (GAS) elements) to initiate transcription of IFNγ response genes

Adapted from Schroder *et al.*, 2004.

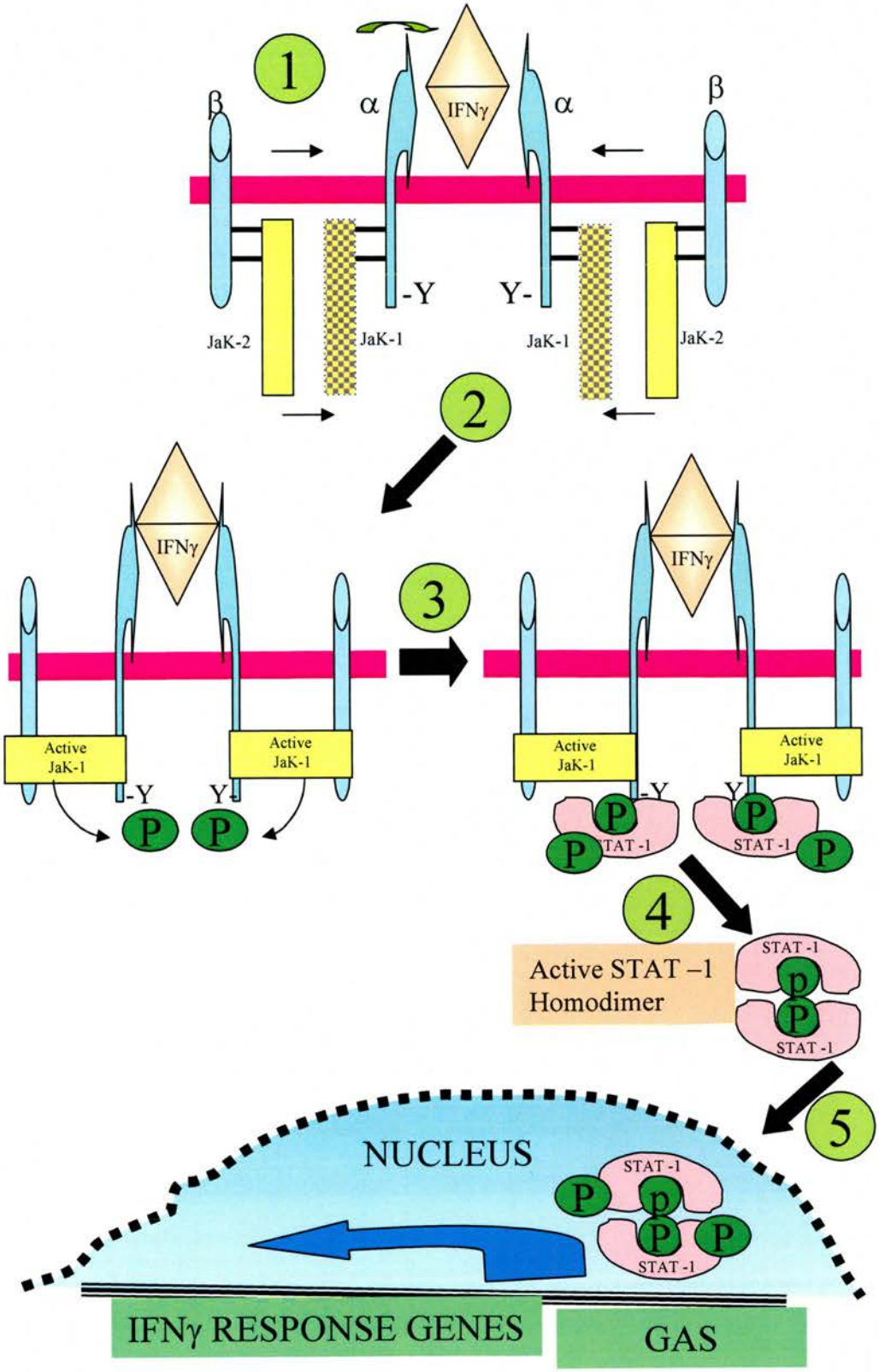

Fig. 1.3. Please see the facing page for legend

proteins. A more recent addition to the list of IFN inducible gene with antiviral effect is the RNA-specific adenosine deaminases (ADAR) (Patterson *et al.*, 1995).

1.4.2.4.1. PROTEIN KINASE (PKR)

PKR is a serine – threonine kinase with multiple functions in the control of transcription and translation (Meurs *et al.*, 1990). PKR is normally inactive, but on binding to dsRNA or other polyanions it undergoes autophosphorylation and subsequent dsRNA – independent phosphorylation of substrates (Meurs *et al.*, 1990;Katze *et al.*, 1991;George *et al.*, 1996). The antiviral effect of PKR is due to its phosphorylation of the initiation factor eIF2α (Meurs *et al.*, 1992). In the initial step of translation, the initiator Met–tRNA is recruited to the 40S ribosomal subunit via an interaction with guanosine triphosphate (GTP) bound eIF2. This complex then interacts with mRNA, other initiation factors and the large ribosomal subunit to form a pre – initiation complex, with subsequent hydrolysis of the GTP molecule bound to eIF2 and release of GDP bound eIF2. In order to participate in another round of translational initiation, the GDP bound to eIF2 must be exchanged for GTP, a reaction that is catalysed by the guanine exchange factor, eIF2B. The phosphorylated eIF2α interacts strongly with eIF2B and traps it such that it cannot mediate the recycling of eIF2 (Ramaiah *et al.*, 1994). Since eIF2B is present in limiting amounts, translation is inhibited. Apoptosis may also play a role in the antiviral effect of PKR [Reviewed in (Tan and Katze, 1999)]. Although there is abundant evidence that PKR plays a major role in regulating virus infection, PKR alone is not sufficient to mediate the full antiviral response. Mice with homozygous disruptions of the PKR gene show resistance to virus infection (Yang *et al.*, 1995;Abraham *et al.*, 1999).

1.4.2.4.2. 2'-5' OLIGOADENYLATE SYNTHETASE (OAS)

The oligoadenylate synthetase system is a multienzyme pathway in which IFN inducible OAS is stimulated by dsRNAs, often of viral origin to produce a series of short 2' – 5' oligoadenylates that activate the 2' – 5' adenylate dependent endoribonuclease L (Rnase L) (Kerr and Brown, 1978). Activation of this

pathway leads to extensive cleavage of single stranded RNA, including mRNA and 28S ribosomal RNA (Wreschner *et al.*, 1981;Floyd-Smith *et al.*, 1981).

1.4.2.4.3. THE MYXOVIRUS RESISTANCE (Mx) PROTEINS

The IFN – inducible Mx proteins are highly conserved large GTPases with homology to dynamin and have been found in all vertebrate species examined so far [Reviewed in (Arnheiter *et al.*, 1996;Staeheli and Haller, 1987)]. Mx proteins interfere with virus replication, probably by causing redistribution of nucleocapsids as shown recently in the case of bunyaviruses (Kochs *et al.*, 2002).

1.4.2.5. GAMMA INTERFERON RECEPTOR KNOCK OUT MICE

Gene knock out mice for IFNγ and either chain of IFNγ receptors have been generated (Huang *et al.*, 1993;Dalton *et al.*, 1993;Lu *et al.*, 1998). All three types of knockout mice showed normal development without any overt anomalies. Among the three different types of knockout mice available, the $IFN\gamma R^{-/-}$ mice with disruption of α chain were used to study the effect of IFNγ in different virus infection models. A few examples of such studies on virus infections and their outcome are presented in table 1.3 [Reviewed in (Tau and Rothman, 1999)]. Surprisingly, such studies on different virus infection models have shown that the antiviral function of IFNγ is partially redundant, may be because they duplicate with that of type I interferons.

1.4.2.6. GAMMA INTERFERON AND MHV-68

The cytokine profile during MHV–68 infection of C57BL/6J strain of mice was evaluated (Sarawar *et al.*, 1996). The cells obtained from spleen, mediastinal and cervical lymph node produced high levels of IL-6, IFNγ and lower levels of IL-2 and IL-10 in an *in vitro* restimulation assay. Production of IL-4 and IL-5 was negligible. The IL-6 and IFNγ levels peaked in correlation with viral clearance from lung at day 10 p.i., although significant amount of cytokine was found from day 3 p.i. Surprisingly, mice that were congenitally deficient in the IFNγ gene ($IFN\gamma^{-/-}$) cleared MHV-68 with similar kinetics with that in wild type mice which suggested that IFNγ is not essential for regulating infection (Sarawar *et al.*, 1997).

Table 1.3. Summary of phenotype of IFNγR$^{-/-}$ mice in comparison to wild type mice in different models of virus infection (Tau and Rothman, 1999)

Pathogen	Phenotype in Wild type mice	Phenotype in IFNγR$^{-/-}$ mice
Pseudorabies virus	Vaccine effective; resistant to rechallenge	Vaccine ineffective; susceptible to rechallenge
Sendai virus	Clear infection	Clear infection
MHV-68	Resistant to splenic fibrosis and large vessel arteritis	Develop splenic fibrosis and large vessel arteritis
Vaccinia virus	Resistant	Increased susceptibility, but normal CTL response
Vesicular stomatitis virus	Mount CTL response	Normal CTL response
LCMV	Transient immunodeficiency phenomenon	No transient immune deficiency
Theiler's virus	Resistant on 129/SV background	Develop chronic disease
Corona virus	Develop hepatitis	More severe hepatitis with increased mortality
Murine cytomegalovirus	Clear infection	develops chronic arteritis Persistent infection

Infection of IFNγR$^{-/-}$ mice with MHV–68 via intranasal route also showed similar kinetics of viral clearance from lung (Dutia *et al.*, 1997). The IFNγR$^{-/-}$ mice showed no difference from wild type mice in the titres of infectious virus in the lungs or in the rate of clearance of the lung infection. However, clear differences were observed in the spleen. By 14 days p.i. spleens from IFNγR$^{-/-}$ mice were

pale, shrunken and fibrous. Histological examination showed that there was an early infiltration of granulocytes followed by widespread destruction of splenic architecture. A marked decrease in the number of splenic B-cells and CD4+ and CD8+ T-cells also occurred. These changes were accompanied by a 10 –100 fold greater load of latently infected cells in the IFNγR$^{-/-}$ mice than in wild type mice at 14 to 17 days p.i, but this was reduced to the levels found in wild type mice by 21 days p.i. Treatment of the mice with the antiviral drug 2$^{'}$–deoxyl – 5 – ethyl – beta – 4$^{'}$ – thiouridine from 6 days p.i did not prevent the occurrence of these changes. The changes were completely reversed by depletion of CD8+ T-cells prior to and during the primary infection. Depletion of CD4+ T-cells also reversed the major pathological and virological changes, although in this case there was evidence of some histological changes (Dutia *et al.*, 1997).

Infection of IFNγR$^{-/-}$ mice with MHV-68 also resulted in fibrosis and atrophy of the mediastinal lymph nodes, interstitial pulmonary fibrosis and fibrotic changes in the liver in addition to the pathological changes in spleen (Ebrahimi *et al.*, 2001). It was also concluded that atrophy and cellular depletion of the spleen in IFNγR$^{-/-}$ mice was not the result of increased cell death. The loss of splenocytes in IFNγR $^{-/-}$ mice, which was most evident on day 23-p.i. correlated with an increase in the number of leukocytes in peripheral blood. At the peak of leukocytosis, peripheral blood cells from infected IFNγR$^{-/-}$ mice were unable to traffic through the fibrosed spleens of IFNγR$^{-/-}$ mice, but were able to enter the spleens of wild type mice. It was also found that cytokines like IFNγ, TNFα, TNFβ, IL-1β, transforming growth factor - β1 (TGFβ1), lymphotactin and MIP-1β were elevated on day 14 after infection whereas the chemokines IP –10 and monokine induced by IFNγ (MIG) were significantly reduced.

1.4.2.6.1. ROLE OF VIRAL GENES IN MHV-68 INDUCED SPLENIC FIBROSIS

In order to explore the role of viral genes in the pathogenesis of splenic fibrosis, mutant virus with specific defects in individual genes were used to infect IFNγR$^{-/-}$ mice. Disruption in the M1 gene with LacZ gene failed to produce splenic

pathology in IFNγR$^{-/-}$ mice even though it produced comparable levels of blood vessel pathology (Clambey *et al.*, 2000) . A mutant virus with deletion of four of the tRNA like sequences along with M1 from the virus genome and a mutant virus with an insertion of green fluorescent protein (gfp) with effective deletion of nucleotides 1-3223 in the left hand end of the genome failed to induce splenic pathology in IFNγR$^{-/-}$ mice (Dutia *et al.*, 2004). The same study also showed that MHV–76 and another mutant virus with specific insertion at vtRNA3 also failed to produce splenic pathology in IFNγR$^{-/-}$ mice.

1.4.2.7. VASCULAR PATHOLOGY AND MHV-68

Tropism of MHV–68 towards blood vessels was highlighted during infection of knock out mice deficient in different components of interferon system (Weck *et al.*, 1997). IFNγR$^{-/-}$ mice intraperitoneally infected with MHV–68 at a dose in the range of 1- 3 x 10^6 PFU was monitored for viral clearance and establishment of latency. Some IFNγR$^{-/-}$ mice survived for several months, but eventually most of them died. Mice, which were 6 weeks of age at the time of infection died more rapidly than those greater than 8 weeks of age at the time of infection. Despite their ability to clear the virus from lung and spleen, the IFNγR$^{-/-}$ mice died 1.5 to 14 weeks after infection. Post-mortem diagnosis was severe large vessel arteritis, with narrowing of aortic lumen by inflammation and thrombus formation.

The arteritis lesions involved all three layers of the great vessels. The inflammatory cells were mainly lymphocytic, although neutrophils were seen in some areas. The lesions were most common and most extensive in the base of the aorta. Lesions were also seen in 75% of pulmonary arteries. Immunostaining with polyclonal rabbit serum against MHV-68 showed viral antigen in association with lesions of arteritis. The antigen deposition was mainly noted in the tunica media of blood vessels. The morphology of infected cells, together with the localisation of viral antigen between elastic lamina strongly suggested virus infection of smooth muscle cells.

The IFNγ$^{-/-}$ mice, B-cell deficient mice (μMT), MHC class II deficient mice and CD8+ T-lymphocyte deficient mice also developed arteritis of varying degrees and intensity following MHV-68 infection. It was shown later that persistent MHV-68 replication in the walls of large elastic arteries is required for the maintenance of arteritis (Dal Canto *et al.*, 2000). The suggested reasons for the persistence of disease in arteries include: a) inefficient clearance of viral infection from the site compared with other organs or other blood vessels and b) failure of T cells and macrophages to enter the virus infected elastic media (Dal Canto *et al.*, 2001).

Tropism of MHV–68 towards blood vessels were also shown in Apolipoprotein E deficient (ApoE$^{-/-}$) mice. ApoE$^{-/-}$ mice on normal diet have high cholesterol levels and spontaneously develop atheroma resembling human disease (Plump *et al.*, 1997). When ApoE$^{-/-}$ mice were infected with MHV- 68, atheroma formation was accelerated over a 24-week period (Alber *et al.*, 2000). Acceleration of atherosclerosis was reduced by antiviral drug administration. Histological analysis of the atheromatous plaques showed no difference between lesions of infected and control mice. Viral mRNA was present in the aortas of infected mice before lesion development on day 5 p.i. This suggests that the virus may initiate endothelial injury, which is believed to be an early event in the development of atherosclerosis. In a further study, the question of whether any virally induced systemic immune response is sufficient to trigger enhanced atheroma formation was addressed. To clarify this hypothesis, ApoE$^{-/-}$ mice were infected with either MHV-68 or HSV–1. Viral message was not detected in the aortas of HSV–1 infected mouse. It was concluded that the systemic immune response to any particular infectious agent is insufficient to induce enhanced atherosclerosis in the ApoE$^{-/-}$ mice and pointed to a specific infection or immune mechanisms mediated by MHV–68 is essential for virally enhanced atherogenesis (Alber *et al.*, 2002).

1.5. FIBROSIS

Forty five percent of human mortality in United States of America is associated with a fibrotic disorder (Wynn, 2004). The major known fibrotic disorders

affecting humans is cirrhosis, interstitial lung disease (ILD) including interstitial pulmonary fibrosis (IPF), systemic sclerosis (SS), atherosclerosis, pancreatic fibrosis, rheumatoid arthritis and glomerulonephritis. Fibrotic diseases represent a large group of heterogeneous disorders without effective remedy at present.

The regenerating capacity of the injured tissue dictates whether repair with regeneration of normal parenchymal cells or fibrosis should follow after excessive tissue loss. Fibrosis is a highly co-ordinated complex tissue response characterised by the deposition of extra cellular matrix (ECM). ECM consists of fibrous protein like collagen, elastin and fibrillin, proteoglycans like decorin and fibromodulin, adhesion molecules like fibronectin, laminin and integrins [Reviewed in (Prockop and Kivirikko, 1995) (Aumailley and Krieg, 1996;Faull, 1995)]. Accumulation of inflammatory cells is a hallmark event in the pathogenesis of fibrosis. The infiltrating cells include platelets, macrophages, eosinophils, plasma cells and T-lymphocytes. The pro-fibrotic cytokines secreted by these infiltrating cells include TGFα, TGFβ, platelet-derived growth factor (PDGF), IL-1α, IL-1β, IL-4 and IL-13. Evidence is emerging to confirm that the polarisation of the immune response towards T-helper-2 (Th2) type involving IL-4 and IL-13 is crucial in this setting [Reviewed in (Wynn, 2004)]. The type of Th cell response controls the magnitude of fibrosis: if it is progressing towards Th1 type response, the fibrotic response is minimal and in the case of Th2 type response, enhanced fibrosis occurs. Such a pattern was observed in various models of fibrosis such as schistosome egg induced liver fibrosis (Wynn *et al.*, 1995), pulmonary fibrosis (Keane *et al.*, 2001) and kidney fibrosis (Oldroyd *et al.*, 1999). Microarray studies on the transcription profile during Th1 or Th2 type immune response confirmed that, at the time of Th2 response the genes involved in fibrosis were up-regulated (Sandler *et al.*, 2003;Hoffmann *et al.*, 2001).

1.5.1. TRANSFORMING GROWTH FACTOR - β (TGFβ)

TGFβ is the key cytokine responsible for the pathogenesis of fibrosis (Branton and Kopp, 1999;Sato *et al.*, 2003). It is the prototype member of the TGFβ super family of about 30 proteins, which include other TGFs, bone morphogenic protein

(BMP), inhibins, myostatin and activin families. Activated lymphocytes, macrophages, dendritic cells, neutrophils and immature haematopoietic cells produce TGFβ. There are three mammalian isoforms of TGFβ (TGFβ1-β3), which are structurally identical (Gorelik and Flavell, 2002). TGFβ is chemoattractive for macrophages and induces the production of other growth factors (Wahl *et al.*, 1987;Chantry *et al.*, 1989).

TGFβ is secreted as a latent form, which needs to be cleaved prior to exerting its action. Two latent forms of TGFβ include a 75 kDa glycoprotein latency associated form and a 135 kDa latent TGFβ binding protein form. Cleavage of N - terminal fragment of TGFβ to liberate the active C-terminal fragment is required after its secretion into extra cellular environment. The cleavage happens through several agents like macrophage derived plasminogen activator, matrix metalloproteinase (MMP), cathepsins, calpain, thrombospondin and integrins or acidification of the local environment by the lysosymal leakage [Reviewed in (Letterio and Roberts, 1998;Massague, 1990)]. The active TGFβ is a 25-kDa-homodimeric polypeptide. TGFβ suppresses T-cell mediated cellular immunity through multiple mechanisms (Gorelik and Flavell, 2002). The inhibitory effect on T-cell proliferation is largely attributed to its ability to suppress IL-2 production (Brabletz *et al.*, 1993). TGFβ is chemoattractive for fibroblasts and it can induce synthesis of collagens (type I, III, VI and XI), fibronectins, matrix glycoproteins including osteopontin, osteonectin, thrombospondin, proteoglycans such as biglycan and decorin (Massague, 1990). TGFβ is a mitogen for fibroblasts and its mitogenic potential is lower than platelet derived growth factor (PDGF) and fibroblast growth factor (FGF). The mitogenic potential of TGFβ is mediated by the autocrine action of PDGF–AA (Yamakage *et al.*, 1992;Battegay *et al.*, 1990) as well as PDGF independent pathways (Seifert *et al.*, 1994).

1.5.1.1. SIGNAL TRANSDUCTION

Signal transduction of TGFβ involves two of its receptors namely TGFβ receptor I and II (TGFβRI and TGFβRII). The receptor complexes are heterotetrameric

consisting of two type II receptors and two type I receptors. The receptors have an N-glycosylated extra cellular domain that is rich in cysteine residues, a transmembrane domain and an intracellular serine/threonine kinase domain. Although both receptors are required for signal transduction, TGFβRII only is enough for binding of ligand (Laiho *et al.*, 1991). TGFβRII is constitutively phosphorylated by its own kinase activity and binding of TGFβ to TGFβRII results in recruitment of type I receptor to the complex and phosphorylation of type I receptor by type II receptor kinase occurs (Wrana *et al.*, 1994). The signal transduction pathway after receptor ligand binding involves SMAD proteins. The SMAD family of proteins originated from Drosophila. The founding member is called MAD [mothers against decapentaplegic (dpp) gene] (Sekelsky *et al.*, 1995). The homologues of MAD proteins in *Caenorhabditis elegans* are called SMA, because their mutation caused small body size (Savage *et al.*, 1996). The homologues in vertebrates were named SMADs as they are related to SMA and MADs (Graff *et al.*, 1996;Hahn *et al.*, 1996).

There are eight different SMAD proteins identified and they fall into three distinct functional groups. The SMAD 1, 2, 3, 5 and 8 fall in the group of receptor activated SMADs (R-SMADs). SMAD-4 is the common mediator SMAD. SMAD 6 and 7 are grouped as inhibitory SMADs (I-SMADs). The R - SMADs are kept in the cytoplasm in the basal state bound to the protein called SMAD anchor for receptor activation (SARA) (Tsukazaki *et al.*, 1998). The type I receptor kinase of the receptor ligand complex will phosphorylate the receptor activated SMADs (SMAD-2 and 3). Upon phosphorylation, R–SMADs are released from SARA and this pathway specific phoshorylated SMADs will hetero-oligomerize with SMAD-4 in the cytoplasm. This complex will translocate into the nucleus by a mechanism involving the cytoplasmic protein called importin where it mediates transcriptional activation of the target genes (Kurisaki *et al.*, 2001;Xiao *et al.*, 2000;Nakao *et al.*, 1997). The binding of this complex with DNA can occur directly or with the help of other co–factors, like cyclic adenosine monophosphate (cAMP) response element binding protein (CREB) -

Binding Protein (CBP)/p300 (Shen *et al.*, 1998). The up-regulated genes include the genes responsible for laying out the ECM including collagen.

Connective tissue growth factor (CTGF) is a molecule released from fibroblasts activated by TGFβ. CTGF is a member of CCN family of proteins [Reviewed in (Perbal, 2004)]. CCN stands for the first three members of this family: cysteine – rich 61 (CYR61/CCN1), connective tissue growth factor (CTGF/CCN2) and nephroblastoma overexpressed (NOV/CCN3). The function of CTGF is to promote fibroblast proliferation, matrix production and granulation tissue formation (Bradham *et al.*, 1991;Shi-wen *et al.*, 2000;Moussad and Brigstock, 2000). The receptor and signal transduction process through which it mediates this function remain to be elucidated.

1.5.2. PLATELET DERIVED GROWTH FACTOR (PDGF)

PDGF is a major mitogen and chemoattractant for connective tissue cells (Yi *et al.*, 1996;Yoshida *et al.*, 1995). α-Granules of the platelets are the major source of PDGF and many other cell type including macrophages can produce PDGF (Shimokado *et al.*, 1985;Martinet *et al.*, 1986). Role of PDGF in fibrotic disorders like atherosclerosis, lung fibrosis, cirrhosis and kidney fibrosis has been reported and in most of these conditions the source of PDGF is from activated macrophages [Reviewed in (Heldin and Westermark, 1999)]. It is a dimeric molecule consisting of structurally similar A and B polypeptides linked by disulfide bonds. It appears as homodimeric or heterodimeric isoforms of A and B (AA, AB, and BB) polypeptide chains. In addition to the mitogenic activity, it has a chemotactic activity as well due to its ability to induce reorganisation of the actin system of the cell. Recently two other forms of PDGF (PDGF–C and PDGF –D) have been identified (Li *et al.*, 2000;Bergsten *et al.*, 2001).

Fibroblasts have around 200000 receptors for PDGF and smooth muscle cells carry 50000 receptors. Activation of receptor by ligand binding causes autophosphorylation of the receptors leading to increased catalytic activity of the kinases and formation of docking sites for signal transduction molecules.

Different signal transduction molecules that contain Src homology -2 (SH2) domains are involved (e.g. Phosphotidyl inositol -3 (PI3) -kinase). PDGF induces the expression of ECM proteins such as collagen type I, III, IV and V as well as collagenase (Chua *et al.*, 1985;Bauer *et al.*, 1985).

1.5.3. Th2 TYPE CYTOKINES

Th2 cytokines include IL-4, IL-5 and IL-13. Receptors for IL-4 were reported from both mouse and human fibroblasts (Sempowski *et al.*, 1994;Doucet *et al.*, 1998). IL-4 can induce collagen synthesis from human fibroblasts (Fertin *et al.*, 1991). Increased level of IL-4 was reported in the broncho alveolar lavage (BAL) fluid obtained from IPF patients. Interstitium of patients suffering from cryptogenic fibrosing alveolitis also showed evidence of IL-4 (Emura *et al.*, 1990;Wallace *et al.*, 1995). Macrophage derived IL-4 was found in higher quantities in pulmonary fibrosis induced in rats by radiation (Buttner *et al.*, 1997).

IL-13 uses the IL-4Rα for inducing signal transduction and shares the biological properties of IL-4 (Zurawski *et al.*, 1993). Although IL-4 and IL-13 share similar biological properties, IL-13 is the dominant cytokine mediating liver fibrosis (Chiaramonte *et al.*, 1999;Chiaramonte *et al.*, 2001). Role of IL-13 in modulating the development of fibrosis was also shown in several models of chronic pulmonary disease (Blease *et al.*, 2001;Zhu *et al.*, 1999;Belperio *et al.*, 2002). In addition to directly stimulating fibroblasts to produce collagen (Oriente *et al.*, 2000), IL-13 also acts in the way of stimulating macrophages to produce TGFβ and MMP-9 (Lee *et al.*, 2001). A recent study showed that IL-13 driven fibrogenesis is completely independent of TGFβ and MMP-9 (Kaviratne *et al.*, 2004).

IL-5 is the third member of the Th2 cytokine family and it is involved in the differentiation, activation and recruitment of eosinophils. Studies on the role of IL-5 in the pathogenesis of fibrosis yielded conflicting results in various models of fibrosis (Sher *et al.*, 1990;Cho *et al.*, 2004;Hao *et al.*, 2000). The role of IL-5 in

the pathogenesis of fibrosis is currently believed to be indirect: by way of promoting the pro- fibrotic cytokines like IL-13 and TGFβ.

1.5.4. ANTI – FIBROTIC CYTOKINES

IFNγ and TNFα are important cytokines with anti–fibrotic activity (Varga *et al.*, 1990;Kahari *et al.*, 1990;Yufit *et al.*, 1995;Higashi *et al.*, 1998). The anti-fibrotic activity of IFNγ is shown to be mediated by the up-regulation of SMAD-7 molecule in fibrosarcoma cells which is an inhibitory SMAD protein able to inhibit the phosphorylation of SMAD-3 and consequent downstream signalling events (Ulloa *et al.*, 1999). However, it has been shown that this inhibitory mechanism is not functional in human skin fibroblasts. It was shown that over expression of transcriptional co-activator p300/CBP suppresses the IFNγ mediated inhibition of TGFβ signalling suggesting that IFNγ activated STAT1 sequestrates endogenous p300/CBP and reduces the interaction with SMAD-3 and suppressing collagen gene transcription (Ghosh *et al.*, 2001). Several transcriptional factors, which will suppress TGFβ signalling, have been described [Reviewed (Ghosh, 2002)]. Another route through which IFNγ exert its anti-fibrotic property is by up-regulating the expression of MMPs. IFNγ can also act as an inhibitor of IL-13 mediated fibrosis by way of up-regulating the production of IL-13Rα2 (Daines and Hershey, 2002). IL-13 binds IL-13Rα2 with high affinity, but does not signal and is considered as a decoy receptor. IFNγ is able to downregulate the phosphorylation of STAT6, the key molecule involved in the signal transduction of IL-4 and IL-13 (Heller *et al.*, 2004). The proposed interaction between TGFβ, IL-13/IL-4 and IFNγ in regulating the collagen gene expression is presented in figure. 1.4.

TNFα is a cytokine with a specific receptor present on a wide population of cells (Schall *et al.*, 1990). Lipopolysacharides (LPS), microbial agents, IL-1, IL-2, and granulocyte macrophage colony stimulating factor (GM-CSF) are able to stimulate macrophages to secrete TNFα. The signal transduction machinery starts with TNF receptor I (TNFRI) and TNFRII. The signalling cascades involve

activation of NF-κB and mitogen activated protein kinase (MAPK) pathways. Adaptor molecules like TNFR associated factor – 1 (TRAF-1) and TRAF-2 also play a key role in mediating the TNFR-I induced activation of NF-κB (Wajant and Scheurich, 2001;Chen and Goeddel, 2002). The anti–fibrotic activity of TNFα is mediated through differential induction of C-Jun and JunB. C-Jun and JunB are transcription factors of the activator protein – 1 (AP-1) family, which have antagonistic transcriptional activities. Induction of C-Jun by cytokines has been shown to directly interfere with SMAD pathway by preventing binding of SMAD-3 to DNA or to sequestrate the transcriptional co-activator p300 (Verrecchia *et al.*, 2003).

1.5.5. BIOSYNTHESIS OF COLLAGEN

Fibroblasts are the main cell responsible for the synthesis of collagen. Heterogeneity in the phenotype of fibroblast in many fibrotic disorders is reported [Reviewed in (Fries *et al.*, 1994)]. α smooth muscle actin (αSMA) expressing myofibroblast is another cell type capable of producing collagen, which has been reported from human patients with IPF and bleomycin model of the disease in mice (Zhang *et al.*, 1994). The cell of similar phenotype seen the case of liver fibrosis is called hepatic stellate cell (HSC) and in the pancreatic fibrosis as pancreatic stellate cell (PSC) (Madro *et al.*, 2004;Ramadori and Saile, 2004).

Transformation of fibroblast to myofibroblast with the expression of αSMA was shown in *in vitro* studies using profibrotic cytokines like TGFβ, IL-4 and IL-13 (Desmouliere *et al.*, 1993;Hashimoto *et al.*, 2001).The origin of these fibroblasts and myofibroblasts at the site of fibrosis was thought to be by proliferation and differentiation of cells in the local site. However, recent evidence shows that there is a population of non-resident circulating cells called fibrocytes as the source of myofibroblasts at the site of fibrosis. These cells express collagen I, CD11b, CD13, CD34, CD45RO, MHC class II and CD86. They constitute 0.1 to 0.5% of the nonerythrocytic cells in the peripheral circulation (Abe *et al.*, 2001). Epithelial mesenchymal transition (EMT) is another possibility for generation of myofibroblasts at the site of fibrosis [Reviewed in (Zeisberg and Kalluri, 2004)].

Figure 1.4. Diagrammatic representation of anti – fibrotic activity of IFNγ.

(1) The signal transduction machinery of TGFβ involves phoshorylation and activation of SMAD2 and 3 and its association with SMAD4 before translocating to the nucleus. SMAD7 is an inhibitory molecule which can prevent the phosphorylation of SMAD2 and 3 and consequent events. IFNγ upregulates the expression of SMAD7 and it is suggested as one of the mechanism by which IFNγ exerts the anti – fibrotic activity (Ullao *et al.,* 1999).

(2) The binding of SMAD complex with DNA can occur directly or with the help of other co – factors, like cyclic adenosine monophosphate (cAMP) response element binding protein (CREB) - Binding Protein (CBP)/p300. It is suggested that, activated STAT1 following IFNγ signal transduction can sequestrate CBP/p300 and can inhibit the pro-fibrotic activity of TGFβ (Ghosh *et al.,* 2001).

(3) IL-13 is another pro- fibrotic cytokine. IL-13 receptor α2 is a decoy receptor for IL-13. IFNγ can upregulate the release of IL-13 R α2 from its cytoplasmic stores. This action is suggested as the mechanism by which IFNγ mediates its anti-fibrotic activity (Daines and Hershey, 2002).

(4) Another mechanism through which IFNγ inhibits IL-13 mediated fibrogenesis is by suppressing the activity of STAT6, the key molecule involved in IL-13 signal transduction (Heller *et al.,* 2004). This effect was demonstrated in lung epithelial cells.

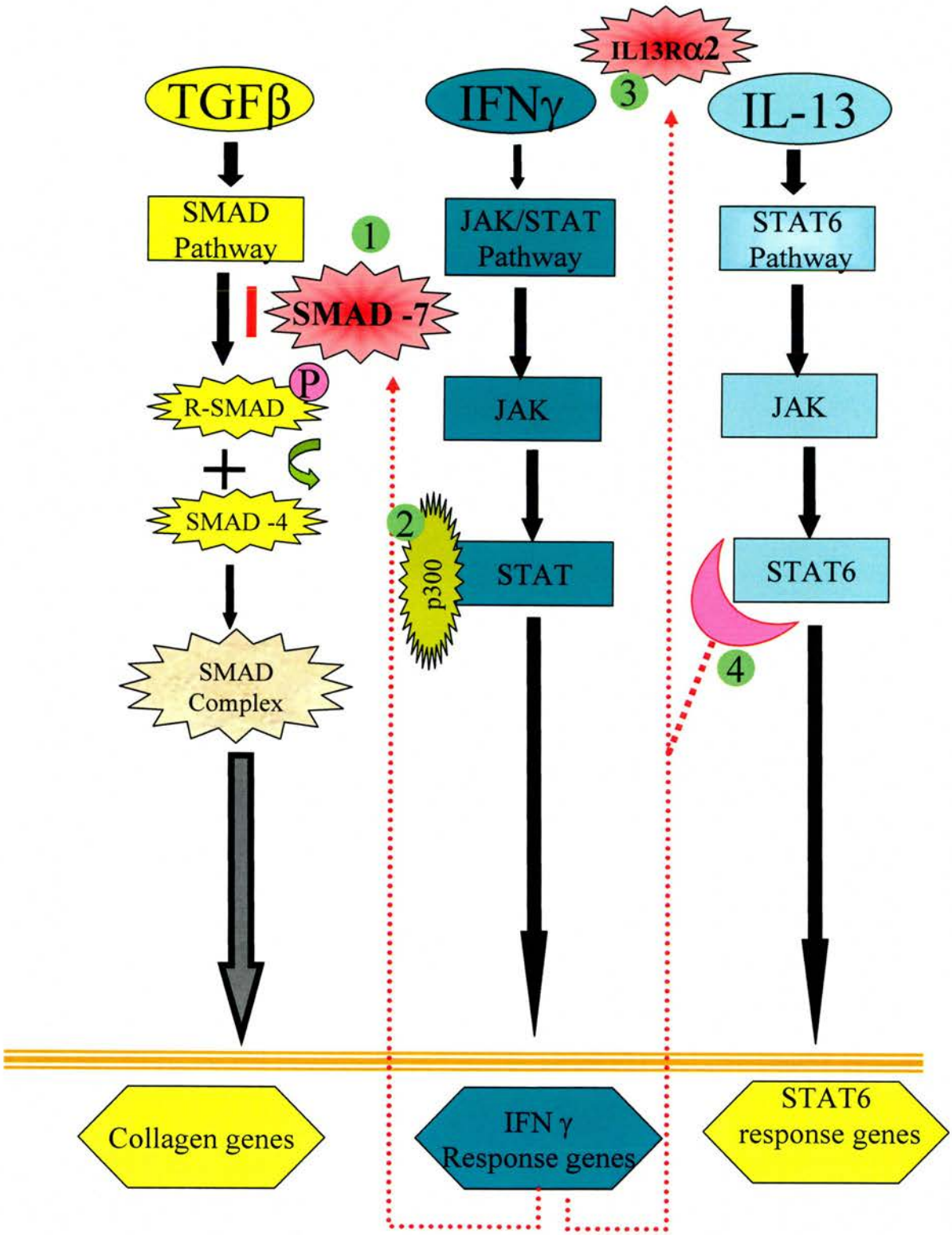

Figure 1.4. Please see the legend on the facing page

The collagen super family of proteins now contains 19 proteins formally defined as collagens and another ten proteins that have collagen like domains. The distinguishing feature of collagen family of proteins is their large domains composed of repeating –Glycine-X-Y- sequence and their unique triple helical structure. Proline is frequently found in the X and hydroxy – proline in the Y position and it makes glycine and proline as the two main amino acids required for the synthesis of collagen. The triple helix structure of collagen is formed from three polypeptide chains that are each coiled into a left – handed helix. Three chains are then coiled around each other into a right-handed helix so that the final structure is like a rope – like rod [Reviewed in (Engel and Prockop, 1991)].The different types of collagen are the product of different genes and some type of collagen are the product of a combination of genes. Different combinations of polypeptide chains determine the type of collagen. A list of known types of collagen, their responsible genes and primary locations are presented in table 1. 4 (Prockop and Kivirikko, 1995). The fibril forming collagens contain large triple – helical domains with about 1000 amino acids or 330 –Gly-X–Y– repeats per chain. These proteins are first synthesised as precursors known as procollagens that need to be cleaved into N-propeptides and C-propeptides by specific proteinases. Type I is the most abundant collagen and it is found in variety of tissues. The type I collagen is composed of two - α1(I) and one-α 2(1) chains. The α1(I) chain is encoded by COL1A1 gene and α 2(1) by COL1A2 gene(de Wet *et al.*, 1983).

1.5.6. RESOLUTION OF FIBROSIS

Resolution of fibrosis is a promising concept. It was believed that fibrosis is non-reversible and it may be true that in reality, complete resolution of fibrosis is not possible. However, evidence is emerging to confirm the ability of effective therapeutic interventions to reverse the phenotype of fibrosis (Arthur, 2002). Removal of etiological agent is the most effective remedial measure to treat many forms of fibrosis. This approach is possible in the case of fibrotic disorders with known etiological factor like alcohol abuse. In reality, there are many fibrotic disorders with unknown etiology. In such instances, intervention of the

Table 1.4. Different types of collagen, their genes and primary locations (Prockop and Kivirikko, 1995).

Type	Gene	Location
I	COL1A1 COL1A2	Most connective tissues, major component of ECM in skin, bone and ligaments
II	COL2A1	Cartilage, vitreous humour
III	COL3A1	Skin, lung and vascular system and most of the connective tissue
IV	COL4A1 COL4A2 COL4A3 COL4A4 COL4A5 COL4A6	Basement membrane
V	COL5A1 COLSA2 COL5A3	Tissues containing Collagen I
VI	COL6A1 COL6A2 COL6A3	Most connective tissue
VII	COL7A1	Anchoring fibrils
VIII	COL8A1 COL8A2	Many tissues, especially endothelium
IX	COL9A1 COL9A2 COL9A3	Tissues containing collagen II
X	COL10A1	Hypertrophic cartilage
XI	COL11A1 COL11A2 COL2A1	Tissues containing collagen II
XII	COL12A1	Tissues containing collagen I
XIII	COL13A1	Many tissues
XIV	COL14A1	Tissues containing collagen I
XV	COL15A1	Many tissues
XVI	COL16A1	Many tissues
XVII	COL17A1	Skin hemidesmosomes
XVIII	COL18A1	Many tissues, especially liver and kidney
XIX	COL19A1	Rabdomyosarcoma cells

the molecular events leading to the fibrogenesis is the most feasible therapeutic approach. Fibrillar collagens (I and III) are degraded by interstitial MMPs. Increase in the activity of MMPs supplemented by decreased activity of tissue inhibitors of MMPs (TIMPs) favours resolution of fibrosis. Apoptosis of collagen secreting cells is another mechanism, which favours resolution of fibrosis.

1.5.7. CIRRHOSIS

Chronic injury to liver from a variety of causes leads to fibrosis of liver. The main causes of liver fibrosis include alcohol abuse, chronic hepatitis C virus (HCV) infection, hepatitis B virus (HBV) infection and non-alcoholic steatohepatitis (NASH). Apoptosis of hepatocytes is being recognised as a major contributory factor in triggering the fibrotic response [Reviewed in (Canbay *et al.*, 2004)]. The distribution of fibrous tissue in the liver parenchyma depends on the type of injury. In the case of chronic viral infection, fibrogenesis begins around the portal tract. In cirrhosis due to chronic alcohol abuse, the deposition of fibrous tissue is seen in the peri-central and peri-sinusoidal areas. However, the fibrosis progresses and bridging fibrosis occurs leading to complete destruction of hepatic architecture. Hepatic stellate cells (HSCs), formerly known as lipocytes, Ito cells or peri-sinusoidal cells were identified as the main collagen producing cells in the liver (Friedman *et al.*, 1985). Other than HSCs, portal myofibroblasts and cells of bone marrow origin also contribute to liver fibrosis (Ramadori and Saile, 2004;Forbes *et al.*, 2004).

1.5.7.1. VIRAL AETIOLOGY OF CIRRHOSIS

Pathogenesis of HCV-induced liver fibrosis is poorly understood. The current hypothesis is that infection of hepatocytes with HCV leads to the release of profibrotic mediators that will activate the neighbouring HSCs to initiate fibrosis. HCV infects a number of cell types, including hepatocytes, monocytes, lymphocytes and salivary glandular cells (Shimizu *et al.*, 1996;Caussin-Schwemling *et al.*, 2001;Arrieta *et al.*, 2001). Recently, it has been shown that recombinant core and NS3 proteins of HCV can directly stimulate the inflammatory and fibrogenic actions of HSCs (Bataller *et al.*, 2004).

HBV, a member of Hepadnaviridae family is another virus associated with pathogenesis of liver fibrosis. Recent estimate shows that this virus throughout the world affects 350 million people. Chronic HBV infection is mainly seen in children infected vertically from their mother. Infection during adulthood normally results in lifelong immunity [Reviewed in (Fattovich, 2003). A successful vaccine is available against HBV infection.

1.5.8. IDIOPATHIC PULMONARY FIBROSIS (IPF)

IPF is a poorly understood chronic human disease characterised by progressive pulmonary fibrosis. Alveolar type II cell injury and apoptosis are thought to be early events in the pathogenesis. Lung injury with bleomycin in laboratory rodents is a popular model for studying this disease condition (Takahashi *et al.*, 2001). The role of myofibroblasts in the pathogenesis of IPF has been recognised in human patients and animal models (Zhang *et al.*, 1994;Kuhn and McDonald, 1991). Bone marrow derived fibrocytes also contribute to lung fibrosis in human patients and bleomycin model of disease (Phillips *et al.*, 2004;Moore *et al.*, 2005). Studies in human patients and animal models have established the protective effect of IFNγ on the development of IPF. Deficiency of IFNγ has been proposed as one of the aetiological factors (Ziesche *et al.*, 1999;Giri *et al.*, 1986). Environmental exposure to dust and association with various viral agents have been proposed as aetiological factors [Reviewed in (Egan *et al.*, 1997) and (Tang *et al.*, 2003)]. Increased level of Th2 cytokines was reported in the lung of patients suffering from IPF (Ando *et al.*, 1999).

1.5.8.1. VIRAL ETIOLOGY OF IDIOPATHIC PULMONARY FIBROSIS

Association of EBV with IPF has been supported by serological, virological and molecular biological data (Kelly *et al.*, 2002;Vergnon *et al.*, 1984;Egan *et al.*, 1995;Stewart *et al.*, 1999;Tang *et al.*, 2003). MHV-68 was demonstrated as a co – factor in the development of pulmonary fibrosis in bleomycin resistant mice (BALB/c) (Lok *et al.*, 2002). Recently, it has been shown that chronic pulmonary infection of IFNγR$^{-/-}$ mice with MHV-68 result in a progressive deposition of interstitial collagen in lung. The infected mice also showed other features of IPF

like increased TGFβ expression, myofibroblast transformation, production of Th2 type cytokines, hyperplasia of type II alveolar epithelial cells and increased expression of MMP-7 (Mora *et al.*, 2005).Hepatitis C virus and adenovirus are the two other suggested viral aetiological agents responsible for IPF (Ueda *et al.*, 1992;Kuwano *et al.*, 1997) .

1.5.9. SYSTEMIC SCLEROSIS (SS)

SS is a disease of unknown aetiology characterised by excessive deposition of collagen in the skin and multiple internal organs [Reviewed in (Jimenez and Derk, 2004). Depending on the clinical severity, there are three recognised form of disease: limited cutaneous SS, diffuse cutaneous SS and fulminant SS. Involvement of gastrointestinal tract, kidney and lung leads to serious complications and are often fatal. The histopathological changes in the skin include marked thickening of the dermis with massive collagen deposition. Early lesions are characterised by infiltration of mononuclear cells in the dermal – adipose tissue interface. The pathogenesis of SS is not clearly defined. Pathological alterations were noticed in fibroblasts, endothelial cells and T and B-lymphocytes. Fibroblasts isolated from SS lesions show persistent activation of collagen and other ECM proteins. Endothelial involvement leads to obliteration of the lumen of small arteries and arterioles. The role of lymphocytes in the pathogenesis of SS is suggested to be through the production of auto antibodies and growth factors to promote the production of fibrous tissue. As the aetiology is currently unknown, several factors including genetic, environmental and infectious agents are suggested as etiological factors. Microchimerism is a novel hypothesis suggested as the cause of SS. During pregnancy, allogenic foetal or maternal cells cross the placenta in both directions and persist in the tissues of mother and child and it is suggested that such foreign cells may become activated by a second event and mount a graft-versus-host reaction which is manifested as SS [Reviewed in (Artlett, 2003)].

1.5.9.1. VIRAL AETIOLOGY OF SYSTEMIC SCLEROSIS

Retrovirus and HCMV are the main infectious agents attributed as the aetiological factors of SS. Anti-Scl-70 antibodies seen in patients with SS is specific for topoisomerase-I antigen. Sequence homology between topisomerase-I and certain retrovirus proteins and the possibility of molecular mimicry is the evidence shown in favour of retrovirus aetiology [Reviewed in (Jimenez *et al.*, 1995)]. Furthermore, antibodies to retroviral proteins have been detected in SS patients (Dang *et al.*, 1991). Evidence in support of HCMV as an aetiological factor is the presence of IgA antibodies specific for HCMV in SS patients and such antibodies are capable of inducing apoptosis in human endothelial cells (Neidhart *et al.*, 1999).

1.6. THE ROLE OF MACROPHAGES IN FIBROSIS

Macrophages play key role in the pathogenesis of fibrosis (see Figure 1.5). Macrophages contribute to the pathogenesis of fibrosis mainly through the following mechanisms: 1) Release of pro – fibrotic cytokines like TGFβ and PDGF upon appropriate stimulation. Removal of apoptotic resident parenchymal or stromal cells by macrophages leads to the release of pro – fibrotic cytokines. 2) The up-regulation of arginase – I in alternatively activated macrophages favours the production of proline, an important component of collagen. In addition to the contribution from arginase – I up-regulation, the agents responsible for alternate activation of macrophages like IL-4 and IL-13 itself can stimulate fibroblasts and myofibroblasts to produce ECM. Macrophages isolated from fibrotic disorders in humans like IPF have been shown to secrete the pro- fibrotic cytokines (Martinet *et al.*, 1987).

1.6.1. ACTIVATION OF MACROPHAGES

Considerable advances have been made on the understanding of activation of macrophages in the past decade [Reviewed in (Mosser, 2003;Duffield, 2003;Mantovani *et al.*, 2004;Gordon, 2003)]. Activated macrophages were defined as cells that secreted inflammatory mediators and killed intracellular pathogens. Advances in the biology of macrophages in the past decade have

Figure 1.5. Role of macrophages in the pathogenesis of fibrosis

(1) Macrophages contribute to the pathogenesis of fibrosis by release of pro-fibrotic cytokines upon appropriate mode of activation. Activation by Th2 type cytokines constitutes the main mechanism by which macrophages secrete pro-fibrotic cytokines. Removal of apoptotic cells is another important mechanism which leads to release of pro-fibrotic cytokines.

(2) Activation of macrophages by Th2 type cytokines is termed as alternate activation of macrophages. The main feature of alternate activation macrophages is selective metabolism of L- arginine by Arginase -1 enzyme, which eventually leads to production of proline, a main amino acid of collagen (for details, please see figure 1.6).

(3) In addition to activating macrophages, the Th2 cytokines, especially IL-13 can directly stimulate collagen producing cells to secrete extra cellular matrix (ECM)

(4) Th1 cytokine like IFNγ antagonise the actions of Th2 cytokines.

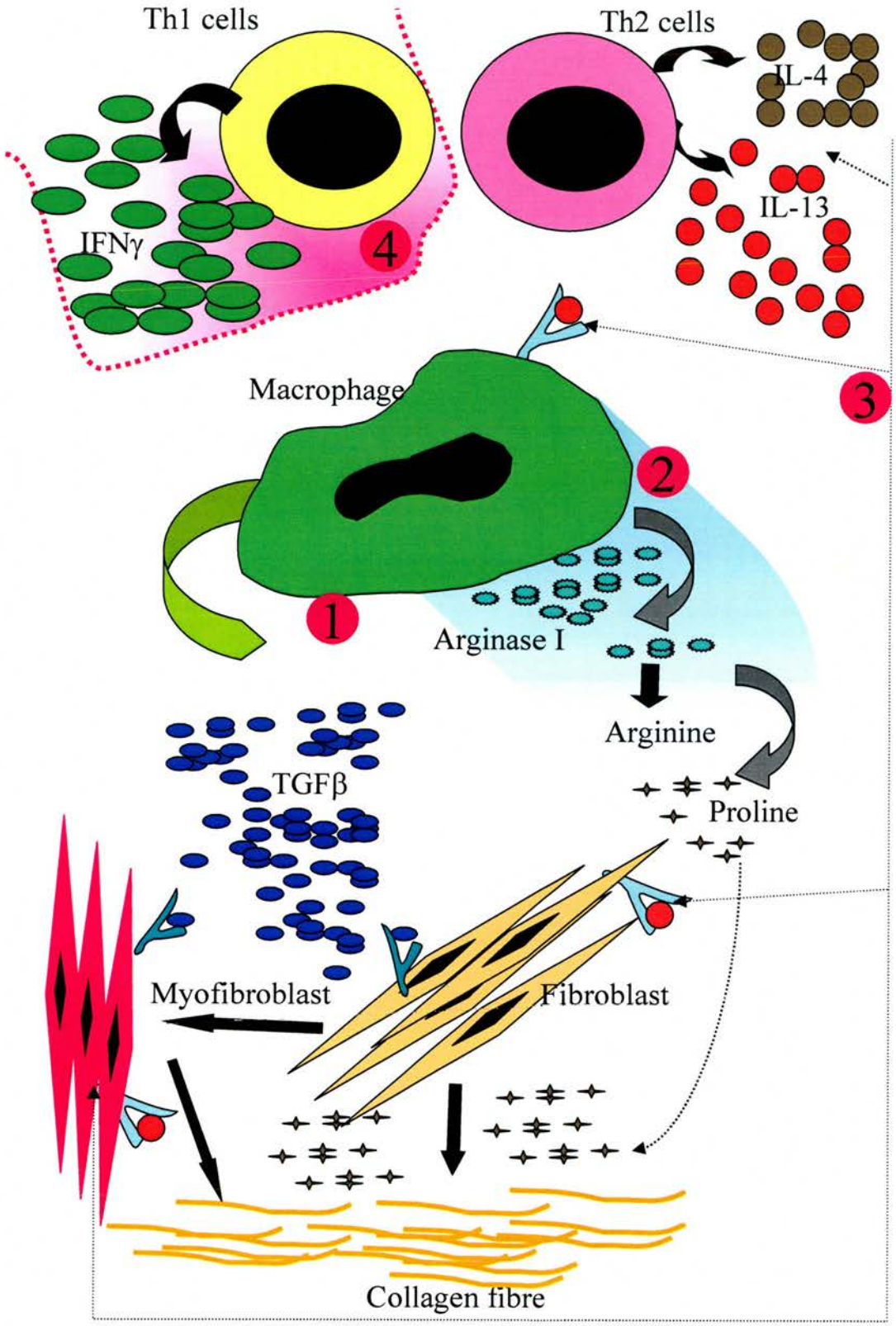

Figure .1.5. Please see the legend on the facing page

revealed that such a definition would not cover all activated macrophages encountered in different tissues during disease. Various endogenous and exogenous stimuli activate macrophages in a different manner manifested by release of cellular factors directed to perform different functions. Three main modes of activation of macrophages have been recognised. They are grouped as: classical activation (Ca), alternate activation (Aa) and type II activation. The Ca macrophages and Aa macrophages are also referred as M1 and M2 macrophages respectively (Mills *et al.*, 2000). The paradigm of polarisation of macrophages in association with tumours was examined and it was concluded that the tumour-associated macrophages (TAM) fall in the group of M2 macrophages (Mantovani *et al.*, 2002). Another proposal to classify activated macrophages on the basis of the intracellular content of glutathione has emerged (Murata *et al.*, 2002). Those macrophages with high glutathione content are defined as reductive macrophages (RM) and those with low glutathione content as oxidative macrophages (OM). The cytokine secretion profile and other features show apparent analogy between RM and Ca macrophage, and between OM and Aa macrophages.

It is suggested that the activation profile of macrophages change with time from one predominated by Ca to the one predominated by Aa macrophages and it is argued that engulfment of apoptotic cells by Ca macrophages contribute to this transformation (Duffield, 2003;Gregory and Devitt, 2004). Recently, it has been shown in a liver fibrosis model by a novel macrophage depletion strategy that functionally distinct subsets of macrophages supporting development and resolution of fibrosis occur during experimental induction and resolution of liver fibrosis (Duffield *et al.*, 2005).

1.6.1.1. CLASSICAL ACTIVATION (Ca)

Macrophages exposed to IFNγ along with stimulation by a microbe or microbial products such as LPS constitute classical activation. Other pro-inflammatory cytokines like TNFα, IL-1, IL-12 and activated T-Lymphocytes through CD40 ligand can also cause Ca of macrophages. Classically activated macrophages show up-regulation of MHC class II molecules, release pro-inflammatory

cytokines like, IL-1, IL-6, IL-12, IL-23 and TNF along with nitric oxide (NO) and reactive oxygen intermediates (ROI) (Ehrt *et al.*, 2001;Hibbs, Jr., 2002;MacMicking *et al.*, 1997). These cells are capable of migrating towards sites of inflammation to attack and degrade pathogens. Ca of macrophages is found in granulomas in association with T-lymphocytes secreting pro-inflammatory cytokines and in immunopathology associated with type I auto immune diseases.

1.6.1.2. ALTERNATE ACTIVATION (Aa)

IL-4 and IL-13 are the principal signals to orchestrate Aa of macrophages through their common receptor chain IL-4Rα (Stein *et al.*, 1992;Gordon, 2003). The role of IL–10 and glucocorticosteroids as the stimulus for Aa of macrophages is controversial (Goerdt and Orfanos, 1999;Gordon, 2003).These activated cells fail to produce NO due to differential metabolism of L- arginine (See below) and consequently are defective in killing intracellular microbes. They up-regulate some MHC class II molecules and in many instances inhibit T-cell proliferation (Schebesch *et al.*, 1997). The signature cytokine produced by this cell is IL-10. The Aa of macrophages also produce the key pro-fibrotic cytokines like TGFβ and PDGF (Mills *et al.*, 2000;Song *et al.*, 2000).Alternatively activated macrophages produce fibronectin and matrix associated protein (Gratchev *et al.*, 2001). In addition to arginase –I expression, which is being recognised as the principal marker molecule, these cells also produce a signature chemokine called alternate macrophage activation associated CC chemokine–1(AMAC-1) (Kodelja *et al.*, 1998). First in Inflammatory Zone – 1 (FIZZ –1) and YM-1 are other two novel molecules associated with Aa of macrophages. However, their functions are not clearly defined (Raes *et al.*, 2002). FIZZ –1 is involved in the transformation of fibroblasts to myofibroblasts (Liu *et al.*, 2004).

A key difference shown by Aa macrophage and Ca macrophage is with regard to the metabolism of L–arginine (Munder *et al.*, 1998;Hesse *et al.*, 2001) (Figure.1.6). In a Ca macrophage, there is up-regulation of nitrous oxide synthase –2 (NOS2) and it metabolises L- arginine into nitric oxide and citrulline. Whereas in the case of Aa macrophages, arginase I is up-regulated and it leads to the

Figure.1.6 Differential metabolism of L-Arginine by classically activated and alternatively activated macrophages.

The top half of the panel highlighted in light green colour represents the classical activation of macrophages. In classically activated macrophages, L-arginine is metabolised by Nitrous oxide synthase –2 (NOS2) to generate nitric oxide, which also inhibit the action of Arginase-1. NOS2 is able to downregulate the expression of Arginase -1 enzyme involved in the alternate activation pathway of macrophage activation. Alternate activation pathway of macrophage activation is highlighted in pink colour on the bottom half of the panel. Alternate activation of macrophages promotes Arginase -1 dependent formation of Proline and polyamines which ultimately promote collagen synthesis and cellular proliferation. Alternatively activated macrophages also produce TGFβ, a key pro-fibrotic cytokine.

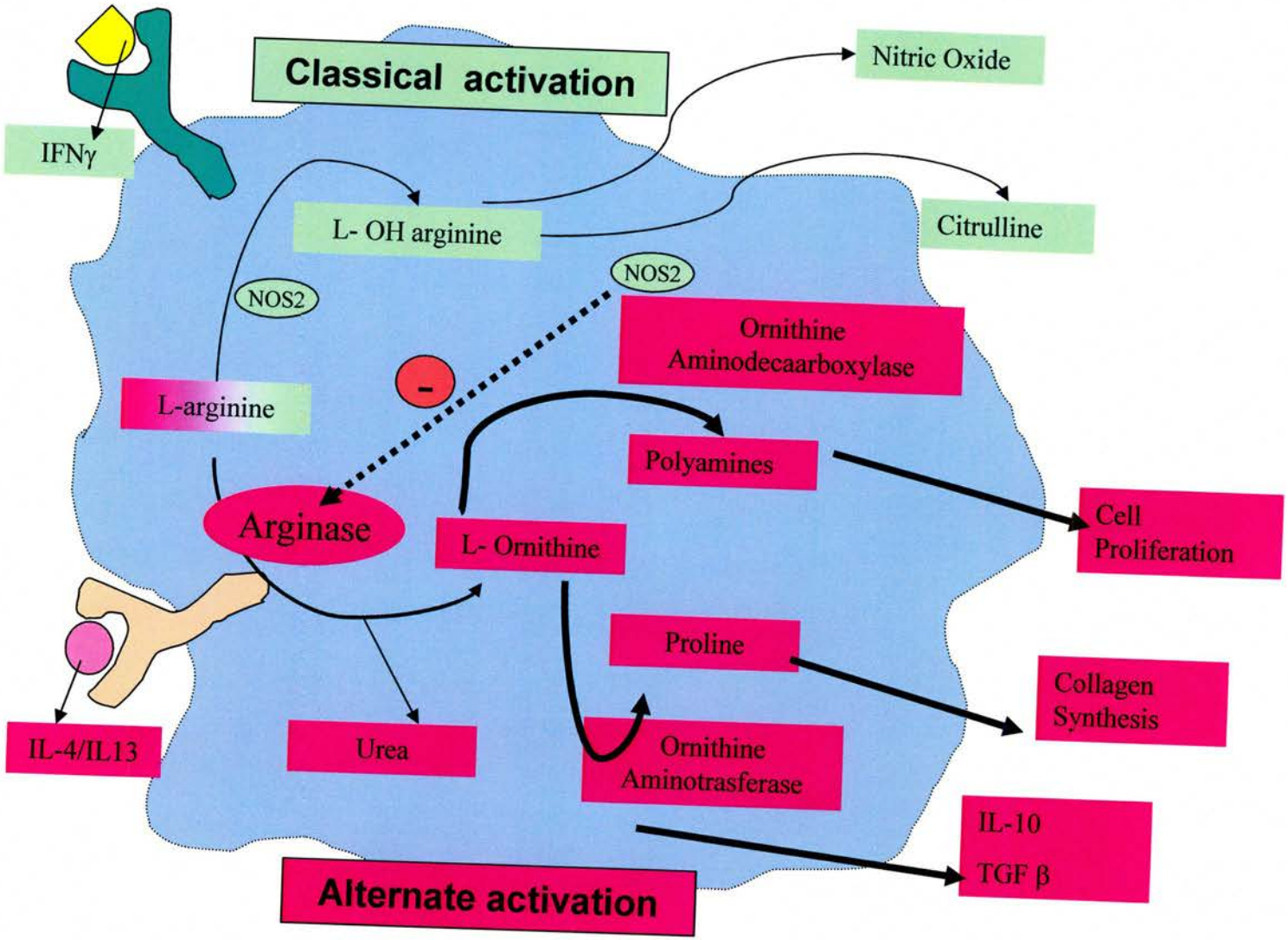

Figure 1.6. Please see the legend on the facing page.

production of L–ornithine and urea from L–Arginine. Arginase–I is the hepatic isoform of arginase involved in the terminal stage of urea cycle. L–Ornithine can be further converted to polyamines by ornithine aminodecarboxylase or proline by ornithine aminotransferase. Proline is an important amino acid required for the synthesis of collagen (see section 1.5.5). Arginase–I up-regulation and enhancement of fibrosis by Aa of macrophages has been shown in the *Schistosoma mansoni* induced liver fibrosis model (Hesse *et al.*, 2001), bleomycin induced IPF model (Endo *et al.*, 2003), peritoneal nematode implantation model of chronic type II inflammation (Nair *et al.*, 2003) and different models of parasitic diseases (Vincendeau *et al.*, 2003). Dendritic cells and fibroblast also show the difference in activation profile shown by macrophages when exposed to either Th1 or Th2 cytokines (Munder *et al.*, 1999;Witte *et al.*, 2002).

1.6.1.3. THE TYPE II ACTIVATION

Ligation of FcRs on macrophages with immune complexes and variety of stimuli suppressed IL-12 production and produced large quantities of IL-10 (Sutterwala *et al.*, 1997;Gerber and Mosser, 2001). Such activated macrophages were called as Type II activated macrophage (Anderson and Mosser, 2002). This mode of activation required another stimulus after FcR ligation to express this phenotype. The secondary stimuli included stimuli that signalled through toll like receptors (TLRs), CD40 and CD44. Type II activated macrophages do not up-regulate arginase –I expression. With the exception of IL-12 and IL-10 the cytokine secretion profile mirrored that of Ca macrophage (Gerber and Mosser, 2001). Type II activated macrophages stimulated T-lymphocytes to secrete IL-4 (Anderson and Mosser, 2002).

1.7. PROJECT OUTLINE

Murine gammaherpesvirus – 68 (MHV–68) infections in laboratory mice is a small animal model for studying the pathogenesis of gammaherpesviruses in their natural host.

A defect in the α chain of gamma interferon receptor ($IFN\gamma R^{-/-}$) renders the host unresponsive to IFNγ, although the mice can produce IFNγ in response to virus infection. Intranasal infection of $IFN\gamma R^{-/-}$ mice with MHV–68 results in fibrosis of spleen. The core objective of this project was to further characterise the pathological changes in the spleen of $IFN\gamma R^{-/-}$ mice infected with MHV-68. To achieve this objective, the study was focussed around the following core areas.

- Sequential gross and histopathological changes
- Characterisation of the cellular events
- Identification of host response genes
- Role of IFNγ responsiveness in pathogenesis
- Assessment of the level of productive and latent infection

In addition to the pathological changes in the spleen, intraperitoneal infection of $IFN\gamma R^{-/-}$ mice with MHV-68 was shown to cause chronic arteritis affecting the major blood vessels. The effect of IFNγ unresponsiveness on the pathology of lung and liver following MHV-68 infections is currently unknown. Therefore, the study was also extended to explore the pathological changes in lung, liver and aorta following intranasal infection of $IFN\gamma R^{-/-}$ mice with MHV-68.

CHAPTER TWO: MATERIALS AND METHODS

2.1. MAINTENANCE OF CELL CULTURES

2.2. PREPARATION OF VIRUS STOCKS AND INOCULUM

2.3. TITRATION OF MHV-68

2.4. INFECTION AND SAMPLING OF MICE

2.5. HISTOPATHOLOGY

2.6. IMMUNOHISTOCHEMISTRY

2.7. *IN SITU* HYBRIDISATION

2.8. EXTRACTION OF RNA FROM SPLEEN

2.9. BONE MARROW CHIMERA EXPERIMENT

2.1. MAINTENANCE OF CELL CULTURES

Baby hamster kidney (BHK-21) cells are a continuous fibroblastoid cell line derived from a Syrian golden hamster. BHK-21 cells were cultured in Glasgow modified eagle's medium (GMEM, Invitrogen, UK) supplemented with 10% (v/v) tryptose phosphate broth (TPB, Invitrogen, UK) and 10% (v/v) new born calf serum (NBCS, Invitrogen, UK), 100U/ml penicillin, 100U/ml streptomycin and 2mM L-glutamine. Cell lines were cultured in sterile plastic-ware (Nunc) and incubated at 37°C in equilibrium with humidified 5% CO_2. For further passaging, adherent cells were maintained in sub-confluent growth. The medium was poured off and the monolayer washed in 0.02% versene. The monolayer was then incubated with 0.25% trypsin (Invitrogen, UK) until the cells could be removed from the surface of the flask by gentle tapping. The trypsin was then diluted in an equal volume of medium and cells with diluted medium were collected in plastic universals pre - rinsed with medium and centrifuged (450*g*, 5mins). The cell pellet was resuspended in appropriate growth medium. For quantification, small aliquot (50µl) was mixed with 50µl 0.1% trypan blue (w/v) and the number of un-stained viable cells was counted using a haemocytometer. Approximately 5 x 10^6 – 1 x 10^7 cells were re-seeded into fresh tissue culture flasks in about 50 ml of medium.

2.2. PREPARATION OF VIRUS STOCKS AND MOCK INOCULUM

Stocks of MHV-68 were generated in BHK-21 cells. Cells were grown in TC175cm^2 flasks (~1x10^7 cells/flask).The cells were harvested and counted as described in section 2.1, resuspended in medium (1x10^7/ml) and infected with MHV-68 at a multiplicity of infection (MOI) of 0.001. The cells were incubated for 1.5 hours at 37°C with shaking to enhance infection and seeded (2x10^6 cells/flask) in TC175cm^2 flasks. The infected cells were incubated at 37°C for 5-7 days or until gross cytopathic effect (CPE) were observed. Once complete CPE was observed, the cells were dislodged from the monolayer by scraping or gentle tapping of the flask and collected in a universal tube pre-rinsed with medium and centrifuged (2000*g*, 20mins, 4°C). The pellet was resuspended in a small volume of sterile phosphate buffered saline (PBS) (5-10ml) and homogenised with 20 - 30 strokes of a chilled Wheaton-Dounce homogeniser. The homogenate was

transferred to a glass universal tube and sonicated in a water-bath for 15 minutes at 4°C. Following centrifugation (2000*g*, 20mins, 4°C) of the homogenate, the supernatant was transferred to a clean universal tube and kept on ice. The pellet was resuspended in 1ml sterile PBS, re-homogenised and centrifuged (2000*g*, 20mins, 4°C). The supernatants were pooled, aliquoted and stored at -70°C. The mock inoculum was prepared from the uninfected BHK- 21 cells by following the same procedure as described above for preparing virus stocks.

2.3. TITRATION OF MHV- 68

Titres of virus stocks were determined using a plaque assay as described previously (Sunil-Chandra *et al.*, 1992a). Duplicate serial dilutions of the virus sample were prepared (10^{-1} to 10^{-8}) in 1.8ml medium. BHK-21 cells ($1x10^6$) were added to each virus dilution and incubated for one hour at 37°C with shaking. The infected cells were transferred to 60mm culture plates and incubated at 37°C for four days. Uninfected BHK-21 cells were also seeded in duplicate plates at the same density as a negative control. Cells were fixed in 4% buffered formal saline (v/v) (BFS) (Surgipath) and stained with 0.1% toluidine blue. Virus plaques were counted using a light microscope and virus titre was calculated as plaque forming units (PFU/ml).

2.4. INFECTION AND SAMPLING OF MICE

Wild type 129/Sv/Ev mice and IFNγR$^{-/-}$ mice on the 129/Sv/Ev background were purchased from Bantin and Kingman, Hull, United Kingdom and bred in house. Age and sex matched mice were anaesthetised with halothane (Merial Animal Health Ltd.) and inoculated intranasally with $4x10^5$ PFU of MHV-68 in 40µl of sterile PBS. Three experiments were conducted to study the sequential pathological changes following intranasal inoculation of virus. The first experiment was to look at the sequential pathological changes on day 8, 10, 12, 14, 16, 18 and 20. The second experiment was conducted to study the pathological changes at later time points. The time points in this experiment were day 12, 20, 30, 35, 40, 45, 50, 60, 80 and 120 p.i. The time point at day 12 and 20 was taken to overlap the first experiment. The third experiment was conducted to clarify the

effect of mock infection on IFNγR$^{-/-}$ mice. Two sets of IFNγR$^{-/-}$ age and sex-matched mice were used for this experiment. One set of mice was infected with $4x10^5$ PFU of MHV-68 in 40 µl of sterile PBS. The other set of mice was instilled with mock inoculum (prepared as described in section 2.2) in 40 µl volume intranasally. The time points taken in this experiment were day 12, 16, 20 and 50.

At various time intervals as indicated above, 3-5 mice were sacrificed by CO_2 asphyxiation. At very few time points, two mice were sacrificed. A detailed post-mortem examination of the mice was carried out. The lung was inflated BFS (Surgipath) *in situ* through trachea and collected in BFS. The spleen and liver was also collected in BFS in separate tubes. The organs collected were processed and used for histopathology, immunohistochemistry (IHC) and *in situ* hybridisation (ISH) studies.

2.5. HISTOPATHOLOGY

The histopathological analysis involves processing of tissue, blocking of tissue into paraffin wax, sectioning of tissue and adhering 5 – 7 µm thick sections on to appropriate glass slides and staining them with haematoxylin and eosin stain or special stains as required. These procedures were carried out at the Veterinary Pathology Unit of the Easter Bush Veterinary Centre, Edinburgh.

2.5.1. TISSUE PROCESSING

The organs fixed in BFS were processed routinely and paraffin blocks were made. Automatic tissue processor was used for processing of tissues. The tissues for processing were placed in a plastic cassette before starting the schedule. The processing schedule involved dehydrating the tissues by passing through ascending grades of alcohol (80% alcohol, 95% alcohol and isopropanol) for 45 minutes at each concentration of solvents. Before moving to xylene for clearing, the tissues were passed through a mixture of isopropanol and xylene (50% each) for 90 minutes. Clearing of tissues was carried out by passing through xylene (Two changes of xylene for 75 and 90 minutes duration). Before embedding in

wax, the cleared tissue was passed through two change of pre – melted wax (60^0C) for 90 minutes and 120 minutes. The wax used for embedding processed tissue was pre-melted overnight (60 ± 5^0C). The processed tissue was placed in a mould tray with melting wax and the tissue was pressed to the base of the mould. The plastic cassette carrying tissue was placed on top of the mould and placed in a cold plate to allow solidification. The block was moved to cold water for complete solidification of the block.

2.5.2. SECTIONING

The paraffin blocks were cut to obtain 5-7 μm sections. Sectioning was carried out in a Rotary microtome. Cut sections were floated out on a water bath set at 48 - 50^0C to facilitate proper spread of section before lifting on to appropriate glass slides. The sections used for routine haematoxylin and eosin stain and special stains were adhered on to normal glass slides. The sections required for IHC and ISH studies were adhered on to snowcoat extra (Surgipath) glass slides to allow firm adhesion of sections to slides. The glass slides with adhered sections were dried by keeping them in an oven set at 55^0C for 30 minutes.

2.5.3. HAEMATOXYLIN AND EOSIN STAINING

The sections mounted on to the glass slides were stained with haematoxylin and eosin in an automatic stainer. The staining procedure involved dewaxing, hydration, staining, dehydration, clearing and mounting. Dewaxing of slides was achieved by passing through two changes of xylene for three minutes each. Then sections were passed through descending grades of alcohol and taken to water. The hydrated sections were stained with Haematoxylin solution for five minutes. The stained sections were washed in water and taken through 1% acid alcohol and Scott's tap water substitute with washing steps in water in between. The cytoplasmic staining was done using eosin solution for two minutes. The stained sections were washed and dehydrated through ascending grades of alcohol. Passing through two changes of xylene for two minutes each cleared the dehydrated sections. The cleared sections were mounted with glass cover slip and

permanent mountant. The mounted slides were allowed to dry for 30 minutes before viewing under microscope.

2.5.4. SPECIAL STAINS

The special staining techniques employed to demonstrate fibrous tissue in the spleen sections were Masson's trichrome (MT), Martius yellow-brilliant crystal scarlet-soluble Blue (MSB), and Picrosirius red. Von Kossa method for demonstration of calcium in the bony metaplasia lesions in the spleen and Perls technique for demonstration of hemosiderin pigment in the spleen were also used in this study.

2.5.4.1. MASSON'S TRICHROME (MT)

The tissue sections were taken to water by passing through two changes of xylene and descending grades of alcohol. Nuclear staining was done in iron haematoxylin solution for five minutes. The washed sections were differentiated in acid alcohol and washed in tap water before staining in acid fuchsin solution for five minutes. The sections were washed in water and differentiated in phosphomolybdic acid solution for five to ten minutes. The sections are washed well in water and counterstained with light green solution for one minute. After counter staining, the sections were washed well in water and dehydrated by passing through ascending grades of alcohol and cleared in xylene and mounted using glass cover slip and vectamount (Vector laboratories).

2.5.4.2. MARTIUS YELLOW-BRILLIANT CRYSTAL SCARLET-SOLUBLE BLUE (MSB)

The dewaxed sections were taken to water and nuclei was stained with iron haematoxylin solution and rinsed in 95% alcohol. The sections were then taken to martius yellow solution for two minutes. The sections were washed briefly in water and stained in brilliant scarlet solution for 10 minutes. After washing in water, the sections were treated with phosphotungstic acid solution for 5-10 minutes. Then the sections were washed in water and stained with aniline blue solution for 10 minutes. The stained sections were dehydrated by passing through

ascending grades of alcohol and cleared in xylene before mounting in Vectamount (Vector laboratories).

2.5.4.3. PICROSIRIUS RED

The sections were dewaxed and hydrated by passing through descending grades of alcohol and taken to water. Nuclear staining was done using Haematoxylin QS (Vector laboratories) for one minute. The washed sections were treated with 0.2% phosphomolybdic acid for two minutes and stained in picrosirius red solution for 90 minutes. The stained sections were dehydrated by passing through ascending grades of alcohol, cleared and mounted in Vectamount (Vector Laboratories).

2.5.4.4. VON KOSSA

The dewaxed sections were taken to water through descending grades of alcohol. The sections were covered with 2% aqueous silver nitrate solution and exposed to bright light for 60 minutes. The sections were then washed in several changes of deionised water and later in tap water and counter stained with 1% aqueous neutral red. The sections were dehydrated, cleared and mounted using Vectamount (Vector laboratories).

2.5.4.5. PERLS STAINING

The dewaxed sections were taken to water through descending grades of alcohol. Equal parts of hydrochloric acid and potassium ferrocyanide solutions were mixed and filtered on to the section. The staining was allowed for 30 minutes with a change of solution after 15 minutes. The sections were washed several times in water. Nuclear staining was done with neutral red solution for five minutes. The sections are dehydrated, cleared and mounted with Vectamount (Vector Laboratories).

2.6. IMMUNOHISTOCHEMISTRY (IHC)

IHC techniques were employed to demonstrate viral antigen and various marker antigens on tissue sections. Indirect double immunoperoxidase technique was used with all primary antibodies.

2.6.1. PRIMARY ANTIBODY

The list of primary antibodies used in this study and their source is presented in table 2.1. A rabbit polyclonal antibody against MHV–68 was used to characterise the presence of viral antigen positive cells in various organs. The cell types studied include B-lymphocytes, T- lymphocytes (CD3) and T-lymphocyte subsets (CD4 and CD8), red pulp macrophages (RPM), marginal zone macrophages (MZM) and marginal metallophils (MM) in spleen. Arginase – I, a key marker of alternatively activated macrophages was investigated with a polyclonal antibody raised in rabbit against human recombinant arginase – I (A gift from Dr.Gotoh, Kumamoto University, Japan). This antibody was shown previously to cross react with mouse arginase –I (Endo *et al.*, 2003). The characterisation of bony metaplasia in the spleen of IFN$\gamma R^{-/-}$ mice was done using an antibody against bone morphogenic protein–4 (BMP-4). BMP-4 is a cytokine involved in the morphogenesis of bone (Chen *et al.*, 2004). Myofibroblasts positive for α- smooth muscle actin (α-SMA) has been shown to contribute to fibrogenesis in many fibrotic disorders and animal models of fibrotic disorders (Grotendorst *et al.*, 2004). The role of myofibroblasts in the model of splenic fibrosis was investigated by IHC with antibody against α-SMA. The negative control included polyclonal serum from the species of animals from which primary antibodies was made.

2.6.2. BLOCKING

BFS fixed and paraffin embedded tissue sections adhered on to snowcoat extra glass slides (Surgipath) were deparaffinised in xylene and taken through descending grades of alcohol. The endogenous peroxidase was quenched by 0.6% H_2O_2 in methanol for 30 minutes. Immersing in deionised water for five minutes hydrated the sections. The antigen unmasking was done using 0.1% protease IV in tris buffered saline (TBS) [PH 7.6]. Blocking of endogenous immunoglobulins was carried out by incubating the sections with 10% normal serum in TBS (Normal serum from the species of animals from which secondary antibodies were made - Blocking serum). In the case of primary antibody of mouse immunoglobulin isotype, mouse immunoglobulin blocking reagent supplied in the

Table 2.1. Primary antibodies used for immunohistochemistry

Sl. No.	Primary antibody	Clone and Dilution [in square brackets]	Source	Reference
1	Anti- MHV-68	Polyclonal antibody raised in Rabbit [1:2000]	Laboratory for Clinical and molecular Virology, Edinburgh	(Sunil-Chandra *et al.*, 1992a)
2	F4/80	Clone A3: 1 (Rat IgG2b) [1:20]	Serotec, United Kingdom.	(Austyn and Gordon, 1981)
3	ER-TR9	Polyclonal antibody raised in rat [1:1000 (1μg/ml)]	BMA Biomedicals, Switzerland	(Dijkstra *et al.*, 1985)
4	MOMA -1	MOMA –1 clone (Rat IgG2a) [1:10]	Serotec, United Kingdom	(Kraal *et al.*, 1988)
5	CD3	Clone CD3-12 (Rat IgG1) [1:200]	Serotec, United Kingdom	(Jones *et al.*, 1993)
6	CD4	Clone YTS -191.1 (Rat IgG2b) [1:1000]	Laboratory for Clinical and molecular Virology, Edinburgh	(Cobbold *et al.*, 1990)
7	CD8	Clone YTS -169.4 (Rat IgG2b) [1:1000]	Laboratory for Clinical and molecular Virology.	(Cobbold *et al.*, 1990)

Sl. No.	Primary antibody	Clone and Dilution [in square brackets]	Source	Reference
8	CD45R/B220	Clone RA3-6B2 (Rat IgG2a) [1:1000]	PharMingen, USA	(Coffman, 1982)
9	Arginase -I	Polyclonal antibody raised in rabbit (Anti-recombinant human arginase – I) [1:250]	Dr. Tomomi Gotoh, Kumomoto University, Japan	(Sonoki *et al.*, 1997)
10	BMP-4	Clone 3H2 (Mouse IgG2b) [1:20]	Novocastra Laboratories, United Kingdom	(Jones *et al.*, 1991)
11	α Smooth muscle actin	Clone αsm-1 (Mouse IgG2a) (Anti – Human α smooth muscle actin) [1:50]	Novocastra laboratories, United Kingdom	(Skalli *et al.*, 1986)

Mouse on Mouse (MOM) kit (Vector laboratories) was used. The incubation time was 30 minutes. After treating the sections with blocking serum/reagent, the primary antibody was applied at the concentrations mentioned in the table 2.1. The primary antibody was diluted in 2% of the blocking serum in TBS and incubated at room temperature for two hours.

2.6.3. SECONDARY ANTIBODY

The sections incubated with primary antibody were thoroughly washed in TBS and treated with biotinylated secondary antibodies. For primary antibodies originating from rabbit the biotinylated secondary antibodies raised in goat against rabbit immunoglobulins were used. When, the primary antibodies were of rat immunoglobulin, the secondary antibodies raised in rabbit against rat

immunoglobulins were used. In the case of mouse monoclonal primary antibody, the biotinylated Anti-mouse IgG reagent supplied in the Mouse on Mouse kit (Vector laboratories) was used. The concentration of biotinylated secondary antibody used was 10μg/ml. The secondary antibody was diluted in 1.5% of the blocking serum in TBS. The incubation time for secondary antibody was 30 minutes.

2.6.4. ENZYME CONJUGATE AND SUBSTRATE

The conjugated complex of antigen, primary antibody and biotinylated secondary antibody was detected by adding ABC reagent (Vector laboratories), streptavidin peroxidase conjugate ready to use solution (Zymed laboratories) or Steptavidin – peroxidase (POD) conjugate (500mU/ml) (Roche molecular biochemicals). The ABC reagent was prepared and kept for thirty minutes as per manufacture's instructions before applying to the sections. The streptavidin – POD conjugate (Roche molecular biochemicals) was prepared in TBS. The incubation time for enzyme conjugate was 30 minutes at room temperature. The substrate solution was applied after washing the sections in TBS. 3, 3'-diaminobenzidine (DAB) or Vector Nova Red (Vector Laboratories) was used as the substrate for detection of peroxidase conjugate. The substrate solution was prepared in deionised water as per the manufactures instruction. The development of colour was monitored under microscope and the incubation time varied between five to ten minutes. Haematoxylin QS (Vector laboratories) was used as the counter stain to demonstrate the nucleus. The counter stain was applied for 45 seconds after thorough washing in water. The counterstained sections were washed in deionised water with two changes of deionised water. The sections were dehydrated by passing through ascending grades of alcohol and cleared in xylene. The stained sections were mounted with glass cover slip using Vectamount (Vector laboratories).

2.7. *IN SITU HYBRIDISATION* (ISH)

The ISH protocol involves generation of riboprobe with a digoxigenin label, hybridisation of probe into RNA in tissue sections and detection of the digoxigenin label by immunoenzymatic techniques.

2.7.1. GENERATION OF RIBOPROBE

Riboprobe was generated from a recombinant plasmid, pEH1.4 (Figure.2.1). pEH1.4 was prepared by inserting 1.4kb *EcoRI-HindIII* sub fragment of *HindIII* – E fragment of MHV-68 genome encoding tRNA1-4 into pBS (Stratagene) (Bowden *et al.*, 1997).

2.7.1.1. QUANTIFICATION OF PLASMID DNA

Plasmid DNA was quantified using a spectrophotometer (Cecil). In a quartz cuvette 99 µl of water and one µl of plasmid DNA was added and optical absorbance measured at 260 nm and 280 nm. The absorbance value obtained at 260 nm was multiplied by 100 to account for the dilution of the DNA and by 50 again to obtain the concentration (µg/ml). This quantification was based on the fact that one absorbance unit at 260 nm is equivalent to approximately 50 µg/ml of double-stranded DNA. The ratio of absorbance values at 260 nm to 280 nm indicated the purity of the DNA. A ratio between 1.7 and 1.9 indicate good purity of DNA (Sambrook *et al.*, 2001).

2.7.1.2. RESTRICTION DIGESTION OF PLASMID

Restriction enzymes were obtained from New England Biolabs and used with the supplied buffers according to the manufacturer's instructions. 25 µg of plasmid DNA was used for restriction digestion reaction. Restriction digestion reactions were carried out in a volume of 100 µl with one unit of enzyme per one µg of DNA for 3 h at 37°C. Two independent reactions were carried out with *HindIII* and EcoRI.

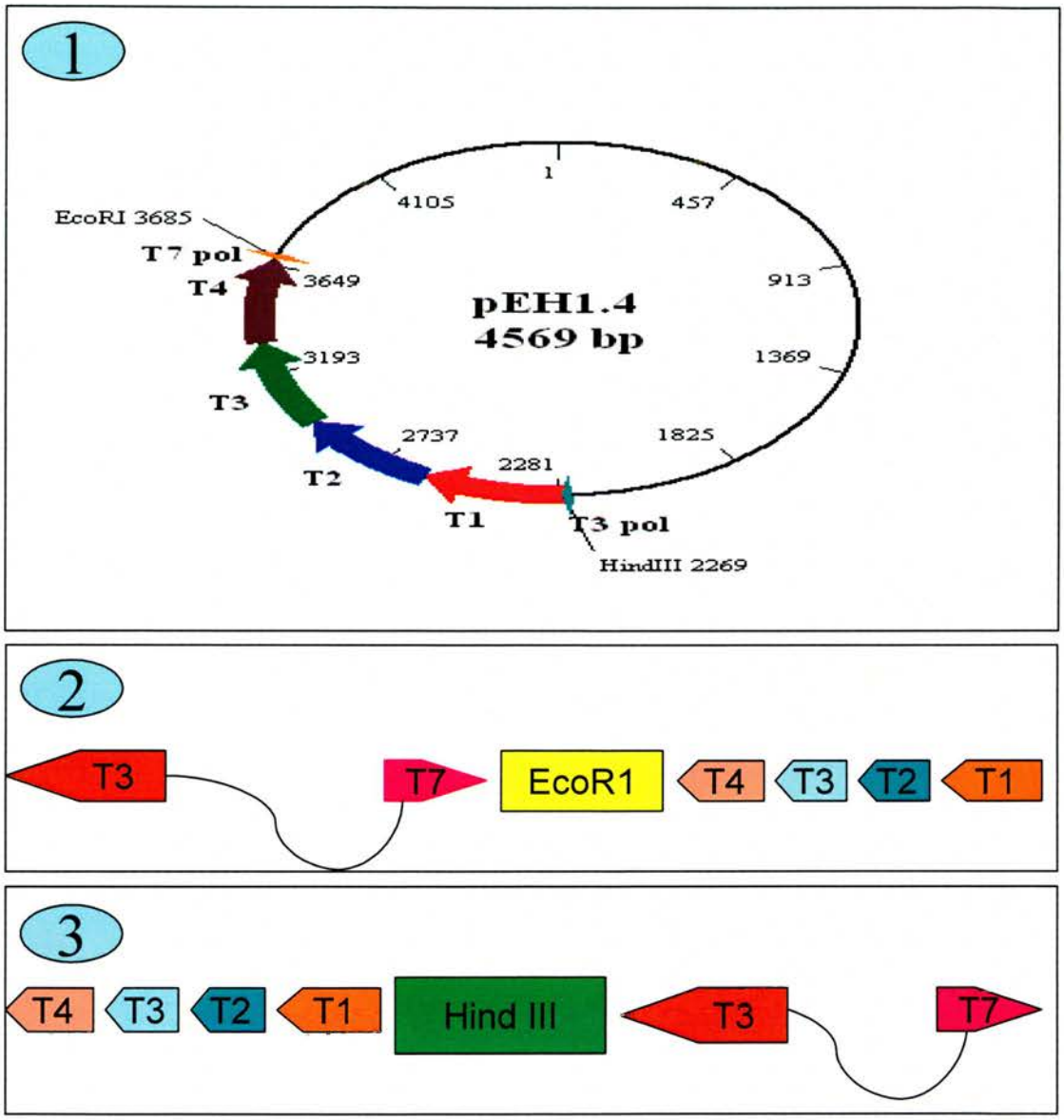

Figure. 2.1. Restriction digestion of pEH1.4. A recombinant plasmid pEH1.4 containing MHV- 68 tRNA 1-4 (As shown in the top panel) is used for making the riboprobe (Bowden *et al.* 1997). The plasmid linearised by restriction digestion with *Hind III* (Panel 2) is used for generating antisense probe by *in vitro* transcription with T7 RNA polymerase. The sense probe was made by linearising the plasmid with *Eco R1 (Panel 3) and in vitro* transcription with T3 RNA polymerase. T1, vtRNA1. T2, vtRNA2. T3, vtRNA3. T4, vtRNA4.

2.7.1.3. PURIFICATION OF THE LINEARISED PLASMID

Phenol – chloroform extraction procedure was used for purification of linearised plasmid. A mixture of phenol [pH 7.9], chloroform and iso-amyl alcohol in a ratio of 25:24:1 (v/v) was added to 0.2 volume of DNA (digested with restriction enzymes in 100µl) in a 1.5ml eppendorf tube. The contents of the tube were thoroughly mixed using a vortex for 30s then centrifuged (9000*g*) for 2mins. The upper aqueous phase containing the DNA was transferred to a clean tube and the procedure was repeated until the interface between the aqueous and non-aqueous solutions became clear. A single chloroform extraction was performed to ensure removal of phenol from the DNA. DNA was precipitated in 2.5 volume of ethanol (96%) and 0.15 volume of 3M sodium acetate [pH 5.5] at ˉ80°C for one hour. The precipitated DNA was centrifuged (9000*g*, 10mins), washed in 70% ethanol and resuspended in 20µl of TE.

2.7.1.4. AGAROSE GEL ELECTROPHORESIS

DNA (typically ≤ 1 µg) was mixed with 3 µl gel loading buffer and 10µl of milli-Q water and loaded onto agarose gels containing 1% agarose (SeaKem®, Flowgen) and 0.5 µg/ml (w/v) ethidium bromide in TAE buffer. Electrophoresis was carried out in a horizontal tank (BIO-RAD) containing TAE buffer at 80V. The size of DNA bands was estimated by comparison with DNA molecular weight markers (1kb Plus DNA ladder, Invitrogen). DNA bands were visualised using a short wave UV transilluminator (UVP Inc.).

2.7.1.5. *IN VITRO* TRANSCRIPTION OF DNA

One microgram of linearised plasmid DNA was used for *in vitro* transcription. The plasmid digested with *HindIII* was used for making run off transcripts of antisense probe with T7 RNA polymerase and the EcoRI cut plasmid for generation of sense probe with T3 RNA polymerase. The *in vitro* transcription procedure incorporates a digoxigenin labelled UTP in every 20 –25th position of the transcript. The *in vitro* transcription reaction was carried out in a volume of 20µl. In addition to one microgram of linearised plasmid DNA, 2µl of 10x DIG RNA labelling mix (Roche Molecular Biochemical), 2µl of 10x Transcription

buffer (Roche Molecular Biochemicals), 2µl of either T7 RNA polymerase or T3 RNA polymerase (Roche Molecular Biochemicals) and enough sterile filtered water to the make up the volume to 20µl was used. The contents of the tube were mixed well and centrifuged before incubation in a water bath at 37^0C for three hours. The template DNA was denatured using 2 U RNase free Dnase I (Roche Molecular Biochemicals) and incubated at 37^0C for 15 minutes. The transcription reaction was stopped by adding 2µl of 0.2M Ethylene diamine tetra acetic acid (EDTA) [pH: 8.0]. The labelled RNA probes in the mixture are precipitated by adding one µl of yeast tRNA (10µg /ml), 2µl of 3M sodium acetate [pH: 5.5] and 50 µl of ice cold absolute alcohol. Incubating the mixture at $^-80^0$C for 30 minutes facilitated the precipitation of RNA. The precipitated RNA was recovered by centrifuging (13000 g) the mixture at 4^0C for 20 minutes. The precipitated RNA was washed in ice - cold 70% ethanol, air-dried and allowed to regain to room temperature. The RNA pellet was resuspended in 45 µl sterile filtered water for 30 minutes. An aliquot of the RNA was run on an ethidium bromide stained agarose gel for checking the presence of transcript.

2.7.1.6. ALKALINE HYDROLYSIS OF THE PROBE

The transcript generated by *in vitro* transcription was about 1.4 kb in size and hence alkaline hydrolysis of the probe was done to regulate the length of the probe. The following formula was used to arrive at the time of incubation during alkaline hydrolysis to regulate the length of the probe.

$$t = \frac{L_0 - L_f}{k \times L_0 \times L_f}$$

t = Time in minutes

L_0 = Initial length of transcript in kb

L_f, Desired probe length in kb;

k = constant = 0.11kb/min

The desired probe length was set at 170 bp and the time required for alkaline hydrolysis was estimated as 47 minutes. The alkaline hydrolysis was carried out

by adding 5 µl of carbonate buffer to 45 µl of riboprobe diluted in sterile filtered water. (The entire amount of riboprobe obtained by in vitro transcription as described in section 2.7.1.5.) The incubation time was 47 minutes at 60^0 C. The hydrolysis was stopped by adding 5 µl of hydrolysis – neutralisation buffer (1:10 volume). The hydrolysed riboprobes were precipitated by adding 2.5 volume of chilled ethanol. The samples were mixed well and incubated at -80^0C for 30 minutes. To precipitate the RNA, the sample was centrifuged at 13000g for 20 minutes at 4^0C. After centrifugation, the absolute alcohol was decanted and the pellet washed with 70% alcohol and centrifuged again at 13000 g for 20 minutes at 4^0C. The pellet was air dried and diluted in 50 µl of sterile filtered water and the aliquots are stored at -70^0 C.

2.7.1.7. ESTIMATING THE YIELD OF DIGOXIGENIN – LABELLED PROBE

The yield of digoxigenin labelled probe was estimated by making serial dilutions of the newly prepared probe and comparing it with dilutions of a standard digoxigenin labelled RNA probe. Digoxigenin labelled "antisense"- Neo RNA, transcribed with T7 RNA polymerase from one µg DNA (Roche Molecular Biochemicals) was used as the standard. The concentration of the probe in the standard solution was approximately 100 µg/ml DIG labelled RNA. The following dilutions of the standard RNA probe were made in TE: 10ng/µl, 1ng/µl, 100pg/µl, 10pg/µl and 1pg/µl. The newly synthesised probe was also diluted with the assumption that in *vitro* transcription of one µg of DNA would have yielded 10 µg of labelled RNA. Five µl each of diluted newly prepared probes and standard solutions were applied on to a nylon membrane (Hybond – N+, Amersham) in parallel. The spots were allowed to air dry and another five µl of the diluted probes were applied to the corresponding original spots in the membrane. The cross linking of nucleic acid to the membrane was achieved by placing the air-dried membrane in a stratalinker at 120 mJ. The membrane was transferred to a plastic container and washed with maleic acid buffer in a shaker. The washing was done three times with change of buffer every five minutes. The membrane was incubated with buffer no.2 for 30 minutes making sure that the

solution was covering the area with spots of probes. The anti-DIG antibody conjugated with alkaline phosphatase (Roche Molecular Biochemicals) diluted in buffer no.2 at a concentration of 1: 5000 was applied to the membrane and incubated for one hour at room temperature. The membrane was washed with washing buffer three times for ten minutes each time in a shaker. The membrane was equilibrated in buffer no.3 for five minutes and substrate solution was applied. The substrate solution was prepared by dissolving one tablet of Sigma Fast substrate (Sigma) in 10 ml of deionised water. The colour development was allowed to occur in dark for two hours and washing the membrane in deionised water for five minutes stopped the colour development. The colour intensities in the control and newly prepared probe were compared and approximate quantification of the newly prepared probe was achieved.

2.7.2. HYBRIDISATION

ISH technique was performed on formalin fixed paraffin embedded tissue sections (5–7 μ thickness) adhered onto Snowcoat extra coated slides (Surgipath). Paraffin wax was removed by passing through xylene for five minutes each with two changes of xylene. The sections were taken to deionised water through descending grades of alcohol. Sections were equilibrated in PBS for five minutes and then treated with 0.1% solution of protease IV for five minutes. Protease treated sections were washed in PBS and passed through two changes (five minutes each) of 0.3M ammonium acetate in absolute alcohol and air dried before application of the pre - hybridisation buffer. The sections covered with pre- hybridisation buffer were incubated at 55^0C for an hour in a hydrated chamber. The salmon sperm DNA (SS DNA) solution was boiled for two minutes prior to adding into the pre-hybridisation and hybridisation buffer. The probe was diluted in hybridisation solution at a concentration of 200 ng/ml. After addition of the probe into the hybridisation buffer, the solution was boiled for two minutes, vortexed, centrifuged and chilled on ice. One-hundredth volume of IM Dithiothreitol (DTT) was added to the probe mix before applying on to the tissue sections. The pre-hybridisation solution was tipped off before applying the probe in the hybridisation solution. 50μl of probe mix was applied to each section and

covered with parafilm to prevent evaporation of the probe mix during over night incubation in a hydrated chamber at 55^0C.

2.7.3. DETECTION OF DIGOXIGENIN LABEL

Digoxigenin label on the hybridised probe was detected by anti–digoxigenin antibody tagged with alkaline phosphatase enzyme. The hybridised sections were immersed in 4x standard saline citrate (SSC) buffer and the adhered parafilm carefully removed. The sections were washed in descending concentration of SSC (2xSSC, 1xSSC and 0.2x SSC with two changes in each dilution for 15 minutes) on a shaking platform set at 37^0C, except for the final wash in 0.2x SSC, which was carried out at 55^0C. The sections were rinsed in PBS before washing in buffer No.1 for three times (five minutes each time). The sections were then incubated in buffer no.2 supplemented with 0.3% (v/v) Titron – X 100 for 30 minutes at room temperature. The Fab fragments anti-digoxigenin antibody tagged with alkaline posphatase also is diluted in the above solution (Buffer no.2 supplemented with 0.3% (v/v) titron –x 100) at a concentration of 1:200 (3750 mU/ml). Incubation of antibody was carried out for two hours in room temperature. After incubation with primary antibody, the sections were washed in buffer no.1 for three times (15 minutes each time) on a shaking platform. After the washing steps, the sections are equilibrated in buffer no.3 for five minutes. Substrate solution was prepared by dissolving Sigma Fast substrate tablet in 10 ml deionised water. After two hours of incubation in the dark, washing the sections thoroughly in deionised water for five minutes stopped the enzyme reaction. The sections were then flooded with nuclear fast red solution (Vector laboratories) and incubated in room temperature for five minutes. The stained sections were washed thoroughly in deionised water and air dried. The air-dried sections were dehydrated by passing through ascending grades of alcohol and cleared by passing through two changes of fresh xylene. The dehydrated and cleared sections were permanently mounted with Vectamount permanent mounting solution (Vector Laboratories)

2.8. EXTRACTION OF RNA FROM SPLEEN

Total RNA was isolated from spleen using the RNeasy® Mini Kit (QIAGEN). Initially, the spleen was disrupted and homogenised in guanidine isothiocyanate (GITC) containing buffer. Disruption of the spleen was achieved by grinding the tissue in a sterile eppendorf tube with 600 µl lysis buffer (Buffer RLT) using a sterile plastic pestle (Sigma). With the twisting action of the pestle, the spleen tissue is made into a viscous lysate. Homogenisation of the lysate was done using a QIAshredder homogeniser (Qiagen). The viscous lysate was loaded on to the QIAshredder spin column sitting in a 2 ml collection tube. The spin column was centrifuged for two minutes at 13000 rpm. The homogenised clear lysate in the collection tube is saved for isolation of RNA. The clear lysate was transferred into a fresh sterile eppendorf tube and centrifuge at 13000 rpm for three minutes. The supernatant was carefully transferred into a new microcentrifuge tube. One volume of 70% ethanol was added to the cleared lysate and mixed immediately by pipetting. 700 µl of the sample was loaded on to the Rneasy mini column placed in a 2 ml collection tube. The tube was closed gently and centrifuged at 10000 rpm for 15 seconds. The flow through was discarded. 700 µl of buffer RW1 was applied to the RNeasy column and tube was closed gently and centrifuged at 10000 rpm for 15 seconds to wash the column and the flow through along with the collection tube was discarded. The RNeasy column was transferred to another 2 ml collection tube and applied 500 µl of buffer RPE on to the column. Centrifuged the samples for 15 seconds and the flow through was discarded. Another 500 µl of buffer RPE was applied to the column and centrifuged again at 10000 rpm for two minutes to dry the silica gel membrane in the spin column. After making sure that the column was dry and free of ethanol, RNA was eluted with 50 µl of RNase free water.

2.8.1. QUANTIFICATION OF RNA

RNA concentration was calculated by measuring the absorbance at 260 nm (A260) in a spectrophotometer (Cecil). An absorbance of 1.0 unit at 260 nm is equivalent to 40µg/ml of RNA. The RNA sample was diluted in the ratio of 1:100

and absorbance was measured at 260 nm and the concentration was calculated by the following formula.

RNA concentration = Absorption at 260nm (A_{260}) × 40 × dilution factor

The purity of the nucleic acid sample, with respect to protein contamination, was assessed using the ratio A_{260}/A_{280}, where a value greater than 1.8 indicates that the sample is free from protein contamination. The RNA was also analysed by gel electrophoresis on a 1% agarose gel prepared in TAE. Representative samples of RNA were also tested in an Agilent 2100 Bioanalyser to check the integrity of RNA.

2.8.2. DNA DECONTAMINATION OF RNA SAMPLES

Decontamination of RNA samples from DNA is absolutely essential for subsequent applications like Reverse Transcriptase - Polymerase Chain Reaction (RT- PCR) and real time RT- PCR. DNA *–free* kit (Ambion) was used for decontamination of RNA samples from DNA. Recombinant DNase - I (rDNase – I) was the principal ingredient of the kit to denature contaminating DNA in the sample. The kit also provides reagents to subsequently remove DNase and divalent cations from sample. DNase treatment was carried out on 10 µl of RNA sample. 0.1 volume of 10x buffer supplied in the kit (1µl) and 1µl of rDNase I (2U/µl) was added to the RNA sample. The solution was incubated at 37^0C for 30 minutes. After 30-minute incubation another 1 µl of rDNase was added and incubated at 37^0C for 30 minutes. DNase inactivation was carried out by adding 2µl of the inactivation reagent. The solution with inactivation reagent was incubated for two minutes at room temperature with occasional mixing. The solution was centrifuged at 10000 g for 1.5 minutes and the supernatant was carefully transferred into a new tube. The quantification of decontaminated RNA was carried out as described above (section 2.8.1). The DNA decontamination of the RNA sample was tested by PCR for murine β- actin gene on RNA samples. Positive control for this PCR reaction was DNA sample extracted from the blood

of a control wild type mouse. The procedure for extraction of DNA from blood of mice will be described later (section 2.8.7).

2.8.3. COMPLIMENTARY DNA (cDNA) SYNTHESIS

cDNA synthesis from RNA was carried out by reverse transcription (RT) reaction. DNase treated RNA was used for RT reaction. The DNA decontamination of RNA was checked by PCR for β-actin. The RNA quantification was carried out after DNase treatment and 1 μg of RNA was used for RT reaction. To the RNA taken in a fresh tube, 200 ng of random primers (Amersham Biosciences, UK) and 1 μl of 10mM dNTP mix were added and the final volume was made up to 12 μl with Rnase free water. The mixture was incubated at 65^0 C for five minutes and quickly transferred to ice for chilling. After chilling, 4μl 5x first strand buffer (Invitrogen, UK) and 1μl of 0.1M DTT were added and mixed gently and centrifuged briefly before incubating at 42^0 C for two minutes. Following this incubation, 200 U (1μl) Superscript II RNase H^- Reverse Transcriptase (Invitrogen, UK) was added and the cDNA synthesis reaction was carried out at 42°C for 50 minutes. Incubating at 70°C for 15 min inactivated the enzyme. The cDNA was stored at -20^0C until further manipulations such as PCR and Real Time PCR. The success of the RT reaction was checked by PCR for β- actin gene. One tenth of the reverse transcribed sample was used in a PCR reaction. Once the success of RT reaction was confirmed by PCR for β- actin gene, PCR for the arginase – 1 gene was carried out. The newly synthesised cDNA was used for down stream analysis by RT-PCR and Quantitative –RT-PCR (Q-RTPCR).

2.8.4. POLYMERASE CHAIN REACTION (PCR)

PCR was typically performed in a volume of 50μl containing a final concentration of 100μM 2'-deoxyadenosine-5'-triphosphate (dATP), 2'-deoxyguanosine-5'-triphosphate (dGTP), 2'-deoxycytidine-5'-triphosphate (dCTP), 2'-deoxythymidine-5'-triphosphate (dTTP) (Ultrapure dNTP set, Amersham Biosceinces, UK), reaction buffer (20mM Tris [pH 8.4], 50mM KCl, Invitrogen, UK), 3 mM $MgCl_2$ (Invitrogen, UK), 50pmol of each primer (MWG Biotech,

Germany), 100 – 500 ng of template DNA and 5U of *Taq* DNA polymerase (Invitrogen, UK). All PCR primers were purchased from MWG – biotech and are shown in table no.2.2. PCR was carried out in thin-walled 0.5ml eppendorf tubes (ThermoHybaid) on an Omnigene thermal cycler (ThermoHybaid). The reactions without *Taq* DNA polymerase were overlaid with mineral oil (Sigma, UK). The reactions were heated to 94°C for 5mins, then held at 80^0 C and *Taq* DNA polymerase was added ("hot-start"), thus limiting non-specific amplification. The block was programmed to repeat 35 cycles of 45s denaturation at 94°C, annealing at 55^0C for 45 sec, 30s extension at 72°C and ending with 5mins at 72°C. PCR products were analysed by agarose gel electrophoresis.

2.8.5. PURIFICATION OF PCR PRODUCTS

Amplified DNA was purified using the QIA quick PCR purification kit (Qiagen) according to the manufacturer's instructions. PCR products were pooled and mixed with five volumes of buffer PB supplied in the kit. The mixture was applied to the QIAquick spin column and centrifuged for one minute at 13000 rpm. The follow through was discarded and 750 µl of buffer PE applied to the spin column assembly. The column assembly was centrifuged for one minute; the follow through was discarded and centrifuged again at 13000 rpm for one minute. The column was placed in a new sterile 1.5 ml eppendorf tube. The purified DNA from the column was eluted with 50µl of buffer EB and stored at $^-20^0$ C until further required.

2.8.6. QUANTITATIVE–RT PCR (Q- RTPCR)

Q-RTPCR was carried out on the cDNA synthesised as per the procedure described above (section 2.8.3.). SYBR Green I dye (Biogene) chemistry method was used for Q-RTPCR. The fluorescence intensity of SYBR Green I dye (Excitation max. 497 nm and emission max. 520 nm) increases 1000 – fold in the presence of dsDNA and does not interfere with DNA amplification during PCR. This characteristic allows the detection of PCR products in real time when the dye is added into the PCR reaction. A Rotor-Gene real time PCR machine (Corbett Research) was used for the analysis.

2.8.6.1. NORMALISATION OF GENE EXPRESSION

β-actin gene was used as the endogenous control to normalise the expression level of the target gene. The transcription of the β-actin gene and target gene from the cDNA samples was assessed by PCR and agarose gel electrophoresis as described above. Two sets of primers were designed by Dr.B.M. Dutia and they were called as 'outer' and 'inner' (Table No. 2.2) primers. The amplicons generated by PCR with the 'outer' set of primers on cDNA obtained from pooled samples was purified and used as the template for PCR with 'inner' set of primers to generate a standard curve. The gene copy number in the sample was estimated in relation to the assigned value of gene copy numbers in the standard. Standard curves were prepared for both target and endogenous control. For each experimental sample, the amount of target and endogenous control was determined from the appropriate standard curve. Then, the target amount was divided by the endogenous control amount to obtain a normalised target value. The normalised amount of target is a unitless number that can be used to compare the relative amount of target in different samples

2.8.6.2. PROTOCOL FOR Q-RTPCR

The 'inner' PCR primers were used for the Q-RTPCR. The target and endogenous control gene amplifications were carried out in separate tubes. The purified PCR product obtained from PCR with 'outer' primers for both endogenous control and target gene were diluted tenfold in duplicate and used to generate standard curve. The experimental samples also assayed concurrently in duplicate and the relative concentration of endogenous control and target gene was determined for each experimental sample. The Q-RTPCR was conducted in 20μl volume and consisted of 10x fast start taq polymerase buffer (Roche Molecular Biochemicals) (2μl), 10mM of each dNTPs (0.4μl), 50pM of primers (0.5μl) each, fast start taq polymerase (0.15μl), SYBR green dye I (0.7μl). The volume was made up to 15μl with Rnase free water and 5μl of diluted template cDNA was added. Two micro litres of cDNA samples were diluted to 10 μl and 5μl each was added in duplicate reactions (cDNA was prepared from 1μg of RNA as described in section 2.9.3. and the final volume of cDNA reaction was 19μl).

Table No. 2.2. Primer pair used in the experiments

Sense (S) Antisense (A)	Primer Pair	Region of the gene
β-Actin S β-Actin A (PCR & RT-PCR)	5' – TGT GAT GGT GGG AAT GGG TCA – 3' 5' – TTT GAT GTC ACG CAC GAT TTC – 3' (Amplicon size: 513 bp)	Nt. 206 – 226 Nt. 719 – 699 (Accession No. NM.007393.1)
β-Actin – (1) S β-Actin –(1) A ('inner')	5'- CGT TGA CAT CCG TAA AGA CC – 3' 5' -CTG GAA GGT GGA CAG TGA – 3' (Amplicon size : 201 bp)	Nt 938 - 957 Nt 1139 –1122 (Accession No. NM.007393.1)
β-Actin –(2) S β-Actin –(2) A ('outer')	5'- GTG GCA TCC ATG AAA CTA CA-3' 5'- GTA CTC CTG CTT GCT GAT CC –3' (Amplicon size : 251 bp)	Nt 895 – 914 Nt 1166- 1147 (Accession No. NM.007393.1)
Arginase –I (I) S Arginase –I (I) A ('inner')	5'- CAG AAG AAT GGA AGA GTC AG –3' 5'- CAG ATA TGC AGG GAG TCA CC – 3' (Amplicon size : 249 bp)	Nt 341 – 360 Nt 590 - 571 (Accession No. NM.007482)
Arginase –I (2) S Arginase –I (2) A ('outer')	5'- GAG TAT GAC GTG AGA GAC CAC -3' 5'- GAA GGT CTC TTC CAT CAC CTT – 3' (Amplicon size : 518 bp)	Nt 209 – 229 Nt 727 – 705 (Accession No. NM.007482)
IFNγR – S IFNγR – A	5'-GAG TGT AAT GAG AGT CTG TG –3' 5'- CTG TCA TCA TGG AAA GGA GGG – 3' (Amplicon size: 148 bp)	Nt 705 – 724 Nt 853 – 833 (Accession No. NM: 010511.1

The amplification cycle was as follows: a melting step of 95^0C for 10 minutes was followed by 45 cycles of 94^0C for 30 seconds, 62^0C for 20 seconds and 72^0C for 20 seconds, followed by a melting analysis step from 65 to 94^0 C at 0.3^0c/20 seconds at first step and 0.3^0c / every second for each step afterwards. The amplification cycle for target gene (Arginase –I) was as follows; a melting step of

95^0 C for 10 minutes was followed by 45 cycles of 94^0 C for 20 seconds, 60^0 C for 20 seconds and 72^0 C for 20 seconds, followed by a melting analysis step from 65 to 99^0 C at 0.5^0 C / second.

2.8.7. EXTRACTION OF DNA FROM BLOOD

Blood was collected from two mice (one IFNγR$^{-/-}$ and one wild type) to extract DNA to use as positive control for PCR to check the DNA contamination of RNA samples extracted from spleen of mice. Blood was also collected from the bone marrow chimera mice made as described in section 2.9.1. to confirm the success of chimera formation. QIAamp DNA Blood Mini kit (Qiagen, UK) was used to extract DNA from blood. 20 µl of proteinase – K (20µg/ml) (Sigma, UK) was taken in a 1.5 ml eppendorf tube and 200 µl of blood sample was added to the enzyme and ensured that the enzyme mixed well with blood. 200 µl of buffer AL was added to the sample and mixed by pulse – vortexing for 15 seconds to make a homogenous solution. The sample was centrifuged briefly and incubated at 56^0 C for 10 minutes. The eppendorf tube was centrifuged briefly after incubation to collect drops of solution from the inside of the lid. 600 µl of 96% ethanol was added to the sample and mixed by pulse vortexing for 15 seconds. The mixture was carefully applied on to a spin column assembly sitting in a 2 ml collection tube and the tube containing filtrate was discarded. The spin column assembly was centrifuged at 8000 rpm for one minute. The collection tube containing the filtrate was discarded and spin column assembly was placed in a new collection tube. 500 µl of buffer AW1 was applied to the spin column assembly without wetting the rim. The spin column assembly was centrifuged at 8000 rpm for one minute. 500 µl of buffer AW2 was applied to the column and centrifuged at 13000 rpm for three minutes. The collection tube containing filtrate was discarded and the spin column assembly was placed in a sterile 1.5 ml eppendorf tube. 200 µl of buffer AE was applied to the membrane in the spin column and incubated at room temperature for five minutes. The DNA adhered to the membrane of the spin column assembly was eluted by centrifugation at 8000 rpm for one minute. The concentration of DNA was estimated as per the same procedure used for quantification of plasmid DNA as described in section 2.7.1.1.

2.9. BONE MARROW CHIMERA EXPERIMENT

In order to study the contribution of bone marrow derived cells in the pathogenesis of splenic fibrosis in IFNγR$^{-/-}$ mice infected with MHV–68, bone marrow chimera mice were generated and pathological changes were investigated in comparison with normal mice following intranasal infection with MHV–68.

2.9.1. GENERATION OF BONE MARROW CHIMERA MICE

Two sets of bone marrow chimera mice were made. The first set of chimeras was made on wild type (129 Sv/Ev) background and the second set on IFNγR$^{-/-}$ background.

To generate bone marrow chimeras in the wild type background, two sets of twelve each wild type 129 Sv/Ev female mice were selected and grouped as recipient. Another two set of nine female mice each in the IFNγR$^{-/-}$ background and wild type 129 Sv/Ev mice was also selected and designated as donor. The donor groups of mice were sacrificed by asphyxiation with $C0_2$ and the femurs collected aseptically in Roswell park memorial institute – 1640 (RPMI –1640) medium supplemented with foetal calf serum (FCS) and stored separately. The bone marrow cells from the femur were squeezed out and collected in fresh batch of RPMI–1640 with FCS. The harvested bone marrow cells from each group were pooled in 40 ml of RPMI-1640. The cells were centrifuged at 1500 rpm for five minutes and resuspended in 40ml of fresh RPMI–1640. 1 X 10^7 cells were injected in to the recipient mice via tail vein in a volume of 100 µl. The recipient mice were subjected to irradiation (920 rad for 47 minutes) before injecting with the bone marrow cells from donor mice. The wild type mice, which received bone marrow cells from IFNγR$^{-/-}$ mice were designated as 'WG' and the other group, which received wild type cells, were designated as 'WW'. To generate bone marrow chimera mice in the IFNγR$^{-/-}$ (129 Sv/Ev) background, the same procedure as above was followed with IFNγR$^{-/-}$ mice as the recipient group. The IFNγR$^{-/-}$ mice, which received bone marrow cells from IFNγR$^{-/-}$ were designated as 'GG' and the IFNγR$^{-/-}$ mice which received cells from wild type 129 Sv/Ev

as 'GG' and the IFNγR$^{-/-}$ mice which received cells from wild type 129 Sv/Ev mice were designated as 'GW'. The recipient mice were maintained on a normal diet for two months before infecting with virus.

2.9.2. INFECTION OF BONE MARROW CHIMERA MICE

The repopulation of peripheral circulation with cells originating from newly received bone marrow cells were confirmed by PCR for IFNγR gene on DNA isolated from blood. The blood was collected from the tail tip and DNA was extracted as per the procedure described in section 2.8.7. The PCR was carried out as per the procedure described in section 2.8.4. by using the primer set as described in table 2.2. After confirming the repopulation of cells in the peripheral circulation with cells originating from newly injected bone marrow cells the mice were infected with 4x 10^5 PFU of MHV –68 in 40µl volume as described in section 2.4. Along with two groups of chimera mice, another group of 12 wild type mice designated as 'WO' was also infected in the similar way as described above in the experiment involving bone marrow chimera mice in the wild type (129 Sv/Ev) background (In total three groups designated as WG, WW and WO). In the experiment involving bone marrow chimera mice in the IFNγR$^{-/-}$ backgrounds, 12 each age matched IFNγR$^{-/-}$ mice and wild type mice were also used and they were designated as G and W respectively (In total four groups designated as GW, GG, W and G). Three mice from each group were sacrificed on day 12, 16, 20 and 35 post infections. Detailed post-mortem examination was carried out. Weight of dead mouse and spleen was estimated and the weight of spleen was expressed as percentage of body weight. The spleen was collected in BFS and processed as described in section 2.5 for histopathological evaluation.

2.10. STATISTICAL ANALYSIS

Mann – Whitney test and 2 sample t- test in the MINITAB Release 14 software was used for statistical analysis of the data.

APPENDIX 1 – CHEMICALS AND SOLUTIONS

All chemicals were obtained from Sigma (Sigma-Aldrich Company Ltd., Fancy Road, Poole, Dorset, BH12 4OH, England) or MERCK BDH (VWR international Ltd, Merck House, Poole, Dorset BH15 1TD, England). The chemicals obtained from other manufactures are specifically mentioned as and when they appear in the text.

Water:

Deionised water (Millipore) was used for making solutions and rinsing glassware used for immunohistochemistry. Sterile filtered water acquired from Sigma was used for preparations of nucleic acid, PCR and RT- PCR. The solutions for *in situ* hybridisation studies were made in Diethyl-pyrocarbonate (DEPC) treated deionised water. The deionised water was treated with DEPC at a level of 0.1% (v/v) and incubated at 37^0 C overnight and autoclaved before use.

TE buffer:

10mM Tris - HCl, 1mM EDTA [pH 8.0].

TAE buffer:

0.04M Tris - acetate, 1mM EDTA [pH 8.0].

TBS:

50mM Tris, 150mM NaCl [pH 7.6].

PBS:

137mM NaCl, 2.7mM KCl, 10 mM Na_2HPO_4, 1.0 mM KH_2PO_4 [pH 7.4]

6x loading buffer:

10% (w/v) Ficoll, 0.25% (w/v) bromophenol blue, 0.25% (w/v) xylene cyanole, 0.4% (w/v) orange G, 10 mM Tris-HCl [pH 7.5], 50 mM EDTA.

SOLUTIONS FOR HAEMATOXYLIN AND EOSIN STAINING

a. Harris's haematoxylin solution

Haematoxylin 5g, Ethyl alcohol 50ml, Potassium alum 100g,

Deionised water 950 ml, Mercuric oxide 2.5g, Glacial acetic acid 40ml.

b. Eosin solution: 1% aqueous solution

c. Acid alcohol: 1% hydrochloric acid in 70% alcohol

SOLUTIONS FOR MASSON'S TRICHROME (MT) STAINING

a. Weigert's Iron Haematoxylin solution

Stock solution A:

Haematoxylin 1g in Alcohol 100ml (95%).

Stock solution B:

30% ferric chloride in water 4ml, Deionised water 95ml, Con. HCl 1ml.

Working solution:

Mix equal parts of solution A and B

b. Acid fuchsin 0.5g, Glacial acetic acid 0.5ml and deionised water 100 ml

c. Phoshomolybdic acid 1.0g and deionised water 100ml

d. Light green 2.0g, Glacial acetic acid 2.0ml and deionised water100ml

(Diluted 1:10 with deionised water prior to use)

SOLUTIONS FOR MARTIUS YELLOW-BRILLIANT CRYSTAL SCARLET-SOLUBLE BLUE (MSB) STAINING

a. 0.5% Martius Yellow in 2% phosphotungstic acid in 95% alcohol

b. 1% brilliant crystal scarlet 6R in 2.6% acetic acid

c. 1% aqueous phosphotungstic acid

d. 0.5% aniline blue in 1% acetic acid

SOLUTIONS FOR PICRO SIRIUS RED STAINING

a. 1% Sirius red F3B (Raymond A Lamb Ltd.) in saturated aqueous picric acid

b. 0.2% Aqueous phosphomolybdic acid

SOLUTIONS FOR VON KOSSA STAINING

a. 2% aqueous silver nitrate

b. 1% aqueous neutral red

SOLUTIONS FOR PERLS STAINING

a. 2% aqueous potassium Ferrocyanide

b. 2% hydrochloric acid

c. 1% aqueous neutral red

SOLUTIONS FOR *IN SITU* HYBRIDISATION

10x DIG RNA labelling Mix [pH: 7.5]:

10mM ATP, 10mM CTP, 10mM GTP, 6.5mM UTP, 3.5mM DIG UTP

10x Transcription buffer: [pH: 8.0]

400mM Tris-HCl, 60mM $MgCl_2$, 100mM DTT, 20mM Spermidine

Carbonate Buffer [pH10.2]:

0.4M $NaHCO_3$, 0.6M Na_2CO_3

Hydrolysis Neutralisation Buffer [pH: 4.6]

3M Sodium Acetate [pH adjusted to 4.6 with glacial acetic acid]

Maleic Acid Buffer [pH: 7.5]:

0.1 M Maleic acid, 0.15 M NaCl

Buffer No.1: [pH 7.5]

0.1M Tris, 0.15 M NaCl

Buffer No.2 (Blocking solution)

0.1% (v/v) Normal Sheep Serum in Buffer No.1.

Buffer No.3: [pH 9.5]

0.1M Tris, 0.1M NaCl, 0.05M $MgCl_2$

Washing Buffer

0.5% (v/v) Tween-20 in Buffer No.1.

20x SSC [pH 7.0]:

3 M NaCl, 0.3 M sodium citrate

20x Salts [pH6.8)

0.1M EDTA, 0.1M Piperazine N, N' – bis (2-ethane sulfonic acid) (PIPES), 3M NaCl

50x Denhardt's solution:

1% (w/v) Ficoll, 1% (w/v) polyvinylpyrrolidone, 1% (w/v) Bovine Serum Albumin (BSA)

Pre hybridisation Solution:

50% (v/v) Formamide, 25% (v/v) 20x Salt solution, 10% (v/v) 50x Denhardt's solution, 2.5% (v/v) Salmon Sperm DNA (11mg/ml), 2.5% (v/v) Yeast tRNA (10mg/ml), 1.0% (v/v) Heparin (2000U/ml), 1.0% (v/v) Sodium Dodecyl sulphate (SDS) – 10% (w/v)

Hybridisation Solution:

50% (v/v) Formamide, 25% (v/v) 20x Salt solution, 10% (v/v) 50x Denhardt's solution, 2.5% (v/v) Salmon Sperm DNA (11mg/ml), 2.5% (v/v) Yeast tRNA (10mg/ml), 1.0% (v/v) Heparin (2000U/ml), 1.0% (v/v) Sodium Dodecyl sulphate (SDS) – 10% (w/v), 10% (v/v) Dextran sulphate (0.5g/ml)

Buffer for Anti-Digoxigenin – AP, Fab fragments: [pH 7.6]

50 mM Triethanolamine, 03 mM NaCl, 01 mM $MgCl_2$, 0.1 mM $ZnCl_2$, 1% BSA (w/v)

Sigma Fast Alkaline Phosphatase Substrate Solution: [pH 9.5]

5-Bromo-4-Choloro-3-Indolyl phosphate (BCIP): 0.15mg/ml,
Nitro Blue Tetrasolium (NBT): 0.30mg/ml, Tris: 10mM, $MgCl_2$: 05mM

APPENDIX 2 - COMMERCIAL SUPPLIERS

Ambion Inc, Ambion (Europe) Ltd, Ermine Business Park, Spitfire Close, Huntingdon, Cambridgeshire PE29 6XY
www.ambion.com

Amersham Biosciences UK Ltd, Amersham Place, Little Chalfont, Buckinghamshire HP7 9NA HP7 9NA
www.amershambiosciences.com

Bantin and Kingman Universal Ltd. Grimston, Aldbrough, Hull HU11 4QE
www.bku.com

Biogene
www.biogene.co.uk

Bio-Rad Laboratories Ltd, Bio-Rad House, Maylands Avenue, Hemel Hempstead, Hertfordshire HP2 7TD
www.bio-rad.com

Biologo, Br. Hartmut Schultheiss e.K. Steindamm 1G-H, 24119 Kronshagen, Germany
www.biologo.de

BMA Biomedicals AG, Rheinstrasse 28-32, 4302 Augst, Switzerland
Email: info@bma.ch

Cecil Instruments Ltd, Milton Technical Centre, Cambridge CB4 6AZ
www.cecilinstruments.com

DakoCytomaton Ltd, Denmark House, Angel Drove, Ely, Cambridgeshire CB7 4ET
www.dakocytomation.com

Flowgen, Findel House, Excelsior Road, Ashby Park, Ashby de la Zouch, Leicestershire LE65 1NG
www.flowgen.co.uk

Invitrogen Ltd, 3 Fountain Dr, Inchinnan Business Park, Paisley PA4 9RF
www.invitrogen.com

Merial Animal Health Ltd, Sandringham House, Harlow Business Park, Harlow, Essex, CM19 5TG http://uk.merial.com

Millipore, 80 Ashby Road, Bedford, Massachusetts, USA
www.millipore.com

MWG Biotech (UK) Ltd, Mill Court, Featherstone Road, Wolverton Mill South, Milton Keynes MK12 5RD
www.mwg-biotech.com

Nalgenunc International, 75 Panorama Creek Drive, Rochester, NY 14625
www.nalgenunc.com

New England Biolabs (UK) Ltd, 73 Knowl Piece, Wilbury Way, Hitchin, Hertfordshire, SG4 OTY
www.neb.com

Novocastra Laboratories Ltd. Balliol Business Park, WestBenton Lane, Newcastle upon TyneNE12 8EW
www.novocastra.co.uk

Pharmingen – BD biosciences Pharmingen, 21 In Between Towns Road, Cowley, Oxford OX4 3LY
www.bdbiosciences.com/pharmingen/

QIAGEN Ltd, Boundary Court, Gatwick Rd, Crawley, West Sussex RH10 9AX
www.QIAGEN.com

Promega UK Ltd, Delta House, Chilworth Research Centre, Southampton SO16 7NS
www.promega.com

Raymond A Lamb Limited. Units 4 5 Parkview, Industrial Estate, Alder Close, Lottbridge Drove, Eastbourne, East Sussex, BN23 6QE.
www.ralamb.co.uk

Roche Molecular Biochemicals, Bell lane, Lewes, East Sussex, BN7 1LG
www.roche.com

Serotec Ltd., 22 Bankside, Station approach, Kidlington, Oxford, OX5 1JE, UK
www.Serotec.co.uk

Sigma-Aldrich Company Ltd, The old Brickyad, New Road, Gillingham, Dorset, England
www.sigma-aldrich.com

Surgipath Europe Ltd., Ventrue park, Stirling Way, Bretton, Peterborough, PE3 8YD, UK.

www.sugipath.com

ThermoHybaid, Action Court, Ashford Road, Ashford, Middlesex, TW15 1XB
www.thermohybaid.com

UVP Ultra Violet Products Ltd, Unit 1, Trinity Hall Farm Estate, Nuffield Road, Cambridge CB4 1TG
www.uvp.com

Vector Laboratories Inc, 30 Ingold Road, Burlingame, CA94010, USA.
www.vectorlabs.com

VWR international Ltd, Merck House, Poole, Dorset BH15 1TD
www.vwr.ltd.uk

CHAPTER THREE: CHARACTERISATION OF SPLENIC FIBROSIS

3. CHARACTERISATION OF SPLENIC FIBROSIS

The spleen is the major organ which shows distinct pathological changes in IFNγR$^{-/-}$ mice infected with MHV–68. The main features of splenic pathology are development and resolution of fibrosis (Dutia et al, 1997, Ebrahimi et al 2001). Characterisation of the virological, cellular and molecular events associated with these pathological processes was the main objective of this study.

The study was structured under the following sub-headings:

3.1. Survey of pathological changes in the spleen

3.2. Characterisation of cellular events

3.3. Alternate activation of macrophages

3.4. Bone marrow chimera experiments

3.5. Role of productive and latent virus infection in the pathogenesis of splenic fibrosis

Each sub-chapter detailing the study under each sub-heading is presented with an introduction, followed by description of the results and a brief summary. Finally, a comprehensive discussion of results is presented with suggestions for future work.

3.1. SURVEY OF PATHOLOGICAL CHANGES IN THE SPLEEN

The sequential pathological changes during the development and resolution of fibrosis in the spleen of IFNγR$^{-/-}$ mice infected with MHV–68 are not known. In this study, a detailed pathological survey was undertaken to delineate these events. As described in the Materials and Methods (section 2.4), three different experiments were carried out with close time intervals between day 8 and 120 and gross and histopathological observations were made.

Fibrosis is a host response to injury of a chronic nature characterised by deposition of extra cellular matrix (ECM). The ECM consists of proteoglycans (e.g. decorin and fibromodulin), adhesion molecules (e.g. fibronectin and laminin) and different types of fibrous proteins (e.g. collagen, elastin and fibrillin). Collagens are the major fibrous protein in the ECM. To date 19 different types of collagens have been described (Ghosh, 2002). Type I collagen, which is a product of two genes (COL1A1 and COL1A2) is the main type of collagen found in many tissues like skin, bone and ligaments. A diverse group of cells (fibroblasts and myofibroblasts) is responsible for the production of ECM proteins including collagen. The cell type responsible for the synthesis of ECM in splenic fibrosis caused by MHV-68 has not been investigated before. The current study investigated whether myofibroblast - type cells characterised by the expression of α smooth muscle actin (αSMA) are involved in the pathogenesis of splenic fibrosis. The expression of αSMA was investigated by immunohistochemical techniques as described in the Materials and Methods section 2.6.

3.1.1. GROSS PATHOLOGY

Splenomegaly was observed as the initial response of the spleen towards virus infection in both IFNγR$^{-/-}$ and 129 Sv/Ev mice. The size and colour of the spleen showed distinct changes during the course of infection, especially in the IFNγR$^{-/-}$ mice (Figure.3.1.1). In IFNγR$^{-/-}$ mice, at the time of splenomegaly during day 10 - 12 p.i., the spleen appeared dark red or brownish black in colour with a glistening smooth surface. During day 14 -18 p.i., the colour changed to yellowish brown,

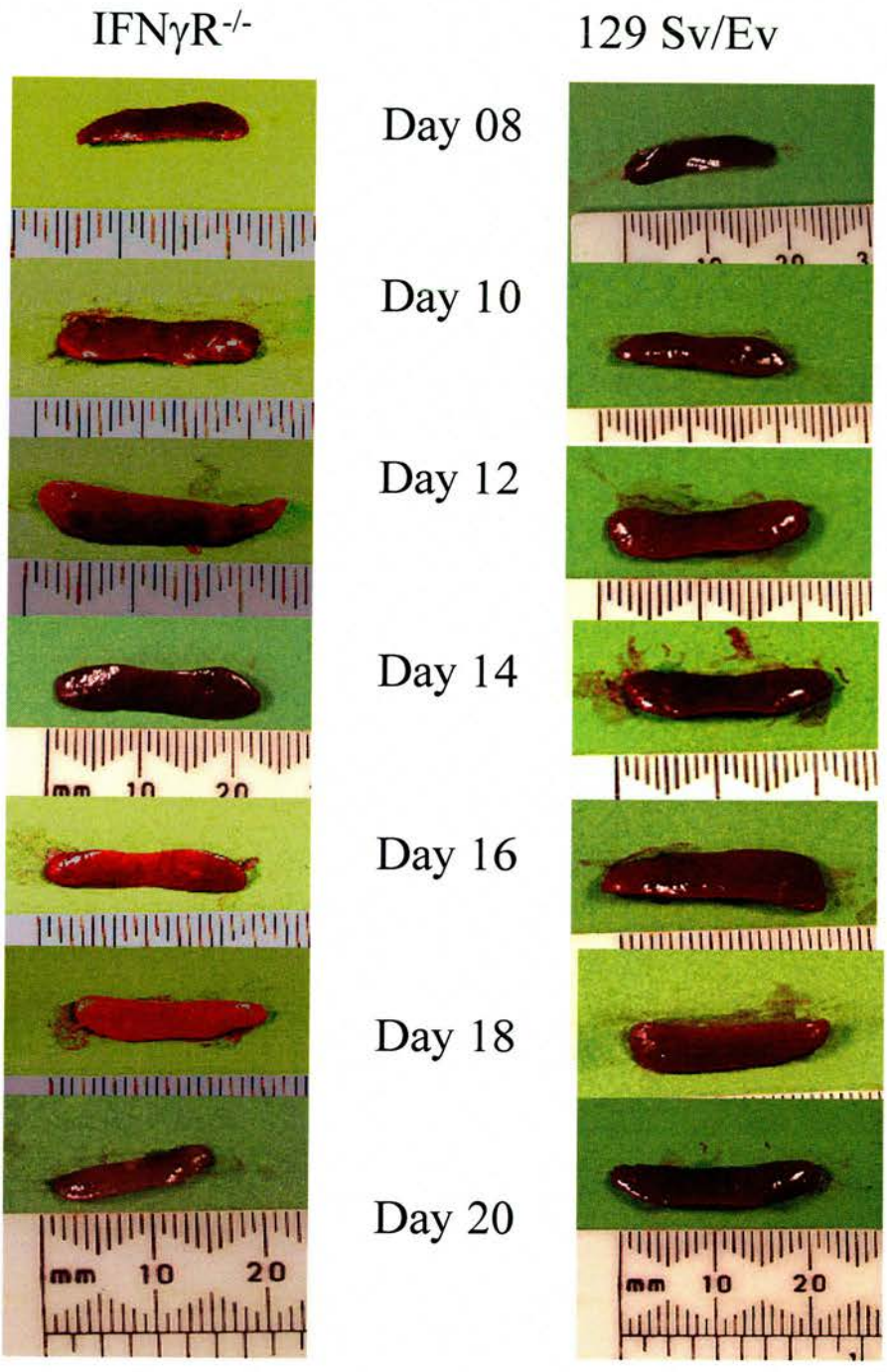

Figure 3.1.1 Gross pathological changes in the spleen of mice infected with MHV-68. A representative image of spleen at each time point is presented. Note the difference in size and colour of spleen from IFNγR$^{-/-}$ and 129 Sv/Ev mice at later time points.

though the spleen appeared enlarged with a smooth glistening capsule. At day 20 p.i. the spleen was shrunken and pale in colour. At day 30 p.i. the colour changed towards reddish brown, although the size of the spleen appeared small. The colour and appearance of the spleen remained the same during the rest of the time points up to day 120 p.i. The spleen of 129 Sv/Ev group of mice appeared dark red or brownish black in colour and enlarged with glistening smooth capsule during the phase of splenomegaly (Day 14- 18 p.i.). Thereafter the spleen regained its normal size and remained in that state until day 120 p.i.

The weight of spleen expressed as a percentage of body weight from two different experiments is presented in Figure. 3.1.2. The spleen showed a progressive increase in weight during the initial time points of the experiment. The weight of the spleen peaked at day 12 p.i. in IFNγR$^{-/-}$ mice and then showed a steep decline. The difference in the weight of the spleen expressed as percentage of body weight at this time point was statistically significant (p value = 0.0131). In 129 Sv/Ev mice, the peak of splenomegaly was observed at day 16 p.i. and then showed a gradual decline. The contrast in the weight of the spleen was marked at day 20 p.i. between two groups with a drastic drop in the weight of the spleens from IFNγR$^{-/-}$ mice compared to 129 Sv/Ev mice. The difference in the weight of the spleen expressed as percentage of body weight at day 20 p.i was statistically significant (p value = 0.0367). The weight of the spleen remained at apparently the same levels in both groups of mice from day 30 up to day 120 p.i. However, the difference in splenic weight expressed as percentage of body weight is not statistically significant at day 30 p.i. (p value = 0.0518) whereas, statistically significant at day 120 p.i. (p value = 0.02). Data for day 12 and day 20 p.i. from experiment No.1 and 2 was pooled for statistical analysis.

In the third experiment conducted to assess the effect of mock infection in IFNγR$^{-/-}$mice, the spleens of mock infected mice did not show any obvious pathological change. Whereas, the MHV-68 infected IFNγR$^{-/-}$ mice showed a similar pattern of pathological changes as observed in experiment no.1 and 2.

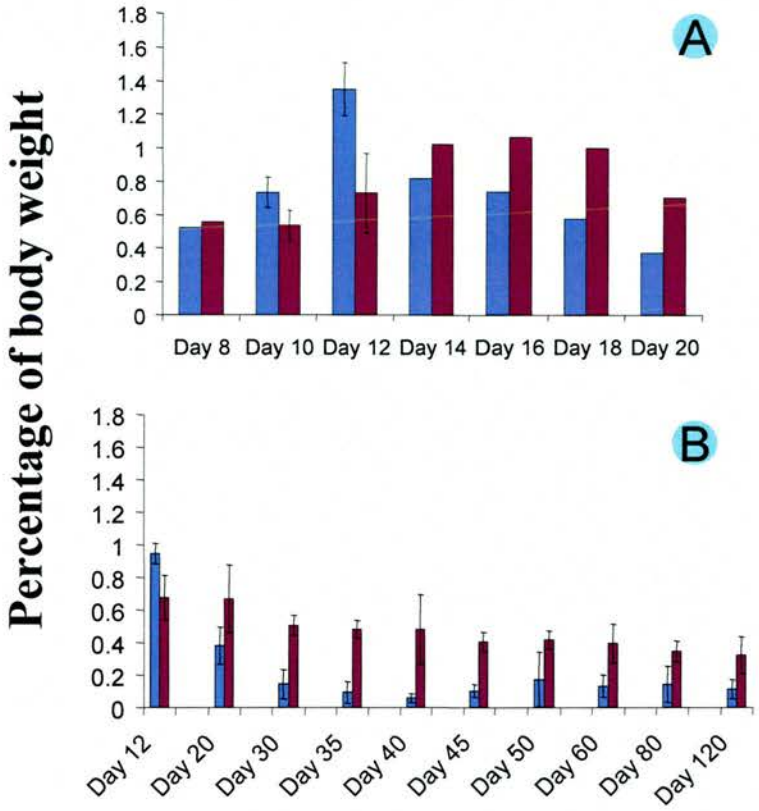

Figure. 3.1.2. Weight of spleen expressed as percentage of body weight :

Experiment 1 (A) (n= 2 each at day 8, 3 each at day 10, 3 each at day 12, 2 each at day 14, 16,18 and 20) Experiment 2 (B) (n= 3 each at day 12 and 20, 4 IFNγR -/- and 3 129 Sv/Ev at day 30, 5 IFNγR -/- and 3 129 Sv/Ev at day 35, 4 IFNγR -/- and 3 129 Sv/Ev at day 40, 3 each at day 45, 50, 60 and 80, 5 IFNγR -/- and 4 129 Sv/Ev at day 120) Each bar represent Mean± Standard Deviation

IFNγR -/- mice infected with MHV-68

129 SV/Ev mice infected with MHV-68

3.1.2. HISTOPATHOLOGY

Histologically, the spleen showed no signs of infection at day 08 p.i in both groups of mice (Figure. 3.1.3A and 3.1.3F). By day 10 p.i. both groups of mice showed germinal centre (GC) formation in the white pulp. GCs develop in response to an antigenic challenge characterised by proliferation of B-lymphocytes. Hyperplasia of the white pulp was characterised by an increase in the number of mitotic figures and tingible body macrophages (TBM) loaded with apoptotic bodies. Transformation of B-lymphocytes towards plasma cells was also evident. The red pulp was congested. In IFNγR$^{-/-}$ mice, by day 12 p.i, there was an expansion of the white pulp with GC and active TBM. TBM were large with many apoptotic bodies. Focal expansion of small lymphocytes was visible in the red pulp area. These changes were moderate in 129 Sv/Ev mice compared to IFNγR$^{-/-}$ mice (Figure. 3.1.3B and 3.1.3G). The appearance of micro-abscesses with a focal collection of neutrophils in the splenic parenchyma was another notable finding at this time point in IFNγR$^{-/-}$ mice. In IFNγR$^{-/-}$ mice, by day 14 p.i., depletion of mature lymphocytes in the white pulp, which were occupied by a heterogeneous mixture of larger mononuclear cells, was noticed. The infiltrating cells showed the morphological features of macrophages. They appeared to be round with slightly irregular cell outlines and slightly acidophilic cytoplasm. In IFNγR$^{-/-}$ mice at day 16 p.i. a mild degree of fibroblast proliferation and collagen deposition was noticed around the white pulp (Figure.3.1.3C). The peak level of fibrosis along with collapsed red pulp and shrunken lymphoid follicles was noticed at day 20 p.i. (Figure. 3.1.3D).

From day 30 p.i. onwards the spleens from IFNγR$^{-/-}$ mice showed signs of recovery with appearance of red blood cells in the red pulp and more dark blue stained small lymphocytes in the lymphoid follicles. The recovery state was more evident at day 35 p.i. The expanding lymphoid follicles pushed the fibrous tissue towards the periphery (Figure 3.1.3E). From day 35 p.i. onwards, the red pulp also carried brown coloured hemosiderin pigments in between the fibrous tissue strands. Some of the macrophages also were laden with hemosiderin pigments

Figure.3.1.3. Histopathological changes in the spleen of MHV -68 infected mice.

Haematoxylin and Eosin staining.

Note the tightly packed small lymphocytes in the lymphoid follicles in both spleens at day 8 p.i. (A and F). At day 12 p.i. the GC formation in the lymphoid follicles of both groups of mice is evident. A number of TBM (arrows) with apoptotic bodies is evident in the IFNγR$^{-/-}$ mice (B). At day 16 p.i. in the IFNγR$^{-/-}$ spleen, the majority of the cells in the lymphoid follicles are lightly stained large cells with increased cytoplasm (macrophage like) compared to normal GC structure in 129 Sv/Ev spleens. Also note the presence of a few spindle shaped cells in the periphery of lymphoid follicles of IFNγR-/- spleen (Highlighted in a rectangle with arrow in C. Magnified version of the area highlighted is presented in the inset). At day 20 p.i. the shrunken lymphoid follicles contain few lymphocytes and TBM in the IFNγR$^{-/-}$ and these are encircled by spindle shaped cells and extra cellular matrix – 'fibrotic cage' formation (D). The dramatic re-appearance of mature lymphocytes in the lymphoid follicles of IFNγR-/- spleen is noticed at day 35 p.i. (E)

GC, Germinal centre. LF, lymphoid follicles. R, Red pulp.

Magnification 200X

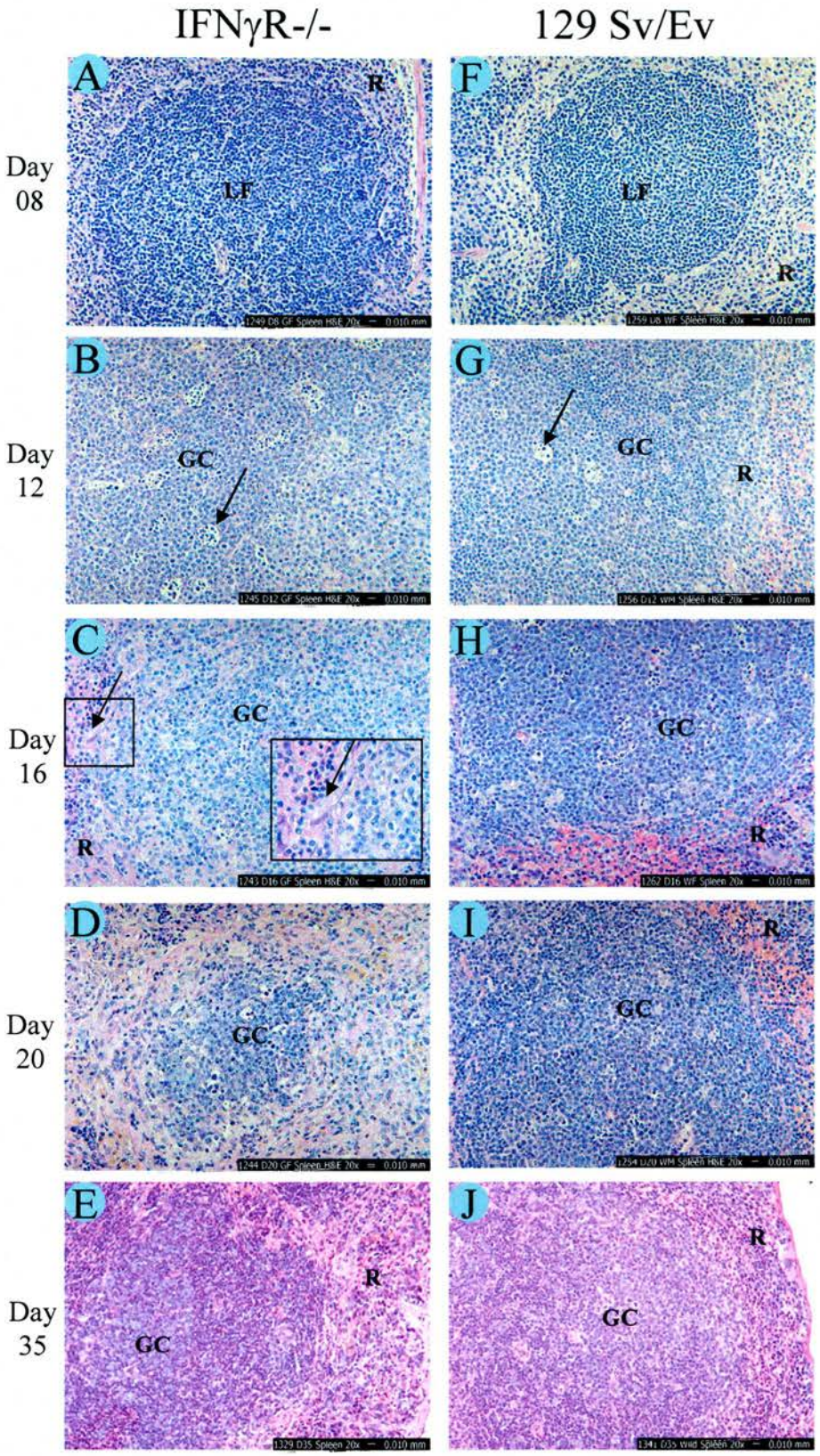

Figure. 3.1.3. Please see the legend on the facing page

(Figure. 3.1.4). By day 45 p.i. the long stretches of fibrous bands appeared broken and smaller bands of fibrous tissue was noticed.

In 129 Sv/Ev mice, from day 10 p.i. onwards, the spleen remained active with GC and TBMs and by day 16 p.i. showed peak levels of antigen responsiveness with features similar to the spleens of IFNγR$^{-/-}$ mice at day 12 p.i. From day 18 p.i. onwards, the spleens of the 129 Sv/Ev mice showed features of resolution with a reduction in the size of lymphoid follicles in the white pulp, decreased cellularity and reduced number of TBMs. The spleen, at later time points until day 120 p.i., did not show any significant changes from the descriptions given above.

No significant pathological changes were observed in the spleen of mock infected IFNγR$^{-/-}$ mice from the third experiment. Whereas, the spleens of MHV-68 infected IFNγR$^{-/-}$ mice showed a similar pattern of pathological changes as observed in experiment no.1 and 2

3.1.3 IDENTIFICATION OF MYOFIBROBLAST–TYPE CELLS IN THE SPLEEN OF IFNγR$^{-/-}$ MICE INFECTED WITH MHV-68

The distribution of collagen in the spleen was initially investigated by various histochemical techniques including Masson's trichrome (MT), Martius yellow – brilliant crystal scarlet – soluble Blue (MSB) and picrosirius red (PSR). The histochemical staining of spleen sections showed the accumulation of collagen and their secreting cells predominantly around the shrinking white pulp lymphoid follicles ('fibrotic cage') and in the capsular area. Strands of collagen were also noticed in the red pulp parenchyma (Figure 3.1.5). Among the cell population, which showed positive staining, the majority of them were spindle shaped with a central elongated nucleus. The positive cells also included round to stellate shaped cells with central round nucleus. The staining for αSMA showed mainly stellate shaped cells with positive staining reaction among the fibrous tissue around the shrunken white pulp lymphoid follicles (Figure 3.1.6).

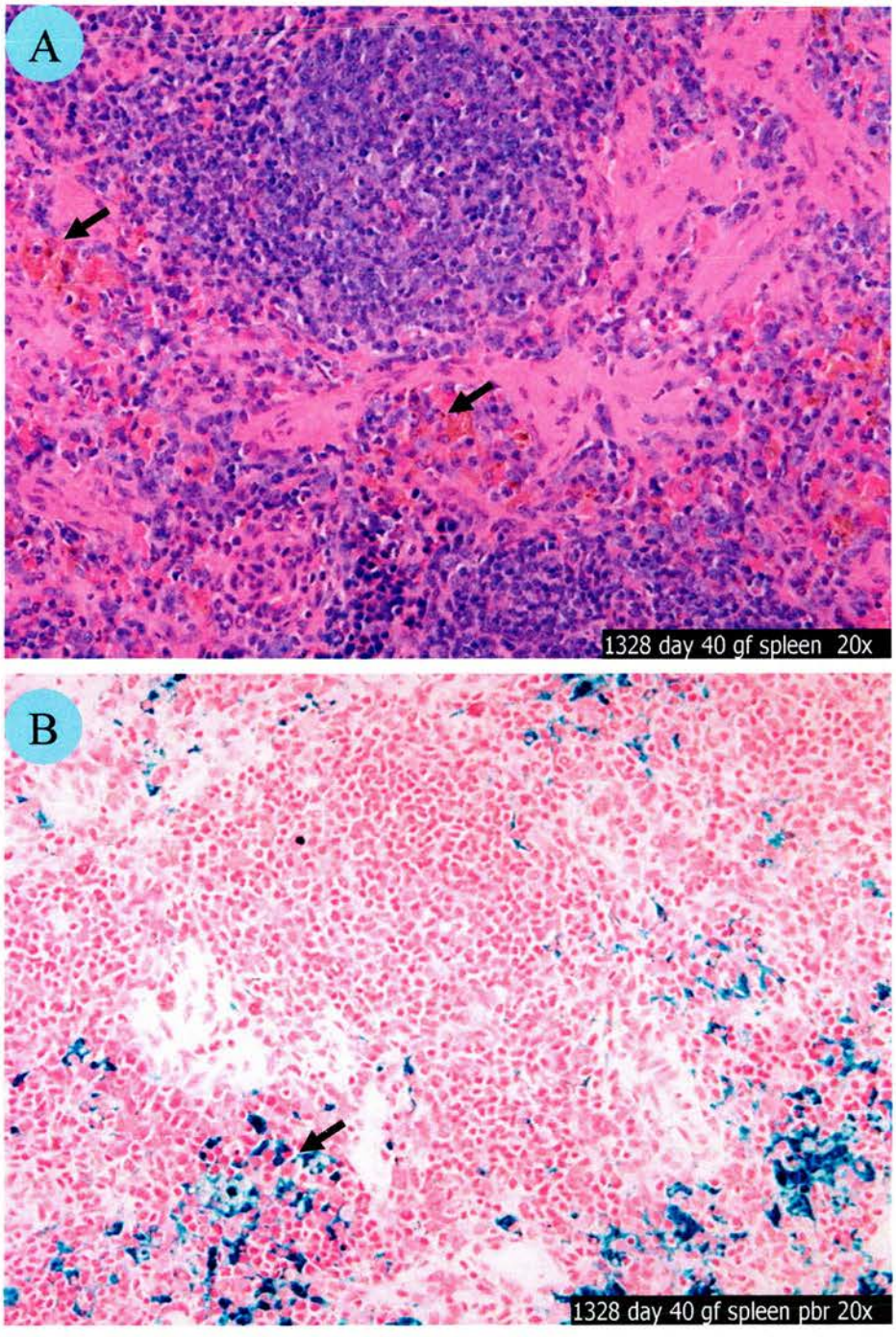

Figure.3.1.4. Hemosiderosis in the spleen of IFNγR-/- mice at day 40 p.i.

A, Haematoxylin & Eosin staining : Note the presence of brown pigments in the red pulp (arrows). B, Perl's staining : Note the presence of blue pigments in the red pulp (Arrow).

Magnification 200X.

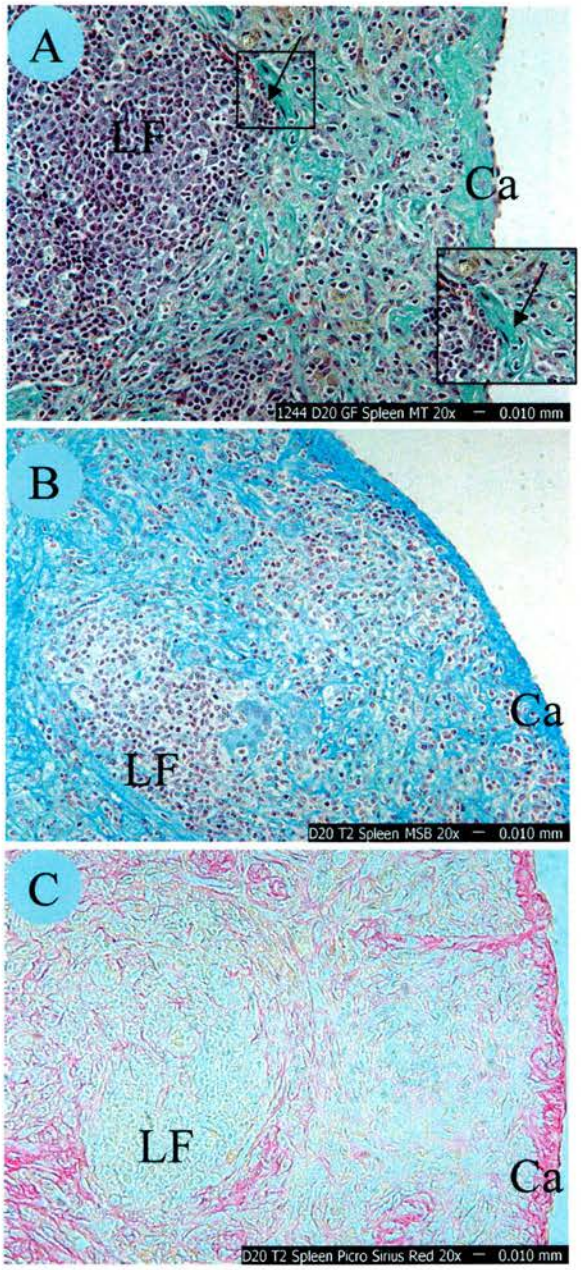

Figure. 3.1.5. Characterisation of fibrosis in the spleen by histochemical techniques.

Formalin fixed paraffin embedded tissue sections of spleen from IFNγR-/- mice infected with MHV-68 and harvested at day 20 p.i. were stained with Masson's trichrome (light green counter stain) (A), Martius yellow – Brilliant crystal scarlet – soluble blue (Blue colour for collagen) (B) and Picrosirius red (Red colour for collagen) (C). Note the predominance of collagen deposition around the shrinking white pulp lymphoid follicles and capsular locations. An area is highlighted in a rectangle to demonstrate spindle shaped cells. The highlighted area is magnified and presented in the inset. LF, lymphoid follicle. Ca, Capsule.

Magnification 200X

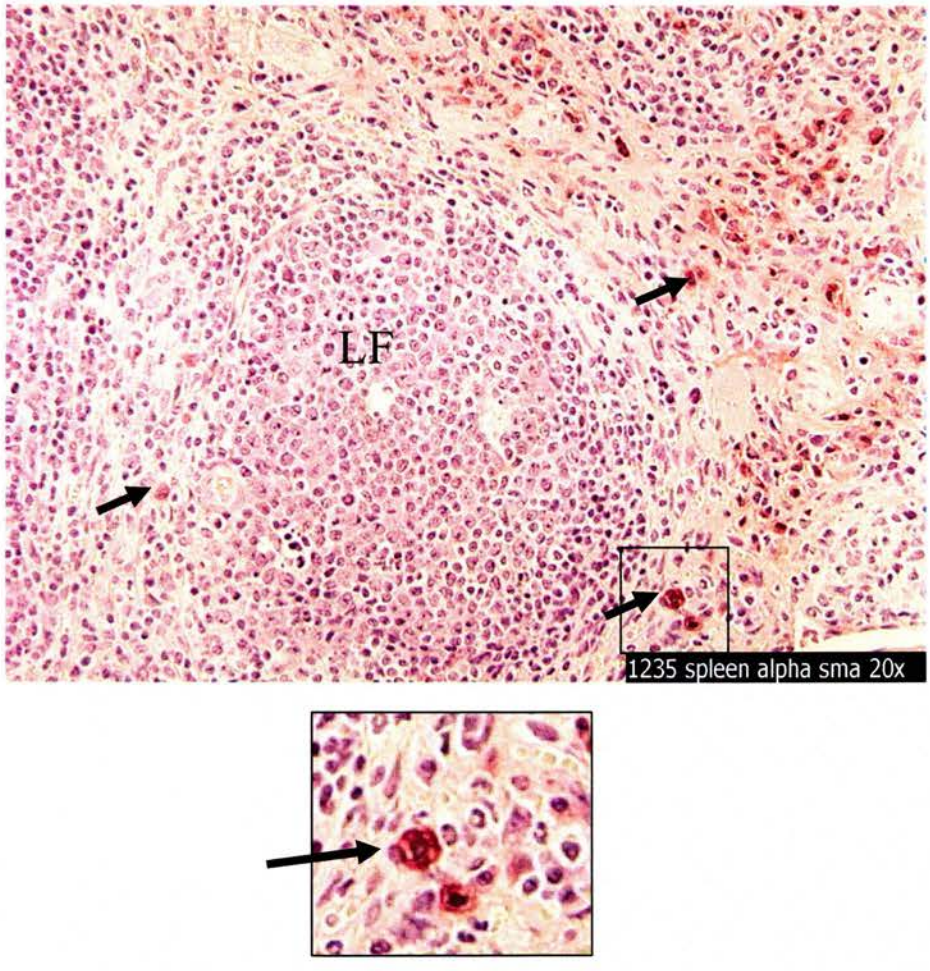

Figure. 3.1.6. Identification of myofibroblast-type cells in the spleen of IFNγR-/- mice infected with MHV-68 and harvested at day 20 p.i.

Alpha smooth muscle actin staining . Red colour indicate positive staining (arrows). LF, lymphoid follicle. A magnified view of the cells in highlighted rectangle is presented below the original image

Magnification 200X

3.1.4. SUMMARY

The survey of pathological changes in the spleen identified key time points, which are relevant to the development and resolution of fibrotic changes in the spleen. Interestingly, the spleen did not show any obvious sign of antigen responsiveness in the form of a GC reaction at day 8 p.i. in either group of mice. The induction period required for development of the GC in lymphoid organs after exposure to an antigen is around three days (Heinen, 2002). Earlier studies on detecting latent viral load in the spleen following MHV–68 infection in immunocompetent mice have recovered latent virus from spleen as early as day 3 p.i.(Sunil-Chandra *et al.*, 1992a) . The current observation of lack of antigen responsiveness in the spleen at day 8 p.i. suggests that the virus may be reaching the spleen in a latent form as early as day 3. p.i. and exposure of viral antigen to the splenic immune system takes place only a few days earlier than day 10 p.i.

In IFNγR$^{-/-}$ mice, the spleens follow a different pattern of events from day 14 p.i., which is characterised by invasion of lymphoid follicles with a heterogeneous mixture of large mononuclear cells morphologically similar to macrophages. This pattern reaches its peak at day 16 p.i. and the majority of the cells in most of the lymphoid follicles at this point are occupied by macrophages. At the same time, fibroblasts also start to appear in the periphery of these lymphoid follicles. From this point onwards the spleens from IFNγR$^{-/-}$ mice showed a drastic change characterised by the collapse of the red pulp occupied by plump fibroblasts and collagen fibres. The lymphoid follicles in the white pulp shrinks and the macrophage - like cells, except for few TBM disappeared from the centre of the lymphoid follicles. Day 20 p.i. is the peak time point where the highest level of fibrotic changes were seen and appeared like a 'fibrotic cage' around the shrunken white pulp nodule mainly carrying tightly packed small lymphocytes. From day 30 p.i. onwards the spleen gradually regained its normal structure, which became clear as early as day 35 p.i. and the spleens maintain this 'recovery' state until the last time point of the experiment.

This part of the study indicated that, gradual depletion in the number of lymphocytes in the lymphoid follicles of the spleen is the primary event associated with the pathogenesis of fibrosis. The recovery phase was characterised by re-population of shrunken lymphoid follicles. The preliminary characterisation of the fibrotic changes in the spleen showed a contribution from myofibroblast-type cells characterised by αSMA expression in the pathogenesis of fibrosis. This is the first description of the αSMA positive myofibroblast type cell in the spleen which we would like to name it as splenic stellate cells (SSc) in line with hepatic stellate cells and pancreatic stellate cells.

3.2. CHARACTERISATION OF CELLULAR EVENTS

Survey of the pathological changes in the spleen at close time intervals following MHV–68 infection of IFNγR$^{-/-}$ mice compared to 129 Sv/Ev mice revealed the nature of sequential pathological changes taking place in the spleen during the development and resolution of fibrosis. To delineate these sequential histopathological changes, cellular characterisation was undertaken with reference to different cell populations in the spleen. The different cell types present in the spleen include B-lymphocytes, T-lymphocyte, follicular dendritic cells and different subsets of macrophages. B-lymphocytes are the primary cells harbouring latent MHV-68 in spleen (Sunil-Chandra *et al.*, 1992b). T-lymphocytes constitute between 5 – 25% of the cells present in the GC (Heinen, 2002) and they have an important role in the regulation of MHV–68 infections (Ehtisham *et al.*, 1993;Doherty *et al.*, 2001). Both CD4+ and CD8+ T-lymphocyte are important in the pathogenesis of splenic fibrosis caused by MHV-68 in IFNγR$^{-/-}$ mice as their depletion prior to and during the course of infection abrogates the pathogenesis (Dutia *et al.*, 1997). Macrophages play a central role in the pathogenesis of fibrosis mainly through the alternate activation pathway (Wynn, 2004). The role of macrophages in the pathogenesis of splenic fibrosis induced by MHV–68 infection of IFNγR$^{-/-}$ mice is not known. The current investigation was undertaken to assess the contribution of these different cell populations to the pathogenesis. Thus the profile and distribution pattern of B-lymphocytes, T-lymphocyte and different subsets of macrophages in the spleen during the course of infection was investigated using immunohistochemical techniques.

3.2.1. B- LYMPHOCYTES

CD45R/B220 staining was used to identify distribution patterns of B-lymphocytes during the course of infection. Sections of spleen from experiments no.1 and 2 were used in this study. As expected, B-lymphocytes were mainly seen in the lymphoid follicles and marginal zone of the spleen (Figure 3.2.1). No difference in the distribution pattern was observed between two groups of mice up to day 10 p.i. At day 12 p.i., in IFNγR$^{-/-}$ mice, in line with peak hyperplasia of the lymphoid follicles and GC formation, a relative increase in the number of B-lymphocytes

Figure.3.2.1. B-lymphocytes in the spleen of MHV-68 infected mice.

CD45R/B220 staining (See Materials and Methods).

Note the tightly packed CD45R/B220 positive B-lymphocytes (Reddish brown colour) in the lymphoid follicles in both spleens at day 8 p.i. (A and F). Expansion of B - lymphocytes with TBM (Arrows) are evident in both groups of mice at day 12 p.i. (B and G), but is more intense in IFNγR$^{-/-}$ mice. At day 16 p.i, in the IFNγR-/- spleen, the numbers of B lymphocytes are reduced in number compared to 129 Sv/Ev spleens (C and H). Note the shrunken lymphoid follicles with few B-lymphocytes in the spleen of IFNγR$^{-/-}$ mice at day 20 p.i. (D and I). The re-appearance of B – lymphocytes in large numbers in to the lymphoid follicles of IFNγR$^{-/-}$ spleen was noticed at day 35 p.i. (E and J)

LF, lymphoid follicles. R, Red pulp
Magnification 200X.

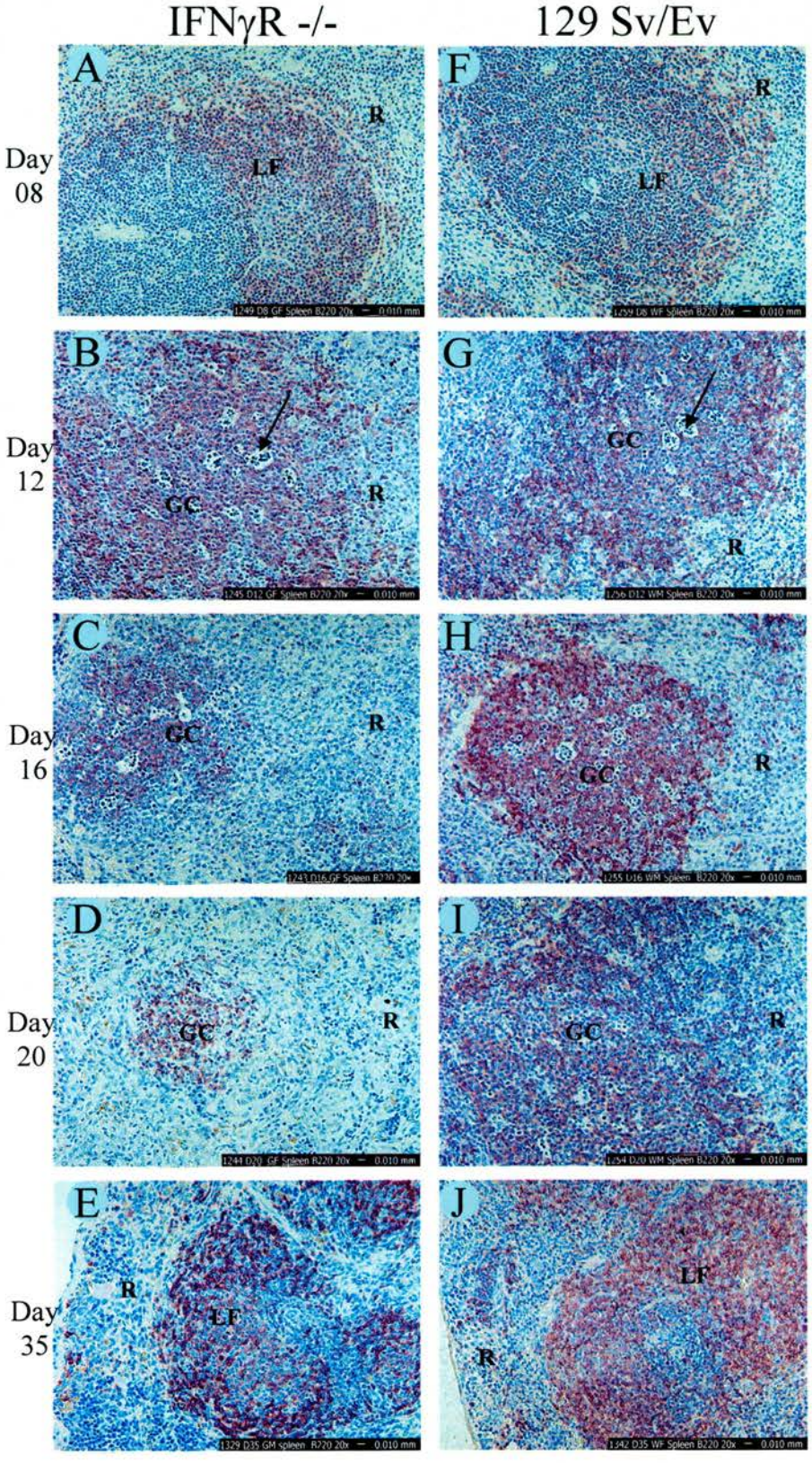

Figure. 3.2.1. Please see the legend on the facing page

was noticed (Figure. 3.2.1B). From day 12 to day 20 p.i. the number of B-lymphocytes showed a gradual decrease in the lymphoid follicles of IFNγR$^{-/-}$ mice. At day 20 p.i. very few B-lymphocytes were present in the contracted spleen (Figure. 3.2.1D). At day 30 p.i., the spleens of IFNγR$^{-/-}$ mice showed a dramatic increase in the number of B-lymphocytes indicating the resolution phase of the fibrotic response. The recovery state was pronounced at day 35 p.i. (Figure 3.2.1E). There was no difference in the distribution pattern in the spleen from day 30 to day 120 p.i. in IFNγR$^{-/-}$ mice. In 129 Sv/Ev mice, the spleens from day 12 to day 16 p.i. showed a gradual increase in the size of the lymphoid follicles with more B-lymphocytes, as well as other features of the GC. From day 16 p.i. onwards the spleens of 129 Sv/Ev mice showed a normal pattern of distribution of B-lymphocytes up to day 120 p.i.

3.2.2. T- LYMPHOCYTES

Serial sections of the spleens from experiment no.1 and 2 were used in this study. T-lymphocytes were identified by CD3 staining and subsets of T-lymphocyte were further characterised by CD4 and CD8 staining. T-lymphocytes are normally seen around the blood vessels in periarteriolar lymphoid sheath (PALS) (Figure. 3.2.2A and 3.2.2F). CD3+T-lymphocyte were detected in the GC throughout the course of the experiment with their notable absence in the lymphoid follicle area of the spleen from IFNγR$^{-/-}$ mice between day 16 and day 20 p.i. (Figure 3 –2.2C and 3.2.2D). From day 35 p.i. onwards T-lymphocyte were mainly seen in the PALS area. Analysis of the sub- population of T-lymphocytes among the infiltrating cells in the GC showed that they included both CD4+ and CD8+ T-lymphocytes with increased numbers present in the spleens of IFNγR$^{-/-}$ mice (Figure. 3.2.3).

3.2.3. SPLENIC MACROPHAGES

There are at least four different sub-populations of macrophages in the spleen (Mebius and Kraal, 2005;Taylor *et al.*, 2005): Red pulp macrophages (RPM), Marginal zone macrophages (MZM), Marginal metallophils (MM) and TBM.

Figure.3.2.2. T- lymphocytes in the spleen of MHV -68 infected mice.

CD3 staining (See Materials and Methods).

Note the presence of CD3+ T lymphocytes (Reddish brown colour) in the PALS in both spleens at day 8 p.i. (A and F). At day 12 p.i presence of T lymphocytes in the germinal centre area of the spleen is observed in both groups of spleen (B and G). CD3 positive T lymphocytes were not seen in the IFNγR$^{-/-}$ spleen at day 16 and 20 p.i. (C and D), whereas T lymphocytes are seen in the 129 Sv/Ev spleen in the PALS and GC (H and I). At day 35 p.i. re-appearance of CD3 positive T lymphocytes in the IFNγR$^{-/-}$ spleen in the PALS (E) and in 129 Sv/Ev spleen T lymphocytes are seen in the PALS and GC.

GC, Germinal Centre. LF, lymphoid follicles. PALS, Peri arteriolar lymphoid sheath. R, Red pulp
Magnification 100X

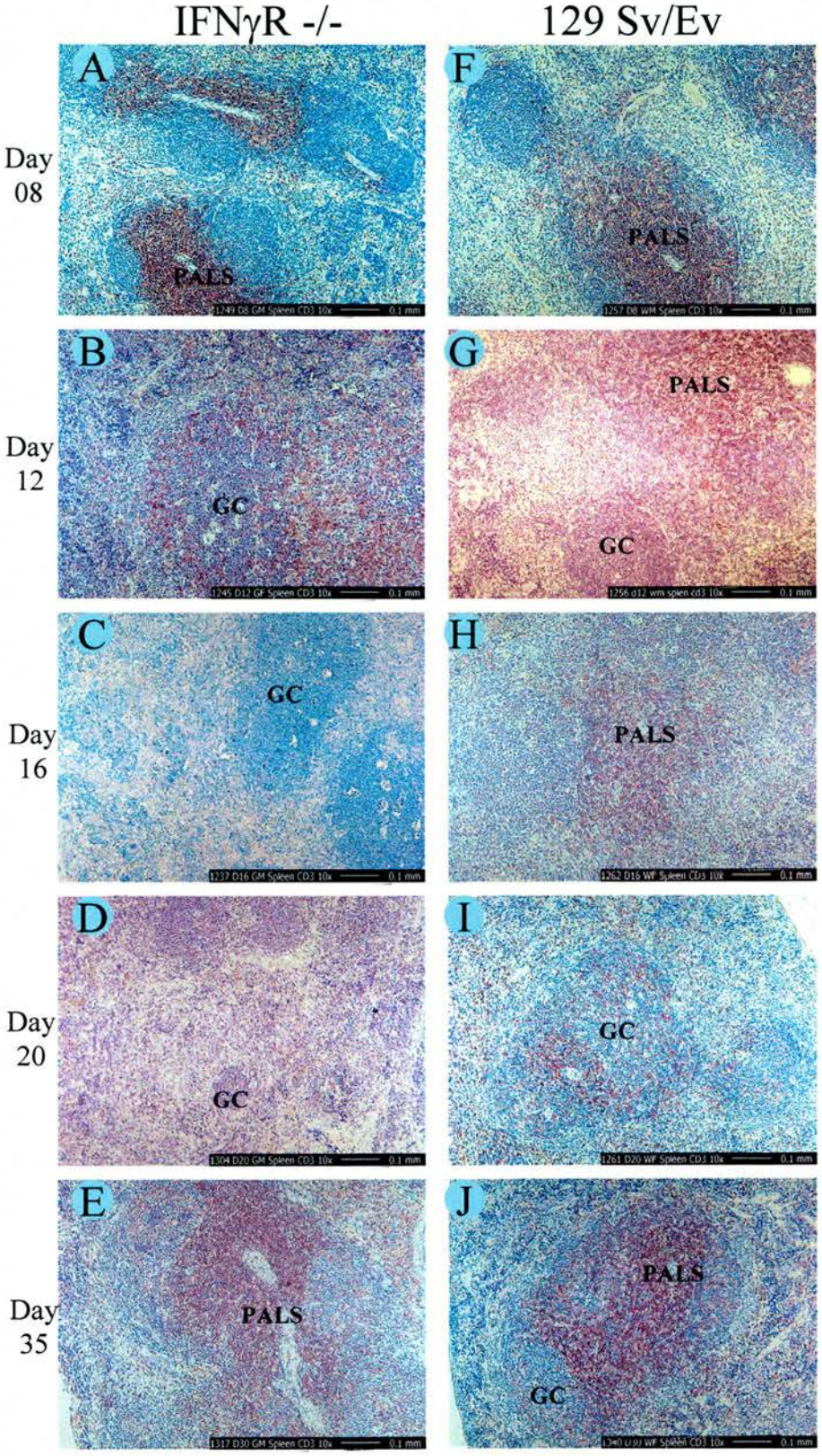

Figure. 3.2.2. Please see the legend on the facing page

IFNγR -/- 129 Sv/Ev

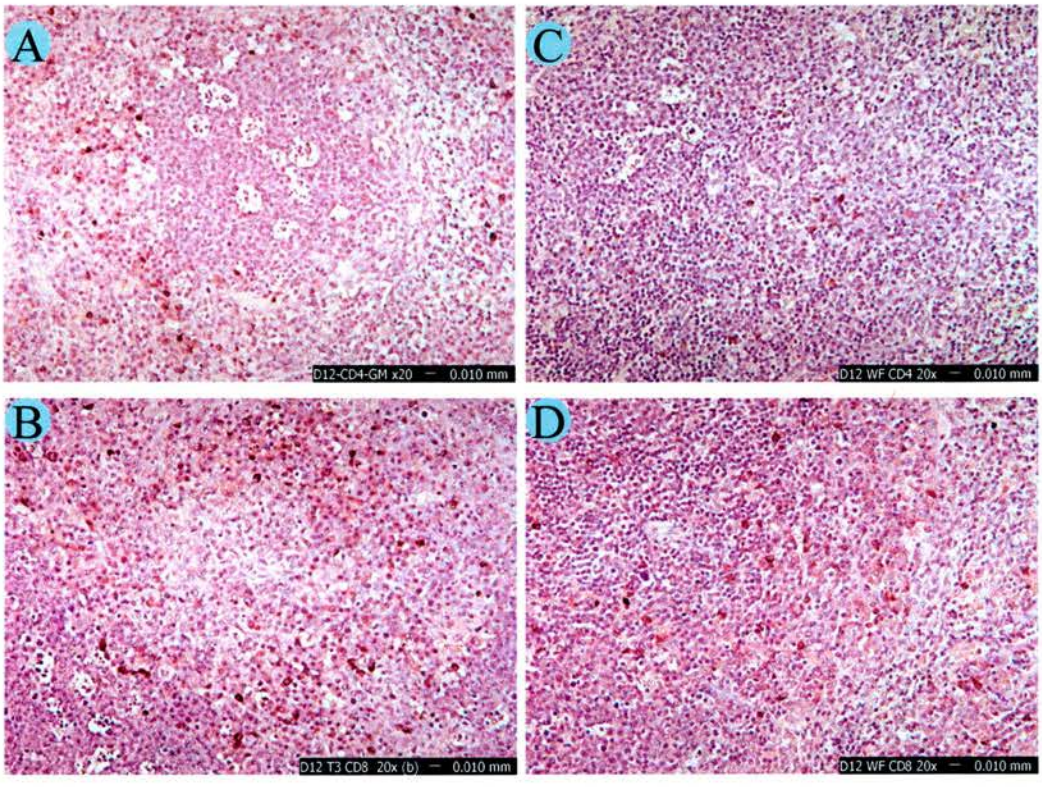

Figure. 3.2.3. T-lymphocyte subsets in the spleen of mice infected with MHV -68 at day 12 post infection. A and B IFNγR -/-. C and D 129 Sv/Ev. A and C CD4 positive lymphocytes. B and D CD8 positive lymphocytes (Red colour)

Magnification 200X

A schematic representation of the subsets of macrophages in the spleen is presented in Figure.3.2.4.

3.2.3.1. RED PULP MACROPHAGES (RPM)

One of the major activities taking place in the splenic red pulp is the filtering and removal of senescent red blood cells. This function is carried out by the RPM lining the red pulp cords. RPM are strongly positive for macrophage specific plasma membrane differentiation antigen F4/80 (Austyn and Gordon, 1981). F4/80 antibody was used to study the profile of RPM in the spleen during the course of MHV-68 infections. At day 8 p.i, the F4/80 positive cells were distributed in the red pulp and in the sub-capsular locations. The morphological features of the macrophages were not clearly visible at this stage in either group of mice. They appeared as syncitium in the red pulp of the spleen (Figure.3.2.5A and 3.2.5F). The distribution pattern of RPM showed dramatic changes during day 12 – 16 p.i. in IFN$\gamma R^{-/-}$ mice (Figure. 3.2.5B – 3.2.5C). On day 12 p.i., F4/80 positive cells were noticed in the white pulp lymphoid follicles. At this time point, the morphological features of the macrophages were round and amoeboid in shape suggesting an activation profile. At day 16 p.i an increased number of positive cells in the white pulp area were observed. By day 18 and 20 p.i., there were only a few positive cells in either red pulp or white pulp (Figure. 3.2.5D). By day 30 p.i. the F4/80 positive cells showed a dramatic return into the red pulp and sub-capsular locations, which were pronounced at day 35 p.i (Figure.3.2.5E). The RPM remained in the red pulp with an activated phenotype throughout the course of experiment until day 120 p.i. In 129 Sv/Ev mice, the RPM always remained in the red pulp and never showed any activated phenotype (Figure 3.2.5F – 3.2.5J).

3.2.3.2. MARGINAL ZONE MACROPHAGES (MZM)

The area immediately surrounding lymphoid follicles and PALS, which demarcate it from red pulp, is called the marginal zone (MZ) of the spleen. The MZ structure is remarkably uniform with a fine reticular network supporting an evenly distributed specific population of cells. MZM are large cells (15 – 20 μm) with well-developed phagocytic activity and close contact between its cell processes

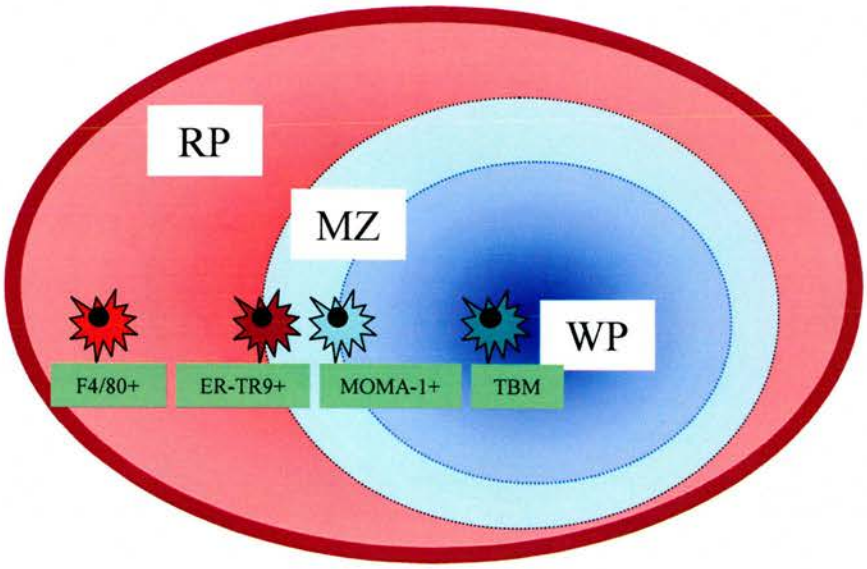

Figure.3.2.4. Schematic representation of different resident macrophage population in the spleen : RP: red pulp contain F4/80 + red pulp macrophages (RPM), MZ: Marginal Zone contains ER-TR9 + Marginal Zone Macrophages (MZM) in the outer zone of MZ and MOMA –1+ Marginal Metallophils (MM) in the inner side of MZ. The resident macrophages in the white pulp (WP) lymphoid follicles are called Tingible Body macrophages (TBM)

Figure.3.2.5. F4/80 positive red pulp macrophages in the spleen of MHV - 68 infected mice.

F4/80 staining (See Materials and Methods).

Note the presence of F4/80 positive macrophages (reddish brown colour) in the red pulp of the spleen in both groups of spleen at day 8 p.i. (A and F). Dramatic movement of activated macrophages are noticed into the germinal centre area (GC) in IFNγR-/- mice at day 12 p.i. (B). At the same time, macrophages were restricted to the red pulp in 129 Sv/Ev mice at all time points (G, H, I and J). In IFNγR-/- mice, the number of F4/80 positive macrophages increases at day 16 p.i (C) and then disappears at the time of peak fibrosis at day 20 p.i. (D). The macrophages show a dramatic return to the red pulp at day 35 p.i. (E)

GC, Germinal Centre. W, White pulp. R, Red pulp
For images A, E, F and J, magnification 10X. For images B, C, D, G, H and I, magnification was 200X.

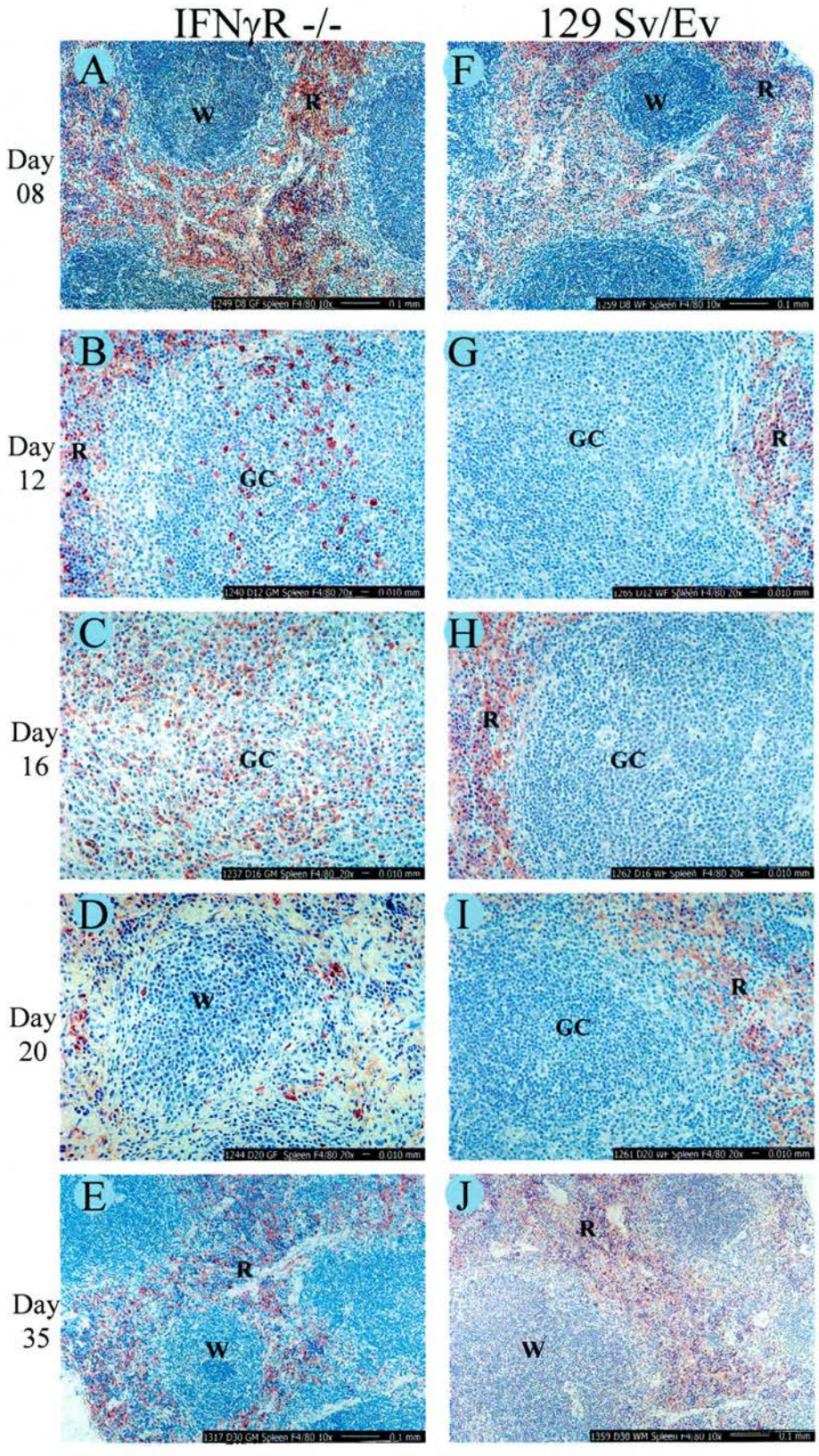

Figure. 3.2.5. Please see the legend on the facing page

and the surrounding marginal zone B (MZB) cells. MZM can selectively take up neutral polysaccharides such as Ficoll (Humphrey and Grennan, 1981), which is used as a distinguishing feature of these macrophages.

The ER-TR9 monoclonal antibody selectively identifies a specific group of macrophages in the marginal zone of the spleen (Van *et al.*, 1985). There has been renewed interest in this sub-population of macrophages in recent years as it has been shown that the antigen recognised by the ER-TR9 antibody is the same as SIGNR1 which is the murine homologue of human dendritic cell specific ICAM – 3 grabbing non Integrin (DC – SIGN) (Geijtenbeek *et al.*, 2002). DC – SIGN is a C – type lectin that binds to an immunoglobulin super-family adhesion molecule, ICAM –3/CD50 expressed specifically on a group of resting T cells (Geijtenbeek *et al.*, 2000b). DC – SIGN was found to bind HIV –1 envelope lipoprotein and transmit the virus to T cells (Geijtenbeek *et al.*, 2000a). This molecule is shown to bind many pathogens including Ebola virus (Alvarez *et al.*, 2002), human cytomegalovirus (Halary *et al.*, 2002), *Leishmania major* (Colmenares et al., 2002) and *Mycobacterium tuberculosis* (Tailleux et al., 2003).

As detailed in the Materials and Methods section, ER-TR9 antibody was used to assess the profile of MZM of spleen from experiment no.1 and 2. MZM appeared as clearly defined round active cells in the MZ. As with RPM, MZM also appeared to increase in number and move into the GC area of the white pulp in IFNγR$^{-/-}$ mice during day 12 and day 16 p.i. (Figure 3.2.6A and 3.2.6B). At day 20 p.i. there were only a few MZM in the spleen of IFNγR$^{-/-}$ mice (Figure 3.2.6C). In contrast, few ER-TR9 positive macrophages were found in the MZ of the spleen of the 129 Sv/Ev mice at day 12 p.i. (Figure 3.2.6D). By day 16 p.i. and day 20 p.i. low numbers of MZM were found in the lymphoid follicles in 129 Sv/Ev mice (Figure 3.2.6E and 3.2.6F). At day 35 p.i. the MZM were mainly confined to the marginal zone in both groups of mice.

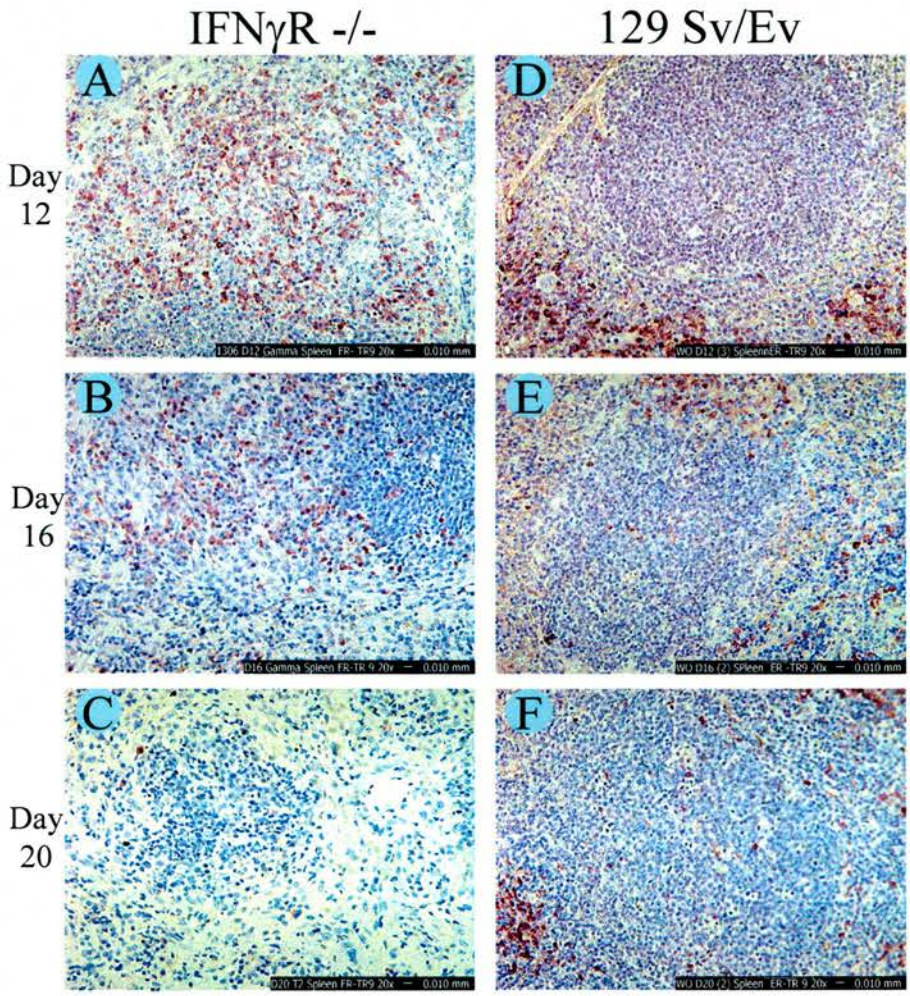

Figure. 3.2.6. Marginal zone macrophages in the spleen of mice infected with MHV-68 at various time points – ER-TR9 staining.

Note the increase in the number and movement of ER-TR9 positive marginal zone macropahges towards the germinal centre area in IFNγR -/- (A and B) wheareas, in wild type mice the MZM are restricted to marginal zone.

Magnification 200X

3.2.3.3. MARGINAL METALLOPHILS (MM)

MM are found in the inner side of the marginal zone with cell processes extending into the white pulp. These macrophages are strongly positive for non-specific esterase (Eikelenboom, 1978) and acid phosphatases, but negative for ER-TR9 and F4/80. These macrophages can take up latex particles and colloidal carbon upon intravenous administration. The MOMA –1 monoclonal antibody (Kraal and Janse, 1986) was used to detect MM in tissue sections in this study. The profile of MM during the course of infection was similar to that of MZM. There was an increase in the number of MM moving towards lymphoid follicles at day 12 and day 16 p.i. infection in IFNγR$^{-/-}$ mice (Figure 3.2.7A and 3.2.7B). In contrast, in 129 Sv/Ev mice, the MM always remained in the marginal zone (Figure 3.2.7C and 3.2.7D). At day 20 p.i, there were only a few MM seen around lymphoid follicles in IFNγR$^{-/-}$ mice.

3.2.3.4. TINGIBLE BODY MACROPHAGES (TBM)

TBM are specialised phagocytic cells present in the GC of lymphoid organs. In the GC, the B-lymphocytes that fail to recognise an antigen or only have low affinity for the antigen are destined to undergo apoptosis and are swiftly removed by TBM. TBM are positive for CD68 (Rabinowitz and Gordon, 1991) and milk fat globule epidermal growth factor (EGF) factor 8 (MFG – E8) (Hanayama *et al.*, 2004). Absence of MFG–E8 on TBM renders them less efficient at engulfing apoptotic B-cells in the GC.

The morphological features of TBM were used to asses the profile of TBM in this study. TBM are large cells with vacuolated cytoplasm carrying numerous apoptotic bodies which gives a 'starry sky' appearance to the secondary lymphoid follicles (see the inset of figure 3.2.8). The number of TBM per 10 random GC per section of spleen from experiment No.1 was counted. The number of TBM peaked at day 12 p.i in IFNγR$^{-/-}$ mice, whereas, the number peaked at day 16 p.i. in 129 Sv/Ev mice in first experiment (Figure 3.2.8). However, the difference in the number of TBM at both time points between IFNγR$^{-/-}$ and 129 Sv/Ev mice was not statistically significant ($p=0.0809$ at day 12 and 1.0 at day 16 p.i.).

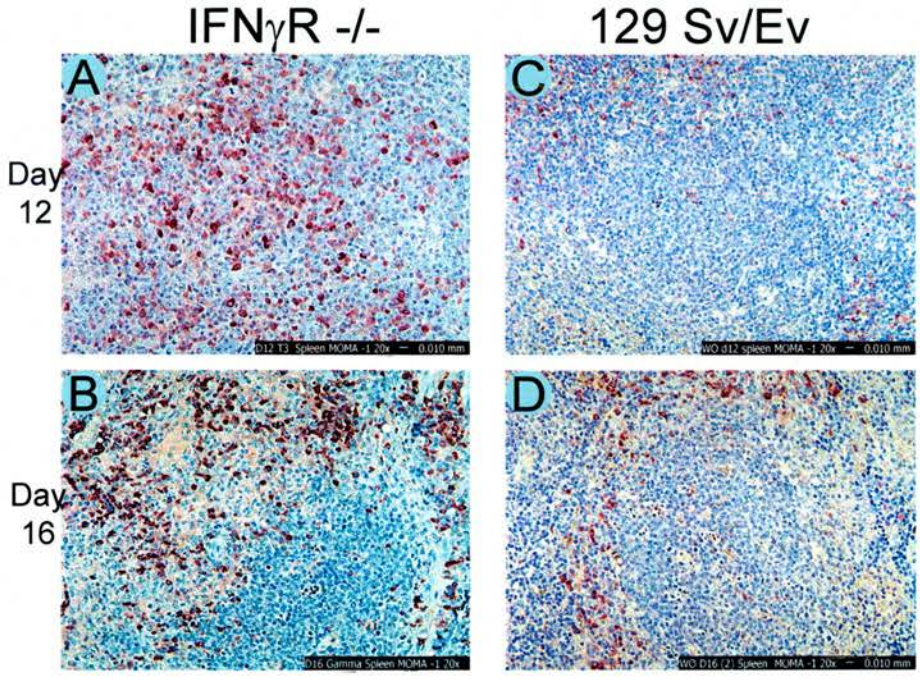

Figure. 3.2.7. Marginal metallophils in the spleen of mice infected with MHV -68 at various time points – MOMA-1 staining.

Note the increase in the number and movement of marginal metallophils towards the germinal centre area in sections A and B.

Magnification 200X.

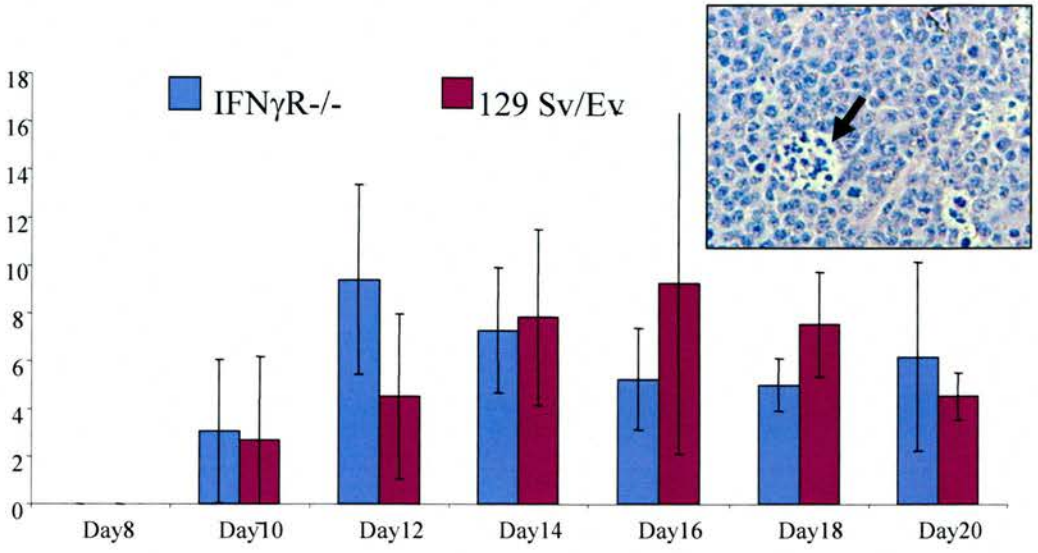

Figure.3.2.8. Tingible body macrophages in the spleen. Ten random germinal centres from each spleen was chosen and the number of TBMs were counted. Each bar represents the average number of TBM with standard deviation for each group of mice at different time points. A representative image of TBM is presented in the inset (arrow). Magnification 400x

3.2.4. SUMMARY

This study was concerned with the dynamics of cell populations in the spleen of IFNγR$^{-/-}$ mice and 129 Sv/Ev mice following MHV-68 infection. The profile of B – lymphocytes during the course of infection supported the observation made during the histopathological examination. In the spleens from IFNγR$^{-/-}$ mice, the B-lymphocyte showed a progressive reduction and only very few B-lymphocytes were present in the lymphoid follicles at day 20 p.i, which was encircled by the 'fibrotic cage'. The recovery phase was characterised by re-population of lymphoid follicles with increased numbers of B-lymphocytes.

The profile of T-lymphocytes identified by immunohistochemistry confirmed their contribution to the development of the GC reaction in both groups of mice. Both CD8 and CD4 positive T lymphocytes were present in the GC. The presence of T-lymphocytes could be a response to latently infected B-lymphocytes. These cells could act as a trigger for the development of fibrosis as seen by Dutia et al (1997). In the absence of IFNγ signalling, the immune response could be shifting towards a Th2/Tc2 type of response. Further characterisation of infiltrating CD8 and CD4 positive T lymphocytes are required to identify the shift in the immune response towards Th2/Tc2 type.

This part of the investigation revealed the activation profile of different subsets of macrophages in the spleen during the course of infection in IFNγR$^{-/-}$ mice prior to the development of fibrosis. This is particularly important as this activation profile is noticed in mice, which are not able to respond to IFNγ, which is considered as the most important classical activator of macrophages. It is possible that the cytokines released by the infiltrating T-lymphocytes may be responsible for the activation of macrophages and their movement towards the lymphoid follicles carrying latently infected cells. This observation indicates the operation of an alternate pathway of activation in this setting. This hypothesis was therefore investigated in the next part of the study (section 3.3).

The quantification of TBM showed no obvious difference between two groups of mice. It is possible that the process of removal of apoptotic cells by phagocytic cells contributes to the pathogenesis of fibrosis by releasing pro-fibrotic cytokines like TGFβ (Savill and Fadok, 2000). In this model, the TGFβ released during this process may be enough to drive the development of fibrosis in the absence of anti-fibrotic effect of IFNγ. In support of this hypothesis, an earlier investigation on the cytokine profile in the spleen of IFNγR$^{-/-}$ mice infected with MHV-68 has shown up-regulation of TGFβ (Ebrahimi *et al.*, 2001).

3.3. ALTERNATE ACTIVATION OF MACROPHAGES

The observation of an activated phenotype and change in the distribution pattern of different subsets of macrophages towards GC in the spleen following MHV-68 infection in IFNγR$^{-/-}$ mice compared to 129Sv/Ev mice suggested a contributory role of these cells in the pathogenesis of fibrosis. This was particularly important, as the mice in which we see these changes are not able to respond to IFNγ, the classical macrophage activator, due to their inherent deficiency of the receptor. This prompted an investigation into the alternate activation of macrophages. The well characterised marker molecule for alternatively activated macrophage is arginase-I (Gordon, 2003). L – arginine can be metabolised by three different enzymes namely, inducible nitric oxide synthase (iNOS), arginase-I and arginase-II. In macrophages, L – arginine is metabolised by iNOS to produce citrulline and nitric oxide, which is one of the principal cytotoxic mechanisms of these cells (Hibbs, Jr. *et al.*, 1987). Alternatively, arginase-I and arginase-II metabolise L – arginine to L – ornithine and urea. L – ornithine can be further metabolised to proline or polyamines. Polyamines aid cellular proliferation and proline is an important amino acid required for collagen synthesis. We investigated the role of arginase-I in this scenario by three different methodologies namely, reverse transcriptase – polymerase chain reaction (RT – PCR), Quantitative RT – PCR (QRT-PCR) and immunohistochemistry.

3.3.1. REVERSE TRANSCRIPTASE–POLYMERASE CHAIN REACTION (RT-PCR)

RT- PCR studies showed the up-regulation of arginase- I in IFNγR$^{-/-}$ mice infected with MHV-68 in a time dependent manner (Figure 3.3.1). In IFNγR$^{-/-}$ mice, arginase-I transcripts were detected reproducibly from day 12, 16 and 20. The bands became faint from day 35 p.i onwards. Faint bands were visible in few mice of the 129 Sv/Ev group at different time points indicating that arginase -1 may be expressed at a reduced level in 129 Sv/Ev mice infected with MHV-68.

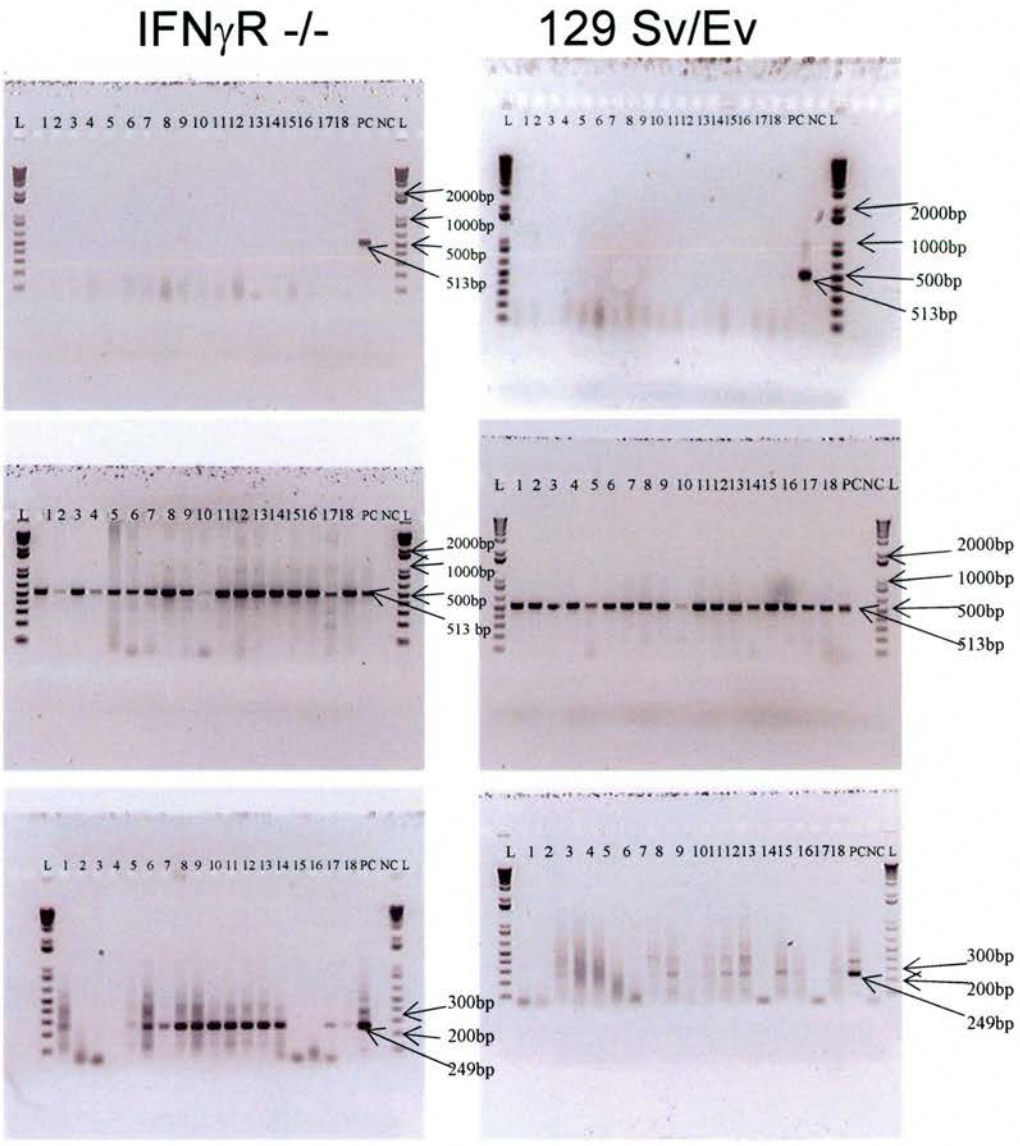

Figure.3.3.1. Reverse Transcriptase – Polymerase chain reaction (RT-PCR) for Arginase – 1 from RNA samples extracted from spleens of mice infected with MHV-68. RNA was extracted from spleens of three mice each at day 0 (lane 1,2,3), day 8 (Lane 4,5,6), day 12 (Lane 7,8,9), day 16 (lane 10, 11, 12), day 20 (Lane 13, 14, 15) and day 35 (Lane 16, 17, 18). Top panel , PCR for β actin gene to confirm removal of DNA from the RNA samples after DNase treatment. Middle panel, RT – PCR for β actin gene after cDNA synthesis to confirm transcription efficiency of RNA. Bottom panel, RT-PCR for arginase – I gene. L, DNA ladder. PC, positive control. NC, Negative control

3.3.2. QUANTITATIVE RT- PCR (QRT-PCR)

To quantify the level of expression of arginase-I in IFNγR$^{-/-}$ mice in comparison to 129 Sv/Ev mice following MHV-68 infection at different time points, QRT-PCR analysis was carried out on RNA samples isolated from the spleen of mice infected with MHV-68. The relative copy number of gene for arginase-I was negligible or below the level of detection in 129 Sv/Ev mice at all time points whereas the copy number of arginase-I in IFNγR$^{-/-}$ mice showed a progressive increase in copy number from day 8 p.i. to day 16 p.i and then it declined at subsequent time points. The fold change in the level of arginase-I is presented in Figure. 3.3.2.

3.3.3. IMMUNOHISTOCHEMISTRY

The antibody against arginase-I used in this study was raised in a rabbit against recombinant human arginase- I. This antibody cross-reacts with rat and mouse arginase-I (Endo *et al.*, 2003) and was a kind gift from Dr. Tomomi Gotoh of Kumamoto University, Japan. Staining of sections of spleen for arginase-I showed cells expressing arginase-I in the spleen at day 12, 16 and 20 p.i from IFNγR$^{-/-}$ mice. A representative image of the sections of spleen taken at day 12 p.i and stained with arginase-I antibody is presented in Figure. 3.3.3. Arginase-I positive cells were noticed in the light area of GC. None of the sections of the spleen from MHV-68 infected 129 Sv/Ev mice or IFNγR$^{-/-}$ mice harvested at day 8 and day 35 p.i showed arginase-I positive cells.

3.3.4. SUMMARY

This study indicated a positive contribution of macrophages in the pathogenesis of fibrosis through their alternate activation pathway characterised by arginase-I expression. The concept of an alternative pathway of macrophage activation by the Th2 type cytokines such as IL-4 and IL–13 has gained credence in the past decade to account for a distinctive macrophage phenotype that is consistent with their role in tissue repair. It is reasonable to assume that in the absence of signalling towards a Th1 response, the immune response following MHV-68 infections may skew towards Th2 type characterised by IL- 4 and IL-13

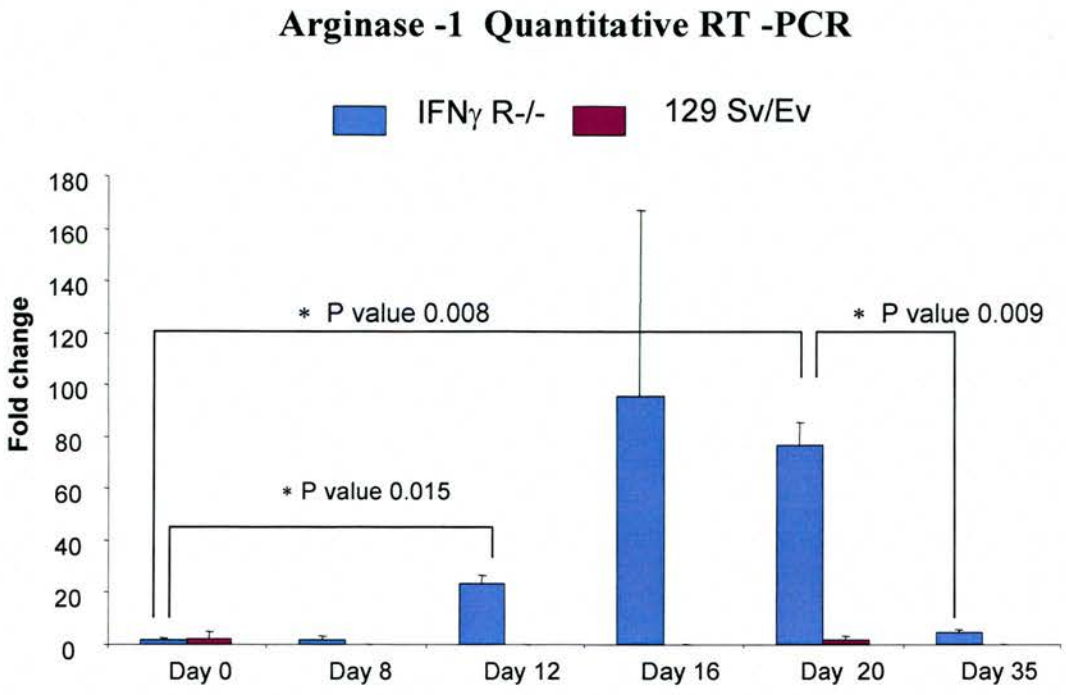

Figure.3.3.2. Quantitative Reverse Transcriptase – Polymerase chain reaction (Q-RTPCR) for arginase – I gene from RNA samples extracted from spleens of mice infected with MHV -68.

RNA was extracted from spleens of three mice each at day 0, day 8, day 12, day 16 , day 20 and day 35 from IFNγR-/- and 129 Sv/Ev mice infected with MHV-68. β actin gene expression was used to normalise the data. Purified PCR product generated with the outer set of primers for arginase-I and β actin gene was used to generate the standard curve. The level of arginase –I gene expression normalised with β actin gene is expressed as fold change (average three values at each time point) in relation to level of gene expression at day 0 post infection.

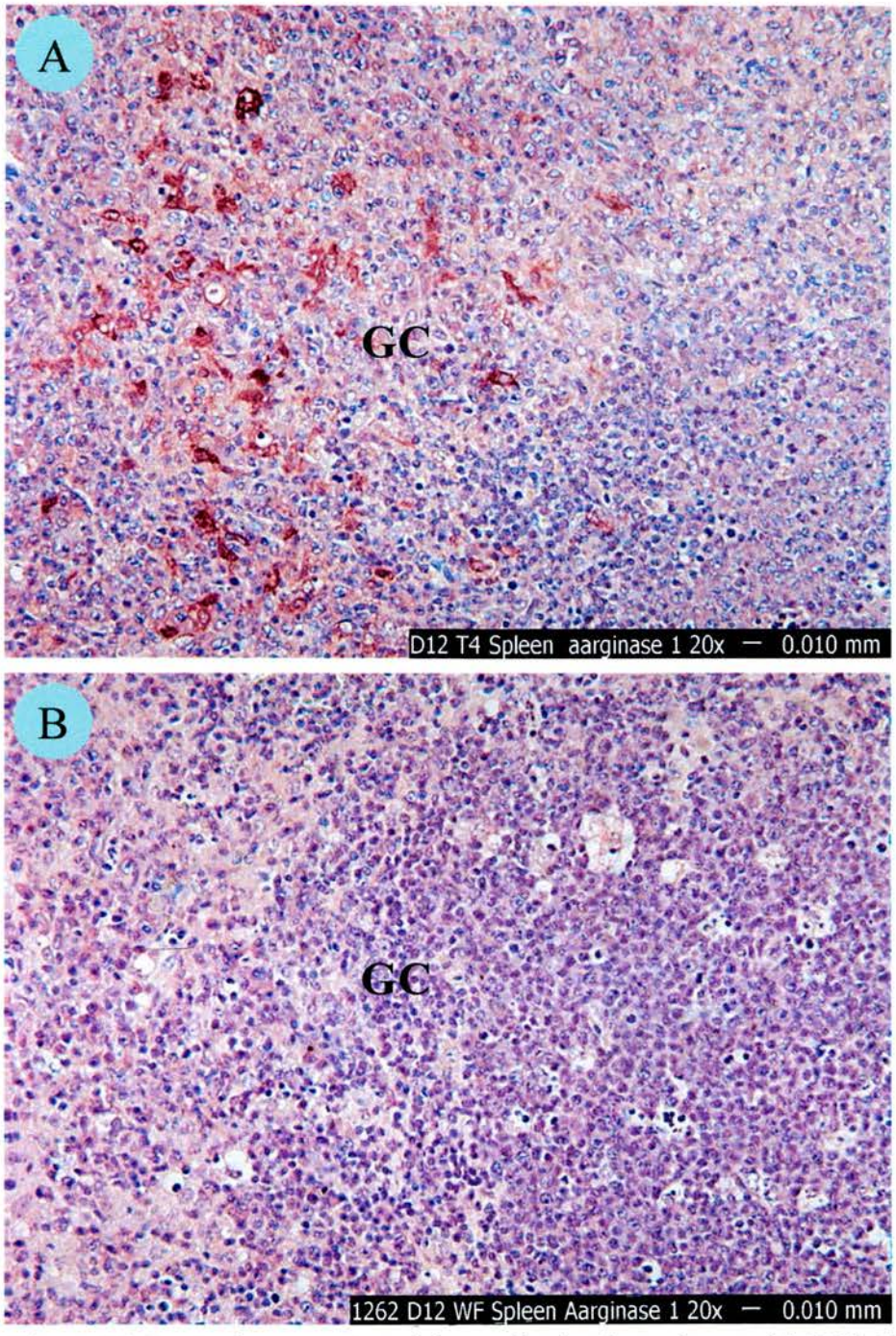

Figure.3.3.3. Arginase – I positive cells in the spleen of MHV-68 infected mice at day 12 p.i. Arginase -1 antibody staining

Arginase -1 staining. A= IFNγR-/-; B= 129/Sv/Ev.

Note the presence of Arginase -1 positive cells in the germinal centre of IFNγR-/- mice. Arginase -1 positive cells are absent in the spleen of 129 Sv/Ev mice. GC, germinal centre

Magnification 200X

expression. Interestingly, earlier studies on infection of IFNγR$^{-/-}$ mice and IFNγ$^{-/-}$ mice with MHV-68 infections have not shown such a switch towards Th2 response (Sarawar *et al.*, 1997;Ebrahimi *et al.*, 2001). In view of the expanding knowledge on the cytokine, chemokine and chemokine receptor homologues encoded by herpesviruses, (Alcami, 2003) it is possible that, a hitherto uncharacterised gene of MHV – 68, as proposed recently (Dutia *et al.*, 2004) may be selectively secreting a molecule to directly activate macrophages. However, a recent study reported that following intranasal infection of IFNγR$^{-/-}$ mice with MHV-68 produced high levels of IL-4, IL-5 and IL-10 in the lung (Mora *et al.*, 2005). It will be useful to assess the cytokine profile in the IFNγR$^{-/-}$ mice following MHV-68 infections with more sensitive techniques to establish the role of Th2 cytokines in pathogenesis.

3.4. BONE MARROW CHIMERA EXPERIMENTS

The role of IFNγ responsiveness of bone marrow derived cells (BMDC) in the pathogenesis of splenic fibrosis was investigated. The approach taken to address this hypothesis was through generation of bone marrow chimera mice (in 129 Sv/Ev background and IFNγR$^{-/-}$ background) and their infection with MHV–68. The procedure adopted for generation of chimera mice is presented in Materials and Methods (section 2.9.1.)

3.4.1. ASSESSMENT OF BONE MARROW CHIMERA FORMATION

The success of bone marrow chimera formation was assessed by PCR on DNA extracted from blood of chimera mice. The IFNγ receptor knock out mouse was generated by inserting a blunted XhoI–SalI fragment of pMC1neopA (Stratagene) (1146bp) into blunted Aat II site on exon V of IFNγ receptor gene (Huang *et al.*, 1993). The primers used for PCR for assessing the success of chimera formation were designed (Table 2.2) to span the insertion site of the neomycin cassette so that the normal gene will provide a small product of 148 bp and the disrupted gene would provide a large product (148 + 1146 = 1294bp).

The PCR for IFNγ receptor gene from IFNγR$^{-/-}$ mice replaced with BMDC from 129 Sv/Ev mice (129Sv/EV⇒ IFNγR$^{-/-}$) showed that almost all of the BMDC were from 129 Sv/Ev mice (Panel A of figure 3.4.1). Lane number 3, 4, 5 and 6 had few faint bands of 1294bp suggesting that few BMDC from IFNγR$^{-/-}$ background are still present in the blood. Those bands may be due to epithelial cell contamination at the time of blood collection. The gel picture of PCR products for IFNγR gene from control gamma chimera (IFNγR$^{-/-}$ ⇒ IFNγR$^{-/-}$) mice shows few non specific bands other than the bands for smaller products (148bp) (Panel B of figure 3.4.1). Lane 2 had no PCR product. This may be because of poor quality of template DNA or inhibitors of PCR in the DNA sample.

The generation of bone marrow chimera mice on the 129 Sv/Ev background (IFNγR$^{-/-}$ ⇒ 129 Sv/EV) was partially successful, as there were faint bands

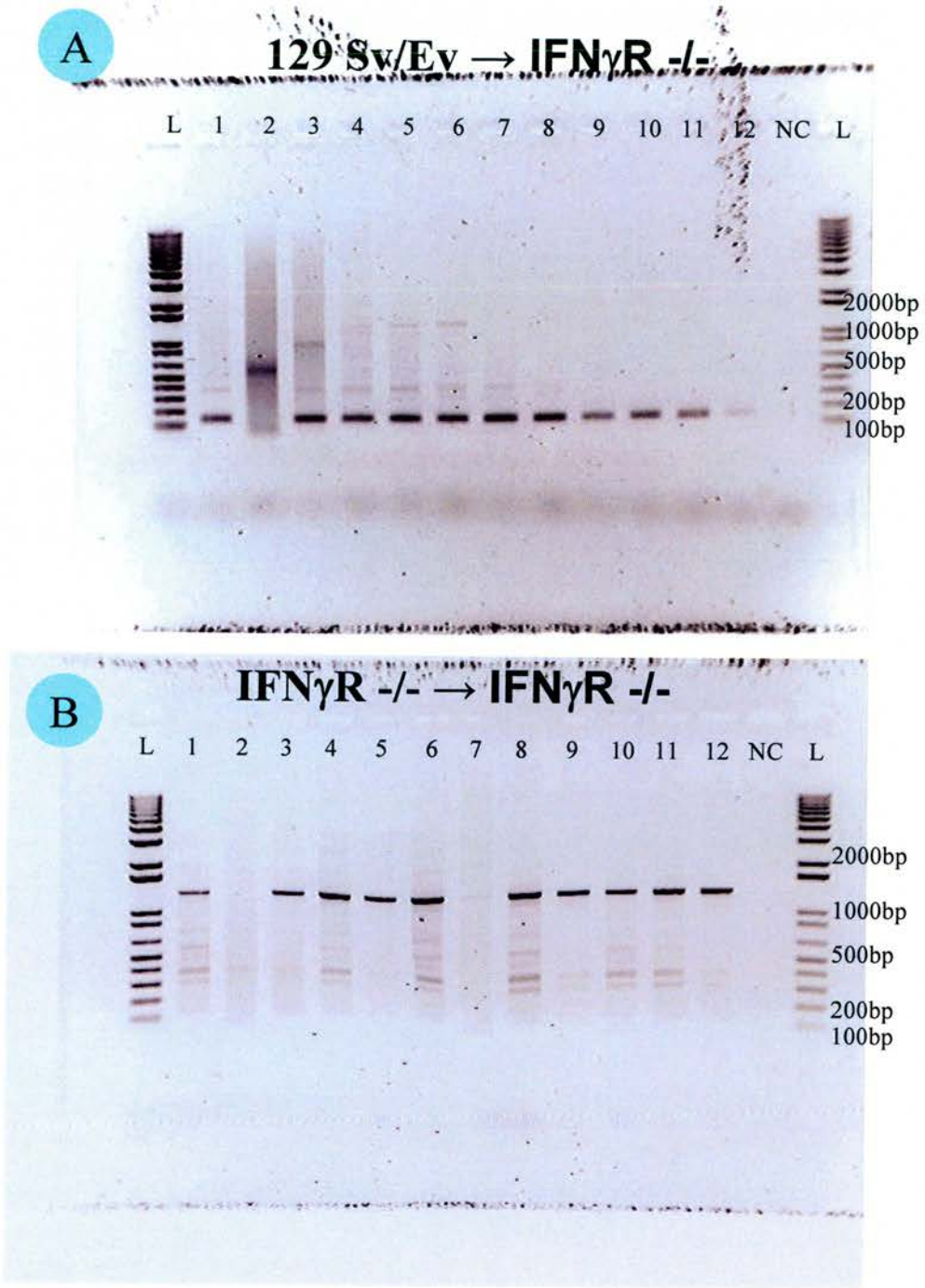

Figure.3.4.1. Polymerase chain reaction (PCR) for IFNγR gene from DNA samples extracted from blood of bone marrow chimera mice in the IFNγR -/- background .

Panel A, IFNγR -/- mice with replaced bone marrow cells from 129 Sv/Ev mice. Panel B, IFNγR -/- mice with replaced bone marrow cells from IFNγR -/- mice as control

L, DNA ladder. NC, Negative control , Each lane represent individual mice

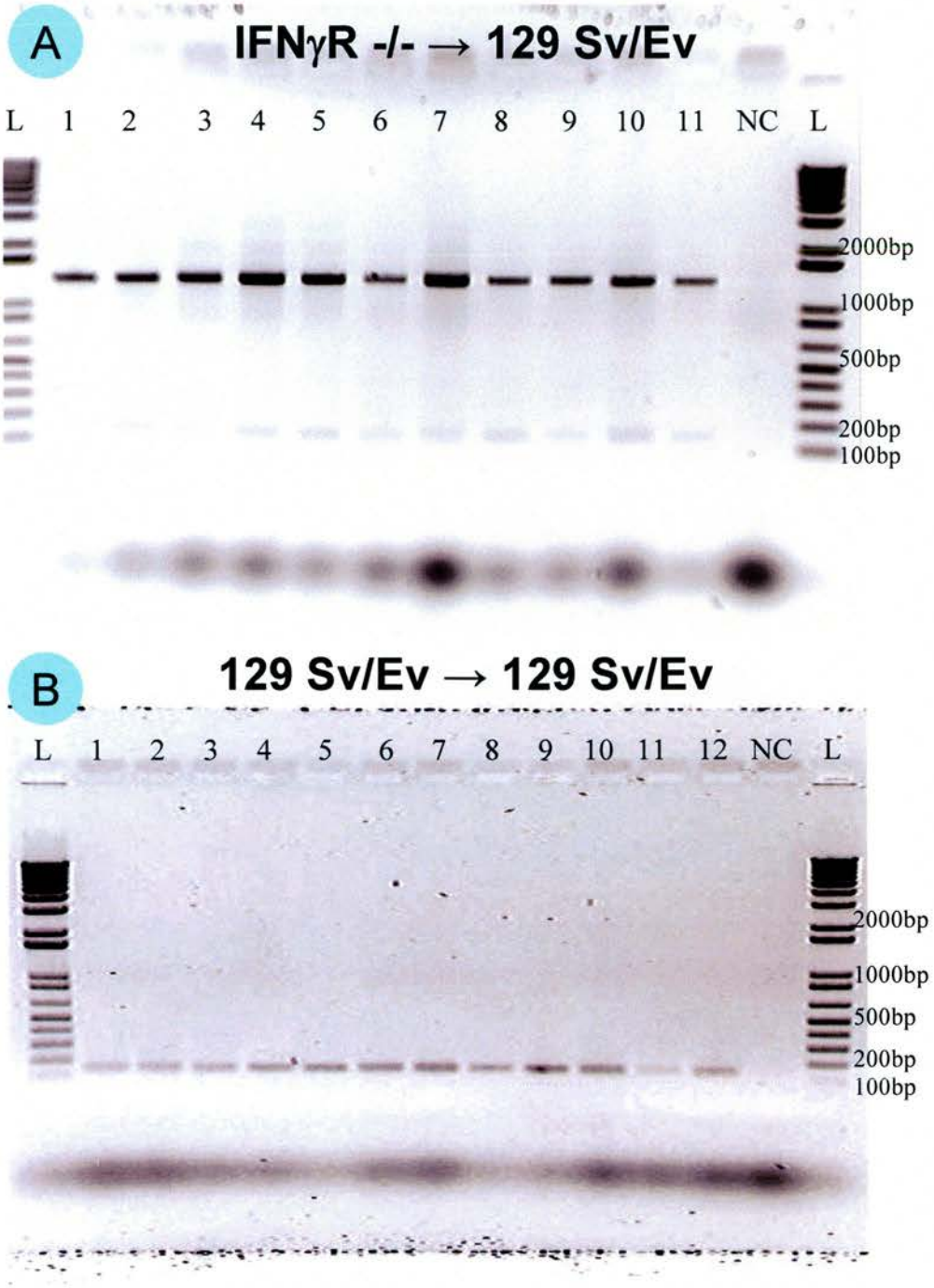

Figure.3.4.2. Polymerase chain reaction (PCR) for IFNγR gene from DNA samples extracted from blood of bone marrow chimera mice in the 129 Sv/Ev background .

Panel A, 129 Sv/Ev mice with replaced bone marrow cells from IFNγR -/- mice. Panel B, 129 Sv/Ev mice with replaced bone marrow cells from 129 Sv/Ev mice as control

L, DNA ladder. NC, Negative control , Each lane represent individual mice

detected for the small PCR products in the blood of 129 Sv/Ev mice with BMDC from IFNγR$^{-/-}$ mice (IFNγR$^{-/-}$ ⇒ 129 Sv/EV). However, the dominant genotype detected was BMDC in the IFNγR$^{-/-}$ background (Panel A of Figure.3.4.2). The control wild type chimera mice (129 Sv/Ev ⇒ 129 Sv/Ev mice) showed PCR products of expected size (148bp) from all animals (Panel B of Figure 3.4.2).

3.4.2. PATHOLOGICAL CHANGES IN CHIMERA MICE IN 129 Sv/Ev BACKGROUND (IFNγR$^{-/-}$ ⇒ 129 Sv/Ev)

At the time of infection, another set of age and sex matched 129 Sv/Ev mice were recruited into the study. All three groups of mice (129 Sv/Ev, 129Sv/Ev ⇒ 129 Sv/Ev and IFNγR$^{-/-}$ ⇒ 129 Sv/Ev) were infected intranasally with 4X10^5 PFU of MHV-68 in 40μl of sterile saline as described in Materials and Methods section 2.4.

Three mice each from three groups were sacrificed on day 12, 16, 20 and 35. There was no difference in the gross and histopathological features of spleen between three groups of mice at all four time points. The weight of spleen expressed as percentage of body weight is presented in Figure 3.4.3. The difference in weight of spleen expressed as a percentage of body weight between three groups of mice [129 Sv/Ev mice, IFNγR$^{-/-}$ ⇒ 129 Sv/Ev, and 129 Sv/Ev ⇒129 Sv/Ev] at all four time points was not statistically significant. Histopathological examination also confirmed the absence of any differences in the structure of spleen between three groups of mice infected with MHV-68. All the spleen showed immune responsiveness in the form of GC reaction with TBM and behaved like the spleens from experiment no.1 and 2.

3.4.3. PATHOLOGICAL CHANGES IN CHIMERA MICE IN IFNγR$^{-/-}$ BACKGROUND (129 Sv/Ev ⇒ IFNγR$^{-/-}$)

As with chimera mice in the 129 Sv/Ev background, control chimera mice were also generated in the IFNγR$^{-/-}$ background (IFNγR$^{-/-}$ ⇒ IFNγR$^{-/-}$). At the time of

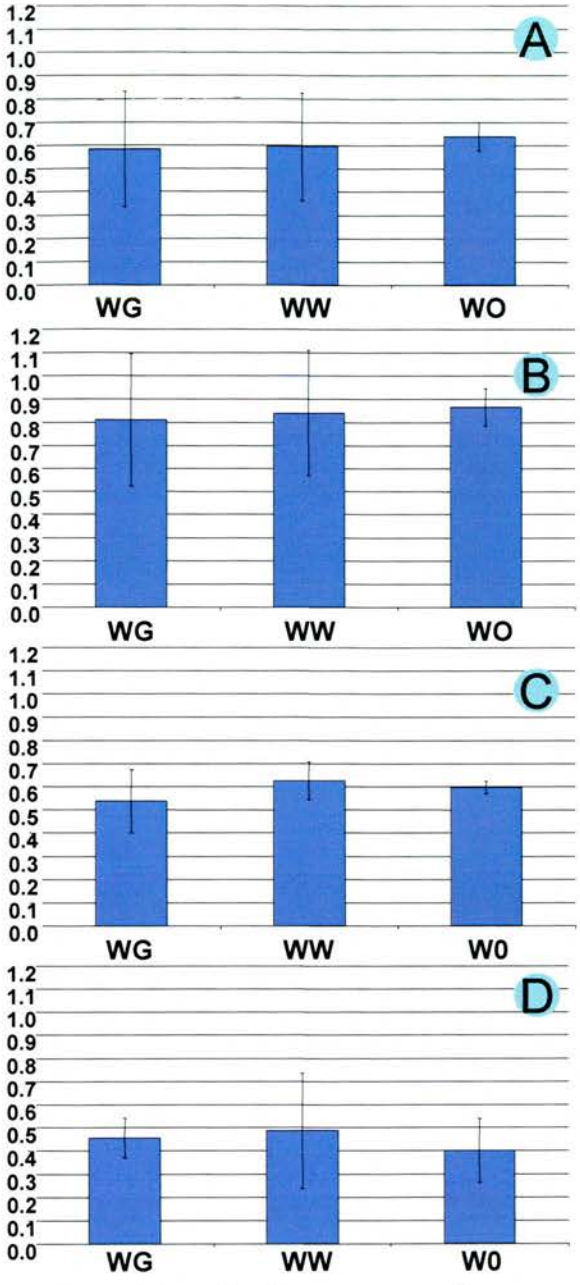

Figure. 3.4.3. Weight of spleen expressed as percentage of body weight from bone marrow chimera experiment in the 129 Sv/Ev background. Mice were intranasally infected with 4x 105 PFU of MHV –68. Panel A, Day 12 P.I. Panel B, Day 16 P.I. Panel C, Day 20 P.I. Panel D, Day 35 P.I. WG, 129 Sv/Ev mice replaced with bone marrow cells from IFNγR -/- mice. WW, 129 Sv/Ev mice with bone marrow cells from 129 Sv/Ev mice (Control). WO, 129 Sv/Ev mice

infection, a group of age and sex matched IFNγR$^{-/-}$ and 129 Sv/Ev mice were recruited in to the study. There were four groups of mice in this experiment [129 Sv/Ev mice, IFNγR$^{-/-}$ mice, 129Sv/Ev ⇒ IFNγR$^{-/-}$ and IFNγR$^{-/-}$ ⇒ IFNγR$^{-/-}$]. The mice were infected intranasally with 4X 10^5 PFU of MHV - 68 in 40µl of sterile saline as described in Materials and Methods section 2.4. The time points in this experiment were day 12, 16, 20 and 35 and three mice each were sacrificed on the stipulated time points and pathological changes in the spleen was investigated.

The weights of spleen expressed as percentage of body weight was not statistically significantly between four groups of mice at all time points (Figure 3.4.4). However, the size, colour and appearance of the spleen from gamma chimera mice (129Sv/Ev ⇒ IFNγR$^{-/-}$) appeared similar to the spleens of 129 Sv/Ev groups of mice rather than the spleen of IFNγR$^{-/-}$ mice at day 12, 16 and more specifically at day 20 p.i. (Figure 3.4.5). At day 35 p.i. the spleens from gamma chimera mice (129Sv/Ev ⇒ IFNγR$^{-/-}$) appeared smaller in size like the spleens of control gamma chimera (IFNγR$^{-/-}$ ⇒ IFNγR$^{-/-}$) and IFNγR$^{-/-}$ mice. Histopathologically, the spleen from gamma chimera mice (129Sv/Ev ⇒ IFNγR$^{-/-}$) at day 12 p.i and day 16 p.i. appeared similar to the spleens of 129 Sv/Ev mice. The features included early GC reaction at day 12 p.i. which progressed to expansion of white pulp lymphoid follicles with extensive GC reaction at day 16 p.i. (Figure 3.4.6C, D, G and H). The histopathological features of spleens from control chimera mice (IFNγR$^{-/-}$ ⇒ IFNγR$^{-/-}$ mice) and IFNγR$^{-/-}$ mice appeared similar. The GC reaction was more intense at day 12 p.i and invasion of white pulp lymphoid follicles with macrophages were evident at day 16 p.i. (Figure 3.4.6A, B, E, and F).

Even though the gross appearance of the spleen from gamma chimera mice (129Sv/Ev ⇒ IFNγR$^{-/-}$) at day 20 p.i. looked similar to the spleen of 129 Sv/Ev mice, a distinct histopathological feature was noticed in the spleen of gamma chimera mice. The red pulp of the spleen was intact with erythrocytes and splenic cords. However, depletion of small lymphocytes in the lymphoid follicles was noticed. The small lymphocytes were replaced by cells with macrophagic and

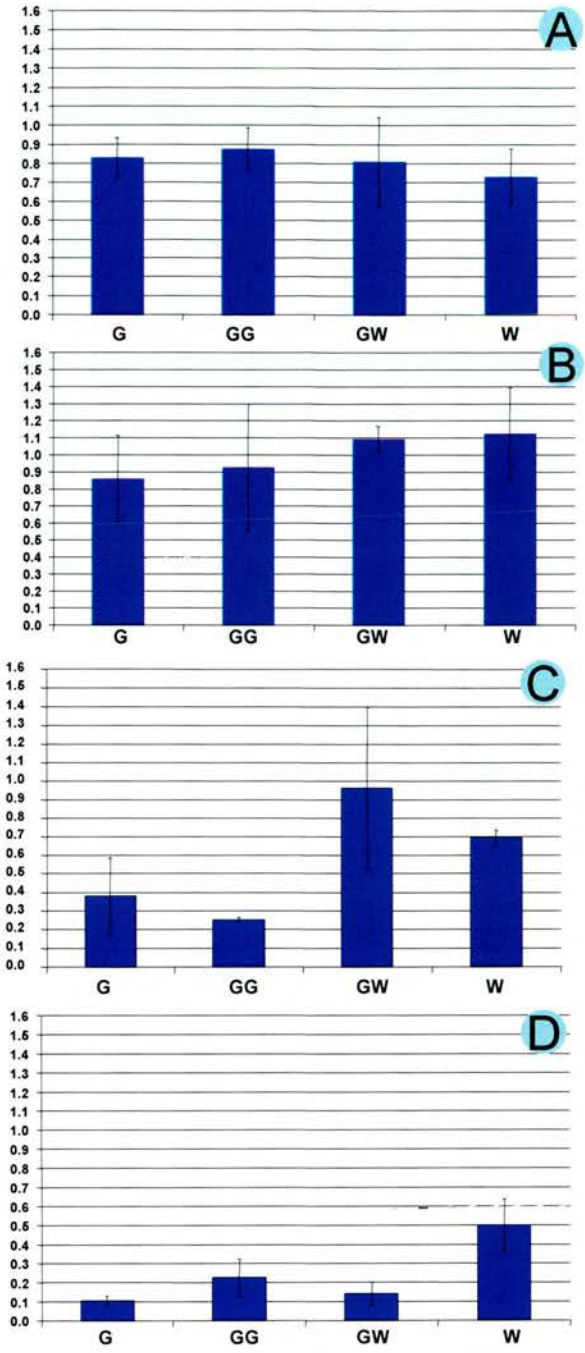

Figure. 3.4.4. Weight of spleen expressed as percentage of body weight from bone marrow chimera experiment in the IFNγR-/- background. Mice were intranasally infected with 4X 105 PFU of MHV –68. Panel A, Day 12 P.I. Panel B, Day 16 P.I. Panel C, Day 20 P.I. Panel D, Day 35 P.I. G, IFNγR -/- mice. GG, IFNγR -/- mice replaced with bone marrow cells from IFNγR -/- mice (Control) GW, IFNγR -/- mice with bone marrow cells from 129 Sv/Ev mice WO, 129 Sv/Ev mice

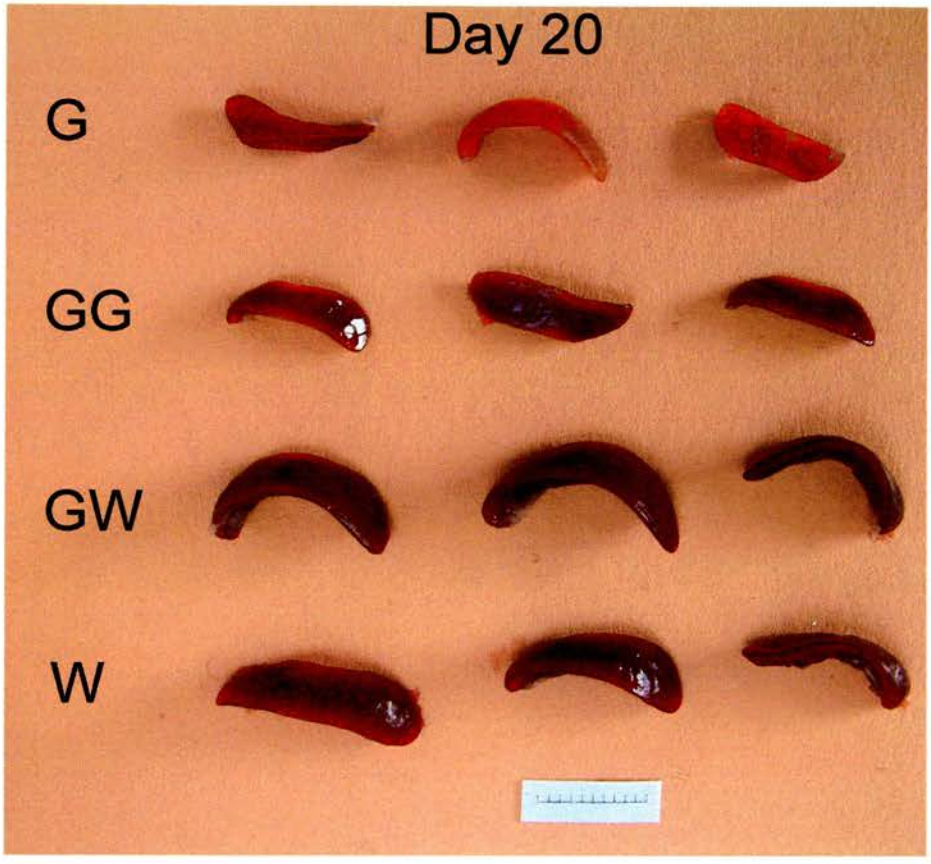

Figure. 3.4.5. Gross pathology of spleen from bone marrow chimera experiment in the IFNγR-/- background at day 20 p.i.. G, IFNγR -/- mice. GG, IFNγR -/- mice replaced with bone marrow cells from IFNγR -/- mice (Control) GW, IFNγR -/- mice with bone marrow cells from 129 Sv/Ev mice W, 129 Sv/Ev mice. Note the difference in the colour and size of the spleen primarily between the group 'G' and 'GW'. Bar = 1cm

Figure.3.4.6. Histopathological changes in the spleen of MHV-68 infected mice in the bone marrow chimera experiment (129 Sv/Ev ⇒ IFNγR-/-) – Day 12 and Day 16 p.i.

Haematoxylin and Eosin staining.

The spleens of control chimera (IFNγR-/- ⇒ IFNγR-/-) (B) showed features of active TBM reaction like that of IFNγR-/- mice (A) at day 12 p.i. The TBM reaction was less intense in gamma chimera (129 Sv/Ev ⇒ IFNγR-/-) and 129 Sv/Ev mice at this time point (C and D). At day 16 p.i. the lymphoid follicle area was occupied by macrophage like cells in control chimera (IFNγR-/- ⇒ IFNγR-/-) and IFNγR-/- mice (E and F). In 129 Sv/Ev mice and gamma chimera mice (129 Sv/Ev ⇒ IFNγR-/-) the TBM reaction was more intense than seen at day 12 p.i (G and H). In summary, control chimera (IFNγR-/- ⇒ IFNγR-/-) and IFNγR-/- mice behaved similar and gamma chimera (129 Sv/Ev ⇒ IFNγR-/-) and 129 Sv/Ev mice behaved similar at both time points (day 12 and day 16 p.i.).

Magnification 200X.

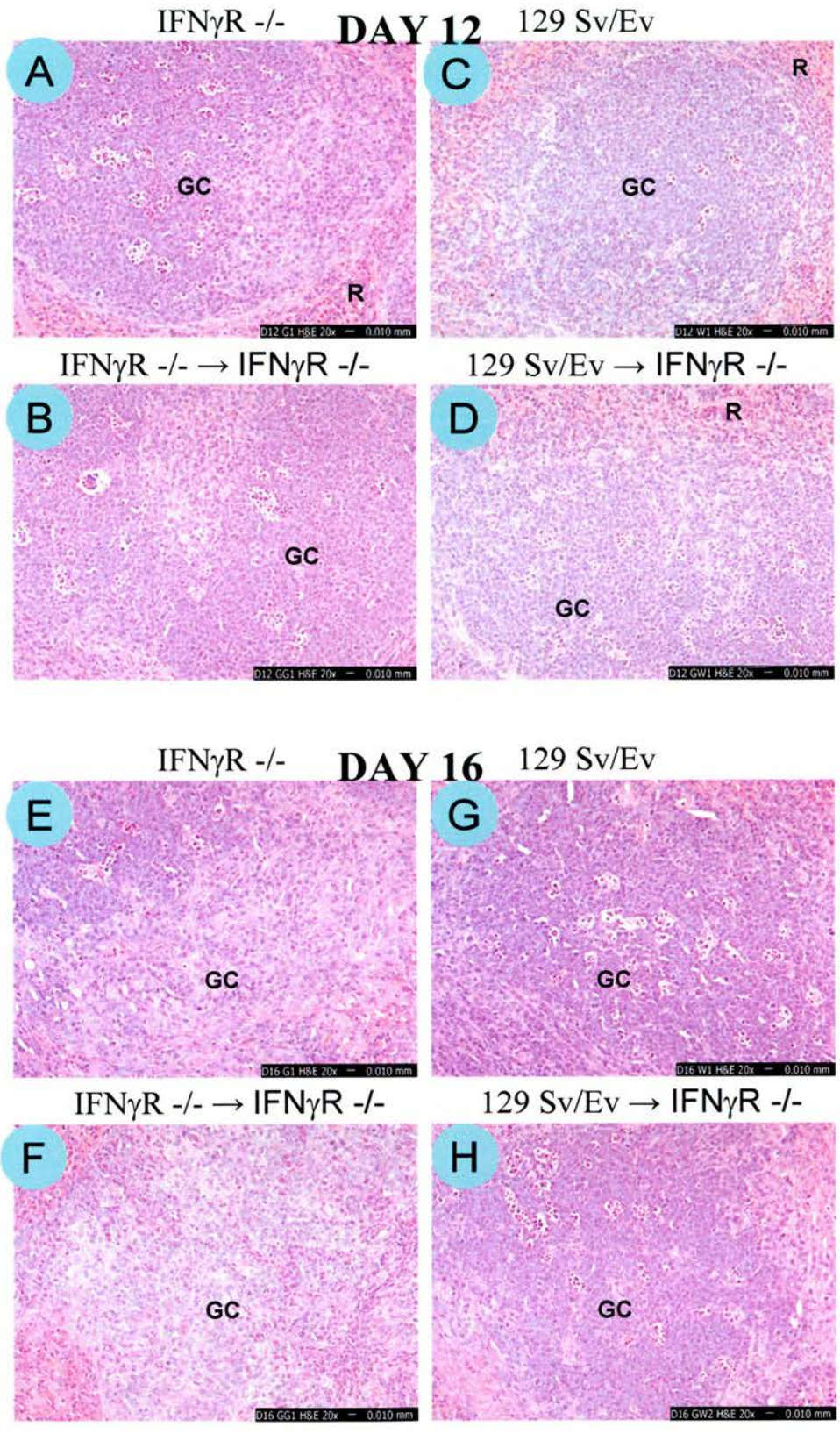

Figure. 3.4.6. Please see the facing page for legend

fibroblastic morphology. A pinkish red amorphous material encircled such disfigured lymphoid follicles (Figure 3.4.7D). At day 20 p.i, the spleens of IFNγR$^{-/-}$ mice and control chimera mice (IFNγR$^{-/-}$ ⇒ IFNγR$^{-/-}$) showed features of splenic fibrosis as described in earlier experiments. At day 35 p.i., the spleens of gamma chimera mice (129Sv/Ev ⇒ IFNγR$^{-/-}$) showed features of recovery with more mature lymphocytes in the lymphoid follicles. Hemosiderin laden macrophages were noticed in the red pulp. Similar changes were noticed in IFNγR$^{-/-}$ mice as well as control chimera mice (IFNγR$^{-/-}$ ⇒ IFNγR$^{-/-}$). The spleen from 129 Sv/Ev mice showed mild GC reaction with very few TBM.

Further characterisation of the histopathological change observed in the spleen of gamma chimera mice (129Sv/Ev ⇒ IFNγR$^{-/-}$) was investigated by histochemical techniques including Masson's trichrome (MT) and Martius yellow-brilliant crystal scarlet-soluble blue (MSB). The MT technique showed that the dark pinkish amorphous material seen around the lymphoid follicles was not collagen (Figure 3.4.8D). The MSB technique confirmed the observation and showed that the pinkish amorphous material was fibrin (Figure 3.4.8E). This shows that replacing the BMDC in IFNγR$^{-/-}$ mice with BMDC from 129 Sv/Ev mice prevented the development of splenic fibrosis following MHV-68 infection. However, it appears that the mechanism by which gamma chimera mice (129Sv/Ev ⇒ IFNγR$^{-/-}$) control the development of fibrosis is not exactly similar to the mechanisms operating in wild type mice. Detailed cellular and virological characterisation of sequential events is required to delineate the underlying mechanism.

3.4.4. SUMMARY

The bone marrow chimera mice experiments further confirmed the contributory role of IFNγ responsiveness of bone marrow derived cells in the pathogenesis of splenic fibrosis. It was more evident in bone marrow chimera mice in the IFNγR$^{-/-}$ background (129Sv/Ev ⇒ IFNγR$^{-/-}$). Replacing the BMDC in IFNγR$^{-/-}$ mice with BMDC from wild type mice prevented the development of fibrosis in the spleen. The histopathological features of the spleen at day 20 p.i. from gamma chimera

Figure.3.4.7. Histopathological changes in the spleen of MHV-68 infected mice in the bone marrow chimera experiment (129 Sv/Ev ⇒ IFNγR-/-) – Day 20 and Day 35 p.i.

Haematoxylin and Eosin staining.

The spleens of IFNγR-/- mice (A) and control chimera mice (IFNγR-/- ⇒ IFNγR-/-) (B) showed features of splenic fibrosis and shrunken lymphoid follicles at day 20 p.i. The gamma chimera mice (129 Sv/Ev ⇒ IFNγR-/-) showed normal red pulp as like 129 Sv/Ev mice at day 20 p.i (C and D). However, the white pulp lymphoid follicles differed significantly with 129 Sv/Ev mice. The lymphoid follicles of gamma chimera mice showed depleted number of lymphocytes which were replaced by macrophage like/ fibroblast like cells. Such disfigured lymphoid follicles were encircled by dense dark pink amorphous material (arrow in 3.5.7D). At day 35 p.i. the spleens from IFNγR-/- mice, control chimera (IFNγR-/- ⇒ IFNγR-/-) and gamma chimera (129 Sv/Ev ⇒ IFNγR-/-) (E, F, and H) showed features of recovery with mature lymphocytes in the lymphoid follicles. Hemosiderin laden macrophages are also present in the red pulp (Brown pigmented cells).The spleen from 129 Sv/Ev mice showed minimal TBM activity (G).

GC, Germinal Centre. R, Red pulp
Magnification 200X.

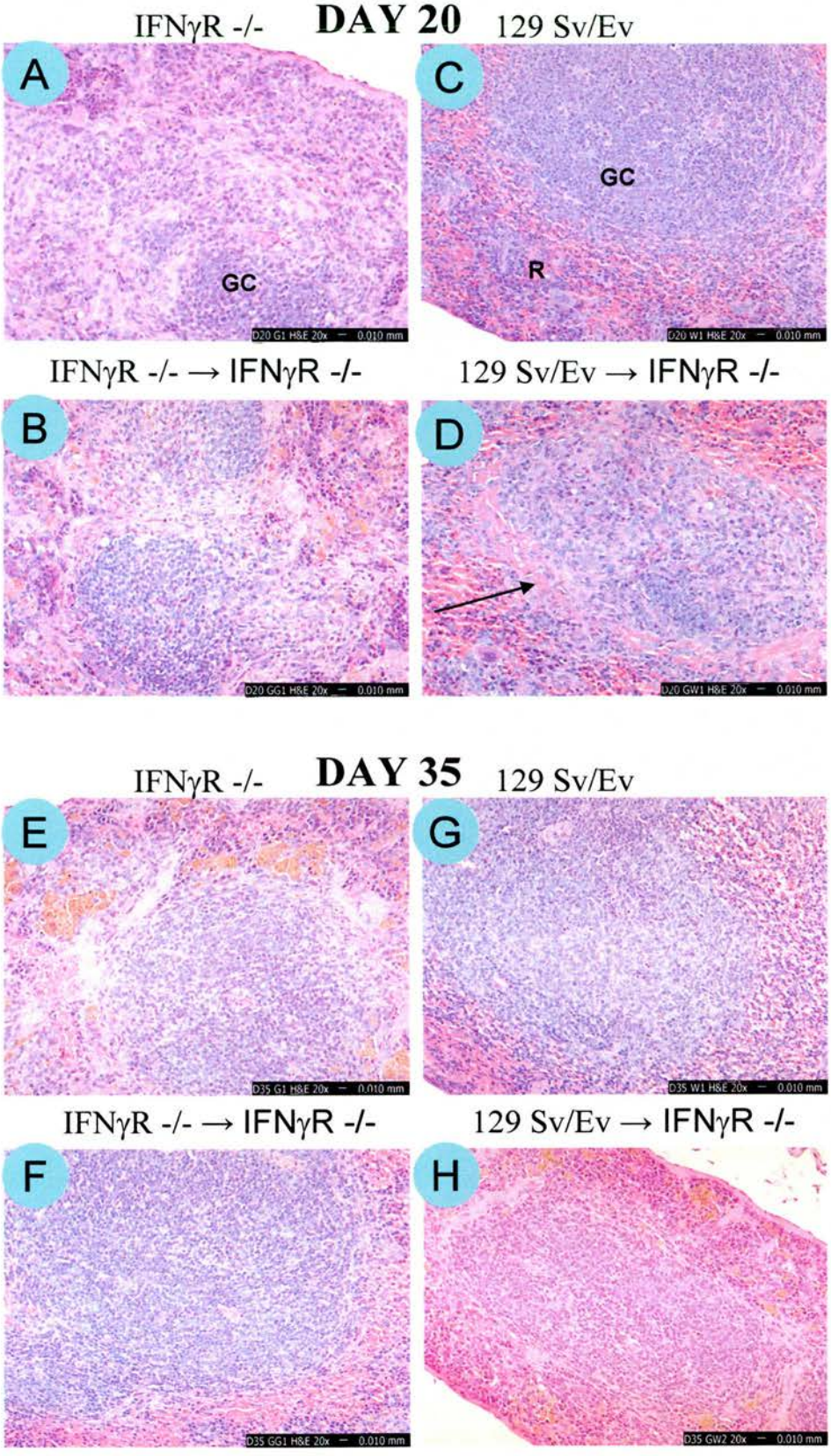

Figure. 3.4.7. Please see the facing page for legend

Figure.3.4.8. Histochemical characterisation of pathological changes in the spleen of MHV-68 infected mice in the bone marrow chimera experiment (129 Sv/Ev ⇒ IFNγR-/-) – Day 20.

Masson's Trichrome stain (Analine blue as the counter stain). A, IFNγR-/- mice, B, control chimera (IFNγR-/- ⇒ IFNγR-/-) C, 129 Sv/Ev mice. D, Gamma chimera - (129 Sv/Ev ⇒ IFNγR-/-).

The spleens of IFNγR-/- mice (A) and control chimera mice (B) showed features of splenic fibrosis in the subcapsular and perifollicular locations. The gamma chimera (129 Sv/Ev ⇒ IFNγR-/-) and 129 Sv.Ev mice did not show positive for collagen except on few strands of trabeculae (C and D). More interestingly, the amorphous pink substance noticed around perifollicular area in H& E sections were not positive for collagen (arrow in D).

The MSB technique confirmed that the amorphous pinkish material was fibrin in nature (Arrow) (E)

Magnification 100X in images A, B C and D. In image E, magnification 200X

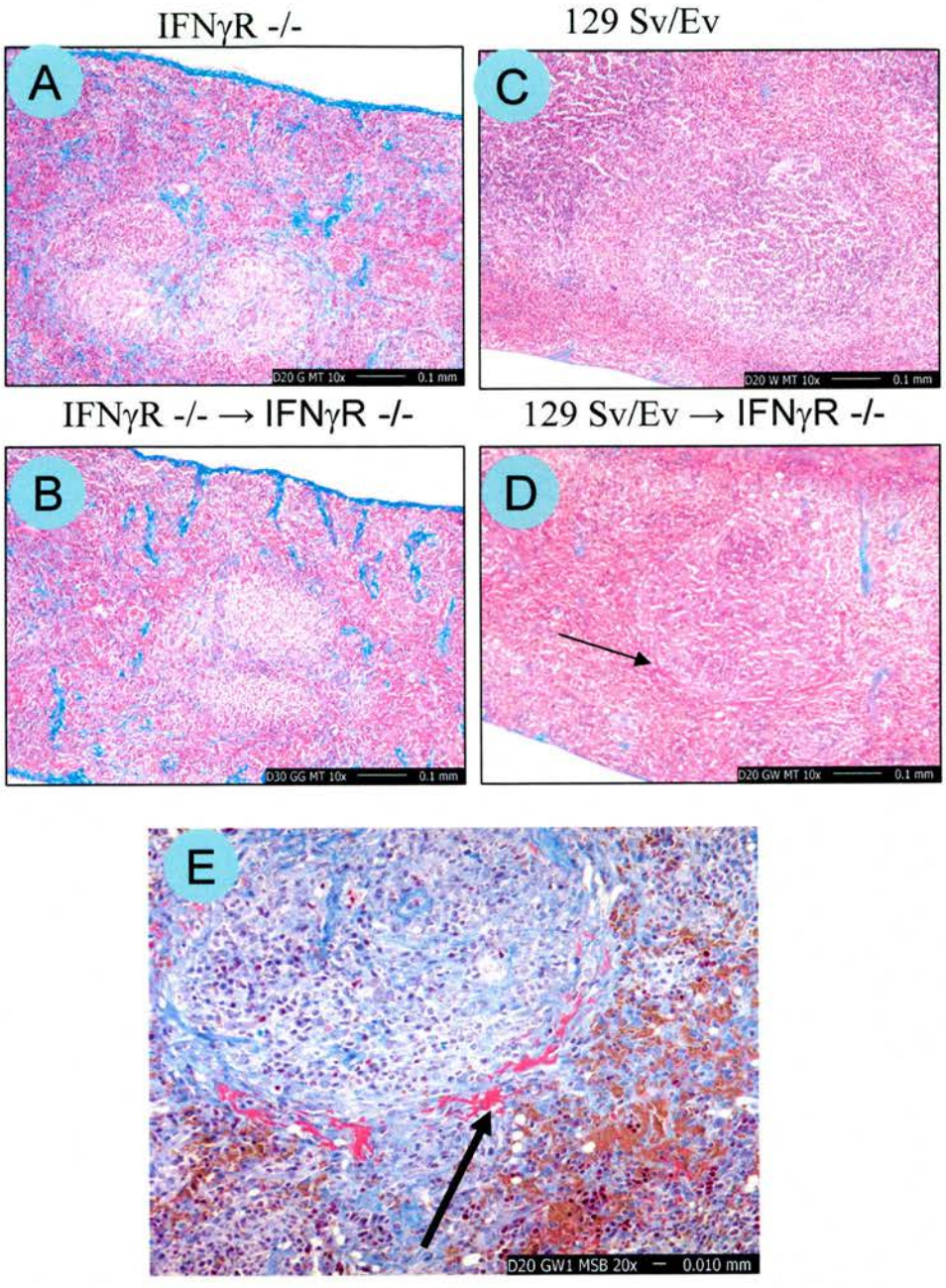

Figure. 3.4.8. Please see the facing page for legend

mice (129Sv/Ev ⇒ IFNγR$^{-/-}$) indicated distinct mechanisms involving the generation of a fibrin meshwork around the lymphoid follicles. Further sequential cellular and virological characterisation is required to understand the exact mechanism involved in this process. It is reasonable to argue that, if the replacement of BMDC from wild type mice into IFNγR$^{-/-}$ mice could prevent the development of splenic fibrosis, replacing the BMDC of wild type mice with bone marrow from IFNγR$^{-/-}$ mice should make the wild type chimera mice (IFNγR$^{-/-}$ ⇒129Sv/Ev) susceptible to the development of splenic fibrosis. However, the wild type chimera mice (IFNγR$^{-/-}$⇒129Sv/Ev) behaved similar to any other wild type mice irrespective of replacement of bone marrow. One of the reasons for such a phenotype in wild type chimera mice (IFNγR$^{-/-}$⇒129Sv/Ev) would be the partial success in the formation of chimera state as noticed in the PCR of DNA from peripheral blood. In other words, it suggests that, inspite of replacing the majority of BMDC in the 129 Sv/Ev mice with cells un-responsive to IFNγ, the remaining few cells with ability to respond to IFNγ could prevent the development of fibrosis in the spleen of wild type chimera mice (IFNγR$^{-/-}$ ⇒129Sv/Ev). It will be interesting to pursue the mechanisms by which the limited number IFNγ responsive cells in the spleen of wild type chimera (IFNγR$^{-/-}$ ⇒129Sv/Ev) mice manage to prevent the development of fibrosis in the spleen.

3.5. ROLE OF PRODUCTIVE AND LATENT VIRUS INFECTION IN THE PATHOGENESIS OF SPLENIC FIBROSIS

The biology of gammaherpesvirus infection in their natural host is not completely understood. From the pathogenesis studies using MHV–68 infections in different strains of mice, it has become apparent that, there are four distinct components of gammaherpesvirus infection in their natural host: (a) acute infection (b) latent infection (c) reactivation from latency and (d) persistent replication. The relationship between these components of infection is not well defined, especially the factors involved in the maintenance of latency and triggers responsible for reactivation of virus.

The role of IFNγ in the control of MHV-68 infection has been extensively studied and it is generally accepted that IFNγ has little role in the control of acute infection in lung, even though the infected mice produce large quantities of IFNγ (Sarawar *et al.*, 1996;Sarawar *et al.*, 1997;Dutia *et al.*, 1997). However, one study reported that infection of IFNγ$^{-/-}$ mice resulted in mortality of one third of infected mice (Kulkarni *et al.*, 1997). The CD4+ T- lymphocyte mediated control of MHV-68 infection in B –lymphocyte deficient mice was shown to be mediated by IFNγ (Christensen *et al.*, 1999). It has been shown that IFNγ controls persistent replication in peritoneal exudate cells (PEC) but not in splenocytes. In this experiment involving intraperitoneal infection of IFNγ$^{-/-}$ mice, ex–vivo reactivation from latency was strikingly low in splenocytes compared to PEC (Tibbetts *et al.*, 2002). Recently, it has been shown that, control of acute and latent MHV-68 infection mediated by CD4+ T lymphocytes require IFNγ (Sparks-Thissen *et al.*, 2005).

The traditional techniques (Plaque assay) used for detection of acute lytic viral infection involved mechanical disruption of cells most commonly by freezing and thawing of organ homogenate, mixing it with a permissive monolayer of cells and observing the development of plaques. Plaques are counted after four to five days of incubation (Sunil-Chandra *et al.*, 1992a). This technique could not detect low level of preformed infectious virus during long term latent infection (Flano *et al.*,

2000;Flano *et al.*, 2002a;Weck *et al.*, 1996;Weck *et al.*, 1999b) except in the case of an immunocompromised host where there is enhanced reactivation from latency or persistent lytic virus replication (Cardin *et al.*, 1996;Dal Canto *et al.*, 2001). Considerable improvement to this technique has been carried out recently to enhance the sensitivity of the assay in the form of mechanical and enzymatic digestion of tissue and mechanical disruption of isolated cells using beads. The virus was then assayed in a one week plaque assay in 12 well plates. The improved assay for lytic virus was able to detect low levels of infectious virus (<100 PFU/tissue) in both spleen and lung during long term latent infection (Flano *et al.*, 1999).

Latency is usually assessed by an 'infectious centre' assay, which measures the ability of viable latently infected cells to reactivate *in vitro* and form plaques on a permissive monolayer (Sunil-Chandra *et al.*, 1992b). Theoretically this technique would detect preformed lytic virus as well. More sensitive limiting dilution assays coupled with PCR for viral DNA in paired samples have shown that non reactivatable latently infected cells are present in higher concentration in latently infected tissues (Weck *et al.*, 1999a).

Immunohistochemical and i*n situ* hybridisation techniques have the ability to implicate the cell types harbouring the infection based on their distribution pattern and morphology of the infected cell. In addition, the *in situ* hybridisation technique will identify the actual number of latently infected cells rather than the latently infected cells reactivating *ex vivo* in an *in vitro* system. In the present study, immunohistochemistry and *in situ* hybridisation technique as detailed in the Materials and Methods section 2.6 and 2.7 were carried out to assess the profile of virus infection in spleen at close time intervals ranging from day 8 p.i. to day 120 p.i. Sections of spleen from experiment no.1 and 2 were used for this purpose.

3.5.1. PRODUCTIVE INFECTION AND PATHOGENESIS OF FIBROSIS

The viral antigen positive cells detected by immunohistochemistry with a polyclonal antibody raised against MHV-68 in rabbit were quantified from all

mice from experiment no.1 and 2. The distribution pattern of viral antigen positive cells was predominant in the marginal zone of the spleen in both groups of mice (Figure 3.5.1). The productively infected cells appeared to be large cells with fairly large cytoplasm and centrally placed large nucleus. The staining was in both nucleus and cytoplasm with intense colour reaction in the nucleus. There were no viral antigen positive cells in both groups of mice at day 8 p.i. Viral antigen positive cells were present at day 10 p.i in both groups of mice and from then onwards the number of viral antigen positive cells showed the same trend in both 129 Sv/Ev mice and IFNγR$^{-/-}$ group of mice with peak of viral antigen positive cells detected at day 14 p.i. However, the number of viral antigen positive cells was higher in IFNγR$^{-/-}$ mice compared with 129 Sv/Ev groups of mice (Figure 3.5.1). In addition, the IFNγR$^{-/-}$ mice never showed any viral antigen positive cells in the spleen after day 20 post infection, whereas in 129 Sv/Ev mice there were viral antigen positive cells at late time points (Day 30, 35, 40 and 45) indicating reactivation of productive infection or low level of persistent infection in the spleen. Interestingly the viral antigen positive cells were seen in the marginal zone of the spleen during this phase of infection as well (Figure. 3.5.2).

3.5.2. LATENT INFECTION AND PATHOGENESIS OF FIBROSIS

A representative sample of spleen from both groups of mice at every time point used in the first and second experiment was assessed for latent infection by *in situ* hybridisation technique with a riboprobe specific for viral tRNA 1-4 of MHV-68. All the latently infected cells were mainly found with in the centre of the lymphoid follicles and the cells were small in size with limited cytoplasm suggestive of lymphocytes. This preliminary analysis suggested significant difference in the biology of latent infection in the spleens of IFNγR$^{-/-}$ mice and 129 Sv/Ev mice. There were no latently infected cells in the spleens of both groups of mice at day 8 p.i. Latently infected cells were detected in both groups of mice from day 10 p.i. In 129 Sv/Ev mice the latently infected cells were found at relatively low levels at later time points. In contrast, in IFNγR$^{-/-}$ mice, higher number of latently infected cells were observed from day 10 p.i. to day 20 p.i.

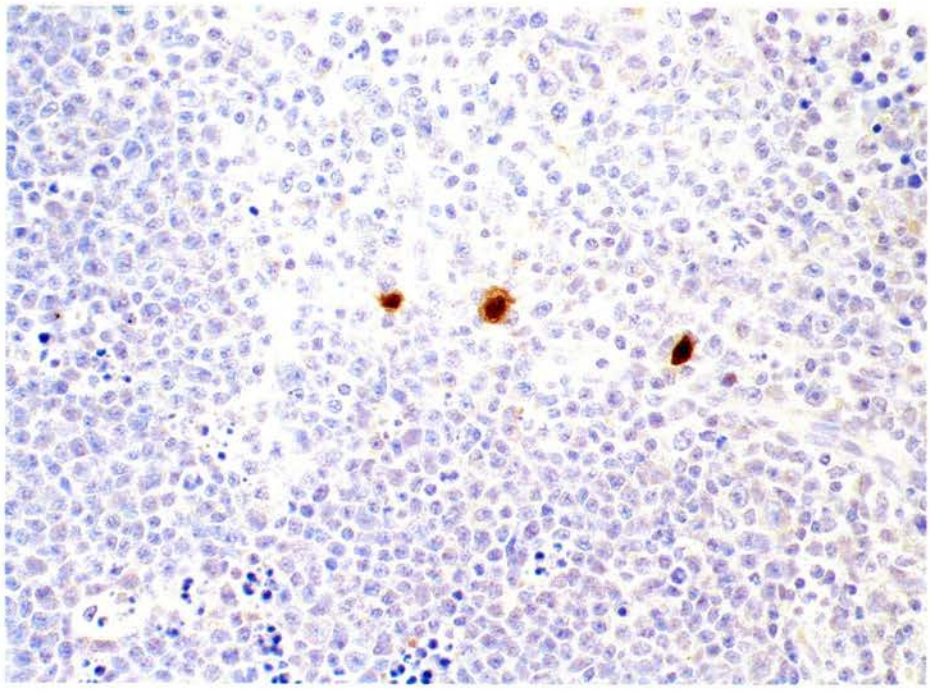

Number of productively infected cells in the spleen - Immunohistochemistry – Experiment No.1

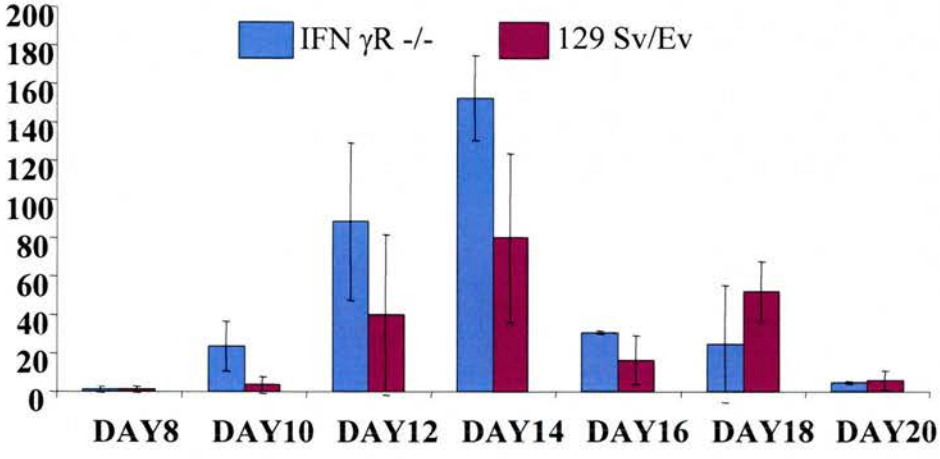

Figure.3.5.1. Number of productively infected cells in the spleen detected by immunohistochemistry using anti–rabbit MHV–68 polyclonal antibody. All the antigen positive cells were counted from all the spleen sections (2-3 mice at each time point) and the average count with standard deviation is presented in the bar diagram. On an average two adjacent spleen sections were stained for viral antigen. A representative section of spleen with viral antigen positive cells (Brown colour) is presented in the top of the page. Objective magnification – 400X

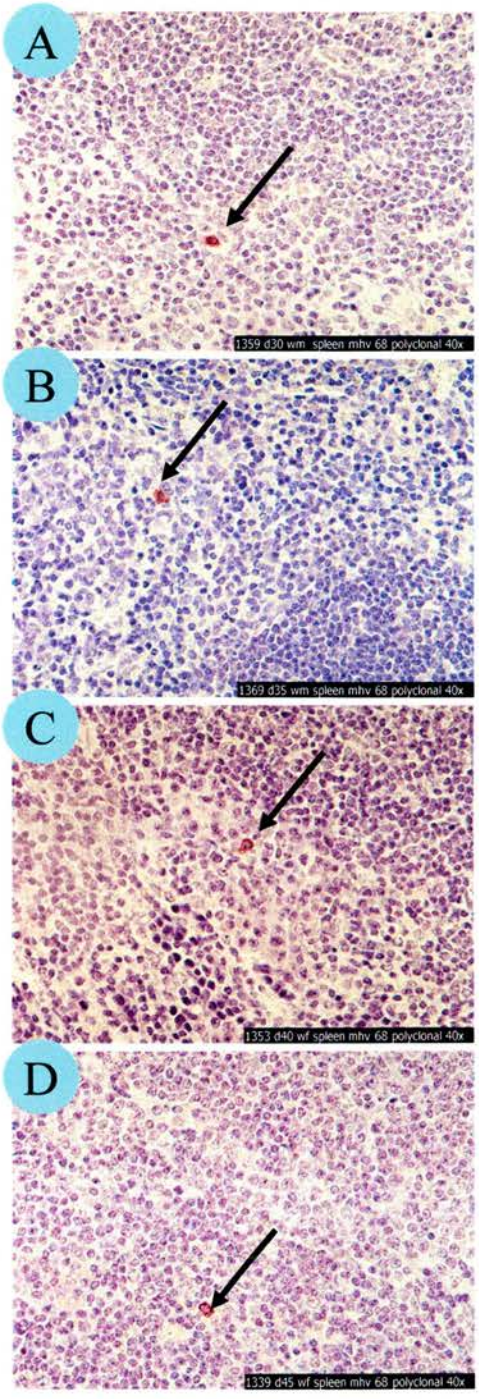

Figure. 3.5.2. Virus antigen positive cells in the spleen of 129 Sv/Ev mice detected by immunohistochemistry using anti – rabbit MHV –68 polyclonal antibody. Panel A, Day 30 P.I. Panel B, Day 35 P.I. Panel C, Day 40 P.I. Panel D, Day 45 P.I. Positive cells are brown in colour and indicated by arrows. Objective magnification 400X

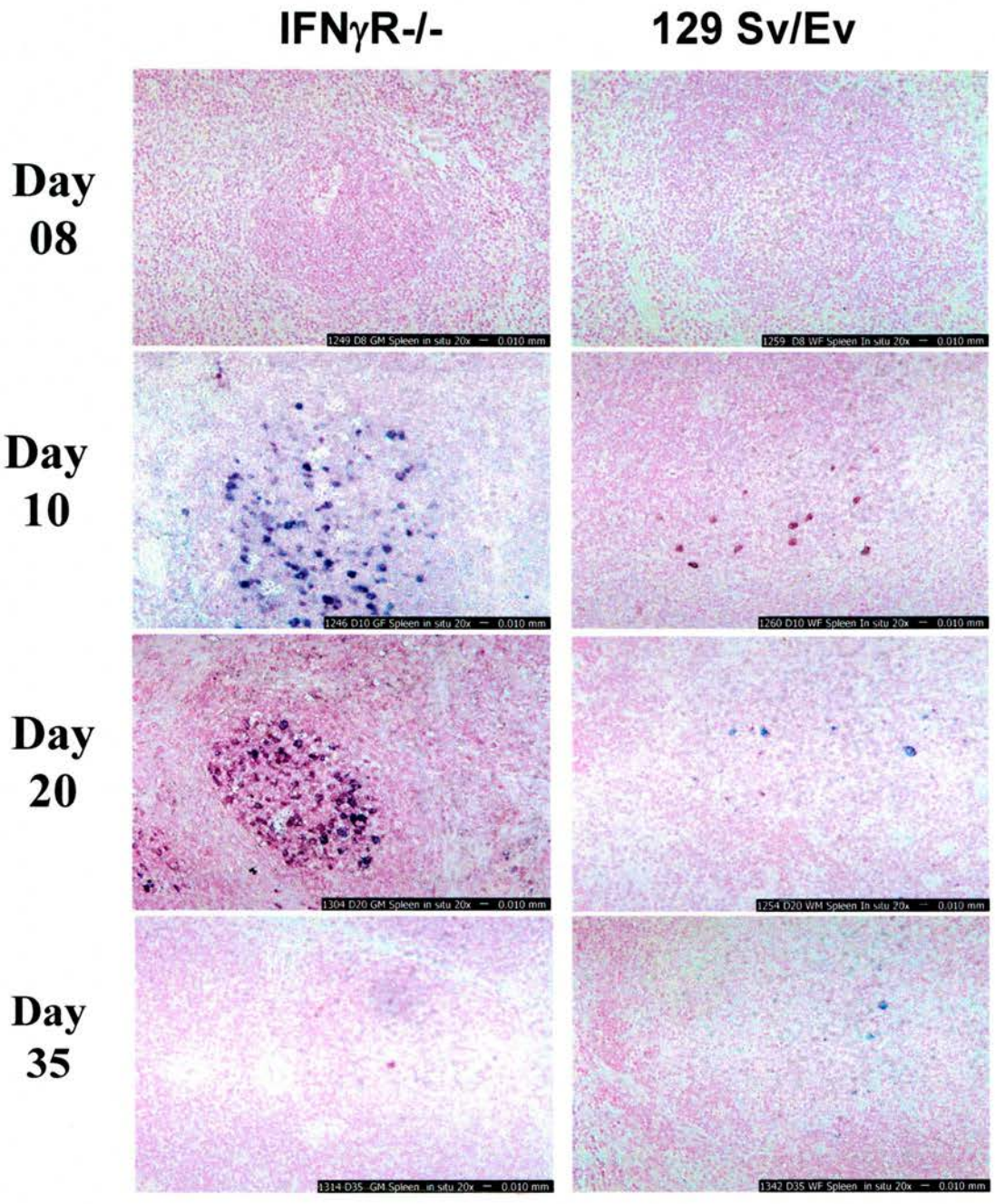

Figure. 3.5.3. *In Situ* Hybridisation with a riboprobe specific for MHV-68 vtRNA 1-4 to detect latently virus infected cells in the spleen . Note the relative increase in the number of latently infected cells in the spleen of IFNγR-/- mice at day 10 and day 20 p.i. A significant reduction in the number of latently infected cells is noticed at day 35 p.i. in IFNγR-/- mice

Magnification 100X

At day 20 p.i. there was marked fibrosis in the spleen along with shrinkage of white pulp lymphoid follicles. Interestingly, there were few or no latently infected cells in the spleen at later time points in IFNγR$^{-/-}$ mice. (Figure 3.5.3.) These observations suggested that fibrosis, as a process was able to contain the expansion of latently infected cells in the spleen. To confirm this hypothesis, an additional experiment was conducted. A set of age and sex matched IFNγR$^{-/-}$ mice and 129 Sv/Ev mice were infected with MHV-68 as described in Materials and Methods section 2.4. This experiment had close time intervals between day 18 p.i and day 30 p.i. and at each time point three mice were used. For 129 Sv/Ev group of mice time point 20 and 30 day p.i. was taken. All the sections of spleen from this experiment were subjected to *in situ* hybridisation with riboprobe against vtRNA 1-4. As shown in Figure 3.5.4, there was a progressive reduction in the number of latently infected cells in the spleen of IFNγR$^{-/-}$ mice from day 18 p.i. to day 30 p.i. At day 18 p.i. all three mice carried latently infected cells in their tightly packed lymphoid follicles and then showed a gradual reduction in the number of lymphoid follicles infected with latent virus, as well as the total number of latently infected cells. As seen in the preliminary experiment the spleens collected at day 30. p.i. had no latently infected cells suggesting that there was a absence of latently infected cells in the spleen by day 30 p.i. All the spleens of 129 Sv/Ev mice at day 20 and 30 p.i. carried moderate numbers of latently infected cells (figure 3.5.5). At least two adjacent sections of the spleen were stained by the *in situ* hybridisation technique. The percentage of lymphoid follicles carrying latently infected cells and total number of latently infected cells from all the spleen sections were estimated by examination of stained sections under a light microscope and the data is presented in table 3.5.1.

3.5.3. SUMMARY

The study for assessing the productive and latent infection in the spleen showed a difference in the level of both forms of infection in the spleen between IFNγR$^{-/-}$ mice and 129 Sv/Ev mice. The levels of productive infection in the lymphoid organs are beyond the level of detection of conventional techniques and hence data on the level of productive infection in the spleen in normal mice is scant.

Table 3.5.1. Latent virus infection in the spleen determined by *in situ* hybridisation technique

Day	Animal No	Percentage of follicles latently infected with MH V-68	Total number of latently infected cells in the spleen section
IFNγR$^{-/-}$			
18	G1	100	864
	G2	100	280
	G3	100	637
22	G1	72.72	526
	G2	42.85	20
	G3	73.3	122
24	G1	50	9
	G2	66.7	53
	G3	76.47	229
26	G1	7.69	1
	G2	0	0
	G3	0	0
28	G1	0	0
	G2	9.1	30
	G3	0	0
30	G1	0	0
	G2	0	0
	G3	0	0
129 Sv/Ev			
20	W1	11.76	32
	W2	68.96	120
	W3	15	6
30	W1	53.84	136
	W2	13.04	80
	W3	27.9	99

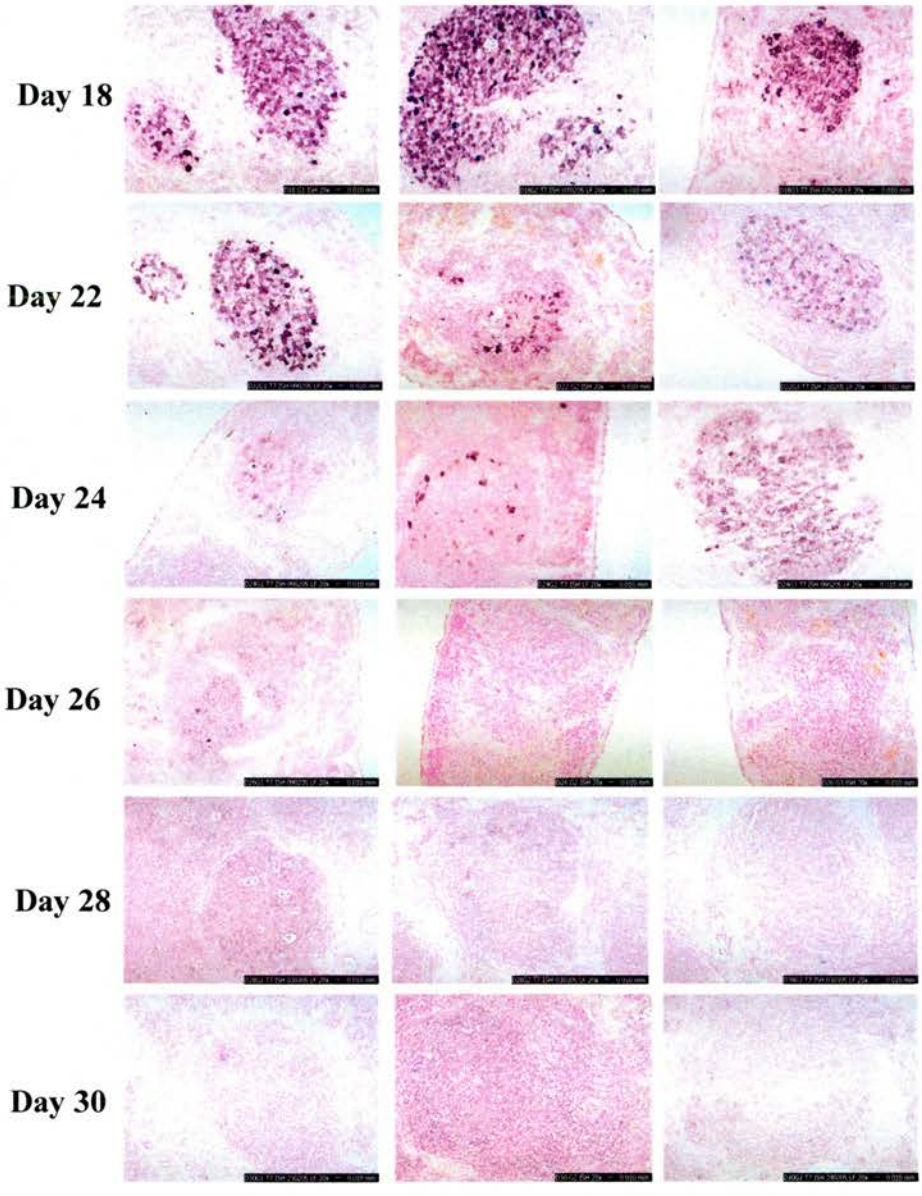

Figure. 3.5.4. *In Situ* Hybridisation with a riboprobe specific for MHV-68 vtRNA 1-4 to detect latently infected cells in the spleen of IFNγR-/- mice infected with MHV-68. (day 18 p.i. to day 30 p.i.). Three mice each in all time points. Note the gradual disappearance of latently infected cells in the spleen with complete absence at day 30 p.i.

Magnification 200X

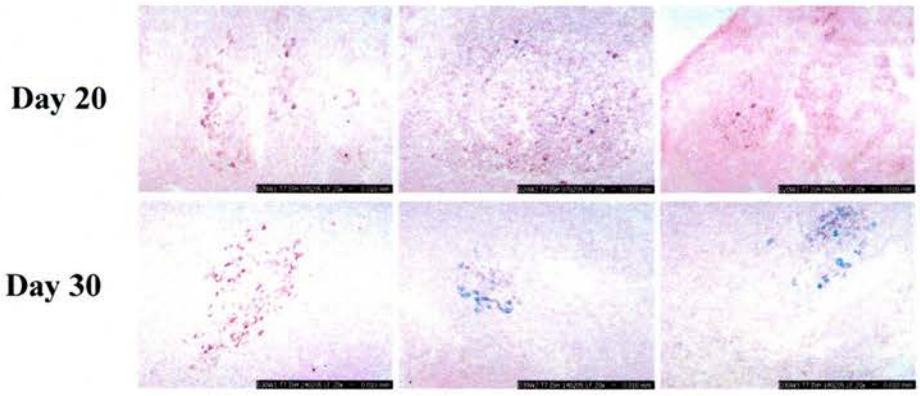

Figure. 3.5.5. *In Situ* Hybridisation with a riboprobe specific for MHV-68 vtRNA 1-4 to detect latently infected cells in the spleen of 129 Sv/Ev mice infected with MH V-68. (day 20 p.i. and day 30 p.i.). Three mice each at both time points. Note the presence of uniform number of latently infected cells in the spleen at day 20 p.i. and day 30 p.i.

Magnification 200X

Dutia *et al* (1997) investigated the level of productive infection in the spleen of IFNγR$^{-/-}$ mice in comparison to 129 Sv/Ev mice following MHV–68 infection by plaque assay and found no evidence of productive infection in 129 Sv/Ev mice at any time point, whereas a low level of infectious virus (< 50 PFU/10^7 cells) was noticed in IFNγR$^{-/-}$ mice. The present study employing immunohistochemistry with a polyclonal antiserum showed productive infection in the spleen from day 10 p.i. The number of productively infected cells showed a similar pattern in both groups of mice with a peak at day 14 p.i. A negligible number of productively infected cells were detected at day 20 p.i. in both groups of mice. However, the number of productively infected cells was invariably higher in IFNγR$^{-/-}$ mice.

The interesting feature of the profile of productive infection is the absence of any productively infected cells in the spleen of IFNγR$^{-/-}$ mice after day 20 p.i. In contrast, in 129 Sv/Ev mice there were a limited number of productively infected cells at day 30, 35, 40 and 45 p.i. suggestive of low grade persistence of productive infection or reactivation from a latent infection. The most interesting feature of the productively infected cells during early times or later in infection is their location within the spleen. At all times, the productively infected cells were seen in the marginal zone of spleen and not in the GC. The earlier description of the location of productively infected cells in the spleen of mice depleted of CD8+ T-lymphocyte prior to infection with MHV-68 was also at the marginal zone of the spleen (Ehtisham *et al.*, 1993).

The profile of latently infected cells showed dramatic differences between the two groups of mice over the course of infection. There were no latently infected cells detectable by the expression of viral tRNA like molecules in the spleen of both groups of mice at day 8 p.i. From day 10 onwards, the number of latently infected cells increased in number in both groups of mice, however the rate of expansion was higher in IFNγR$^{-/-}$ mice compared to 129 Sv/Ev mice. The number of latently infected cells reached a peak around day 18 - day 22 p.i, which is mirrored, by the peak of fibrotic changes in the spleen. The exponential increase in the number of latently infected cells showed a dramatic decline to negligible numbers at day 30

p.i and subsequent time points. Interestingly, this decline in latently infected cells is mirrored by the re-population of the spleen with new cell populations in their respective locations. These observations suggest the following: 1) Fibrosis as a host response mechanism is able to contain the expansion of latently infected cells in the spleen. 2) Presence of latently infected cells in the spleen might be the factor responsible for triggering the fibrosis development. 3) Loss of latently infected cells in the spleen is the trigger for re-population of the spleen.

3.6. DISCUSSION

The ability of the body to replace dead cells is a primary requirement for survival. The response towards the loss of cells in tissues is broadly classified as regeneration and fibrosis. Fibrosis is defined as the replacement of the normal structural elements of the tissue by distorted, non-functional and excessive accumulation of scar tissue (Diegelmann and Evans, 2004). The cascade of events leading to the development of fibrosis include excessive tissue injury and cell loss, infiltration of inflammatory cells, generation of growth factors, attraction and proliferation of extra cellular matrix (ECM) producing cells, laying down and organisation of ECM. The cellular response and micro–environment following tissue injury and cell loss are also critical in the pathogenesis of fibrosis. It has been recognised that the Th2 type of T-lymphocyte response and subsequent alternate activation of macrophages are crucial in the genesis and maintenance of a strong fibrotic response (Wynn, 2004)

The cellular, virological and molecular events taking place in the spleen during the development and resolution of fibrosis described earlier is schematically presented in figure 3.6.1. The observations made during the current investigation on splenic fibrosis will be discussed around the following themes.

1. Cell loss as a trigger
2. The role of gamma interferon
3. Alternate activation of macrophages
4. The role of virus

3.6.1. CELL LOSS AS A TRIGGER FOR SPLENIC FIBROSIS

Earlier studies on splenic fibrosis following MHV-68 infection in IFNγR$^{-/-}$ mice reported that there were 10-100 fold fewer cells in the fibrotic spleen at the height of fibrosis. The drop in cell numbers occurred in B-cell, CD4+ and CD8+ T-lymphocyte populations (Dutia *et al.*, 1997;Ebrahimi *et al.*, 2001). Though all the three subsets of lymphocytes showed a reduction, consideration of their relative number in the spleen suggested that loss of B-lymphocytes would have

Figure 3.6.1. The cellular, virological and molecular events involved in the pathogenesis and resolution of splenic fibrosis in MHV-68 infected IFN$\gamma R^{-/-}$ mice.

Day 08 – The spleen does not show any obvious changes in the spleen. Note the presence of different cell populations in their respective normal locations (B-lymphocytes in lymphoid follicles, T-lymphocytes in PALS , erythrocytes in the red pulp and macrophages mainly in the red pulp and marginal zone)

Day 12 – The spleen shows significant changes in the architecture of spleen. Note the presence of latently infected cells in the spleen along with invasion of T-lymphocytes and alternatively activated macrophages. Productively infected cells can be seen in the marginal zone of spleen.

Day 20 – The spleen shows 'fibrotic cage' formation around the shrunken lymphoid follicles packed with latently infected cells.

Day 35 – The spleen shows recovery phase characterised by re-population of lymphoid follicles with B-lymphocytes and absence of latently infected cells. Re- appearance of other cell – populations in their respective locations is also evident.

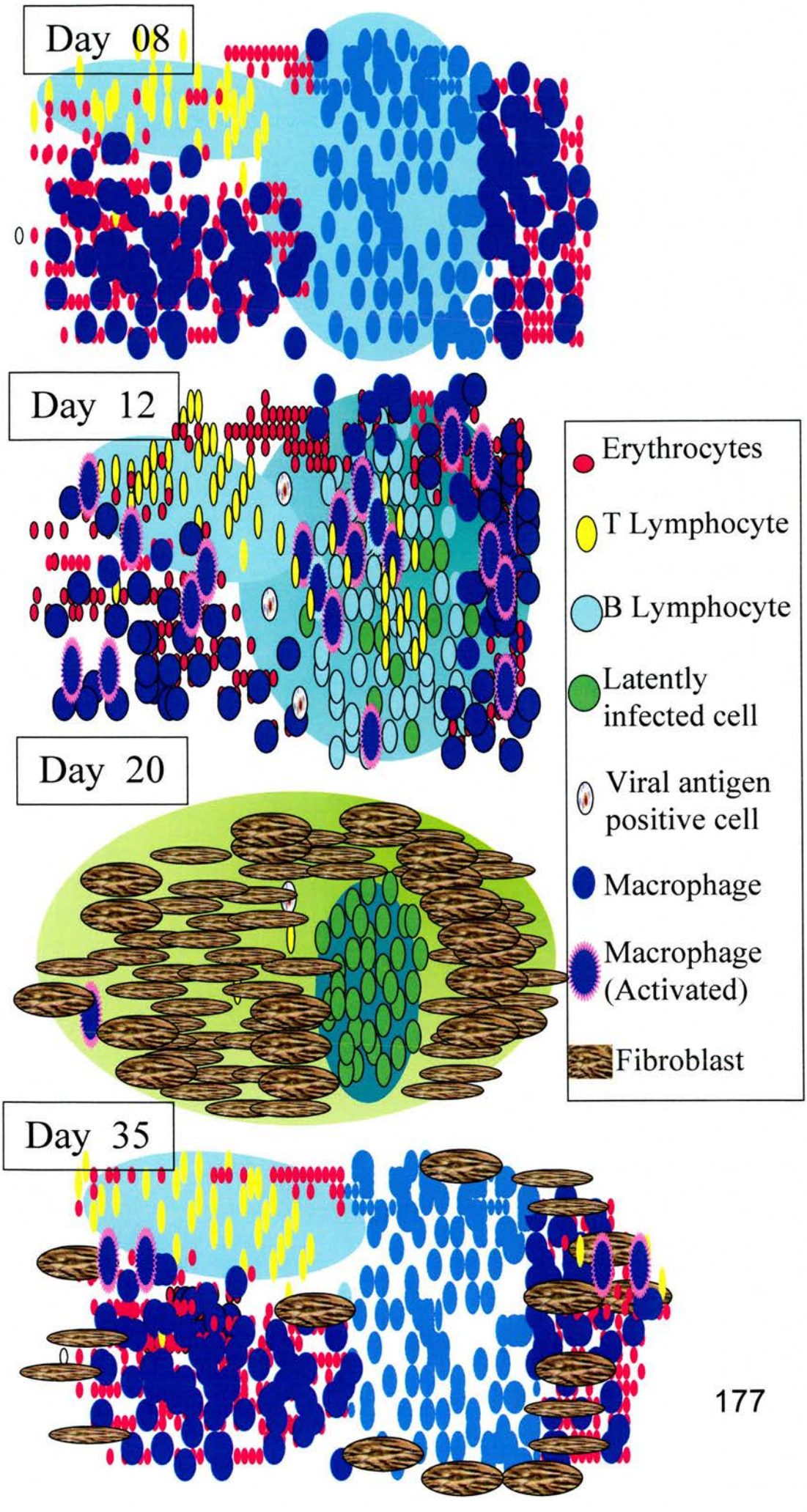
Day 08
Day 12
Day 20
Day 35
Erythrocytes
T Lymphocyte
B Lymphocyte
Latently infected cell
Viral antigen positive cell
Macrophage
Macrophage (Activated)
Fibroblast

more impact than other sets of lymphocytes. The survey of histopathological changes and cellular characterisation in the spleen during the current investigation identified key events, which are relevant to the development and resolution of fibrosis in the spleen. One of the key observations was the sequential reduction in the size of lymphoid follicles in the spleen and development of fibrosis centred on the shrinking lymphoid follicles ('fibrotic cage'). Day 20 p.i. is the peak time point where the highest level of fibrotic changes were seen coupled with shrunken white pulp nodules. The majority of the cell population in the shrinking lymphoid follicles are B-lymphocytes. From day 30 p.i. onwards the spleen gradually regains its normal structure, which became clear as early as day 35 p.i. and maintains this 'recovery' state until the last time point of the experiment. The recovery phase is characterised by re-population of different subsets of cells in the spleen and most profoundly, the B-lymphocytes in the lymphoid follicles. These observations underline the fact that gradual depletion and subsequent re-population of mainly B–lymphocytes is the primary event taking place during the development and resolution of fibrosis respectively. Thus, one possibility is that the sequential reduction in the number of B-lymphocytes in the spleen is the primary trigger for the development of fibrosis.

3.6.2. THE ROLE OF GAMMA INTERFERON

Failure in the signalling of IFNγ is absolutely central to the pathogenesis of splenic fibrosis following MHV-68 infections. Splenic fibrosis is not observed in mice with a normal IFNγ signalling system. In the bone marrow chimera experiments, replacing the BMDC in the IFNγR$^{-/-}$ mice with normal cells with ability to respond to IFNγ could prevent the development of fibrosis in the spleen following MHV-68 infection. Even though the replacement of BMDC from wild type mice into IFNγR$^{-/-}$ mice could prevent the development of splenic fibrosis, replacing the BMDC of wild type mice with BMDC from IFNγR$^{-/-}$ mice showed no obvious effect following MHV-68 infection. The reason for such a phenotype in wild type chimera mice (IFNγR$^{-/-}$ ⇒ 129 Sv/Ev) could be the partial success in the formation of chimera state. In other words, presence of a comparatively lower

number of BMDC with ability to respond to IFNγ could prevent the development of fibrosis.

In the light of above argument, the questions to be considered on the role of IFNγ in the pathogenesis, specifically for the initial trigger of cell loss include: 1) whether the absence of IFNγ signalling contributes to the actual increased cell loss? Or 2) is absence of IFNγ response contributing to prevent the signalling required for the stimulation of haematopoietic stem cells (HSC) in the bone marrow and subsequent transfer of cells to the spleen?

The number of productively infected cells detected by immunohistochemical techniques was comparatively low to account for a massive cell loss. Moreover, the location of productively infected cells in the spleen was mainly in the marginal zone and the main area of cellular depletion was noticed in the lymphoid follicles. The majority of latently infected cells are found in the lymphoid follicles and latent infection is not known to cause cytolytic destruction of cells. In fact, the strategy adopted by gammaherpesvirus during the establishment of latency is to provide survival signals in the form of specific viral gene products to promote the survival of infected cells. The IFNγR$^{-/-}$ mice infected with MHV-68 show a progressive increase in the number of latently infected cells during the development of fibrosis. Thus, it appears that, either productive or latent virus infection of the splenocytes as such is not responsible for enhanced cell loss observed in IFNγR$^{-/-}$ mice following infection with MHV-68

IFNγ is a cytokine with anti–fibrotic activity. The known mechanisms by which IFNγ acts as an anti–fibrotic cytokine is by interfering with the downstream signalling of pro-fibrotic cytokines like TGFβ and IL-13 (See figure 1.4). While considering the role, if any of defective IFNγ signalling contributing to the increased cell loss in the lymphoid follicles, it is necessary to assess the type of cell loss taking place in the lymphoid follicles responding to an antigen. The lymphoid follicles respond to an invading antigen in the form of GC reaction. The GC is a dynamic micro–environment where B-lymphocytes responding to

adequate antigenic signals rapidly expand and differentiate through a pathway of centroblasts and centrocytes to either plasma cells or memory B cells. T-lymphocyte and follicular dendritic cells contribute immensely to sustain this response. B-lymphocytes, which do not receive adequate signals in this micro-environment, undergo cell death in the form of apoptosis. TBM, the resident professional scavengers in the GC will quickly remove the apoptotic cells in this environment (Guzman-Rojas *et al.*, 2002). During the process of B-cell transformation, somatic hyper- mutation of IgV_H and isotype switching from IgM to other isotypes take place. IFNγ is involved in the process of immunoglobulin isotype regulation (Snapper and Paul, 1987). $IFN\gamma R^{-/-}$ mice immunised with live attenuated pseudorabies virus produced highly reduced IgG2a type antibody confirming the role of IFNγ in isotype switching of immunoglobulin during immune response (Huang *et al.*, 1993). Reduced levels of IgG2a type antibody was also reported in $IFN\gamma R^{-/-}$ mice immunised with type II collagen in a study to determine the role of gamma interferon signalling in collagen induced arthritis (Kageyama *et al.*, 1998).

MHV–68 elicits virus-specific antibody, and non-specifically activates B-cells to produce antibody through a CD4+ T-cell dependent process. The antibody response is predominated by IgG2a and IgG2b isotypes (Sangster *et al.*, 2000). The influence of defective IFNγ signalling on the level and type of antibody response following MHV-68 infections was not investigated. Such an investigation would clarify the role of IFNγ in the stimulation of B-cells for antibody production following MHV-68 infections. The possibilities with regard to type of antibody response in the absence of IFNγ signalling include reduced IgG2 type antibody response and/or shifting of the antibody response towards IgG1 type characterised by Th2 type cytokine stimulation. If the antibody response had shifted to similar levels of IgG1 type, it can be assumed that the B-cells are receiving sufficient stimulatory signals of a different kind required for their survival. On the other hand, if the antibody response had not shifted towards IgG1 type and remained at a low level of the IgG2 type, this would suggest that the population of B-cells not receiving adequate signals required for their

transformation and survival would undergo apoptosis. This hypothetical scenario would support a contributory role for the absence of IFNγ signalling leading to enhanced cell death in the spleen.

The level of apoptosis among splenocytes during the course of infection with MHV-68 in IFNγR$^{-/-}$ mice was investigated by the terminal deoxynucleotide transferase–mediated dUTP nick end labelling (TUNEL) technique and concluded that the tempo, level and location of TUNEL positive cells in the spleen was similar in IFNγR$^{-/-}$ mice and wild type mice (Ebrahimi *et al.*, 2001). This observation suggests that splenic cell loss is not the result of increased cell death through the apoptotic pathway. The current investigation also approached the issue of increased cell death in the spleen during the development of fibrosis by way of estimating the average number of TBM in the spleen and found that, there was no obvious difference in the number of TBM in the spleen of IFNγR$^{-/-}$ mice and 129 Sv/Ev infected mice. This observation supports the earlier conclusion that increased cell death is not responsible for the cell loss in the spleen. However, it should be noted that the techniques employed in the current investigation as well as the TUNEL technique are not conclusive enough to estimate the level of apoptosis in an *in vivo* system. The histological snapshots detected by TUNEL staining and TBM counting techniques definitely give a flavour of apoptosis taking place in a tissue. However, the kinetics of apoptotic cell death and their phagocytic removal remains to be completely characterised in lymphoid organs where routine apoptosis of non-responsive lymphocytes and their subsequent removal are taking place. Based on the available evidence so far, it is possible to conclude that, defective IFNγ signalling is not contributing to enhanced splenic cell death in mice infected with MHV-68.

Another issue to be considered is: whether the absence of IFNγ signalling during MHV-68 infection in the spleen is responsible for preventing the stimulation of bone marrow haematopoietic stem cells (HSC) required for replacing the lost cells in the spleen? This aspect was considered earlier by measuring the cellularity of the femoral bone marrow during infection of IFNγR$^{-/-}$ mice with MHV-68 and

concluded that bone marrow cellularity was comparable between wild type and IFNγR$^{-/-}$ mice (Ebrahimi *et al.*, 2001). This observation suggests that bone marrow suppression is not a reason for splenic cell loss either. Viral infections responsible for lymphopenia are known to cause bone marrow suppression as well. For example, Human immunodeficiency virus (HIV) infection, which causes progressive CD4+T-lymphocyte depletion in the peripheral circulation, also causes bone marrow suppression responsible for chronic cytopenia and progression to the acquired immune deficiency syndrome (AIDS). The bone marrow suppression observed during HIV infection is due to infection of bone marrow cells themselves, HIV suppressive proteins and altered cytokine milieu, which shifts towards a Th2 type response [Reviewed in (Panoskaltsis and Abboud, 1999)]. Even though, there was no difference observed in the bone marrow cellularity between IFNγR$^{-/-}$ mice and wild type mice infected with MHV -68 infections (Ebrahimi *et al.*, 2001), it would be worthwhile examining the infection status of bone marrow cells during intranasal infection of mice with MHV-68.

In spite of the lack of a difference in the cellularity of the bone marrow, profound leukocytosis characterised by neutrophilia at day 10 p.i and lymphocytosis at day 14 p.i which peaked at day 23 p.i was reported during MHV-68 infection of IFNγR$^{-/-}$ mice (Ebrahimi *et al.*, 2001). Furthermore, cross transfer studies with peripheral blood leukocytes (PBL) taken from IFNγR$^{-/-}$ mice infected with MHV-68 (at day 23 p.i.) showed that, PBL were unable to enter the spleen of infected IFNγR$^{-/-}$ mice at the height of fibrosis indicating that a basic defect exists in the trafficking of lymphocytes back in to the spleen. In contrast, PBL were able to reach the spleen in IFNγR$^{-/-}$ mice prior to the development of fibrosis at day 10 p.i. The factors responsible for such a defective trafficking of lymphocytes into the spleen needs to be identified. These factors could be viral gene products under the strict regulatory control of IFNγ.

In summary, the contributory role of defective IFNγ signalling during MHV–68 infections for excessive cell loss as an initiator of fibrosis remains to be

delineated. The role of IFNγ as an anti–fibrotic cytokine inhibiting the signalling of pro- fibrotic cytokines like TGF-β and IL–13 also should be taken into consideration.

3.6.3. ALTERNATE ACTIVATION OF MACROPHAGES

Infiltration of inflammatory cells is a characteristic feature of the pathogenesis of fibrosis. In IFNγR$^{-/-}$ mice infected with MHV-68, the invasion of lymphoid follicles with T-lymphocyte (both CD4+ and CD8+) and different subsets of splenic macrophages was noticed from day 12 p.i. Depletion of T–lymphocytes prior to and during the course of infection of IFNγR$^{-/-}$ mice with MHV-68 abrogated the development of fibrosis (Dutia *et al.*, 1997). Several studies have shown the role of the T-lymphocyte in the development of different forms of pulmonary fibrosis. Intratracheal administration of bleomycin in rodents, a model for IPF results in interstitial fibrosis accompanied by a significant infiltration of T and B-lymphocytes (Zhu *et al.*, 1996). In this model of IPF, it has been also demonstrated that the depletion of lymphocytes inhibited the development of fibrosis (Sharma *et al.*, 1996).

The current investigation identified the activation profile of different subsets of macrophages during the course of infection in IFNγR$^{-/-}$ mice prior to the development of fibrosis. This observation indicates the operation of the alternate pathway of activation of macrophages. This study confirmed the positive contribution of macrophages in the pathogenesis of fibrosis through their alternate activation pathway characterised by arginase–I expression. The concept of an alternative pathway of macrophage activation by the Th2 type cytokines [Interleukin – 4 (IL- 4) and IL – 13] has gained credence in the past decade to account for a distinctive macrophage phenotype that is consistent with their role in tissue repair. It is reasonable to assume that in the absence of signalling towards a Th1 response, the immune response following MHV-68 infections is skewed towards a Th2 type response. However, earlier study on infection of IFNγR$^{-/-}$ mice with MHV-68 did not show an obvious switch to a Th2 response (Ebrahimi *et al.*, 2001). In this context, it would be important to further characterise the T-

lymphocytes identified (both CD4+ and CD8+) in the GC of the spleens from IFNγR$^{-/-}$ mice infected with MHV-68 to delineate their Th1/Tc1 or Th2/Tc2 polarisation. It is highly likely that the different subsets of T-lymphocytes observed in the GC of spleen are polarised towards Th2/Tc2 type. Interestingly, a recent study identified transcripts of IL-13 in the spleen of IFNγR$^{-/-}$ mice infected with MHV-68 (Personal communication from Dr. B.Ebrahimi, University of Liverpool, United Kingdom). In addition, a recent study reported that following intranasal infection of IFNγR$^{-/-}$ mice with MHV-68, high levels of IL-4, IL-5 and IL-10 were produced in the lung (Mora *et al.*, 2005).

Gammaherpesviruses are known to encode chemokine homologues capable of driving Th2 type immune response [reviewed in (Alcami, 2003)]. It is possible that, MHV-68 may be encoding gene products which may facilitate the attraction of Th2 polarised lymphocytes into the GC. The conclusive evidence shown in this study for arginase-I expression strongly indicates the shift of immune response towards Th2 type. The up-regulation of arginase-1 in IFNγR$^{-/-}$ mice following MHV-68 infection has other roles than supporting the development of fibrosis. Arginase-I up-regulation has been shown to protect against infection with HSV and pseudorabies virus by depleting the source of arginine required for virus replication (Mistry *et al.*, 2001;Wang *et al.*, 2005). The other contribution of arginase-I is in the regulation of T-lymphocyte activation. It has been shown that macrophages stimulated to produce arginase-I cause rapid depletion of extracellular levels of arginine leading to diminished proliferation of T-lymphocytes and decreased expression of CD3ξ. (Rodriguez *et al.*, 2003). Thus it could be argued that arginase-I up-regulation is a different type of host response mechanism important in controlling the activation of T-lymphocyte and expansion of viral load. The role of arginase-I expression in down regulating the CD3 expression on T-lymphocyte could explain our inability to detect CD3 positive lymphocytes in the spleen of IFNγ$^{-/-}$ mice infected with MHV–68 at day 16 p.i and day 20 p.i. A further possibility is that failure to detect CD3 positive lymphocytes may be due to their absence in the GC during these time points.

Tingible Body Macrophages

The quantification of TBM showed no obvious difference between two groups of mice over the initial course of infection from day 8 to 20 p.i. The process of removal of apoptotic cells by phagocytic cells can contribute to the pathogenesis of fibrosis by releasing pro-fibrotic cytokines like TGFβ (Savill and Fadok, 2000). It would be possible to explain the development of fibrosis in spleen of the IFNγR$^{-/-}$ mice with the contribution from TGFβ released through this process in the absence of anti-fibrotic effect from IFNγ.

The role of macrophages in this scenario is further complicated due to their latent infection with MHV-68 (Flano *et al.*, 2000). Around 1/10^4 splenic macrophages at 14 day p.i. with MHV-68 are infected with virus (Marques *et al.*, 2003). Interestingly, infected macrophages showed a different profile of latent viral gene transcription compared with B-lymphocytes. The transcripts of latency associated genes like ORF73 was not detected in macrophages whereas, ORF 50 and ORF 6 transcripts were detected, which are lytic and reactivation associated. It was also shown that, the ligand responsible for stimulating CD8+ T-cells which is expressed in latently infected GC activated B-cells is not present in latently infected macrophages (Flano *et al.*, 2000). The infection status of macrophages in mice deficient in IFNγR has not been determined. In the current study, the productively infected cells were detected by immunohistochemical techniques in the marginal zone of the spleen. The productively infected cells could be MZM, MM or MZB-lymphocytes. These observations warrant further detailed study on the role of macrophages to delineate their status of latent infection and activation profile.

3.6.4. ROLE OF VIRUS

The profile of latently infected cells showed dramatic differences between two groups of mice over the course of infection. The number of latently infected cells reached a peak around day 18 to 22 p.i, which is mirrored by the peak of fibrotic changes in the spleen. This exponential increase in the number of latently infected cells shows a dramatic decline to negligible numbers at day 30 p.i and

subsequent time points. Interestingly, this decline in latently infected cells is mirrored by the re-population of spleen. This information suggests that the presence of virus in the centre of the lesion maintains the fibrotic state and its removal leads to recovery of fibrosis characterised by re-population of different subsets of cells in the spleen especially the follicular area with B–lymphocytes. This observation highlights a direct cause effect relationship of virus and pathogenesis of fibrosis.

The aetiological role of virus in the pathogenesis was further confirmed by our recent studies with mutant viruses (Appendix. 3). Four independent mutant viruses with insertions and/or deletions in the left hand end of the MHV-68 genome failed to induce splenic fibrosis in spite of their ability to establish latency in the spleen of IFNγR$^{-/-}$ mice (Dutia *et al.*, 2004). The study utilised the following MHV-68 mutant viruses: MHV–76, which lacks the M1, M2, M3, M4 and tRNA molecules in the left hand end of the viral genome (Macrae *et al.*, 2001), V1 virus which has an insertion at viral tRNA3, V2 virus which lack M1 and vtRNA 1-4 (Simas *et al.*, 1998) and LHΔgfp virus, which has an insertion of gfp cassette in place of nucleotide 1- 3223 at the left hand end of the genome . Interestingly, though the mutant viruses were able to establish latency detected by infective centre assay, they did not show an exponential increase in the number of latently infected cells shown by wild type virus in IFNγR$^{-/-}$ mice. This suggests that the mere presence of latent virus in the spleen is not sufficient to cause the fibrosis; instead it is the number of latent cells that matter in fibrosis induction. More interestingly, Northern analysis of RNA extracted from the viruses grown in an *in vitro* system has identified two novel transcripts in the wild type virus with their notable absence in mutant viruses (Dutia *et al.*, 2004). Further characterisations of these novel transcripts and their effect in an *in vivo* system will clarify their role in the pathogenesis of splenic fibrosis.

In summary, this investigation has emphasised the positive contribution from the virus, especially during the latent phase of infection in the pathogenesis of splenic fibrosis in IFNγR$^{-/-}$ mice infected with MHV-68. The viral gene products could

contribute at two points in the cascade of events leading to the development of fibrosis. The first is at the level of preventing the re-population of lymphoid follicles. Homing of B-lymphocytes into lymphoid follicles of spleen is regulated by a well characterised chemokine system. The stromal tissues in the lymphoid follicle, especially follicular dendritic cells (FDC) express B-lymphocyte chemoattractant (BLC)/B-cell attracting chemokine-1 (BCA-1)/CXCL13 and B-lymphocytes express its receptor, CXCR5. The interaction between CXCL13 and CXCR5 is critically important in homing of B-lymphocytes into lymphoid follicles (Legler *et al.*, 1998;Ansel *et al.*, 2000). It is possible that, intervention of this chemokine network by antagonising either the chemokine or its receptor would disrupt the chemokine gradient and prevent the re-population of lymphoid follicles with B-lymphocytes.

MHV–68 encodes two gene products which could interfere with the chemokine network. M3 gene is one of the MHV-68 specific genes, and its product is a well characterised secretary protein with ability to bind a wide range of chemokines (Parry *et al.*, 2000;Van Berkel *et al.*, 2000). Interestingly, M3 protein is capable of binding to C, CC and CX3C chemokines but showed binding with limited or lower affinity to CXC group of chemokines except human CXCL8. Considering the lower affinity of M3 gene product to bind CXC chemokines, its ability to interfere with the chemokine network responsible for the homing of B-lymphocytes into lymphoid follicles is limited. However, it will be interesting to extend the investigation on the binding ability of M3 to CXCL13 (BCA-1) to explore its potential role in preventing the homing of B-lymphocytes into lymphoid follicles. The MHV–GPCR encoded by ORF74 shows significant homology (28%) with CXCR2, which binds to CXCL8. MHV–GPCR can bind with ^{125} I labelled CXCL1 (Verzijl *et al.*, 2004) and its ability to bind other chemokines has not been investigated in detail. However, the related human gammaherpesvirus, KSHV encoded GPCR (KSHV-GPCR), though constitutively active (Arvanitakis *et al.*, 1997) showed binding ability to a wide range of CXC chemokines such as growth related oncogene-α (Gro-α/CXCL1), epithelial cell derived neutrophil activating-78 (ENA-78/CXCL5), neutrophil activating peptide-

2 (NAP-2/CXCL7) and stromal cell derived factor-1 (SDF-1/CXCL12) [Reviewed in (Couty and Gershengorn, 2004)]. In addition, KSHV-GPCR can bind to CC chemokines such as CCL1 and CCL5. Considering the capacity of KSHV–GPCR to bind a wide range of chemokines, it appears highly likely that MHV–GPCR may bind CXCL13 and disrupt the chemokine gradient required for the homing of B-lymphocytes into the lymphoid follicles. MHV-GPCR is expressed during the latent stage of *in vivo* infection in laboratory mice (Wakeling *et al.*, 2001) and the current investigation indicated that viral gene products expressed during latency are likely to play a role in the pathogenesis of fibrosis. Investigation into the antagonising ability of MHV- GPCR on murine CXCL13 is required to prove this hypothesis.

The second area in which the viral gene products could influence the pathogenesis of splenic fibrosis would be in driving the immune response towards a Th2 type response. Macrophage inflammatory proteins (MIP) are highly related members of chemokine family. KSHV encodes three MIP homologues (ORF K6 – vMIP-I /vMIP1α; ORF4–vMIP-II/vMIP -1β and ORF 4.1 – vMIP-III). One of the general functional properties of MIP homologues is their ability to block Th1 polarised lymphocyte driven immune responses. vMIP-II selectively attracts Th2 polarised lymphocytes expressing CCR3 (Sozzani *et al.*, 1998). vMIP-I and vMIP–III bind CCR8 and CCR4 respectively which are Th2 lymphocyte associated chemokine receptors (Dairaghi *et al.*, 1999;Endres *et al.*, 1999;Stine *et al.*, 2000). Homologues of MIPs were not identified in MHV-68. However, there are unique genes in the left hand end of the genome like M1 and M4 as well as other uncharacterised transcripts (Dutia *et al.*, 2004) for which a function is yet to be defined. The current study identified the alternate pathway of activation of splenic macrophages of IFNγR$^{-/-}$ mice indicative of a Th2 polarised immune response. It is possible that, MHV-68 encodes a protein similar to MIP homologues encoded by KSHV, which might be responsible for attracting Th2 type cells into the splenic lymphoid follicles. Further characterisation of CD4+ and CD8+ lymphocytes observed in the splenic germinal centres are required to identify their Th1/Th2 phenotype.

In addition to delineating the cellular, virological and molecular mechanisms involved in the pathogenesis and resolution of fibrosis in the spleen of MHV-68 infected IFNγR$^{-/-}$ mice, the study also highlighted a significant observation with regard to the host response towards latent gammaherpesvirus infection. The fibrosis generated with significant contribution from alternatively activated macrophages was able to contain the expansion of latently infected cells in the spleen. This is a novel observation. Fibrosis as a host response mechanism is known to occur against bacterial, fungal and parasitic pathogens specifically to contain the expansion of pathogens. Such a response against latent gammaherpesvirus infection has not been documented before. The molecular mechanism by which the fibrotic response achieves this containment of expansion of latent virus infection would be an interesting area for future study.

CHAPTER FOUR: OTHER PATHOLOGICAL CHANGES IN IFN$\gamma R^{-/-}$ MICE INFECTED WITH MHV-68

4. OTHER PATHOLOGICAL CHANGES IN IFNγR$^{-/-}$ MICE INFECTED WITH MHV-68

In addition to causing fibrotic changes in spleen, intranasal infection of IFNγR$^{-/-}$ mice with MHV-68 also causes other pathological changes in spleen, mediastinal lymph node, lung, and liver. The documented pathological change other than fibrosis in the spleen of IFNγR$^{-/-}$ mice infected with MHV–68 includes bony metaplasia (Dutia *et al.*, 1997). Resolving fibrotic changes in the mediastinal lymph node, lung and liver was also reported following intranasal infection of IFNγR$^{-/-}$ mice with MHV-68 (Ebrahimi *et al.*, 2001). The primary feature of IFNγR$^{-/-}$ mice infected with MHV-68 via the intraperitoneal route is chronic arterits affecting the base of the aorta leading to significant mortality (Weck *et al.*, 1997).

The current study investigated the pathological changes in the lung, liver, base of the aorta and bony metaplasia in the spleen of IFNγR$^{-/-}$ mice intranasally infected with MHV-68.

4.1. PATHOLOGICAL CHANGES IN THE LUNG

The intranasal infection of MHV-68 in laboratory mice results in a productive infection of the lung, the virus being associated mainly with alveolar epithelium (Sunil-Chandra *et al.*, 1992a). Long-term persistence/latency in the alveolar epithelium has also been reported (Stewart *et al.*, 1998b;Sunil-Chandra *et al.*, 1992a). The kinetics of a productive virus infection in the lung of IFNγR$^{-/-}$ mice followed the same pattern as in wild type mice. Similar to 129 Sv/Ev mice, no infectious virus was detected by plaque assay in the lung of IFNγR$^{-/-}$ mice beyond day 10 p.i. (Dutia *et al.*, 1997). Interstitial fibrosis accompanied by pulmonary phlebitis was reported in IFNγR$^{-/-}$ mice with severe pathological changes occurring at day 14 p.i. and resolving by day 45 p.i. (Ebrahimi *et al.*, 2001). More recently, it was shown that IFNγR$^{-/-}$ mice on the C57BL/6 background intranasally infected with MHV-68 developed progressive and multifocal pulmonary fibrosis. The lung developed sub-pleural fibrosis by day 45 p.i that changed to interstitial fibrosis by day 150 p.i. Thickening of the alveolar wall and pleura was much more evident at day 180 p.i. There was no evidence of fibrosis in wild type mice infected with MHV-68 and the fibrosis that developed in IFNγR$^{-/-}$ mice did not show spontaneous resolution (Mora *et al.*, 2005).

In the current study, the pathological changes in the lung of mice intranasally infected with MHV–68 were evaluated from day 8 p.i to day 120 p.i (Experiment No.1 and 2 as described in Materials and Methods section 2.4). The investigation focused on the extent of histopathological changes with reference to interstitial fibrosis, characterisation of cellular infiltrates in the lung during the course of infection and the level of productive virus infection determined by immunohistochemical techniques using a polyclonal antibody against MHV-68.

4.1.1. HISTOPATHOLOGICAL CHANGES IN THE LUNG OF MICE INFECTED WITH MHV-68

Multifocal to coalescing areas of interstitial pneumonia (IP) was observed at day 8 p.i in both groups of mice. The changes were more intense and extensive in IFNγR$^{-/-}$ mice compared to 129 Sv/Ev mice (Figure. 4.1.1A and B).

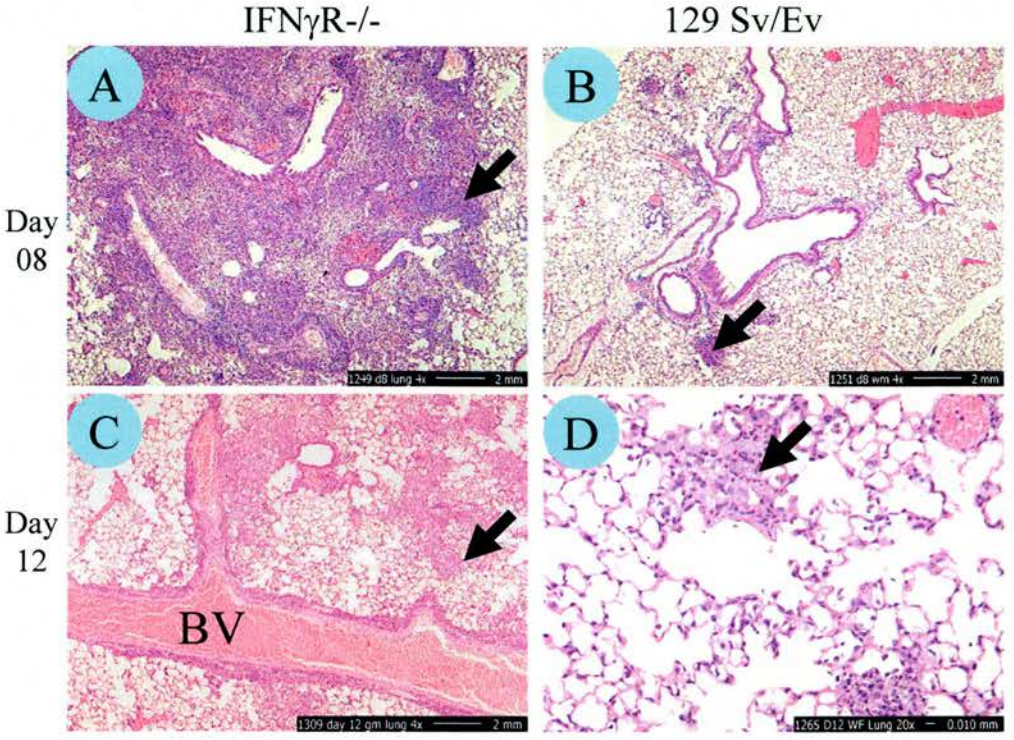

Figure.4.1.1. Histopathological changes in the lung of mice infected with MHV-68

Haematoxylin and Eosin staining.

The focus of interstitial pneumonia (arrows) is more intense and extensive in IFNγR-/- mice compared to 129 Sv/Ev mice at day 08 p.i. On day 12 p.i. in IFNγR-/- mice in addition to the interstitial pneumonia and foci of interstitial fibrosis, intense perivascular cuffing of pulmonary blood vessels (BV) was noticed (C). In 129 Sv/Ev mice at day 12 p.i., the lung is relatively clear with occassional foci of IP (D).

For images, A, B and C, Magnification 40X. For image D, magnification 200X

The coalescing areas of IP were seen adjacent to the bronchial lumen suggestive of bronchointerstitial pneumonia, which was more pronounced in IFNγR$^{-/-}$ mice. The inflammatory cells in the interstitium contained mainly lymphocytes and macrophages. Desquamated alveolar epithelium and inflammatory cells were also seen in the alveolar lumen. By day 10 p.i., there were more macrophage/ mesenchymal type cells in the interstitium in both groups of mice.

The extent of IP was minimal from day 12 p.i onwards in 129 Sv/Ev groups of mice and some had no lesions at all. The odd mouse at day 40 p.i., and day 50 p.i. showed areas of type II pneumocyte hyperplasia and a mild degree of interstitial fibrosis. Occasionally, a focus of alveolar adenoma was observed in 129 Sv/Ev mice at day 120 p.i. The foci appeared as a circumscribed, unencapsulated mass. The cells were arranged in tubular or acinar pattern and were relatively uniform in size with round hyperchromatic nuclei and acidophilic cytoplasm. Mitotic figures were rare.

Perivascular and peribronchiolar cuffing by inflammatory cells along with foci of IP and interstitial fibrosis was the prominent feature in the lung of IFNγR$^{-/-}$ mice at day 12 p.i (Figure. 4.1.1C and D). The infiltrating cells mainly consisted of mononuclear cells and occasional focal collections of neutrophils. One of the mice in IFNγR$^{-/-}$ group showed an area of necrosis of the bronchiolar epithelium surrounded by inflammatory exudates and fibroblasts. Another focus had an area of chronic abscess with necrotic mass in the centre encircled by fibroblast type cells. The IFNγR$^{-/-}$ mice at day 14 and 16 p.i. showed focal areas of fibroblast proliferation in the alveolar wall. In addition, at day 16 p.i. a few of the pulmonary vessels showed trafficking of inflammatory cells mainly neutrophils across the vessel wall suggestive of vasculitis. The perivascular and peribronchiolar infiltration of inflammatory cells was present until day 20 p.i. and showed resolution of these changes from day 30 p.i. onwards (Figure.4.1.2). Occasional foci of IP, type II pneumocyte hyperplasia and alveolar fibrosis were noticed at later time points.

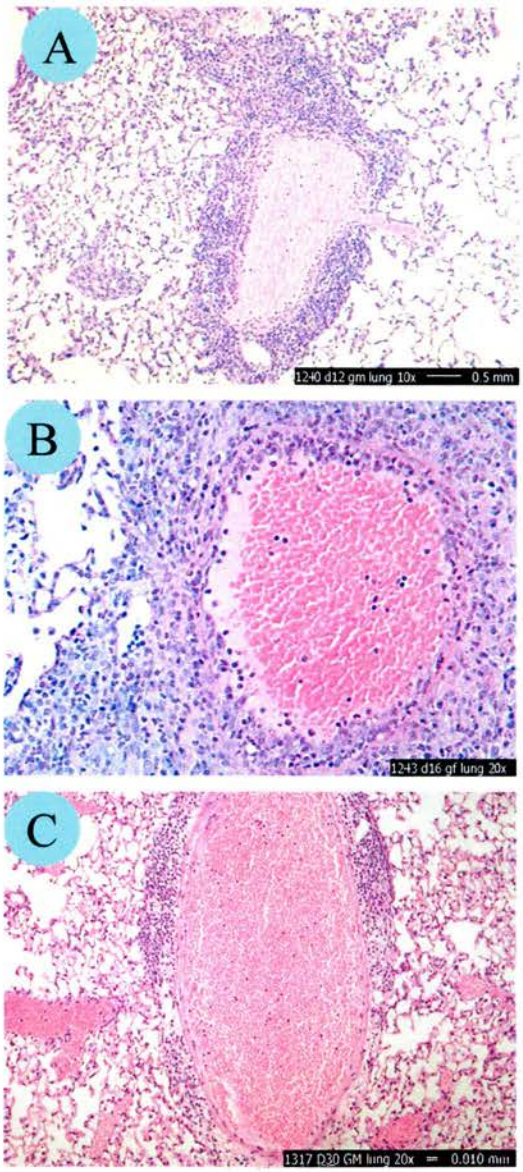

Figure. 4.1.2. Vasculitis in the lungs of IFNγR-/- mice infected with MHV-68

Haematoxylin and Eosin staining.

A, Day 12 p.i. B, Day 16 p.i. C, Day 30 p.i. Note the presence of infiltrating inflammatory cells around the blood vessels. Crossing over of the vessel wall with inflammatory cells is more prominent at day 16 p.i.(B) Clearing of perivascular lesion noticed from day 30 p.i. onwards (C).

For image A, magnification 100X. For images B and C, magnification 200X

4.1.2. CHARACTERISATION OF CELLULAR INFILTRATION IN THE LUNG OF MICE INFECTED WITH MHV-68

All the lung sections of mice from experiment no.1 and 2 were stained for F4/80 (macrophages), CD45R/B220 (B–lymphocytes) and CD3 (T–lymphocytes) as described in Materials and Methods section 2.6. to characterise the cellular changes taking place in the lungs during the course of infection.

The infiltrating cells mainly consisted of B and T-lymphocytes and macrophages during early infection (Day 8 p.i. and Day 10 p.i) in IFNγR$^{-/-}$ mice and T-lymphocytes and macrophages in 129Sv/EV mice (Figure 4.1.3). The macrophages were always found around the blood vessels. The number of infiltrating B-lymphocytes and macrophages were negligible in 129 Sv/Ev mice during the entire course of infection. The perivascular and peribronchial infiltration phase of the infection in IFNγR$^{-/-}$ group of mice included mainly B and T-lymphocytes with occasional macrophages (Figure.4.1.4).

4.1.3. DISTRIBUTION OF VIRUS INFECTED CELLS IN THE LUNG OF MICE INFECTED WITH MHV-68

All sections of lung from both groups of mice from experiment No.1 and 2 were stained with polyclonal rabbit anti-MHV-68 antiserum. The level of virus-infected cells were scored (0 to ++++, see table legend for details) and the data from experiment no.1. is presented in table 4.1. The level of infection in the lung was separately scored for the positivity of alveolar epithelial cells and infiltrating mononuclear cells in the lung using the above scoring system.

In IFNγR$^{-/-}$ mice, viral antigen positive cells could be seen up to day 20 p.i., although there was a clear shift in the tropism of virus infection from alveolar epithelial cells towards infiltrating mononuclear cells around the blood vessels (Figure 4.1.5). In 129 Sv/Ev groups of mice, viral antigen positive cells were mainly confined to alveolar epithelial cells and rarely found after day 10 p.i. suggestive of clearing of the infection. In experiment No.2, viral antigen positive cells were seen up to day 30 p.i. in IFNγR$^{-/-}$ mice but were not observed at later

Table 4.1. Viral antigen positive cells/foci in the lung and incidence of interstitial fibrosis - Experiment No.1.

Day	Animal Number	Alveolar	Mononuclear	Fibrosis
IFNγR-/-				
8	GM1241	0	0	
	GF1249	++++	+	
10	GM1242	+++	++	
	GM1236	++	+	
	GF1246	+	+	
12	GM1240	+	+++	✓
	GM1234	+	++	✓
	GF1245	+	++	✓
14	GM1238	++	+++	✓
	GF1247	0	+++	✓
16	GM1237	+	++	✓
	GF1243	0	++	✓
18	GM1239	0	+	
	GF1248	0	+	
20	GM1235	0	+	
	GF1244	0	++	
129 Sv/Ev				
8	WM1257	++++	+	
	WF1259	++++	+	
10	WM1258	0	0	
	WM1252	++	0	
	WF1260	++	0	
12	WM1256	0	0	
	WM1253	0	0	
	WF1265	0	0	
14	WM1251	0	0	
	WF1263	0	0	
16	WM1255	0	0	
	WF1262	0	0	
18	WM1250	0	0	
	WF1264	0	0	
20	WM1254	0	0	
	WF1261	0	0	

0 = No positive cells, + Occasional positive cells, ++ Few positive cells/foci, +++ Large number of positive cells/foci, ++++ Very large number of positive cells/foci
GM - IFNγR$^{-/-}$ male, GF - IFNγR$^{-/-}$ female,
WM- 129 Sv/Ev male, WF – 129 Sv/Ev female

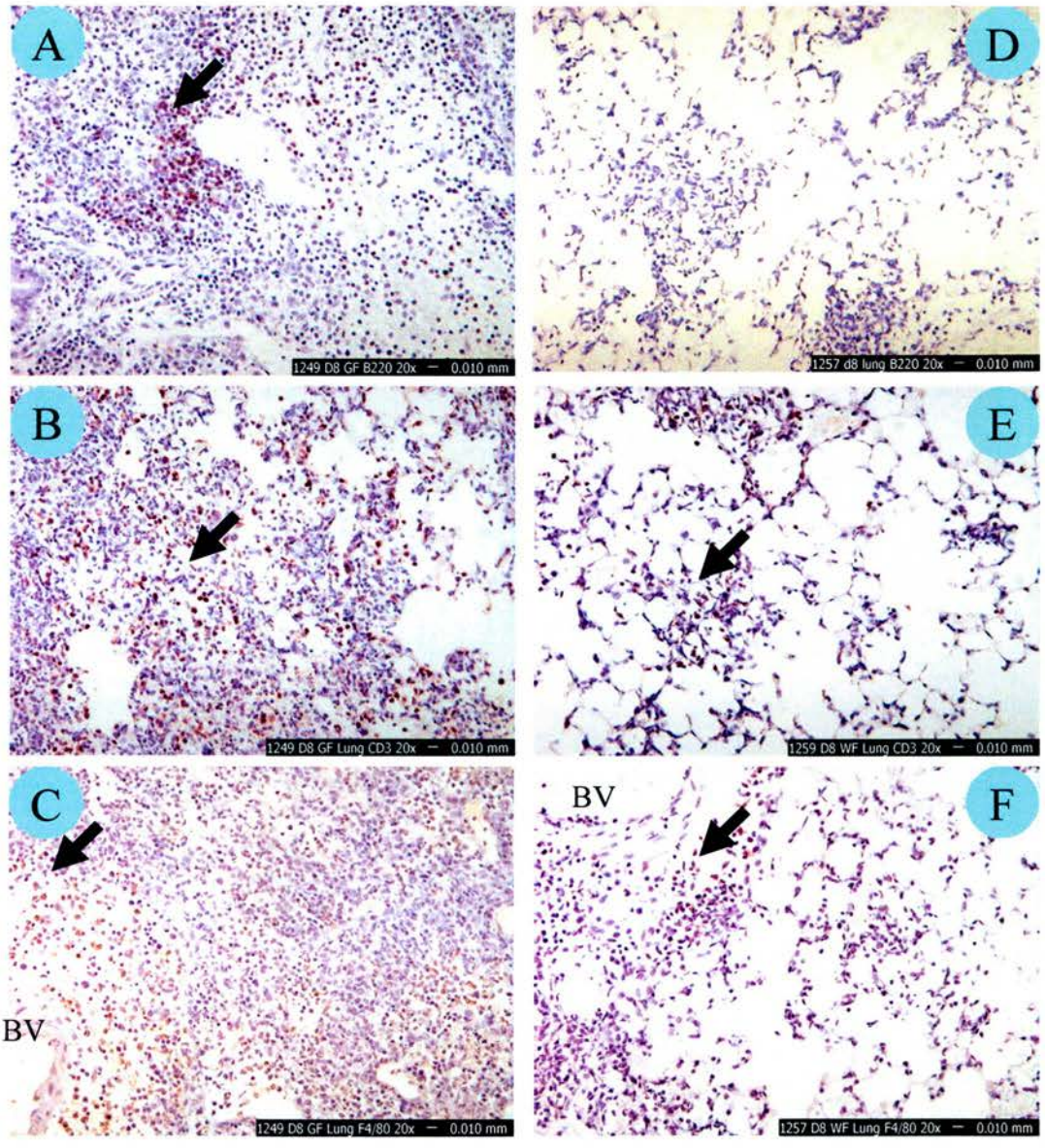

Figure. 4.1.3. Characterisation of cellular infiltrates in the lungs of mice infected with MHV-68 at day 8 p.i.

A,B and C, IFNγR-/- mice D, E and F, 129 Sv/Ev mice. A and D, CD45R/B220 staining . B and E, CD3 staining . C and F, F4/80 staining. BV, Blood vessel. Red colour in A,B, E and F indicate positive staining (Vector novared). Brown colour in C indicate positive staining (DAB). Arrows indicate areas of positive staining.

Magnification 200X

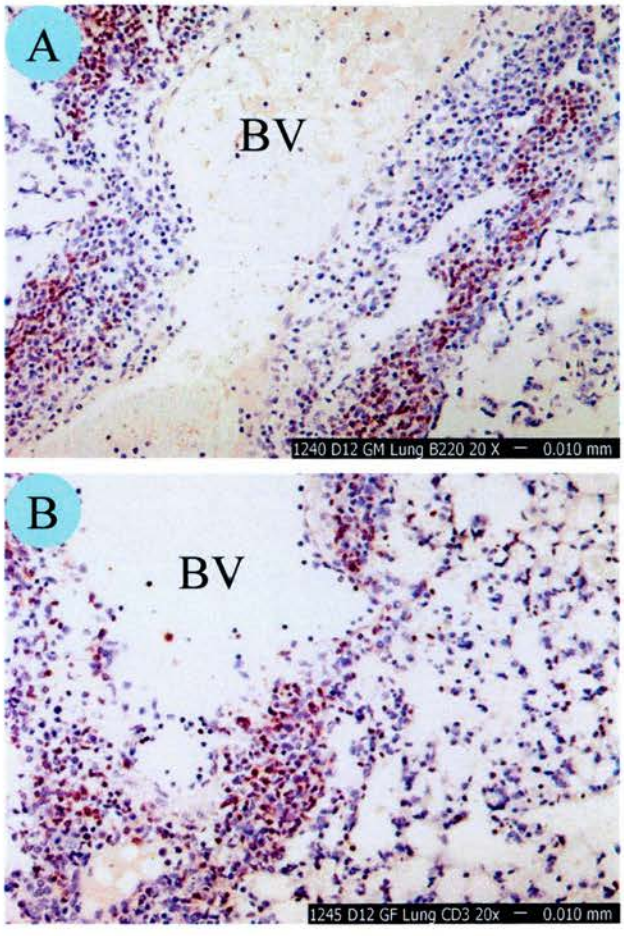

Figure.4.1.4. Characterisation of cellular infiltrates in the lungs of IFNγR-/- mice infected with MHV-68 at day 12 p.i.

A,CD45R/B220 staining. B, CD3 staining. BV, Blood vessel. Note the infiltrating cells around the blood vessels. Red colour indicate positive staining.

Magnification 200X

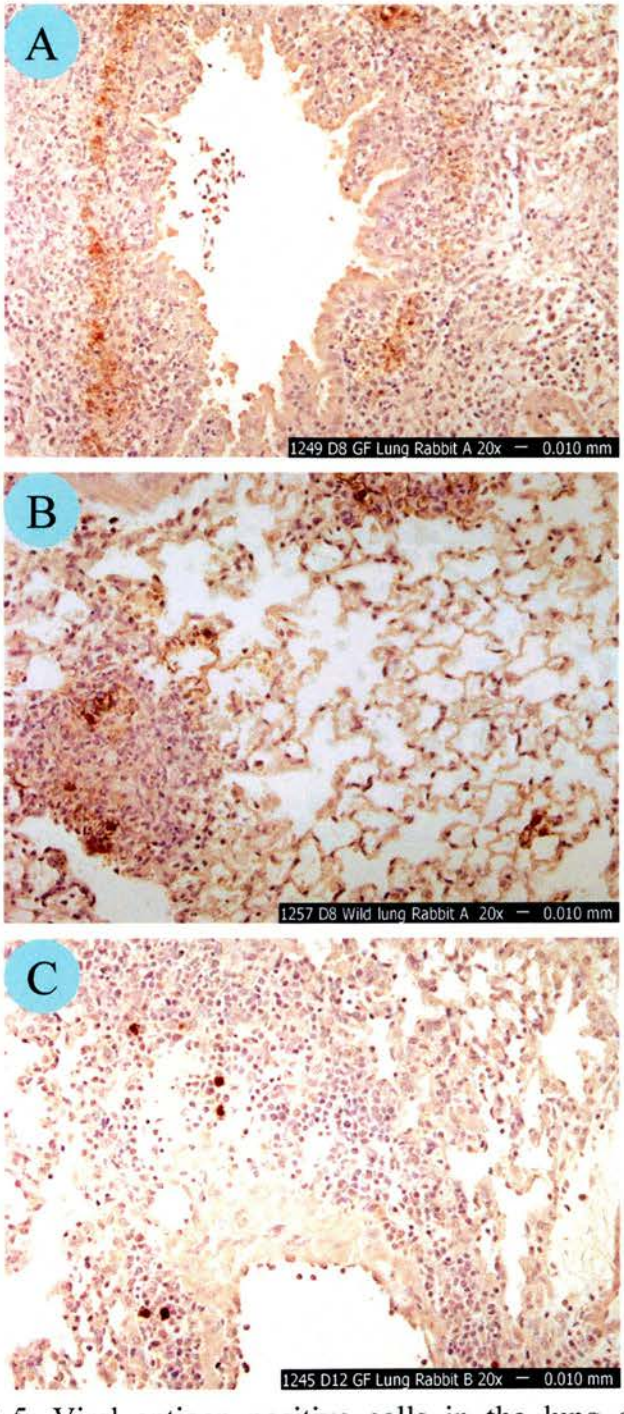

Figure.4.1.5. Viral antigen positive cells in the lung of mice infected with MHV-68

Immunohistochemistry with polyclonal antiserum against MHV -68 raised in rabbit. A and C IFNγR-/- mice. B, 129 Sv/Ev mice. A and B day 8 p.i. C, Day 12 p.i. Note the presence of productively infected mononuclear cells (Brown colour) around the blood vessels in IFNγR-/- mice at day 12 p.i. (C).

Magnification 200X

time points, whereas in 129 Sv/Ev mice viral antigen positive cells were seen among epithelial cells in one mouse at day 60 p.i., possibly indicative of reactivation from a latent infection

The incidence of interstitial fibrosis was also tabulated along with the level of viral antigen positive cells in the lung (Table No. 4.1.). It appeared that there was a window of time p.i. (between day 12 p.i and day 16 p.i.), which correlated with the infection of mononuclear cells in the lung and development of interstitial fibrosis.

4.1.4. DISCUSSION

The pathological changes in the lung of IFNγR$^{-/-}$ mice were more intense and extensive than 129/Sv/Ev mice, especially around day 8 to day 10 p.i. In addition, the lungs of IFNγR$^{-/-}$ mice also showed distinct pathological features at day 12 p.i such as degeneration and necrosis of bronchiolar epithelium, cuffing of blood vessels and bronchial lumen by lymphocytes (both T and B-lymphocytes) and multiple foci of interstitial fibrosis. Taken together, it appears that, the absence of IFNγ signalling is responsible for more severe as well as distinct pathological changes in the lung in comparison to 129 Sv/Ev mice.

It has been previously reported that infection of IFNγR$^{-/-}$ mice with MHV-68 resulted in interstitial fibrosis accompanied by pulmonary phlebitis which peaked at day 14 p.i and was resolved by day 45 p.i. (Ebrahimi *et al.*, 2001). The current observations agree with this report. A recent report showed that, intranasal infection of IFNγR$^{-/-}$ mice on the C57/B6 background developed chronic unresolving fibrosis in the lung (Mora *et al.*, 2005). The observations made in our study do not support this observation. The identification of a window of time correlating with the infection of mononuclear cells and development of interstitial fibrosis is interesting. It may be possible that, infection of mononuclear cells with MHV-68 causes the release of pro-fibrotic cytokines leading to the development of fibrosis. The cell type infected during the mononuclear phase of infection needs to be identified. A recent study showed that, in addition to type II alveolar

epithelial cells, alveolar macrophages were also productively infected with MHV–68 following intranasal infection (Mora *et al.*, 2005).

An earlier study on the kinetics of viral titres in the lung of IFNγR$^{-/-}$ mice and 129/Sv/Ev mice showed no significant difference between the two groups of mice with complete clearance of productive infection at day 10 p.i. (Dutia *et al.*, 1997). The current study with immunohistochemical techniques to investigate the profile of productively infected cells also showed a similar trend at day 8 and day 10 p.i. between the two groups of mice. However, in IFNγR$^{-/-}$ mice, the virus persisted up to day 30 p.i. primarily among mononuclear cells seen around the pulmonary blood vessels. It is surprising to note that, in spite of the difference in the extent of pathological changes in the lung between two groups of mice, the level of productively infected cells detected by immunohistochemistry in the current study and virus load estimated by conventional plaque assay (Dutia *et al.*, 1997) showed little difference. It implies that, in spite of a similar level of virus replication in both groups of mice, the pathological damage in the lung of mice is linked to a failure in the IFNγ response or biasing of the immune system towards a Th2 type cytokine profile.

A distinct pathological change observed in the lung of IFNγR$^{-/-}$ mice from day 12 p.i. onwards was a clear targeting of pulmonary blood vessels and bronchial tree by T and B-lymphocytes and occasional collections of polymorphonuclear (PMN) cells. Some of the neutrophils were seen crossing over the intimal layer of blood vessels. These observations support the vascular tropism of the virus, which is mainly expressed in the absence of IFNγ signalling. The gammaherpesviruses are known to have a tropism for vascular structures. A major microscopic pathology of MCF, a disease caused by AlHV-1 or OvHV-2 in ruminants is characterised by lymphoid proliferation and infiltration associated with necrotising vasculitis (Liggitt and DeMartini, 1980).Considering the sporadic clinical outbreaks of this condition in natural situations, it would be interesting to explore the contribution of any defect in the IFNγ responsiveness as a susceptibility factor for MCF.

4.2. PATHOLOGICAL CHANGES IN THE LIVER

Per oral and/or intranasal infection of outbred laboratory mice of various age groups (suckling to 21 days old) with MHV–68 resulted in recovery of virus from liver at later times p.i. Occasional viral antigen positive parenchymatous and Kupffer cells in the liver were detected by immunofluorescence studies (Blaskovic *et al.*, 1984;Rajcani *et al.*, 1985). Infection of BALB/c mice through the intranasal route did not result in hepatic infection; however infectious virus could be recovered from the liver following intravenous infection with MHV-68 (Sunil-Chandra *et al.*, 1992a).

The current study was undertaken to assess the pathological changes in the liver during the course of infection from day 8 p.i. to day 120 p.i. with special emphasis on histopathological changes, characterisation of cellular infiltrates and distribution of virally infected cells detected by immunohistochemical and *in situ* hybridisation techniques.

4.2.1. HISTOPATHOLOGICAL CHANGES IN THE LIVER OF MICE INFECTED WITH MHV-68

Multifocal non-zonal mixed inflammation was the prominent histopathological change in mice of both groups at day 8 and 10 p.i, although the intensity of the response was greater in IFNγR$^{-/-}$ mice. In IFNγR$^{-/-}$ mice, from day 12 p.i. onwards the mixed inflammatory reaction showed targeting to the portal area with mononuclear and neutrophilic infiltration. The infiltrating cells were seen mainly around the bile ducts. Proliferation of bile ducts around the major intrahepatic and occasional extrahepatic bile ducts was noticed from around day 16 p.i. in IFNγR$^{-/-}$ mice. Hyperplastic bile ducts were surrounded by inflammatory cells composed of focal collection of neutrophils among the mononuclear cell infiltrates. In IFNγR$^{-/-}$ mice, the bile duct hyperplasia around the major intrahepatic bile ducts was a consistent feature from day 20 p.i. (Figure 4.2.1A and table no.4.2.1). Some of the proliferating bile ducts showed degenerative changes and infiltration of inflammatory cells predominated by neutrophils.

Table 4.2.1. Incidence of bile duct lesions in the liver

Sl.No.	Day	IFNγR-/-		129 Sv/Ev	
		Intrahepatic bile duct proliferation and inflammation	Intrahepatic bile duct degeneration and encircling fibrosis	Intrahepatic bile duct proliferation and inflammation	Intrahepatic bile duct degeneration and encircling fibrosis
Experiment No.1					
1	8	0/2	0/2	0/2	0/2
2	10	0/3	0/3	0/3	0/3
3	12	0/3	0/3	0/3	0/3
4	14	0/2	0/2	0/2	0/2
5	16	1/2	0/2	0/2	0/2
6	18	2/2	0/2	0/2	0/2
7	20	2/2	0/2	0/2	0/2
Experiment No.2					
1	12	0/3	0/3	0/3	0/3
2	20	2/3	0/3	0/3	0/3
3	30	1/4	0/4	0/3	0/3
4	35	5/5	0/5	0/3	0/3
5	40	4/4	0/4	1/4	1/4
6	45	1/3	0/3	0/3	0/3
7	50	3/3	1/3	1/3	1/3
8	60	3/3	1/3	0/3	0/3
9	80	3/3	1/3	0/3	0/3
10	120	5/5	2/5	1/4	1/4
Total		32/52 (61.5%)	5/52 (9.61%)	3/48 (6.25%)	3/48 (6.25%)

'Onion Skin' type fibrosis around the necrotic bile ducts in the intrahepatic location was also observed at later time points. Mononuclear cells encircled the fibrotic foci. (Figure 4.2.1B and table 4.2.1.). Bile duct hyperplasia was occasionally observed in some of the 129 Sv/Ev mice at later time points. One mouse each at day 40 p.i., day 50 p.i and day 120 p.i. showed a focus of necrotic bile duct surrounded by inflammatory cells and 'onion skin' like fibrosis (Table. 4.2.1).

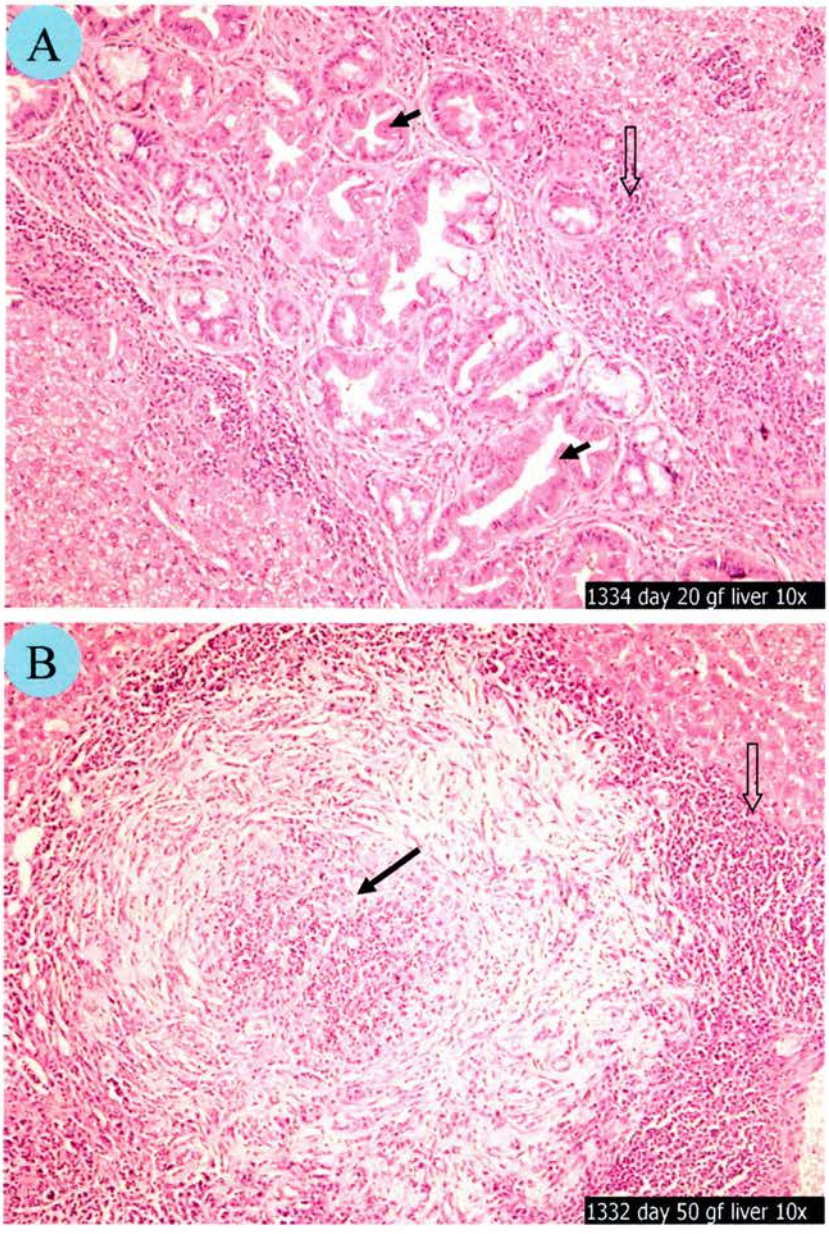

Figure. 4.2.1. Histopathological changes in the liver of IFNγR-/- mice infected with MHV-68

Haematoxylin and Eosin staining. A, Day 20 p.i. B, Day 50 p.i.

At day 20 p.i., the prominent feature is proliferation of intrahepatic bile ducts (Arrow) and infiltration of inflammatory cells around them (hollow arrow). At later time points some of the bile ducts undergo necrotic changes (arrow) and encircling 'onion skin' type fibrosis was noticed . In the periphery of the fibrous tissue mononuclear cells are observed (hollow arrow)

Magnification 100X

4.2.2. CHARACTERISATION OF CELLULAR INFILTRATE IN THE LIVER OF MICE INFECTED WITH MHV-68

The cellular infiltrates around the proliferating bile ducts of IFNγR$^{-/-}$ mice were characterised with special reference to B and T-lymphocytes and macrophages. The results are shown in Figure 4.2.2. No specific chronological order was observed in the appearance of different subsets of mononuclear cells into the lesion. The observation of both B-lymphocytes and macrophages at this site is interesting in the context of spread of infection. Both B–lymphocytes and macrophages in the spleen are latently infected with MHV-68 (Sunil-Chandra *et al.*, 1992b;Flano *et al.*, 2000). Infection status of these macrophages and B–lymphocytes are required to clarify this point. The T-lymphocytes noticed at this site also needs to be further characterised to identify their Th1/Th2 polarisation.

4.2.3 DISTRIBUTION OF PRODUCTIVELY AND LATENTLY INFECTED CELLS IN THE LIVER OF MICE INFECTED WITH MHV-68

All the liver sections of both groups of mice from experiment no.1 and 2 were stained with polyclonal antibody against MHV-68 raised in rabbits. Very few positive cells were identified in the liver. The hepatocytes or cholangiocytes were never found positive for viral antigen. The positive staining was observed among the occasional mononuclear cells in the hepatic sinusoids and infiltrating cells in the portal area (Figure. 4.2.3A). *In situ* hybridisation with riboprobe specific for viral tRNA 1-4 to detect latently infected cells in the liver of IFNγR$^{-/-}$ mice from experiment 1 and 2 was also carried out. The hepatocytes and cholangiocytes were negative for latent virus infection. Occasional collections of latently infected mononuclear cells were observed among the infiltrating cells around the proliferating intrahepatic bile ducts (Figure. 4.2.3B)

4.2.4. DISCUSSION

The inflammation and fibrosis around the bile ducts seen in the IFNγR$^{-/-}$ mice infected with MHV-68 shows similarity to primary sclerosing cholangitis (PSC) in human beings. PSC is a chronic cholestatic liver disease of unknown cause

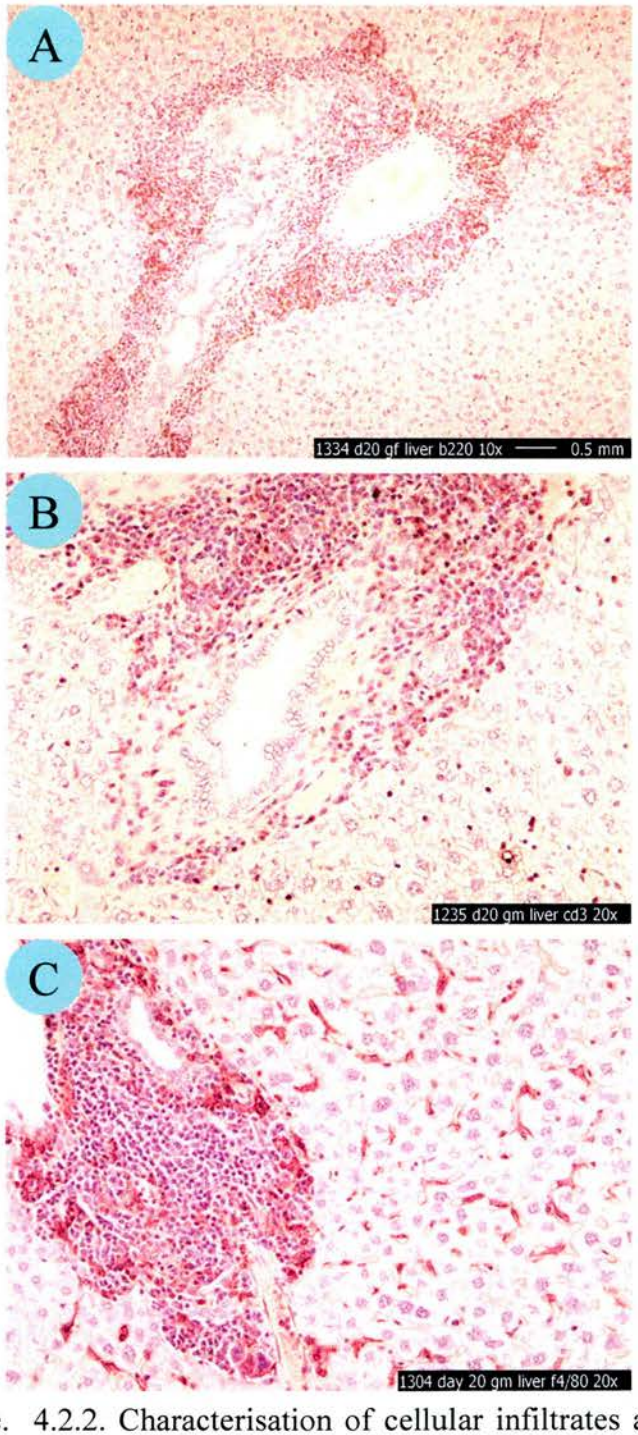

Figure. 4.2.2. Characterisation of cellular infiltrates around the proliferating bile ducts of IFNγR-/- mice infected with MHV-68 .

A representative sample of liver sections from mice at day 20 p.i. is presented. The infiltrating cells included B-lymphocytes (A), T- lymphocytes (B) and macrophages (C) . For image A, magnification 10x. For image B and C, magnification 200x

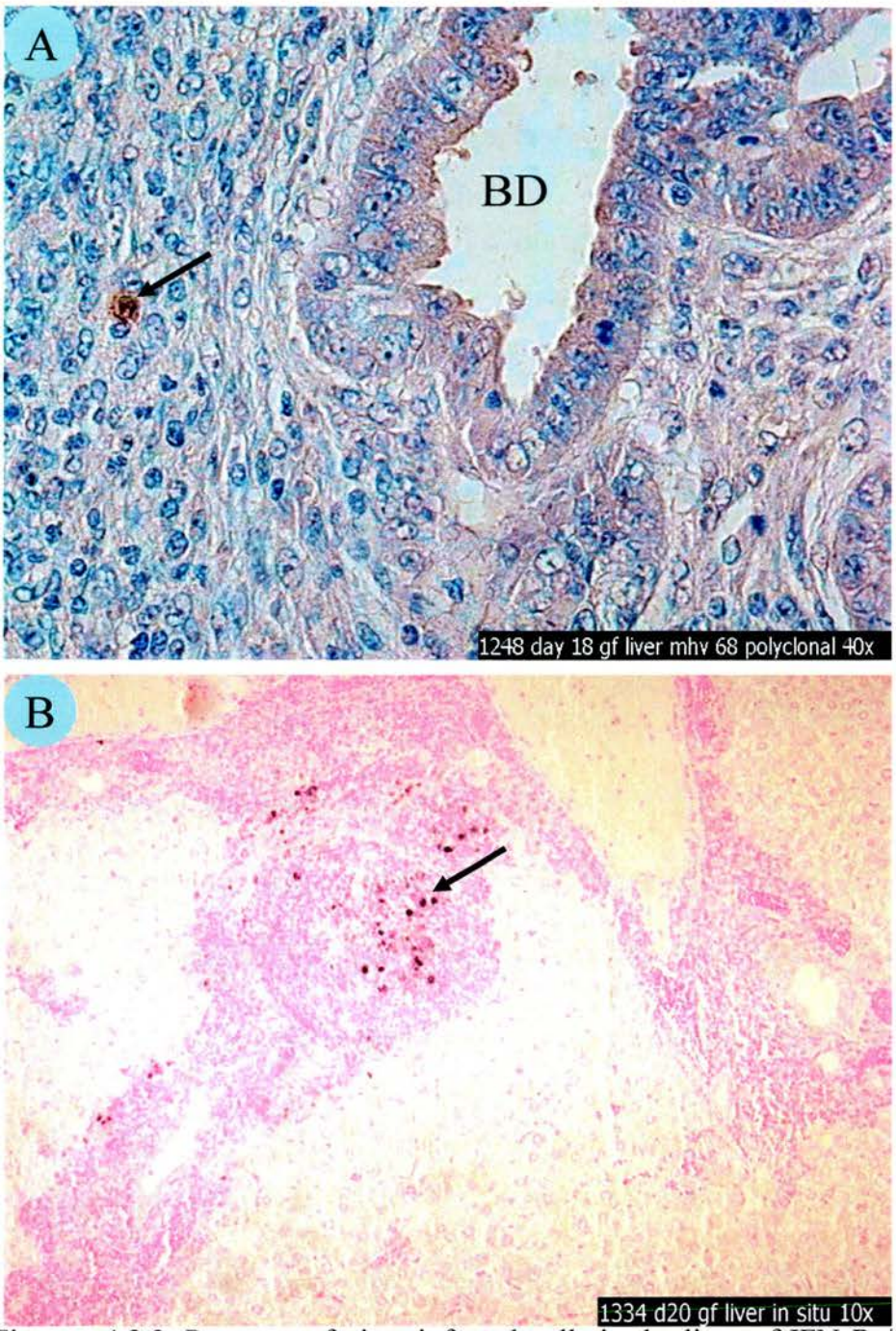

Figure. 4.2.3. Presence of virus infected cells in the liver of IFNγR-/- mice infected with MHV-68

A, Immunohistochemistry with anti rabbit anti-MHV-68 serum showed occasional viral antigen positive cells (arrow) among the mononuclear infiltrate around the bile duct (BD). The image obtained from the liver of mice sacrificed at day 18 p.i. magnification 400X. B, *In situ* hybridisation with a riboprobe against vt RNA 1-4 molecule of MHV -68 showed latently viral infected mononuclear cells among the infiltrating cells (Arrow). The images obtained from the liver of mice sacrificed on day 20 p.i. magnification 100X

characterised by ongoing inflammation, destruction and fibrosis of intrahepatic and extrahepatic bile ducts [Reviewed in (Lee and Kaplan, 1995)]. Bile ducts are the major targets in both acute and chronic hepatic graft versus host disease (GVHD) and the histological features of intrahepatic bile ducts resemble that of primary biliary cirrhosis (PBC) (Epstein *et al.*, 1980). There is considerable overlap between the clinical, biochemical and histological features of PBC and PSC (Wiesner *et al.*, 1992). GVHD is initiated by alloreactive donor T-cells recognising major and/or minor histocompatability antigen of the host. (Nonomura *et al.*, 1998) proposed a mouse model of GVHD across minor histocompatibility barriers, which characteristically exhibits bile duct histology resembling PSC. They injected spleen and bone marrow cells (9:1) of congenic B10.D2 mice into sublethally irradiated BALB/c mice and the histological features of liver were studied for up to 14 months after transplantation. Both intrahepatic and extrahepatic bile ducts were severely involved in the GVHD process and showed histological features resembling PSC.

The immunohistochemical and *in situ* hybridisation studies to detect viral infection in the liver showed very few numbers of cells positive for MHV-68. The hepatocytes or cholangiocytes were never positive for viral antigen. The positive cells were the mononuclear cells present in the sinusoids and portal area of liver. This shows the absence of tropism for the main parenchymal cells of the liver for MHV-68. In the absence of a direct correlation of infectious agent, the hepatic lesions of mice from our study could also be the result of an immunopathological mechanism. It is known that MHV-68 infection leads to the generation of an IM like syndrome. The IM like disease initiated by MHV-68 is unique in the manner of MHC haplotype independent expansion of CD8+ cells, the majority of which utilise Vβ4 chains in the αβ TCR. The ligand driving the Vβ4 expansion is unknown (Hardy *et al.*, 2000). Further characterisation of the cellular infiltrates around the proliferating bile ducts are required to be carried out to clarify whether the cellular infiltrates and CD8+ T–lymphocytes found in the peripheral circulation during IM phase of infection are similar.

4.3. CHRONIC ARTERITIS

Severe large vessel pan - arteritis was the phenotype reported in the IFNγR$^{-/-}$ mice infected intraperitonealy with MHV-68 (Weck *et al.*, 1997). Severe large vessel arteritis was also observed in mice with a null mutation in IFNγ gene also infected intraperitoneally with MHV-68. Studies on IFNγR$^{-/-}$ mice or IFNγ$^{-/-}$ mice intranasally infected with MHV–68 had not reported pathological changes in blood vessels (Dutia *et al.*, 1997;Sarawar *et al.*, 1997). However, infection of apolipoprotein E deficient mice (apoE$^{-/-}$) (which shows a naturally high rate of atherosclerosis) with MHV–68 showed an accelerated rate of atherosclerosis lesion development with virus present in the lesion (Alber *et al.*, 2000;Alber *et al.*, 2002). This observation further confirms the vascular tropism of MHV-68.

During the course of this investigation, one of the IFNγR$^{-/-}$ mice in the experiment No.2 was found dead on day 34 p.i. Detailed post mortem examination and histopathological examination confirmed severe chronic arteritis primarily targeting the base of the aorta as the cause of death. Hence, it was decided to study the pathology of the base of the aorta in mice at subsequent time points of that experiment (Day 35, 40, 45, 50, 60, 70, 80 and 120 p.i.) as well as experiment No.3 (see Materials and Methods section 2.4.).

4.3.1. INCIDENCE AND PATHOLOGY OF CHRONIC ARTERITIS IN IFNγR$^{-/-}$ MICE INFECTED WITH MHV-68

The incidence of chronic arteritis observed in the base of aorta of IFNγR$^{-/-}$ mice from part of experiment no.2 and experiment No.3 is presented in table 4.3.1. None of the mice in the 129 Sv/Ev group showed any sign of arteritis in the base of the aorta. Out of the four cases of arteritis observed in this study, only one caused the death of a mouse and others were observed during histopathological examination.

The primary pathological change was noticed in the tunica media of the blood vessel. There were necrotic patches restricted to the tunica media throughout the course of the blood vessel. A chronic inflammatory response resulted in

Table 4.3.1. Incidence of chronic arteritis

Experiment No.	Days post infection	Number of mice	Positive for Chronic arteritis
	35	5	1 (died on day 34 p.i.)
	40	4	0
	45	3	0
	50	3	0
	60	3	1
	80	3	0
	120	5	1
Total		26	3 (11.5%)
3	12	4	0
	16	4	0
	20	4	0
	50	4	1
Total		16	1 (6.25%)

thickening of the blood vessel wall resulting in a narrowing of the lumen. The inflammatory cells in the tunica adventitia mainly consisted of lymphocytes and a few neutrophils. The immunohistochemical staining with anti-rabbit polyclonal MHV-68 antibody showed viral antigen positive cells in the tunica media of the blood vessel. The morphological features of the some of the viral antigen positive cells suggested a smooth muscle cell phenotype (Figure. 4.3.1).

4.3.2. DISCUSSION

The observation of chronic arteritis lesions in IFNγR$^{-/-}$ mice infected with MHV-68 suggests the tropism of the virus towards the blood vessels and role of IFNγ signalling in regulating this tropism. This observation has added significance as it has been seen in mice intranasally infected with the virus, which mirrors the most probable natural route of infection rather than the earlier report of chronic arteritis in IFNγR$^{-/-}$ mice infected with MHV-68 via intraperitoneal route (Weck *et al.*, 1997). The incidence of chronic arteritis and associated mortality was much lower than that reported in mice infected via intraperitoneal route. Thirty of 30 IFNγR$^{-/-}$ mice (infected via intraperitoneal route) that died 1.5 to 14 weeks after infection had large vessel arteritis. In the current experiment, only one mouse died of chronic arteritis and others were detected during histopathological examination after sacrificing the mice at stipulated time points.

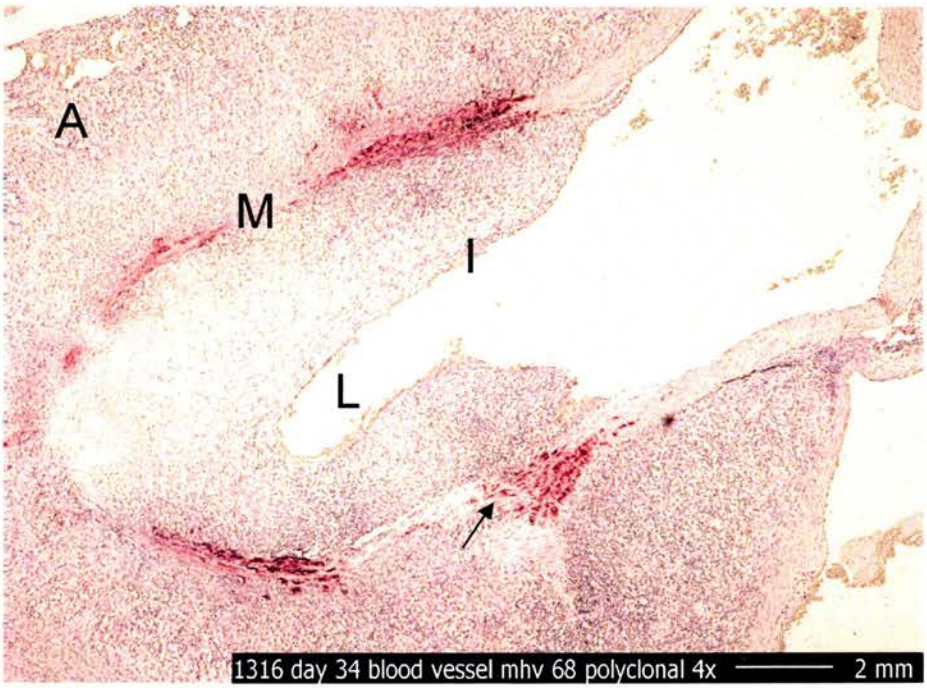

Figure. 4.3.1. Chronic arteritis in the base of the aorta in IFNγ R-/- mice infected with MHV-68.

Formalin fixed paraffin embedded tissue sections of the base of aorta from IFNγR-/- mice infected with MHV -68 were stained with polyclonal antiserum against MHV -68 raised in rabbit. Note the viral antigen positive splindle shaped cells (arrow) in the tunica media of the blood vessel (M). Infiltration of chronic inflammatory cells in the tunica adventitia (A) and thickening of the tunica intima (I) and subsequent narrowing of the lumen (L) is present.
Magnification 40X

The role of IFNγ responsiveness in regulating the tropism of the virus to the large blood vessels is interesting. It has been shown that IFNγ itself can elicit arteriosclerosis in SCID/beige mice (Tellides *et al.*, 2000) and IFNγ potentiates atherosclerosis in apoE$^{-/-}$ mice (Gupta *et al.*, 1997). The interesting feature of chronic arteritis observed in the IFNγR$^{-/-}$ mice infected with MHV–68 is its similarity to the pathology of Takayasu arteritis. Takayasu arteritis is a chronic vascular inflammatory disease of unknown aetiology mainly involving the aorta. The prevalence of this condition is particularly high in south Asian women, even though the condition is reported in other parts of the world. The pathological changes involve all layers of the blood vessel and destruction of medial layer is a common feature (Iwai *et al.*, 2000). Hence, the infection of IFNγR$^{-/-}$ mice with MHV-68 is a potential small animal model to explore the aetiological relationship of human gammaherpesviruses and Takayasu arteritis.

4.4. BONY METAPLASIA IN SPLEEN

The first report on splenic fibrosis induced by MHV–68 in IFNγR$^{-/-}$ mice also reported that in one of the mice at day 31 p.i. showed areas of bony metaplasia (Dutia *et al.*, 1997). The current study extended this information to ascertain the incidence of this condition in the spleen of mice (both IFNγR$^{-/-}$ mice and 129 Sv/Ev mice) irrespective of whether they are infected with MHV-68 or not . The sections of spleen from various experiments were used as the material for studying the incidence of bony metaplasia (Table 4.4.1).

The histogenesis of the bony metaplasia observed in the spleen of MHV–68 infected IFNγR-/- mice had not been investigated before. Ectopic bone formation is a serious disease condition affecting different tissues in humans with conditions such as fibrodysplasia ossificans progressive (FOP) (Virdi *et al.*, 1999). One possibility for the development of these lesions is the trans-differentiation of adult parenchymal cells to osteogenic cells. The other possibility is the differentiation of locally present or recruited adult mesenchymal stem cells to osteoblast series cells and the development of bone. The recently identified mesenchymal stem cells in the spleen with committed lineage to osteogenic potential (Kodama *et al.*, 2005) suggests that the resident stem cells present in the spleen may be responding to the altered micro-environment for its differentiation. The type of micro – environment favouring such differentiation of stem cells in the spleen was shown to involve IL-5. A major phenotype shown by the mice constitutively over expressing IL-5 from their T-lymphocyte is bone nodule formation mainly in the spleen along with perturbations in the normal bone metabolism (Macias *et al.*, 2001).

One of the signalling molecules favouring the osteogenic differentiation of stem cells is bone morphogenic protein–4 (BMP–4). BMP–4 is a member of the BMP group of TGFβ super family [Reviewed in (Wozney, 2002)]. Apparently, in an *in vivo* system, interaction between different BMPs and other cellular factors may be involved in the sequential events leading to mature bone formation. Significant molecules to be considered in this context are TGFβ and CTGF. It has been

shown recently that CTGF has opposing effects on BMP-4 and TGFβ. CTGF can antagonise BMP-4 activity by preventing its binding to receptors and promotes the activity of TGFβ by enhancing its receptor binding (Abreu *et al.*, 2002).

In the current study, in addition to ascertaining the incidence of bony metaplasia lesion in the spleens of MHV–68 infected and uninfected mice, the expression pattern of BMP – 4 in the spleen was studied by immunohistochemical methods.

4.4.1. INCIDENCE OF BONY METAPLASIA IN THE SPLEEN OF MICE

The incidence of bony metaplasia in the spleen was estimated by the histopathological evaluation of spleen sections from three independent groups of infected mice and an uninfected group of mice (Table No. 4.4.1.). The study showed that, the incidence of bony metaplasia was higher in IFNγR$^{-/-}$ mice infected with MHV–68 (12.5% in experiment No.1, 16.6% in experiment No.2 and 25% in experiment no.3). In 129 Sv/Ev mice infected with MHV-68, the incidence was 0% in experiment no.1 and 6.45% in experiment no. 2. None of the uninfected control mice from both groups of mice (donor mice in the bone marrow chimera experiment) showed bony metaplasia in their spleen. However, IFNγR$^{-/-}$ mice mock infected with uninfected BHK lysate developed bony metaplasia. The development of bony metaplasia lesions occurred very late during the infection in 129 Sv/Ev mice (Day 80 p.i). Whereas, the IFNγR$^{-/-}$ mice showed bony metaplasia as early as day 12 p.i. These observations suggest that bony metaplasia lesion observed in the spleen can develop independent of fibrosis.

4.4.2. CHARACTERISATION OF BONY METAPLASIA

Some of the bony metaplasia lesions were observed grossly as small pinhead shaped white nodules on the surface of the spleen and others were observed during routine histopathological examination. The bony metaplastic lesion in the spleen showed a focal distribution pattern with only one or two foci of bony metaplasia in the whole section of spleen. The individual focus of the lesion varied in size and level of mineralization.

Table 4.4.1. Incidence of bony metaplasia in spleen

Days post infection	IFNγ $R^{-/-}$	129/Sv/Ev
Experiment No.1		
8	0/2	0/2
10	0/3	0/3
12	0/3	0/3
14	0/2	0/2
16	1/2	0/2
18	1/2	0/2
20	0/2	0/2
Overall incidence	2/16 (12.5%)	0/16 (0%)
Experiment No. 2		
12	1/3	0/3
20	0/3	0/3
30	1/4	0/3
35	0/5	0/3
40	0/4	0/3
45	0/3	0/3
50	0/3	0/3
60	0/3	0/3
80	2/3	2/3
120	2/5	0/4
Overall incidence	6/36 (16.6%)	2/31 (6.45%)
Bone marrow Chimera experiment (Donor mice - uninfected)		
0	0/9	0/9
Overall incidence	0/9 (0%)	0/9 (0%)
Experiment No. 3		
Days post infection	IFNγ$R^{-/-}$ mice infected with MHV-68	IFNγ$R^{-/-}$ mice mock infected with BHK lysate
12	0/4	0/4
16	0/4	0/4
20	2/4	0/4
50	2/4	2/4
Overall incidence	4/16 (25%)	2/16 (12.5%)

The maximum size of the lesion covered more than two third width of the spleen at a given point of bony metaplasia. The bony tissue was demarcated from the surrounding cells of the splenic parenchyma. Osteoid matrix of the bony tissue carried irregularly placed osteocytes as embedded within the calcified matrix (Figure 4.4.1A). The presence of calcium in the bony tissue was demonstrated with the Van Kossa method of staining (Figure 4.4.1B).

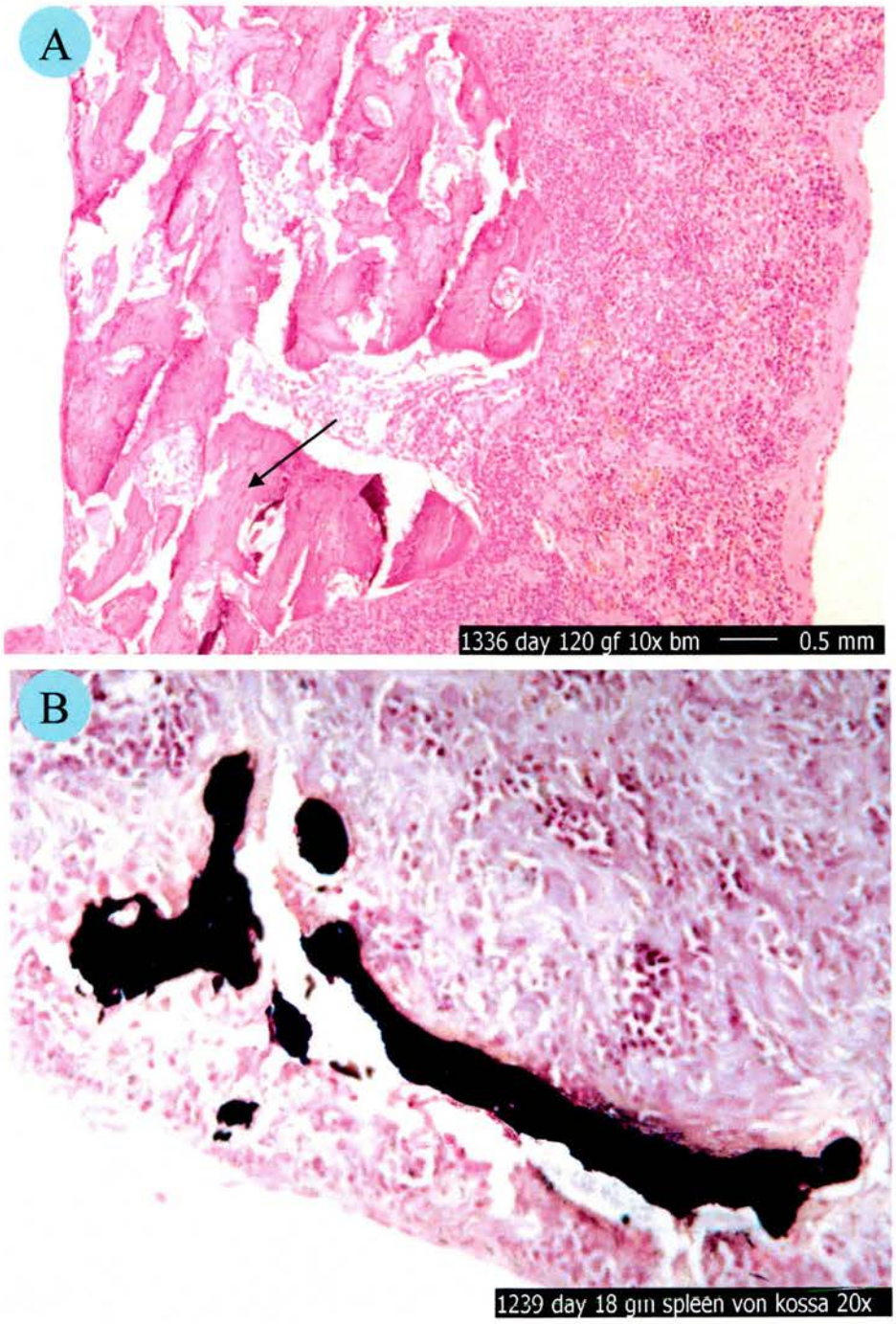

Figure. 4.4.1 . Bony metaplasia in the spleen .

A, Haematoxylin and Eosin staining. IFNγR-/- mice infected with MHV-68, day 120 p.i. Note the presence of osteocytes embedded in the osteoid (arrow). B, Von Kossa method of staining to demonstrate calcium in the bony tissue (Black colour) . IFNγR-/- mice infected with MHV-68, day 18 p.i. For image A, magnification 10X. For Image B, magnification 200x.

4.4.3. EXPRESSION OF BONE MORPHOGENIC PROTEIN–4 IN THE SPLEEN OF IFNγR$^{-/-}$ MICE INFECTED WITH MHV-68

The presence of BMP–4 positive cells in the spleen from all spleens of IFNγR$^{-/-}$ mice from experiment no.2 was investigated by immunohistochemical methods. Large numbers of BMP– 4 positive cells were noticed in the red pulp of the spleen in clusters (Figure. 4.4.2). The BMP– 4 positive cells were seen in close proximity to bony tissue as well as elsewhere in the splenic parenchyma. The positive cells were round to oval and spindle in shape with centrally placed nucleus. The morphology and distribution pattern of these positive cells suggest them as red pulp macrophages.

The number of BMP– 4 positive cells in the spleen sections was scored in a scale of 0 to ++++ is presented in table 4.4.2. (0 for absence of positive cells, + for small number of positive cells and ++++ for large number of positive cells). The score for BMP-4 positive cells in the spleen with bony metaplasia ranged from 0 to ++++, even though the majority of the spleens with bony metaplasia lesion had a score of ++++. More interestingly, the spleens without any visible bony metaplasia lesion had BMP-4 positive cells in the range of 0 to ++++. This indicates that there is no direct correlation between the presence of BMP-4 positive cells and the incidence of bony metaplasia. It may be because the signalling through BMP-4 molecule for the differentiation of putative stem cells to osteoblast series of cells is complex involving interaction with various other factors. It may also be due to delay in the expression of BMP-4 and development of bony metaplasia. Since there was no direct correlation between the presence of BMP-4 positive cells and the incidence of bony metaplasia lesion in IFNγR$^{-/-}$ mice infected with MHV-68, further staining of the sections from 129Sv/Ev mice was not carried out.

4.4.4. DISCUSSION

The current investigation revealed that the development of bony metaplasia lesion is not confined to the spleens of IFNγR$^{-/-}$ mice infected with MHV-68 alone.

Table 4.4.2. Distribution of BMP-4 positive cells in the spleen of IFNγR$^{-/-}$ mice infected with MHV-68

Day	Animal	Score	Bony metaplasia	Day	Animal	Score	Bony metaplasia
08	GM 1241	0		35	GM 1316	+	
	GF 1249	0			GM 1314	++	
10	GM 1242	0			GM 1322	++	
	GM 1236	0			GF 1329	+++	√
	GF 1246	0			GF 1327	+++	
12	GM 1240	0		40	GM 1303	+++	
	GM 1234	+++			GM 1309	+++	
	GF 1245	++++			GF 1328	++++	
	GM 1309	++++	√		GF 1325	+	
	GM 1306	++++		45	GM 1313	++	
	GF 1326	0			GM 1318	+++	
14	GM 1238	++++			GF 1330	+	
	GF 1247	+++		50	GM 1308	+++	
16	GM 1237	++++	√		GM 1310	++	
	GF 1243	++++			GF 1332	++	
18	GM 1239	+	√	60	GM 1320	+++	
	GF 1248	0			GM 1312	++	
20	GM 1235	++++			GF 1337	++	
	GF 1244	+++		80	GM 1321	++	√
	GM 1311	++			GM 1319	++	√
	GM 1304	0			GF 1323	+	
	GF 1334	0		120	GM 1301	+	
30	GM 1315	++			GM1302	0	
	GM 1317	+++	√		GM1305	+	
	GF 1331	+++			GF1336	0	√
	GF 1338	++			GF 1324	+	√

Bony metaplasia lesions were observed in IFNγR$^{-/-}$ mice mock infected with BHK cell lysate and in 129Sv/Ev mice infected with MHV-68, but at a lower incidence compared to IFNγR$^{-/-}$ mice infected with MHV-68. The detection of bony metaplasia lesions as early as day 12 p.i in IFNγR$^{-/-}$ mice as well as in 129 Sv/Ev mice infected with MHV-68 suggest that the development of bony metaplasia

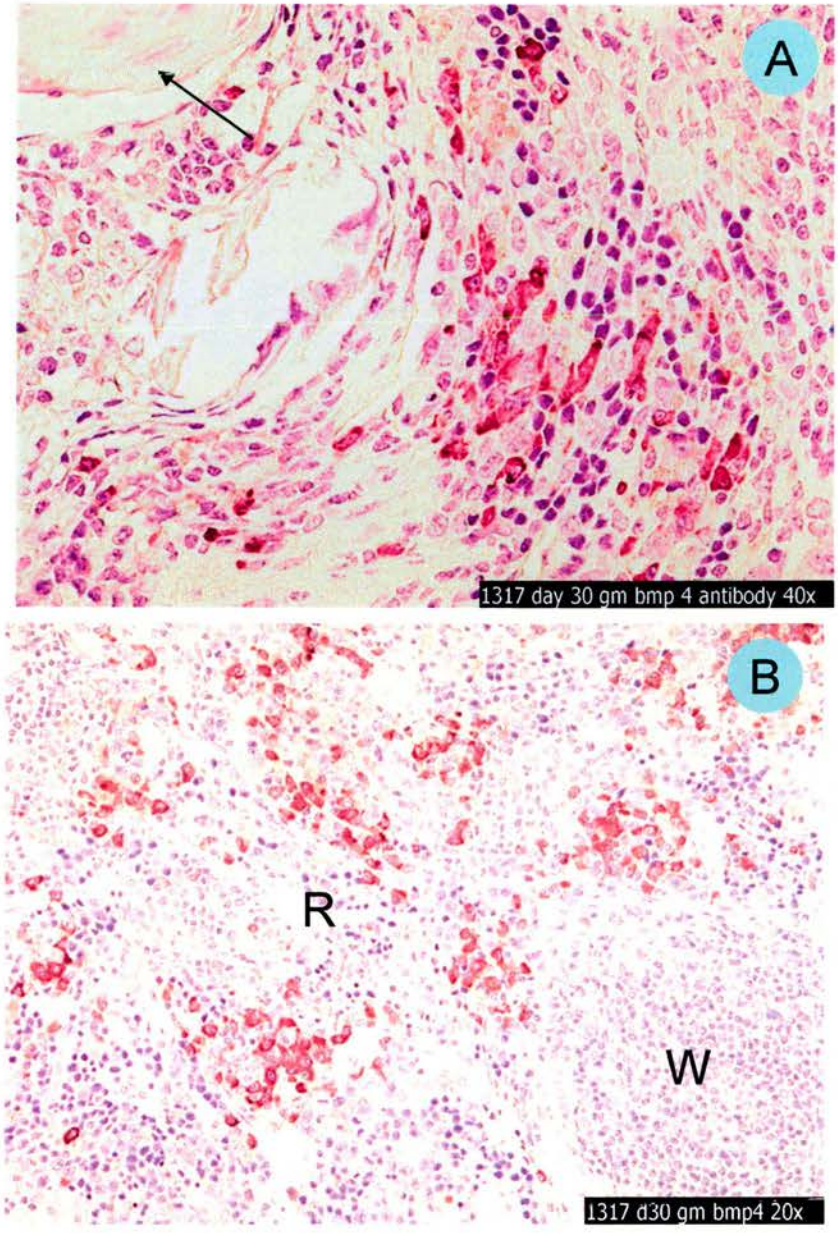

Figure. 4.4.2. Bone morphogenic protein – 4 (BMP-4) expression in the spleen of IFNγ R-/- mice infected with MHV-68 at day 30 p.i.

Collection of BMP-4 positive cells were seen in the red pulp of the spleen both in association with bony tissue (arrow) (A) as well as independent of bony tissue (B). W, White pulp. R, Red pulp. Magnification 400X for image A and 200X for image B

lesion is independent of fibrosis. The observation of increased incidence of bony metaplasia lesion in the spleen of IFNγR$^{-/-}$ mice infected with MHV-68 also argues that, the cytokine micro-environment conducive to the alternate activation of macrophages (Th2 cytokines, IL-5 is an example) is a favourable micro–environment for the differentiation of mesenchymal stem cells in the spleen towards osteogenic lineage.

BMP-4 has important roles in both embryonic development and bone formation. It has been shown recently that transfection of a retroviral vector encoding human BMP-4 into muscle derived stem cells (MDSC) can produce functional BMP-4 and initiate differentiation of stem cells to an osteogenic lineage (Wright *et al.*, 2002). BMP-4 is found in primitive mesenchymal and chondrocytic cells, the cambium layer of the periosteum, the marrow cavity and the muscles adjacent to the fracture site (Nakase *et al.*, 1994). There has been no description of BMP-4 secreting cells in the spleen. It needs to be explored whether the BMP-4 positive cells detected in the spleen are actual mesenchymal stem cells or macrophages in the red pulp. The absence of any clear correlation between the detection of bony metaplasia lesion and presence of BMP-4 positive cells in the spleen indicate the complex *in vivo* signalling mechanisms involved in the osteogenic differentiation. This *in vivo* system of infection of IFNγR$^{-/-}$ mice with MHV-68 provides a suitable small animal model system to study the biology of signalling reactions required for the differentiation of mesenchymal stem cells present in the spleen.

CHAPTER FIVE: DISCUSSION

5. DISCUSSION

The objective of the current study was to investigate the role of IFNγ in the pathogenesis of MHV-68. The investigation was carried out in a knock out mice with a defect in responding to IFNγ ($IFN\gamma R^{-/-}$mice) (Huang *et al.*, 1993). Infection of $IFN\gamma R^{-/-}$ mice with MHV-68 develops significant pathological changes in spleen and large elastic arteries (Dutia *et al.*, 1997;Weck *et al.*, 1997). The emphasis of the current investigation was to delineate the cellular, molecular and virological events associated with the pathological changes occurring in the spleen following intranasal infection of $IFN\gamma R^{-/-}$ mice with MHV-68. In addition to investigating the pathological changes in the spleen, the study was also extended to investigate the pathological changes in the lung, liver and aorta.

Fibrosis was the main pathological change observed in the spleen of $IFN\gamma R^{-/-}$ mice infected with MHV-68. The pathogenesis of fibrosis involves three overlapping phases. An acute or chronic injury is the initiating event. The injurious agent could be mechanical, infectious or an aberrant autoimmune reaction. An inflammatory phase intimately follows injury and the character of the inflammatory reaction directs the tissue response towards fibrosis. T-helper-2 (Th2) cell response mainly promotes a pro-fibrotic response. In contrast, Th1 type immune response driven by cytokines such as IFNγ is antagonistic towards a fibrotic response. Polymorphisms in the IFNγ gene as well as IFNγ receptor gene in human beings are pre-disposing factors leading to severe fibrotic disease following *Schistosoma mansoni* infection in endemic areas (Dessein *et al.*, 1999;Chevillard *et al.*, 2003). The final phase in the pathogenesis of fibrosis involves attraction and proliferation of ECM producing cells, production and lying down of ECM.

'The injury' phase of the splenic fibrosis induced by MHV-68 in $IFN\gamma R^{-/-}$ mice is characterised by the depletion of B-lymphocytes in the lymphoid follicles, which constitute the major type of cells in the spleen. The reduction in the number of B-lymphocytes could be either due to enhanced cell death or defective production

and trafficking of new cells into the spleen. The enhanced cell death in the splenic GC could arise either due to massive infection of splenocytes and subsequent cytolysis or due to massive apoptosis of B-lymphocytes which are unable to respond to an antigenic stimulus. The reduced level of B-lymphocyte turnover from the bone marrow could occur in the event of bone marrow suppression. The last possibility would be a defective trafficking of cells into the spleen due to disruption of a chemokine gradient required for homing of cells into the spleen. All the above possibilities were investigated during earlier studies and concluded that defective trafficking of cells to the spleen occurs at the height of splenic fibrosis (Dutia *et al.*, 1997;Ebrahimi *et al.*, 2001). The current study re-examined the role of productive infection and apoptosis of B-cells in the spleen by different techniques such as immunohistochemistry and counting of TBM respectively. The conclusions from these studies concurred with earlier observations.

As discussed in section 3.6, the GPCR homologue encoded by MHV-68 could potentially interfere with the chemokine gradient required for homing of lymphocytes into the spleen. Why do these events occur only in mice with defect in IFNγ signalling? Whether cellular IFNγ response gene products are able to regulate the transcription and/or translation of the proposed viral gene product or the IFNγ response gene products are able to directly nullify the actions of these putative viral gene products? Interestingly, murine IFNγ inducible protein-10 (IP-10), a key IFNγ response gene product can inhibit the actions of MHV-GPCR (Verzijl *et al.*, 2004) similar to human IP-10 inhibiting the constitutive signalling of KSHV–GPCR (Geras-Raaka *et al.*, 1998). The ability of IP-10 to inhibit the actions of virus encoded GPCR would explain the development of fibrotic changes occurring more specifically in lymphoid organs like spleen in the MHV-68 infected mice, in the absence of IFNγ signalling.

Characterisation of the cellular and molecular events taking place in the spleen of IFNγR$^{-/-}$ mice infected with MHV-68 showed a shifting of the immune response towards Th2 type. Shifting of immune response towards Th2 type was characterised by alternate activation of macrophages recognised by the up-

regulation of marker molecule, arginase -1 at both transcript and protein level. This was further confirmed by detection of transcripts of key Th2 cytokine, IL-13 in the spleen of MHV-68 infected IFNγR$^{-/-}$ mice (Personal communication from Dr. B.Ebrahimi, University of Liverpool, United Kingdom). This observation implies that immune response against a gammaherpesvirus infection can shift towards Th2 type in the event of a defect in driving an immune response towards Th1 type.

The immune response to viruses is predominantly Th1 type. A viral infection in a host with an already polarised Th2 type immune response or a genetic defect in mounting a Th1 type of response presents an awkward scenario to the host immune system. Such a scenario of natural viral infection of humans and animals are always possible. For example, patients with an overload of helminths and other multicellular parasites are likely to have an already tuned immune response towards Th2 type. The congenital defect in the system of IFNγ response can occur at multiple levels ranging from the defect in IL-12 production, the ability of cells to respond to IL-12 and produce IFNγ, polymorphism in the molecule of IFNγ, its ability to bind to the receptor, defect in the receptor units, failure in the signal transduction machinery and finally production of IFNγ response gene products from IFNγ responding cell populations. All the above situations would ultimately result in the failure of the host towards mounting a Th1 type immune response. Th1 responses following tetanus toxoid injections were found to be subdued in subjects living in endemic areas of schistosomiasis or onchocerciasis (Sabin *et al.*, 1996;Cooper *et al.*, 1997). Intracellular pathogens, which require a Th1 type response to control the infection in patients with Th2 biased immune response or defective Th1 type immune response has shown to develop more severe disease (Lienhardt *et al.*, 2002;Actor *et al.*, 1993).

The decision to mount either a Th1 or Th2 immune responses rests with the host. Various factors are involved in such a decision making process. It is argued that the type of polarisation begins at the level of antigen presenting cells (APC) itself, which subsequently bias the T-lymphocyte response according to its polarisation

(Moser and Murphy, 2000). Most importantly, properties of the pathogen dictate the type of immune response mounted against it. For example, multicellular pathogens mount a Th2 type response (Urban, Jr. *et al.*, 1992). In contrast, bacterial organisms like Listeria induces the production of IL-12 that drives a Th1 type immune response (Hsieh *et al.*, 1993). Antigen dose may be a factor involved in the choice of effector functions. Increasing the antigen dose may switch the immune response from type 1 to type 2 and vice versa (Hosken *et al.*, 1995). Soluble or particulate nature of antigen is another factor involved in the decision. The chemokines and their receptor expression also modulate the shift of immune response towards Th1 or Th2 type. Genetic background of the host is another major factor involved in the decision to drive the immune response to either Th1 or Th2 type. For example, BALB/c mice tend to produce a Th2 type response against *Leishmania major*. At the same time B6 and C3H strain of mice mount a Th1 polarised immune response against the same pathogen (Wilson *et al.*, 2005). Reversal of polarisation from Th1 to Th2 or vice versa in an *in vivo* situation is controversial. It is argued that, such a reported reversal of polarisation may be from the naïve T–lymphocytes [Reviewed in (Lafaille, 1998)]. However, shifting of the immune response from Th1 type to Th2 type is reported during granuloma development following schistosoma infection (Wynn *et al.*, 1993).

It would be interesting to explore the factors contributing to the shifting of the immune response towards Th2 type against MHV-68 in IFNγR$^{-/-}$ mice. Progressive increase in the number of latently infected cells noticed in the spleen would have contributed to the shift of immune response. As the virus remains in a 'hidden' form during latent infection, the selectively expressed viral gene products during latency would be the ideal candidate to contribute to such a shift of immune response. Such putative viral gene products may be directly influencing the chemokine gradient required for selective attraction of Th2 type cells. In wild type mice, CD4+ T-lymphocytes are induced during MHV-68 infection and are critically important for the control of replication and latency (Christensen *et al.*, 1999;Flano *et al.*, 2001;McClellan *et al.*, 2004;Sparks-Thissen *et al.*, 2004). More specifically, it has been shown recently that IFNγ producing

Th1 polarised CD4+ T-cells are sufficient for control of MHV-68 infection (Sparks-Thissen *et al.*, 2005). By comparison, relatively little is known about the role of Th2 type responses in MHV-68 infections. As discussed above, in the absence of IFNγ signalling to drive Th1 type immune response, the immune response in the spleen of IFNγR$^{-/-}$ mice following MHV-68 infection has shifted towards Th2 type characterised by secretion of IL-13 and alternate activation of macrophages. Other than artificially biasing the immune response towards Th2 type as a result of defect in the IFNγ receptor, viral gene products also could favour shifting of immune response towards Th2 type. For example, KSHV encoded vMIP-II is a promiscuous chemokine homologue capable of binding to many CC and CXC chemokine receptors and most of such chemokine receptor interactions are antagonistic (Kledal *et al.*, 1997). vMIP-II antagonises CCR5 and CXCR3, which is used by IP-10 to attract Th1 polarised lymphocytes, thereby driving the immune response towards Th2 type (Lindow *et al.*, 2003;Singh *et al.*, 2004). MIP homologues are not identified in MHV-68. Functions of the putative homologue of MIP-II in MHV-68 could contribute to the Th2 type immune response generated in the spleen of IFNγR$^{-/-}$ mice infected with MHV-68.

Invasion of lymphoid follicles carrying latently infected cells with Th2 polarised T-lymphocytes and alternatively activated macrophages were observed in the spleen from day 12 p.i to day 16 p.i. At the same time, marked expansion in the number of latently infected cells in the spleen of mice until day 18 – 22 day p.i compared to wild type controls. This suggests that, the Th2 type cellular response as such is not able to control the expansion of latently infected cells. However, another type of tissue response mediated by Th2 type immune response characterised by fibrosis was able to control the expansion of latently infected cells. This is a novel observation. The molecular mechanism by which fibrosis as a host response achieves this phenomenal effect needs to be investigated. The possibilities include stress induced apoptosis operating in the tightly packed latently infected cells trapped within the 'fibrotic cage'. The stress may be due to the limited supply of nutrients entering into the spleen at the height of fibrosis.

Other pathological manifestations seen the IFNγR$^{-/-}$ mice infected with MHV-68 appears to have bearing on a Th2 type immune response generated in the host. One of the other significant pathological changes observed in the spleen of IFNγR$^{-/-}$ mice infected with MHV-68 was bony metaplasia. The only other documented evidence of bony metaplasia occurring in the spleen of mice was in transgenic mice constitutively expressing IL-5, a key Th2 type cytokine (Macias *et al.*, 2001). This suggests that the constitutive expression of Th2 type cytokine is driving the differentiation of mesenchymal stem cells in the spleen towards an osteogenic lineage. Our data argues that the induced Th2 cytokine milieu developed in the spleen of MHV-68 infected mice may be responsible for the differentiation of mesenchymal stem cells in the spleen. The incidence of bony metaplasia was much higher in IFNγR$^{-/-}$ mice infected with MHV-68 which has mounted a Th2 type immune response compared to wild type mice infected with the virus.

The pathological changes observed in the liver of IFNγR$^{-/-}$ mice infected with MHV-68 showed similarities to the lesions seen in the liver of patients with PSC. PSC is a chronic cholestatic liver disease characterised by intrahepatic and/or extrahepatic bile duct proliferation and concentric fibrosis around necrotic bile ducts. Approximately 75% of patients with PSC have inflammatory bowel disease. The suggested model of etiopathogenesis of PSC involves memory T–lymphocytes generated in the colon during an inflammatory reaction directed against a foreign antigen binding to biliary epithelial cells in response to the same foreign antigen. This binding initiates a strong lymphocytic response. The proliferating T–lymphocytes secrete multiple chemokines and cytokines, predominantly TNFα. The cascade also initiates B–lymphocytes to secrete immunoglobulins including autoantibodies against biliary epithelial cells [Reviewed in (Aoki *et al.*, 2005)]. The lesions seen in the liver of IFNγR$^{-/-}$ mice infected with MHV-68 also appears to be lymphocyte mediated. Characterisation of lymphocyte population around the proliferating intrahepatic bile ducts showed both T and B-lymphocytes. It is possible that the memory T-lymphocytes generated against MHV-68 infected splenocytes may be binding to the biliary

epithelial cells in association with the viral antigen or through a process of 'molecular mimicry' and initiates the cascade of events leading to the development to PSC like lesions in the liver. Epitope mapping of the T-lymphocytes observed around the proliferating bile ducts need to be carried out to prove this hypothesis.

Chronic arteritis and cuffing of pulmonary blood vessels observed in IFNγR$^{-/-}$ mice infected with MHV-68 suggest tropism of the virus towards vascular structures in the absence of protective effect from IFNγ. Tunica media of blood vessels is an immunoprivileged site due to the inability of T–lymphocytes and macrophages to enter the site (Dal Canto *et al.*, 2001). The altered tropism of the virus to an immunoprivileged site in the absence of IFNγ signalling may be a consequence of spleen becoming a 'no go area' for the virus after elimination of latently infected cells mediated by the fibrotic response. Whether spleen has become a 'no go area' for the virus needs to tested by re-infecting the recovered animals with higher dose of virus to compromise the neutralising viral antibodies in the system.

In conclusion, it appears that shifting of immune response towards Th2 type in IFNγR$^{-/-}$ mice infected with MHV-68 resulted in mounting a fibrotic response, which in turn was able to control the expansion of latently infected cells in the spleen. This control of expansion of latently infected cells resulted in recovery phase characterised by re-population of different subsets of resident cells in the spleen. This system of induction of fibrosis and recovery following the elimination of virus infected cells from the centre of the lesion provides an excellent model system to explore the potential link between gammaherpesvirus infection and fibrosis, both at the level of induction and resolution. Other pathological changes observed in the spleen, aorta and liver also deserves further attention as a model system for important disease conditions affecting humans. Diseases such as primary sclerosing cholangitis and Takayasu arteritis are important disease conditions without a known aetiological factors and hence effective therapy. The fact that pathological manifestations mimicking those

disease conditions were observed following infection of a host with defect in the immune system suggest that inherent defects in the chain of IFNγ production to response may be a pre-disposing factor in the pathogenesis of these disease conditions in humans. It is highly likely to be true as gammaherpesviruses are widely prevalent in adult human population (>95%) and only very tiny fraction of carriers of the virus develops these disease during the course of their life time.

REFERENCES

Abe,R., Donnelly,S.C., Peng,T., Bucala,R., and Metz,C.N. (2001) Peripheral blood fibrocytes: differentiation pathway and migration to wound sites. *J Immunol* **166**: 7556-7562.

Ablashi,D.V., Levine,P.H., Prasad,U., and Pearson,G.R. (1983) Fourth international symposium on nasopharyngeal carcinoma application of field and laboratory studies to the control of NPC. *Cancer Res* **43**: 2375-2378.

Abraham,N., Stojdl,D.F., Duncan,P.I., Methot,N., Ishii,T., Dube,M. *et al.* (1999) Characterization of transgenic mice with targeted disruption of the catalytic domain of the double-stranded RNA-dependent protein kinase, PKR. *J Biol Chem* **274**: 5953-5962.

Abreu,J.G., Ketpura,N.I., Reversade,B., and De Robertis,E.M. (2002) Connective-tissue growth factor (CTGF) modulates cell signalling by BMP and TGF-beta. *Nat Cell Biol* **4**: 599-604.

Actor,J.K., Shirai,M., Kullberg,M.C., Buller,R.M., Sher,A., and Berzofsky,J.A. (1993) Helminth infection results in decreased virus-specific CD8+ cytotoxic T-cell and Th1 cytokine responses as well as delayed virus clearance. *Proc Natl Acad Sci U S A* **90**: 948-952.

Adler,H., Messerle,M., and Koszinowski,U.H. (2001) Virus reconstituted from infectious bacterial artificial chromosome (BAC)-cloned murine gammaherpesvirus 68 acquires wild-type properties in vivo only after excision of BAC vector sequences. *J Virol* **75**: 5692-5696.

Adler,H., Messerle,M., Wagner,M., and Koszinowski,U.H. (2000) Cloning and mutagenesis of the murine gammaherpesvirus 68 genome as an infectious bacterial artificial chromosome. *J Virol* **74**: 6964-6974.

Aguet,M., Dembic,Z., and Merlin,G. (1988) Molecular cloning and expression of the human interferon-gamma receptor. *Cell* **55**: 273-280.

Alber,D.G., Powell,K.L., Vallance,P., Goodwin,D.A., and Grahame-Clarke,C. (2000) Herpesvirus infection accelerates atherosclerosis in the apolipoprotein E-deficient mouse. *Circulation* **102**: 779-785.

Alber,D.G., Vallance,P., and Powell,K.L. (2002) Enhanced atherogenesis is not an obligatory response to systemic herpesvirus infection in the apoE-deficient mouse: comparison of murine gamma-herpesvirus-68 and herpes simplex virus-1. *Arterioscler Thromb Vasc Biol* **22**: 793-798.

Albrecht,J.C., Nicholas,J., Biller,D., Cameron,K.R., Biesinger,B., Newman,C. *et al.* (1992) Primary structure of the herpesvirus saimiri genome. *J Virol* **66**: 5047-5058.

Alcami,A. (2003) Viral mimicry of cytokines, chemokines and their receptors. *Nat Rev Immunol* **3**: 36-50.

Allison,J.P. (1994) CD28-B7 interactions in T-cell activation. *Curr Opin Immunol* **6**: 414-419.

Alvarez,C.P., Lasala,F., Carrillo,J., Muniz,O., Corbi,A.L., and Delgado,R. (2002) C-type lectins DC-SIGN and L-SIGN mediate cellular entry by Ebola virus in cis and in trans. *J Virol* **76**: 6841-6844.

Anderson,C.F., and Mosser,D.M. (2002) A novel phenotype for an activated macrophage: the type 2 activated macrophage. *J Leukoc Biol* **72**: 101-106.

Ando,M., Miyazaki,E., Fukami,T., Kumamoto,T., and Tsuda,T. (1999) Interleukin-4-producing cells in idiopathic pulmonary fibrosis: an immunohistochemical study. *Respirology* **4**: 383-391.

Ansel,K.M., Ngo,V.N., Hyman,P.L., Luther,S.A., Forster,R., Sedgwick,J.D. *et al.* (2000) A chemokine-driven positive feedback loop organizes lymphoid follicles. *Nature* **406**: 309-314.

Antman,K., and Chang,Y. (2000) Kaposi's sarcoma. *N Engl J Med* **342**: 1027-1038.

Aoki,C.A., Bowlus,C.L., and Gershwin,M.E. (2005) The immunobiology of primary sclerosing cholangitis. *Autoimmun Rev* **4**: 137-143.

Arnheiter,H., Frese,M., Kambadur,R., Meier,E., and Haller,O. (1996) Mx transgenic mice--animal models of health. *Curr Top Microbiol Immunol* **206**: 119-147.

Arrieta,J.J., Rodriguez-Inigo,E., Ortiz-Movilla,N., Bartolome,J., Pardo,M., Manzarbeitia,F. *et al.* (2001) In situ detection of hepatitis C virus RNA in salivary glands. *Am J Pathol* **158**: 259-264.

Arthur,M.J. (2002) Reversibility of liver fibrosis and cirrhosis following treatment for hepatitis C. *Gastroenterology* **122**: 1525-1528.

Artlett,C.M. (2003) Microchimerism and scleroderma: an update. *Curr Rheumatol Rep* **5**: 154-159.

Arvanitakis,L., Geras-Raaka,E., Varma,A., Gershengorn,M.C., and Cesarman,E. (1997) Human herpesvirus KSHV encodes a constitutively active G-protein-coupled receptor linked to cell proliferation. *Nature* **385**: 347-350.

Arzul,I., Renault,T., Thebault,A., and Gerard,A. (2002) Detection of oyster herpesvirus DNA and proteins in asymptomatic Crassostrea gigas adults. *Virus Res* **84**: 151-160.

Aumailley,M., and Krieg,T. (1996) Laminins: a family of diverse multifunctional molecules of basement membranes. *J Invest Dermatol* **106**: 209-214.

Austyn,J.M., and Gordon,S. (1981) F4/80, a monoclonal antibody directed specifically against the mouse macrophage. *Eur J Immunol* **11**: 805-815.

Babcock,G.J., Hochberg,D., and Thorley-Lawson,A.D. (2000) The expression pattern of Epstein-Barr virus latent genes in vivo is dependent upon the differentiation stage of the infected B cell. *Immunity* **13**: 497-506.

Baer,R., Bankier,A.T., Biggin,M.D., Deininger,P.L., Farrell,P.J., Gibson,T.J. *et al.* (1984) DNA sequence and expression of the B95-8 Epstein-Barr virus genome. *Nature* **310**: 207-211.

Ballestas,M.E., Chatis,P.A., and Kaye,K.M. (1999) Efficient persistence of extrachromosomal KSHV DNA mediated by latency-associated nuclear antigen. *Science* **284**: 641-644.

Banks,T.A., Rouse,B.T., Kerley,M.K., Blair,P.J., Godfrey,V.L., Kuklin,N.A. *et al.* (1995) Lymphotoxin-alpha-deficient mice. Effects on secondary lymphoid organ development and humoral immune responsiveness. *J Immunol* **155**: 1685-1693.

Bataller,R., Paik,Y.H., Lindquist,J.N., Lemasters,J.J., and Brenner,D.A. (2004) Hepatitis C virus core and nonstructural proteins induce fibrogenic effects in hepatic stellate cells. *Gastroenterology* **126**: 529-540.

Battegay,E.J., Raines,E.W., Seifert,R.A., Bowen-Pope,D.F., and Ross,R. (1990) TGF-beta induces bimodal proliferation of connective tissue cells via complex control of an autocrine PDGF loop. *Cell* **63**: 515-524.

Bauer,E.A., Cooper,T.W., Huang,J.S., Altman,J., and Deuel,T.F. (1985) Stimulation of in vitro human skin collagenase expression by platelet-derived growth factor. *Proc Natl Acad Sci U S A* **82**: 4132-4136.

Baumann,M., Mischak,H., Dammeier,S., Kolch,W., Gires,O., Pich,D. *et al.* (1998) Activation of the Epstein-Barr virus transcription factor BZLF1 by 12-O-tetradecanoylphorbol-13-acetate-induced phosphorylation. *J Virol* **72**: 8105-8114.

Bellows,D.S., Chau,B.N., Lee,P., Lazebnik,Y., Burns,W.H., and Hardwick,J.M. (2000) Antiapoptotic herpesvirus Bcl-2 homologs escape caspase-mediated conversion to proapoptotic proteins. *J Virol* **74**: 5024-5031.

Belperio,J.A., Dy,M., Burdick,M.D., Xue,Y.Y., Li,K., Elias,J.A., and Keane,M.P. (2002) Interaction of IL-13 and C10 in the pathogenesis of bleomycin-induced pulmonary fibrosis. *Am J Respir Cell Mol Biol* **27**: 419-427.

Belz,G.T., Liu,H., Andreansky,S., Doherty,P.C., and Stevenson,P.G. (2003) Absence of a functional defect in CD8+ T cells during primary murine gammaherpesvirus-68 infection of I-A(b-/-) mice. *J Gen Virol* **84**: 337-341.

Belz,G.T., Stevenson,P.G., Castrucci,M.R., Altman,J.D., and Doherty,P.C. (2000) Postexposure vaccination massively increases the prevalence of gamma-herpesvirus-specific CD8+ T cells but confers minimal survival advantage on CD4-deficient mice. *Proc Natl Acad Sci U S A* **97**: 2725-2730.

Bergsten,E., Uutela,M., Li,X., Pietras,K., Ostman,A., Heldin,C.H. *et al.* (2001) PDGF-D is a specific, protease-activated ligand for the PDGF beta-receptor. *Nat Cell Biol* **3**: 512-516.

Blasdell,K., McCracken,C., Morris,A., Nash,A.A., Begon,M., Bennett,M., and Stewart,J.P. (2003) The wood mouse is a natural host for Murid herpesvirus 4. *J Gen Virol* **84**: 111-113.

Blasig,C., Zietz,C., Haar,B., Neipel,F., Esser,S., Brockmeyer,N.H. *et al.* (1997) Monocytes in Kaposi's sarcoma lesions are productively infected by human herpesvirus 8. *J Virol* **71**: 7963-7968.

Blaskovic,D., Stancekova,M., Svobodova,J., and Mistrikova,J. (1980) Isolation of five strains of herpesviruses from two species of free living small rodents. *Acta Virol* **24**: 468.

Blaskovic,D., Stanekova,D., and Rajcani,J. (1984) Experimental pathogenesis of murine herpesvirus in newborn mice. *Acta Virol* **28**: 225-231.

Blease,K., Jakubzick,C., Westwick,J., Lukacs,N., Kunkel,S.L., and Hogaboam,C.M. (2001) Therapeutic effect of IL-13 immunoneutralization during chronic experimental fungal asthma. *J Immunol* **166**: 5219-5224.

Boname,J.M., and Stevenson,P.G. (2001) MHC class I ubiquitination by a viral PHD/LAP finger protein. *Immunity* **15**: 627-636.

Bornkamm,G.W., Delius,H., Fleckenstein,B., Werner,F.J., and Mulder,C. (1976) Structure of Herpesvirus saimiri genomes: arrangement of heavy and light sequences in the M genome. *J Virol* **19**: 154-161.

Bowden,R.J., Simas,J.P., Davis,A.J., and Efstathiou,S. (1997) Murine gammaherpesvirus 68 encodes tRNA-like sequences which are expressed during latency. *J Gen Virol* **78**: 1675-1687.

Brabletz,T., Pfeuffer,I., Schorr,E., Siebelt,F., Wirth,T., and Serfling,E. (1993) Transforming growth factor beta and cyclosporin A inhibit the inducible activity of the interleukin-2 gene in T cells through a noncanonical octamer-binding site. *Mol Cell Biol* **13**: 1155-1162.

Bradham,D.M., Igarashi,A., Potter,R.L., and Grotendorst,G.R. (1991) Connective tissue growth factor: a cysteine-rich mitogen secreted by human vascular

endothelial cells is related to the SRC-induced immediate early gene product CEF-10. *J Cell Biol* **114**: 1285-1294.

Branton,M.H., and Kopp,J.B. (1999) TGF-beta and fibrosis. *Microbes Infect* **1**: 1349-1365.

Bridgeman,A., Stevenson,P.G., Simas,J.P., and Efstathiou,S. (2001) A secreted chemokine binding protein encoded by murine gammaherpesvirus-68 is necessary for the establishment of a normal latent load. *J Exp Med* **194**: 301-312.

Bridgen,A., and Reid,H.W. (1991) Derivation of a DNA clone corresponding to the viral agent of sheep-associated malignant catarrhal fever. *Res Vet Sci* **50**: 38-44.

Brooks,J.W., Hamilton-Easton,A.M., Christensen,J.P., Cardin,R.D., Hardy,C.L., and Doherty,P.C. (1999) Requirement for CD40 ligand, CD4(+) T cells, and B cells in an infectious mononucleosis-like syndrome. *J Virol* **73**: 9650-9654.

Brooks,L., Yao,Q.Y., Rickinson,A.B., and Young,L.S. (1992) Epstein-Barr virus latent gene transcription in nasopharyngeal carcinoma cells: coexpression of EBNA1, LMP1, and LMP2 transcripts. *J Virol* **66**: 2689-2697.

Burkitt,D. (1963) A childrens cancer with geographical limitations. *Cancer Prog* **92**: 102-113.

Buttner,C., Skupin,A., Reimann,T., Rieber,E.P., Unteregger,G., Geyer,P., and Frank,K.H. (1997) Local production of interleukin-4 during radiation-induced pneumonitis and pulmonary fibrosis in rats: macrophages as a prominent source of interleukin-4. *Am J Respir Cell Mol Biol* **17**: 315-325.

Buxton,D., Jacoby,R.O., Reid,H.W., and Goodall,P.A. (1988) The pathology of "sheep-associated" malignant catarrhal fever in the hamster. *J Comp Pathol* **98**: 155-166.

Buxton,D., and Reid,H.W. (1980) Transmission of malignant catarrhal fever to rabbits. *Vet Rec* **106**: 243-245.

Caldwell,R.G., Wilson,J.B., Anderson,S.J., and Longnecker,R. (1998) Epstein-Barr virus LMP2A drives B cell development and survival in the absence of normal B cell receptor signals. *Immunity* **9**: 405-411.

Callan,M.F., Fazou,C., Yang,H., Rostron,T., Poon,K., Hatton,C., and McMichael,A.J. (2000) CD8(+) T-cell selection, function, and death in the primary immune response in vivo. *J Clin Invest* **106**: 1251-1261.

Callan,M.F., Steven,N., Krausa,P., Wilson,J.D., Moss,P.A., Gillespie,G.M. *et al.* (1996) Large clonal expansions of CD8+ T cells in acute infectious mononucleosis. *Nat Med* **2**: 906-911.

Callan,M.F., Tan,L., Annels,N., Ogg,G.S., Wilson,J.D., O'Callaghan,C.A. *et al.* (1998) Direct visualization of antigen-specific CD8+ T cells during the primary immune response to Epstein-Barr virus In vivo. *J Exp Med* **187**: 1395-1402.

Canbay,A., Friedman,S., and Gores,G.J. (2004) Apoptosis: the nexus of liver injury and fibrosis. *Hepatology* **39**: 273-278.

Carbone,A., Gaidano,G., Gloghini,A., Larocca,L.M., Capello,D., Canzonieri,V. *et al.* (1998) Differential expression of BCL-6, CD138/syndecan-1, and Epstein-Barr virus-encoded latent membrane protein-1 identifies distinct histogenetic subsets of acquired immunodeficiency syndrome-related non-Hodgkin's lymphomas. *Blood* **91**: 747-755.

Cardin,R.D., Brooks,J.W., Sarawar,S.R., and Doherty,P.C. (1996) Progressive loss of CD8+ T cell-mediated control of a gamma-herpesvirus in the absence of CD4+ T cells. *J Exp Med* **184**: 863-871.

Cathomas,G. (2003) Kaposi's sarcoma-associated herpesvirus (KSHV)/human herpesvirus 8 (HHV-8) as a tumour virus. *Herpes* **10**: 72-77.

Caussin-Schwemling,C., Schmitt,C., and Stoll-Keller,F. (2001) Study of the infection of human blood derived monocyte/macrophages with hepatitis C virus in vitro. *J Med Virol* **65**: 14-22.

Cella,M., Scheidegger,D., Palmer-Lehmann,K., Lane,P., Lanzavecchia,A., and Alber,G. (1996) Ligation of CD40 on dendritic cells triggers production of high levels of interleukin-12 and enhances T cell stimulatory capacity: T-T help via APC activation. *J Exp Med* **184**: 747-752.

Chan,A.T., Teo,P.M., and Huang,D.P. (2004) Pathogenesis and treatment of nasopharyngeal carcinoma. *Semin Oncol* **31**: 794-801.

Chang,Y., Cesarman,E., Pessin,M.S., Lee,F., Culpepper,J., Knowles,D.M., and Moore,P.S. (1994) Identification of herpesvirus-like DNA sequences in AIDS-associated Kaposi's sarcoma. *Science* **266**: 1865-1869.

Chantry,D., Turner,M., Abney,E., and Feldmann,M. (1989) Modulation of cytokine production by transforming growth factor-beta. *J Immunol* **142**: 4295-4300.

Chelbi-Alix,M.K., and Thang,M.N. (1986) Multiple molecular forms of interferon display different specific activities in the induction of the antiviral state and 2'5' oligoadenylate synthetase. *Biochem Biophys Res Commun* **141**: 1042-1050.

Chen,D., Zhao,M., and Mundy,G.R. (2004) Bone morphogenetic proteins. *Growth Factors* **22**: 233-241.

Chen,G., and Goeddel,D.V. (2002) TNF-R1 signaling: a beautiful pathway. *Science* **296**: 1634-1635.

Cheng,E.H., Kirsch,D.G., Clem,R.J., Ravi,R., Kastan,M.B., Bedi,A. *et al.* (1997a) Conversion of Bcl-2 to a Bax-like death effector by caspases. *Science* **278**: 1966-1968.

Cheng,E.H., Nicholas,J., Bellows,D.S., Hayward,G.S., Guo,H.G., Reitz,M.S., and Hardwick,J.M. (1997b) A Bcl-2 homolog encoded by Kaposi sarcoma-associated virus, human herpesvirus 8, inhibits apoptosis but does not heterodimerize with Bax or Bak. *Proc Natl Acad Sci U S A* **94**: 690-694.

Chevillard,C., Moukoko,C.E., Elwali,N.E., Bream,J.H., Kouriba,B., Argiro,L. *et al.* (2003) IFN-gamma polymorphisms (IFN-gamma +2109 and IFN-gamma +3810) are associated with severe hepatic fibrosis in human hepatic schistosomiasis (Schistosoma mansoni). *J Immunol* **171**: 5596-5601.

Chiaramonte,M.G., Cheever,A.W., Malley,J.D., Donaldson,D.D., and Wynn,T.A. (2001) Studies of murine schistosomiasis reveal interleukin-13 blockade as a treatment for established and progressive liver fibrosis. *Hepatology* **34**: 273-282.

Chiaramonte,M.G., Donaldson,D.D., Cheever,A.W., and Wynn,T.A. (1999) An IL-13 inhibitor blocks the development of hepatic fibrosis during a T-helper type 2-dominated inflammatory response. *J Clin Invest* **104**: 777-785.

Cho,J.Y., Miller,M., Baek,K.J., Han,J.W., Nayar,J., Lee,S.Y. *et al.* (2004) Inhibition of airway remodeling in IL-5-deficient mice. *J Clin Invest* **113**: 551-560.

Christensen,J.P., Cardin,R.D., Branum,K.C., and Doherty,P.C. (1999) CD4(+) T cell-mediated control of a gamma-herpesvirus in B cell-deficient mice is mediated by IFN-gamma. *Proc Natl Acad Sci U S A* **96**: 5135-5140.

Christensen,J.P., and Doherty,P.C. (1999) Quantitative analysis of the acute and long-term CD4(+) T-cell response to a persistent gammaherpesvirus. *J Virol* **73**: 4279-4283.

Chua,C.C., Geiman,D.E., Keller,G.H., and Ladda,R.L. (1985) Induction of collagenase secretion in human fibroblast cultures by growth promoting factors. *J Biol Chem* **260**: 5213-5216.

Ciampor,F., Stancekova,M., and Blaskovic,D. (1981) Electron microscopy of rabbit embryo fibroblasts infected with herpesvirus isolates from Clethrionomys glareolus and Apodemus flavicollis. *Acta Virol* **25**: 101-107.

Cinquina,C.C., Grogan,E., Sun,R., Lin,S.F., Beardsley,G.P., and Miller,G. (2000) Dihydrofolate reductase from Kaposi's sarcoma-associated herpesvirus. *Virology* **268**: 201-217.

Clambey,E.T., Virgin,H.W., and Speck,S.H. (2000) Disruption of the murine gammaherpesvirus 68 M1 open reading frame leads to enhanced reactivation from latency. *J Virol* **74**: 1973-1984.

Cobbold,S.P., Martin,G., and Waldmann,H. (1990) The induction of skin graft tolerance in major histocompatibility complex-mismatched or primed recipients: primed T cells can be tolerized in the periphery with anti-CD4 and anti-CD8 antibodies. *Eur J Immunol* **20**: 2747-2755.

Coffey,A.J., Brooksbank,R.A., Brandau,O., Oohashi,T., Howell,G.R., Bye,J.M. *et al.* (1998) Host response to EBV infection in X-linked lymphoproliferative disease results from mutations in an SH2-domain encoding gene. *Nat Genet* **20**: 129-135.

Coffman,R.L. (1982) Surface antigen expression and immunoglobulin gene rearrangement during mouse pre-B cell development. *Immunol Rev* **69**: 5-23.

Colmenares,M., Puig-Kroger,A., Pello,O.M., Corbi,A.L., and Rivas,L. (2002) Dendritic cell (DC)-specific intercellular adhesion molecule 3 (ICAM-3)-grabbing nonintegrin (DC-SIGN, CD209), a C-type surface lectin in human DCs, is a receptor for Leishmania amastigotes. *J Biol Chem* **277**: 36766-36769.

Cook,C.G., and Splitter,G.A. (1988) Lytic function of bovine lymphokine-activated killer cells from a normal and a malignant catarrhal fever virus-infected animal. *Vet Immunol Immunopathol* **19**: 105-118.

Cook,J.R., Emanuel,S.L., Donnelly,R.J., Soh,J., Mariano,T.M., Schwartz,B. *et al.* (1994) Sublocalization of the human interferon-gamma receptor accessory factor gene and characterization of accessory factor activity by yeast artificial chromosomal fragmentation. *J Biol Chem* **269**: 7013-7018.

Cooper,P.J., Guderian,R.H., Nutman,T.B., and Taylor,D.W. (1997) Human infection with Onchocerca volvulus does not affect the T helper cell phenotype of the cellular immune response to mycobacterial antigen. *Trans R Soc Trop Med Hyg* **91**: 350-352.

Coppola,M.A., Flano,E., Nguyen,P., Hardy,C.L., Cardin,R.D., Shastri,N. *et al.* (1999) Apparent MHC-independent stimulation of CD8+ T cells in vivo during latent murine gammaherpesvirus infection. *J Immunol* **163**: 1481-1489.

Corbellino,M., Parravicini,C., Aubin,J.T., and Berti,E. (1996) Kaposi's sarcoma and herpesvirus-like DNA sequences in sensory ganglia. *N Engl J Med* **334**: 1341-1342.

Costanzo,F., Campadelli-Fiume,G., Foa-Tomasi,L., and Cassai,E. (1977) Evidence that herpes simplex virus DNA is transcribed by cellular RNA polymerase B. *J Virol* **21**: 996-1001.

Coulter,L.J., Wright,H., and Reid,H.W. (2001) Molecular genomic characterization of the viruses of malignant catarrhal fever. *J Comp Pathol* **124**: 2-19.

Couty,J.P., and Gershengorn,M.C. (2004) Insights into the viral G protein-coupled receptor encoded by human herpesvirus type 8 (HHV-8). *Biol Cell* **96**: 349-354.

Daines,M.O., and Hershey,G.K. (2002) A novel mechanism by which interferon-gamma can regulate interleukin (IL)-13 responses. Evidence for intracellular stores of IL-13 receptor alpha -2 and their rapid mobilization by interferon-gamma. *J Biol Chem* **277**: 10387-10393.

Dairaghi,D.J., Fan,R.A., McMaster,B.E., Hanley,M.R., and Schall,T.J. (1999) HHV8-encoded vMIP-I selectively engages chemokine receptor CCR8. Agonist and antagonist profiles of viral chemokines. *J Biol Chem* **274**: 21569-21574.

Dal Canto,A.J., Swanson,P.E., O'Guin,A.K., Speck,S.H., and Virgin,H.W. (2001) IFN-gamma action in the media of the great elastic arteries, a novel immunoprivileged site. *J Clin Invest* **107**: R15-R22.

Dal Canto,A.J., Virgin,H.W., and Speck,S.H. (2000) Ongoing viral replication is required for gammaherpesvirus 68-induced vascular damage. *J Virol* **74**: 11304-11310.

Dalton,D.K., Pitts-Meek,S., Keshav,S., Figari,I.S., Bradley,A., and Stewart,T.A. (1993) Multiple defects of immune cell function in mice with disrupted interferon-gamma genes. *Science* **259**: 1739-1742.

Damania,B. (2004) Oncogenic gamma-herpesviruses: comparison of viral proteins involved in tumorigenesis. *Nat Rev Microbiol* **2**: 656-668.

Dang,H., Dauphinee,M.J., Talal,N., Garry,R.F., Seibold,J.R., Medsger,T.A., Jr. *et al.* (1991) Serum antibody to retroviral gag proteins in systemic sclerosis. *Arthritis Rheum* **34**: 1336-1337.

de Lima,B.D., May,J.S., Marques,S., Simas,J.P., and Stevenson,P.G. (2005) Murine gammaherpesvirus 68 bcl-2 homologue contributes to latency establishment in vivo. *J Gen Virol* **86**: 31-40.

de Wet,W.J., Chu,M.L., and Prockop,D.J. (1983) The mRNAs for the pro-alpha 1(I) and pro-alpha 2(I) chains of type I procollagen are translated at the same rate in normal human fibroblasts and in fibroblasts from two variants of osteogenesis imperfecta with altered steady state ratios of the two mRNAs. *J Biol Chem* **258**: 14385-14389.

Decker,T., Kovarik,P., and Meinke,A. (1997) GAS elements: a few nucleotides with a major impact on cytokine-induced gene expression. *J Interferon Cytokine Res* **17**: 121-134.

Deiss,L.P., and Frenkel,N. (1986) Herpes simplex virus amplicon: cleavage of concatemeric DNA is linked to packaging and involves amplification of the terminally reiterated a sequence. *J Virol* **57**: 933-941.

Derynck,R., Leung,D.W., Gray,P.W., and Goeddel,D.V. (1982) Human interferon gamma is encoded by a single class of mRNA. *Nucleic Acids Res* **10**: 3605-3615.

Desmouliere,A., Geinoz,A., Gabbiani,F., and Gabbiani,G. (1993) Transforming growth factor-beta 1 induces alpha-smooth muscle actin expression in granulation tissue myofibroblasts and in quiescent and growing cultured fibroblasts. *J Cell Biol* **122**: 103-111.

Dessein,A.J., Hillaire,D., Elwali,N.E., Marquet,S., Mohamed-Ali,Q., Mirghani,A. *et al.* (1999) Severe hepatic fibrosis in Schistosoma mansoni infection is controlled by a major locus that is closely linked to the interferon-gamma receptor gene. *Am J Hum Genet* **65**: 709-721.

Diamond,C., Brodie,S.J., Krieger,J.N., Huang,M.L., Koelle,D.M., Diem,K. *et al.* (1998) Human herpesvirus 8 in the prostate glands of men with Kaposi's sarcoma. *J Virol* **72**: 6223-6227.

Diefenbach,A., Schindler,H., Donhauser,N., Lorenz,E., Laskay,T., MacMicking,J. *et al.* (1998) Type 1 interferon (IFNalpha/beta) and type 2 nitric oxide synthase regulate the innate immune response to a protozoan parasite. *Immunity* **8**: 77-87.

Diegelmann,R.F., and Evans,M.C. (2004) Wound healing: an overview of acute, fibrotic and delayed healing. *Front Biosci* **9**: 283-289.

Dijkstra,C.D., van Vliet,E., Dopp,E.A., van der Lelij,A.A., and Kraal,G. (1985) Marginal zone macrophages identified by a monoclonal antibody: characterization of immuno- and enzyme-histochemical properties and functional capacities. *Immunology* **55**: 23-30.

Dittmer,D., Lagunoff,M., Renne,R., Staskus,K., Haase,A., and Ganem,D. (1998) A cluster of latently expressed genes in Kaposi's sarcoma-associated herpesvirus. *J Virol* **72**: 8309-8315.

Doherty,P.C., Christensen,J.P., Belz,G.T., Stevenson,P.G., and Sangster,M.Y. (2001) Dissecting the host response to a gamma-herpesvirus. *Philos Trans R Soc Lond B Biol Sci* **356**: 581-593.

Doherty,P.C., Tripp,R.A., Hamilton-Easton,A.M., Cardin,R.D., Woodland,D.L., and Blackman,M.A. (1997) Tuning into immunological dissonance: an experimental model for infectious mononucleosis. *Curr Opin Immunol* **9**: 477-483.

Doucet,C., Brouty-Boye,D., Pottin-Clemenceau,C., Jasmin,C., Canonica,G.W., and Azzarone,B. (1998) IL-4 and IL-13 specifically increase adhesion molecule and inflammatory cytokine expression in human lung fibroblasts. *Int Immunol* **10**: 1421-1433.

Duffield,J.S. (2003) The inflammatory macrophage: a story of Jekyll and Hyde. *Clin Sci (Lond)* **104**: 27-38.

Duffield,J.S., Forbes,S.J., Constandinou,C.M., Clay,S., Partolina,M., Vuthoori,S. *et al.* (2005) Selective depletion of macrophages reveals distinct, opposing roles during liver injury and repair. *J Clin Invest* **115**: 56-65.

Dupin,N., Diss,T.L., Kellam,P., Tulliez,M., Du,M.Q., Sicard,D. *et al.* (2000) HHV-8 is associated with a plasmablastic variant of Castleman disease that is linked to HHV-8-positive plasmablastic lymphoma. *Blood* **95**: 1406-1412.

Dutia,B.M., Allen,D.J., Dyson,H., and Nash,A.A. (1999) Type I interferons and IRF-1 play a critical role in the control of a gammaherpesvirus infection. *Virology* **261**: 173-179.

Dutia,B.M., Clarke,C.J., Allen,D.J., and Nash,A.A. (1997) Pathological changes in the spleens of gamma interferon receptor-deficient mice infected with murine gammaherpesvirus: a role for CD8 T cells. *J Virol* **71**: 4278-4283.

Dutia,B.M., Roy,D.J., Ebrahimi,B., Gangadharan,B., Efstathiou,S., Stewart,J.P., and Nash,A.A. (2004) Identification of a region of the virus genome involved in murine gammaherpesvirus 68-induced splenic pathology. *J Gen Virol* **85**: 1393-1400.

Ebrahimi,B., Dutia,B.M., Brownstein,D.G., and Nash,A.A. (2001) Murine gammaherpesvirus-68 infection causes multi-organ fibrosis and alters leukocyte trafficking in interferon-gamma receptor knockout mice. *Am J Pathol* **158**: 2117-2125.

Efstathiou,S., Ho,Y.M., Hall,S., Styles,C.J., Scott,S.D., and Gompels,U.A. (1990a) Murine herpesvirus 68 is genetically related to the gammaherpesviruses Epstein-Barr virus and herpesvirus saimiri. *J Gen Virol* **71 (Pt 6)**: 1365-1372.

Efstathiou,S., Ho,Y.M., and Minson,A.C. (1990b) Cloning and molecular characterization of the murine herpesvirus 68 genome. *J Gen Virol* **71 (Pt 6)**: 1355-1364.

Egan,J.J., Stewart,J.P., Hasleton,P.S., Arrand,J.R., Carroll,K.B., and Woodcock,A.A. (1995) Epstein-Barr virus replication within pulmonary epithelial cells in cryptogenic fibrosing alveolitis. *Thorax* **50**: 1234-1239.

Egan,J.J., Woodcock,A.A., and Stewart,J.P. (1997) Viruses and idiopathic pulmonary fibrosis. *Eur Respir J* **10**: 1433-1437.

Ehrt,S., Schnappinger,D., Bekiranov,S., Drenkow,J., Shi,S., Gingeras,T.R. *et al.* (2001) Reprogramming of the macrophage transcriptome in response to interferon-gamma and Mycobacterium tuberculosis: signaling roles of nitric oxide synthase-2 and phagocyte oxidase. *J Exp Med* **194**: 1123-1140.

Ehtisham,S., Sunil-Chandra,N.P., and Nash,A.A. (1993) Pathogenesis of murine gammaherpesvirus infection in mice deficient in CD4 and CD8 T cells. *J Virol* **67**: 5247-5252.

Eikelenboom,P. (1978) Characterization of non-lymphoid cells in the white pulp of the mouse spleen: an in vivo and in vitro study. *Cell Tissue Res* **195**: 445-460.

Ellis,J.A., O'Toole,D.T., Haven,T.R., and Davis,W.C. (1992) Predominance of BoCD8-positive T lymphocytes in vascular lesions in a 1-year-old cow with concurrent malignant catarrhal fever and bovine viral diarrhea virus infection. *Vet Pathol* **29**: 545-547.

Emura,M., Nagai,S., Takeuchi,M., Kitaichi,M., and Izumi,T. (1990) In vitro production of B cell growth factor and B cell differentiation factor by peripheral blood mononuclear cells and bronchoalveolar lavage T lymphocytes from patients with idiopathic pulmonary fibrosis. *Clin Exp Immunol* **82**: 133-139.

Endo,M., Oyadomari,S., Terasaki,Y., Takeya,M., Suga,M., Mori,M., and Gotoh,T. (2003) Induction of arginase I and II in bleomycin-induced fibrosis of mouse lung. *Am J Physiol Lung Cell Mol Physiol* **285**: L313-L321.

Endres,M.J., Garlisi,C.G., Xiao,H., Shan,L., and Hedrick,J.A. (1999) The Kaposi's sarcoma-related herpesvirus (KSHV)-encoded chemokine vMIP-I is a specific agonist for the CC chemokine receptor (CCR)8. *J Exp Med* **189**: 1993-1998.

Engel,J., and Prockop,D.J. (1991) The zipper-like folding of collagen triple helices and the effects of mutations that disrupt the zipper. *Annu Rev Biophys Biophys Chem* **20**: 137-152.

Ensser,A., Pflanz,R., and Fleckenstein,B. (1997) Primary structure of the alcelaphine herpesvirus 1 genome. *J Virol* **71**: 6517-6525.

Epstein,M.A., ACHONG,B.G., and Barry,Y.M. (1964) Virus particles in cultured lymphoblasts from Burkitt's lymphoma. *Lancet* **15**: 702-703.

Epstein,O., Thomas,H.C., and Sherlock,S. (1980) Primary biliary cirrhosis is a dry gland syndrome with features of chronic graft-versus-host disease. *Lancet* **1**: 1166-1168.

Farrar,W.L., Birchenall-Sparks,M.C., and Young,H.B. (1986) Interleukin 2 induction of interferon-gamma mRNA synthesis. *J Immunol* **137**: 3836-3840.

Farrell,P.J., Rowe,D.T., Rooney,C.M., and Kouzarides,T. (1989) Epstein-Barr virus BZLF1 trans-activator specifically binds to a consensus AP-1 site and is related to c-fos. *EMBO J* **8**: 127-132.

Fattovich,G. (2003) Natural history of hepatitis B. *J Hepatol* **39 Suppl 1**: S50-S58.

Faull,R.J. (1995) Adhesion molecules in health and disease. *Aust N Z J Med* **25**: 720-730.

Fertin,C., Nicolas,J.F., Gillery,P., Kalis,B., Banchereau,J., and Maquart,F.X. (1991) Interleukin-4 stimulates collagen synthesis by normal and scleroderma fibroblasts in dermal equivalents. *Cell Mol Biol* **37**: 823-829.

Fickenscher,H., and Fleckenstein,B. (2001) Herpesvirus saimiri. *Philos Trans R Soc Lond B Biol Sci* **356**: 545-567.

Fingeroth,J.D., Weis,J.J., Tedder,T.F., Strominger,J.L., Biro,P.A., and Fearon,D.T. (1984) Epstein-Barr virus receptor of human B lymphocytes is the C3d receptor CR2. *Proc Natl Acad Sci U S A* **81**: 4510-4514.

Fiorentino,D.F., Bond,M.W., and Mosmann,T.R. (1989) Two types of mouse T helper cell. IV. Th2 clones secrete a factor that inhibits cytokine production by Th1 clones. *J Exp Med* **170**: 2081-2095.

Flano,E., Husain,S.M., Sample,J.T., Woodland,D.L., and Blackman,M.A. (2000) Latent murine gamma-herpesvirus infection is established in activated B cells, dendritic cells, and macrophages. *J Immunol* **165**: 1074-1081.

Flano,E., Kim,I.J., Woodland,D.L., and Blackman,M.A. (2002a) Gamma-herpesvirus latency is preferentially maintained in splenic germinal center and memory B cells. *J Exp Med* **196**: 1363-1372.

Flano,E., Woodland,D.L., and Blackman,M.A. (2002b) A mouse model for infectious mononucleosis. *Immunol Res* **25**: 201-217.

Flano,E., Woodland,D.L., Blackman,M.A., and Doherty,P.C. (2001) Analysis of virus-specific CD4(+) t cells during long-term gammaherpesvirus infection. *J Virol* **75**: 7744-7748.

Flano,E., Hardy,C.L., Kim,I.J., Frankling,C., Coppola,M.A., Nguyen,P. *et al.* (2004) T Cell Reactivity during Infectious Mononucleosis and Persistent Gammaherpesvirus Infection in Mice. *J Immunol* **172**: 3078-3085.

Flano,E., Woodland,D.L., and Blackman,M.A. (1999) Requirement for CD4+ T Cells in V{beta}4+CD8+ T Cell Activation Associated with Latent Murine Gammaherpesvirus Infection. *J Immunol* **163**: 3403-3408.

Floyd-Smith,G., Slattery,E., and Lengyel,P. (1981) Interferon action: RNA cleavage pattern of a (2'-5')oligoadenylate--dependent endonuclease. *Science* **212**: 1030-1032.

Forbes,S.J., Russo,F.P., Rey,V., Burra,P., Rugge,M., Wright,N.A., and Alison,M.R. (2004) A significant proportion of myofibroblasts are of bone marrow origin in human liver fibrosis. *Gastroenterology* **126**: 955-963.

Foreman,K.E., Friborg,J., Jr., Kong,W.P., Woffendin,C., Polverini,P.J., Nickoloff,B.J., and Nabel,G.J. (1997) Propagation of a human herpesvirus from AIDS-associated Kaposi's sarcoma. *N Engl J Med* **336**: 163-171.

Fowler,P., Marques,S., Simas,J.P., and Efstathiou,S. (2003) ORF73 of murine herpesvirus-68 is critical for the establishment and maintenance of latency. *J Gen Virol* **84**: 3405-3416.

Friedman,S.L., Roll,F.J., Boyles,J., and Bissell,D.M. (1985) Hepatic lipocytes: the principal collagen-producing cells of normal rat liver. *Proc Natl Acad Sci U S A* **82**: 8681-8685.

Fries,K.M., Blieden,T., Looney,R.J., Sempowski,G.D., Silvera,M.R., Willis,R.A., and Phipps,R.P. (1994) Evidence of fibroblast heterogeneity and the role of fibroblast subpopulations in fibrosis. *Clin Immunol Immunopathol* **72**: 283-292.

Fukuda,M., and Longnecker,R. (2004) Latent membrane protein 2A inhibits transforming growth factor-beta 1-induced apoptosis through the phosphatidylinositol 3-kinase/Akt pathway. *J Virol* **78**: 1697-1705.

Gaidano,G., Carbone,A., and Dalla-Favera,R. (1998) Genetic basis of acquired immunodeficiency syndrome-related lymphomagenesis. *J Natl Cancer Inst Monogr*: 95-100.

Gandhi,M.K., Tellam,J.T., and Khanna,R. (2004) Epstein-Barr virus-associated Hodgkin's lymphoma. *Br J Haematol* **125**: 267-281.

Gangappa,S., van Dyk,L.F., Jewett,T.J., Speck,S.H., and Virgin,H.W. (2002) Identification of the in vivo role of a viral bcl-2. *J Exp Med* **195**: 931-940.

Geijtenbeek,T.B., Groot,P.C., Nolte,M.A., van Vliet,S.J., Gangaram-Panday,S.T., van Duijnhoven,G.C. *et al.* (2002) Marginal zone macrophages express a murine homologue of DC-SIGN that captures blood-borne antigens in vivo. *Blood* **100**: 2908-2916.

Geijtenbeek,T.B., Kwon,D.S., Torensma,R., van Vliet,S.J., van Duijnhoven,G.C., Middel,J. *et al.* (2000a) DC-SIGN, a dendritic cell-specific HIV-1-binding protein that enhances trans-infection of T cells. *Cell* **100**: 587-597.

Geijtenbeek,T.B., Torensma,R., van Vliet,S.J., van Duijnhoven,G.C., Adema,G.J., van Kooyk,Y., and Figdor,C.G. (2000b) Identification of DC-SIGN, a novel dendritic cell-specific ICAM-3 receptor that supports primary immune responses. *Cell* **100**: 575-585.

George,C.X., Thomis,D.C., McCormack,S.J., Svahn,C.M., and Samuel,C.E. (1996) Characterization of the heparin-mediated activation of PKR, the interferon-inducible RNA-dependent protein kinase. *Virology* **221**: 180-188.

Geras-Raaka,E., Varma,A., Ho,H., Clark-Lewis,I., and Gershengorn,M.C. (1998) Human interferon-gamma-inducible protein 10 (IP-10) inhibits constitutive signaling of Kaposi's sarcoma-associated herpesvirus G protein-coupled receptor. *J Exp Med* **188**: 405-408.

Gerber,J.S., and Mosser,D.M. (2001) Reversing lipopolysaccharide toxicity by ligating the macrophage Fc gamma receptors. *J Immunol* **166**: 6861-6868.

Ghosh,A.K. (2002) Factors involved in the regulation of type I collagen gene expression: implication in fibrosis. *Exp Biol Med (Maywood)* **227**: 301-314.

Ghosh,A.K., Yuan,W., Mori,Y., Chen,S., and Varga,J. (2001) Antagonistic regulation of type I collagen gene expression by interferon-gamma and transforming growth factor-beta. Integration at the level of p300/CBP transcriptional coactivators. *J Biol Chem* **276**: 11041-11048.

Giri,S.N., Hyde,D.M., and Marafino,B.J., Jr. (1986) Ameliorating effect of murine interferon gamma on bleomycin-induced lung collagen fibrosis in mice. *Biochem Med Metab Biol* **36**: 194-197.

Goerdt,S., and Orfanos,C.E. (1999) Other functions, other genes: alternative activation of antigen-presenting cells. *Immunity* **10**: 137-142.

Gong,M., and Kieff,E. (1990) Intracellular trafficking of two major Epstein-Barr virus glycoproteins, gp350/220 and gp110. *J Virol* **64**: 1507-1516.

Gordon,S. (2003) Alternative activation of macrophages. *Nat Rev Immunol* **3**: 23-35.

Gorelik,L., and Flavell,R.A. (2002) Transforming growth factor-beta in T-cell biology. *Nat Rev Immunol* **2**: 46-53.

Graff,J.M., Bansal,A., and Melton,D.A. (1996) Xenopus Mad proteins transduce distinct subsets of signals for the TGF beta superfamily. *Cell* **85**: 479-487.

Gratchev,A., Guillot,P., Hakiy,N., Politz,O., Orfanos,C.E., Schledzewski,K., and Goerdt,S. (2001) Alternatively activated macrophages differentially express fibronectin and its splice variants and the extracellular matrix protein betaIG-H3. *Scand J Immunol* **53**: 386-392.

Gray,P.W., and Goeddel,D.V. (1982) Structure of the human immune interferon gene. *Nature* **298**: 859-863.

Gray,P.W., and Goeddel,D.V. (1983) Cloning and expression of murine immune interferon cDNA. *Proc Natl Acad Sci U S A* **80**: 5842-5846.

Gray,P.W., Leong,S., Fennie,E.H., Farrar,M.A., Pingel,J.T., Fernandez-Luna,J., and Schreiber,R.D. (1989) Cloning and expression of the cDNA for the murine interferon gamma receptor. *Proc Natl Acad Sci U S A* **86**: 8497-8501.

Gray,P.W., Leung,D.W., Pennica,D., Yelverton,E., Najarian,R., Simonsen,C.C. *et al.* (1982) Expression of human immune interferon cDNA in E. coli and monkey cells. *Nature* **295**: 503-508.

Gregory,C.D., and Devitt,A. (2004) The macrophage and the apoptotic cell: an innate immune interaction viewed simplistically? *Immunology* **113**: 1-14.

Grotendorst,G.R., Rahmanie,H.A.M.E., and Duncan,M.R. (2004) Combinatorial signaling pathways determine fibroblast proliferation and myofibroblast differentiation. *FASEB J* **18**: 469-479.

Gupta,S., Pablo,A.M., Jiang,X., Wang,N., Tall,A.R., and Schindler,C. (1997) IFN-gamma potentiates atherosclerosis in ApoE knock-out mice. *J Clin Invest* **99**: 2752-2761.

Guzman-Rojas,L., Sims-Mourtada,J.C., Rangel,R., and Martinez-Valdez,H. (2002) Life and death within germinal centres: a double-edged sword. *Immunology* **107**: 167-175.

Hahn,S.A., Schutte,M., Hoque,A.T., Moskaluk,C.A., da Costa,L.T., Rozenblum,E. *et al.* (1996) DPC4, a candidate tumor suppressor gene at human chromosome 18q21.1. *Science* **271**: 350-353.

Halary,F., Amara,A., Lortat-Jacob,H., Messerle,M., Delaunay,T., Houles,C. *et al.* (2002) Human cytomegalovirus binding to DC-SIGN is required for dendritic cell infection and target cell trans-infection. *Immunity* **17**: 653-664.

Hanayama,R., Tanaka,M., Miyasaka,K., Aozasa,K., Koike,M., Uchiyama,Y., and Nagata,S. (2004) Autoimmune disease and impaired uptake of apoptotic cells in MFG-E8-deficient mice. *Science* **304**: 1147-1150.

Hao,H., Cohen,D.A., Jennings,C.D., Bryson,J.S., and Kaplan,A.M. (2000) Bleomycin-induced pulmonary fibrosis is independent of eosinophils. *J Leukoc Biol* **68**: 515-521.

Haque,T., Wilkie,G.M., Taylor,C., Amlot,P.L., Murad,P., Iley,A. *et al.* (2002) Treatment of Epstein-Barr-virus-positive post-transplantation lymphoproliferative disease with partly HLA-matched allogeneic cytotoxic T cells. *Lancet* **360**: 436-442.

Hardy,C.L., Silins,S.L., Woodland,D.L., and Blackman,M.A. (2000) Murine gamma-herpesvirus infection causes V(beta)4-specific CDR3-restricted clonal expansions within CD8(+) peripheral blood T lymphocytes. *Int Immunol* **12**: 1193-1204.

Hashimoto,S., Gon,Y., Takeshita,I., Maruoka,S., and Horie,T. (2001) IL-4 and IL-13 induce myofibroblastic phenotype of human lung fibroblasts through c-Jun NH2-terminal kinase-dependent pathway. *J Allergy Clin Immunol* **107**: 1001-1008.

Hatfull,G., Bankier,A.T., Barrell,B.G., and Farrell,P.J. (1988) Sequence analysis of Raji Epstein-Barr virus DNA. *Virology* **164**: 334-340.

Heinen,E. (2002) Encyclopedia of life sciences Macmillan Publishers limited, pp. 142-147.

Heldin,C.H., and Westermark,B. (1999) Mechanism of Action and In Vivo Role of Platelet-Derived Growth Factor. *Physiol Rev* **79**: 1283-1316.

Heller,N.M., Matsukura,S., Georas,S.N., Boothby,M.R., Rothman,P.B., Stellato,C., and Schleimer,R.P. (2004) Interferon-gamma inhibits STAT6 signal transduction and gene expression in human airway epithelial cells. *Am J Respir Cell Mol Biol* **31**: 573-582.

Hemmi,S., Bohni,R., Stark,G., Di,M.F., and Aguet,M. (1994) A novel member of the interferon receptor family complements functionality of the murine interferon gamma receptor in human cells. *Cell* **76**: 803-810.

Henderson,S., Huen,D., Rowe,M., Dawson,C., Johnson,G., and Rickinson,A. (1993) Epstein-Barr virus-coded BHRF1 protein, a viral homologue of Bcl-2, protects human B cells from programmed cell death. *Proc Natl Acad Sci U S A* **90**: 8479-8483.

Hershey,G.K., and Schreiber,R.D. (1989) Biosynthetic analysis of the human interferon-gamma receptor. Identification of N-linked glycosylation intermediates. *J Biol Chem* **264**: 11981-11988.

Hesse,M., Modolell,M., La Flamme,A.C., Schito,M., Fuentes,J.M., Cheever,A.W. *et al.* (2001) Differential regulation of nitric oxide synthase-2 and arginase-1 by type 1/type 2 cytokines in vivo: granulomatous pathology is shaped by the pattern of L-arginine metabolism. *J Immunol* **167**: 6533-6544.

Hibbs,J.B., Jr. (2002) Infection and nitric oxide. *J Infect Dis* **185 Suppl 1:S9-17.**: S9-17.

Hibbs,J.B., Jr., Taintor,R.R., and Vavrin,Z. (1987) Macrophage cytotoxicity: role for L-arginine deiminase and imino nitrogen oxidation to nitrite. *Science* **235**: 473-476.

Hibino,Y., Mariano,T.M., Kumar,C.S., Kozak,C.A., and Pestka,S. (1991) Expression and reconstitution of a biologically active mouse interferon gamma receptor in hamster cells. Chromosomal location of an accessory factor. *J Biol Chem* **266**: 6948-6951.

Higashi,K., Kouba,D.J., Song,Y.J., Uitto,J., and Mauviel,A. (1998) A proximal element within the human alpha 2(I) collagen (COL1A2) promoter, distinct from the tumor necrosis factor-alpha response element, mediates transcriptional repression by interferon-gamma. *Matrix Biol* **16**: 447-456.

Hoffmann,K.F., McCarty,T.C., Segal,D.H., Chiaramonte,M., Hesse,M., Davis,E.M. *et al.* (2001) Disease fingerprinting with cDNA microarrays reveals distinct gene expression profiles in lethal type 1 and type 2 cytokine-mediated inflammatory reactions. *FASEB J* **15**: 2545-2547.

Hoge,A.T., Hendrickson,S.B., and Burns,W.H. (2000) Murine gammaherpesvirus 68 cyclin D homologue is required for efficient reactivation from latency. *J Virol* **74**: 7016-7023.

Hosken,N.A., Shibuya,K., Heath,A.W., Murphy,K.M., and O'Garra,A. (1995) The effect of antigen dose on CD4+ T helper cell phenotype development in a T cell receptor-alpha beta-transgenic model. *J Exp Med* **182**: 1579-1584.

Hsieh,C.S., Macatonia,S.E., Tripp,C.S., Wolf,S.F., O'Garra,A., and Murphy,K.M. (1993) Development of TH1 CD4+ T cells through IL-12 produced by Listeria-induced macrophages. *Science* **260**: 547-549.

Huang,S., Hendriks,W., Althage,A., Hemmi,S., Bluethmann,H., Kamijo,R. *et al.* (1993) Immune-Response in Mice That Lack the Interferon-Gamma Receptor. *Science* **259**: 1742-1745.

Humphrey,J.H., and Grennan,D. (1981) Different macrophage populations distinguished by means of fluorescent polysaccharides. Recognition and properties of marginal-zone macrophages. *Eur J Immunol* **11**: 221-228.

Husain,S.M., Usherwood,E.J., Dyson,H., Coleclough,C., Coppola,M.A., Woodland,D.L. *et al.* (1999) Murine gammaherpesvirus M2 gene is latency-associated and its protein a target for CD8(+) T lymphocytes. *Proc Natl Acad Sci U S A* **96**: 7508-7513.

Iwai,T., Inoue,Y., Matsukura,I., Sugano,N., and Numano,F. (2000) Surgical technique for management of Takayasu's arteritis. *International Journal of Cardiology* **75**: S135-S140.

Jacob,R.J., and Roizman,B. (1977) Anatomy of herpes simplex virus DNA VIII. Properties of the replicating DNA. *J Virol* **23**: 394-411.

Jacoby,M.A., Virgin,H.W., and Speck,S.H. (2002) Disruption of the M2 gene of murine gammaherpesvirus 68 alters splenic latency following intranasal, but not intraperitoneal, inoculation. *J Virol* **76**: 1790-1801.

Jacoby,R.O., Buxton,D., and Reid,H.W. (1988a) The pathology of wildebeest-associated malignant catarrhal fever in hamsters, rats and guinea-pigs. *J Comp Pathol* **98**: 99-109.

Jacoby,R.O., Reid,H.W., Buxton,D., and Pow,I. (1988b) Transmission of wildebeest-associated and sheep-associated malignant catarrhal fever to hamsters, rats and guinea-pigs. *J Comp Pathol* **98**: 91-98.

Jenner,R.G., and Boshoff,C. (2002) The molecular pathology of Kaposi's sarcoma-associated herpesvirus. *Biochim Biophys Acta* **1602**: 1-22.

Jensen,K.K., Chen,S.C., Hipkin,R.W., Wiekowski,M.T., Schwarz,M.A., Chou,C.C. *et al.* (2003) Disruption of CCL21-induced chemotaxis in vitro and in vivo by M3, a chemokine-binding protein encoded by murine gammaherpesvirus 68. *J Virol* **77**: 624-630.

Jimenez,S.A., and Derk,C.T. (2004) Following the molecular pathways toward an understanding of the pathogenesis of systemic sclerosis. *Ann Intern Med* **140**: 37-50.

Jimenez,S.A., Diaz,A., and Khalili,K. (1995) Retroviruses and the pathogenesis of systemic sclerosis. *Int Rev Immunol* **12**: 159-175.

Johnson,H.M., Russell,J.K., and Torres,B.A. (1986) Second messenger role of arachidonic acid and its metabolites in interferon-gamma production. *J Immunol* **137**: 3053-3056.

Johnson,H.M., and Torres,B.A. (1984) Interleukin 2 enhancement of lymphokine secretion by established T cell clones. *J Immunol* **133**: 2278.

Jones,C.M., Lyons,K.M., and Hogan,B.L. (1991) Involvement of Bone Morphogenetic Protein-4 (BMP-4) and Vgr-1 in morphogenesis and neurogenesis in the mouse. *Development* **111**: 531-542.

Jones,M., Cordell,J.L., Beyers,A.D., Tse,A.G., and Mason,D.Y. (1993) Detection of T and B cells in many animal species using cross-reactive anti-peptide antibodies. *J Immunol* **150**: 5429-5435.

Kageyama,Y., Koide,Y., Yoshida,A., Uchijima,M., Arai,T., Miyamoto,S. *et al.* (1998) Reduced susceptibility to collagen-induced arthritis in mice deficient in IFN-gamma receptor. *J Immunol* **161**: 1542-1548.

Kahari,V.M., Chen,Y.Q., Su,M.W., Ramirez,F., and Uitto,J. (1990) Tumor necrosis factor-alpha and interferon-gamma suppress the activation of human type I collagen gene expression by transforming growth factor-beta 1. Evidence for two distinct mechanisms of inhibition at the transcriptional and posttranscriptional levels. *J Clin Invest* **86**: 1489-1495.

Kasahara,T., Djeu,J.Y., Dougherty,S.F., and Oppenheim,J.J. (1983) Capacity of human large granular lymphocytes (LGL) to produce multiple lymphokines: interleukin 2, interferon, and colony stimulating factor. *J Immunol* **131**: 2379-2385.

Katze,M.G., He,Y., and Gale,M., Jr. (2002) Viruses and interferon: a fight for supremacy. *Nat Rev Immunol* **2**: 675-687.

Katze,M.G., Wambach,M., Wong,M.L., Garfinkel,M., Meurs,E., Chong,K. *et al.* (1991) Functional expression and RNA binding analysis of the interferon-induced, double-stranded RNA-activated, 68,000-Mr protein kinase in a cell-free system. *Mol Cell Biol* **11**: 5497-5505.

Kaviratne,M., Hesse,M., Leusink,M., Cheever,A.W., Davies,S.J., McKerrow,J.H. *et al.* (2004) IL-13 activates a mechanism of tissue fibrosis that is completely TGF-beta independent. *J Immunol* **173**: 4020-4029.

Keane,M.P., Belperio,J.A., Burdick,M.D., and Strieter,R.M. (2001) IL-12 attenuates bleomycin-induced pulmonary fibrosis. *Am J Physiol Lung Cell Mol Physiol* **281**: L92-L97.

Kelly,B.G., Lok,S.S., Hasleton,P.S., Egan,J.J., and Stewart,J.P. (2002) A rearranged form of Epstein-Barr virus DNA is associated with idiopathic pulmonary fibrosis. *Am J Respir Crit Care Med* **166**: 510-513.

Kerr,I.M., and Brown,R.E. (1978) pppA2'p5'A2'p5'A: an inhibitor of protein synthesis synthesized with an enzyme fraction from interferon-treated cells. *Proc Natl Acad Sci U S A* **75**: 256-260.

Kilger,E., Kieser,A., Baumann,M., and Hammerschmidt,W. (1998) Epstein-Barr virus-mediated B-cell proliferation is dependent upon latent membrane protein 1, which simulates an activated CD40 receptor. *EMBO J* **17**: 1700-1709.

Kim,I.J., Flano,E., Woodland,D.L., Lund,F.E., Randall,T.D., and Blackman,M.A. (2003) Maintenance of long term gamma-herpesvirus B cell latency is dependent on CD40-mediated development of memory B cells. *J Immunol* **171**: 886-892.

Kitamura,D., Roes,J., Kuhn,R., and Rajewsky,K. (1991) A B cell-deficient mouse by targeted disruption of the membrane exon of the immunoglobulin mu chain gene. *Nature* **350**: 423-426.

Kledal,T.N., Rosenkilde,M.M., Coulin,F., Simmons,G., Johnsen,A.H., Alouani,S. *et al.* (1997) A broad-spectrum chemokine antagonist encoded by Kaposi's sarcoma-associated herpesvirus. *Science* **277**: 1656-1659.

Knight E Jr (1976b) Interferon: purification and initial characterization from human diploid cells. *Proc Natl Acad Sci U S A* **73**: 520-523.

Knight E Jr (1976a) Antiviral and cell growth inhibitory activities reside in the same glycoprotein of human fibroblast interferon. *Nature* **262**: 302-303.

Knipe,D.M., Howley,P.M., Griffin,d.E., Martin,M.A., Lamb,R.A., Roizman,B., and Straus,S.E. (2001) Fields Virology. Philadelphia. Baltimore. New York,

London. Buenos Aires. Hong Kong. Sydney. Tokyo.: Lippincott Williams & Wilkins, pp. 2381-2848.

Kochs,G., Janzen,C., Hohenberg,H., and Haller,O. (2002) Antivirally active MxA protein sequesters La Crosse virus nucleocapsid protein into perinuclear complexes. *Proc Natl Acad Sci U S A* **99**: 3153-3158.

Kodama,S., Davis,M., and Faustman,D.L. (2005) Diabetes and stem cell researchers turn to the lowly spleen. *Sci Aging Knowledge Environ* **2005**: e2.

Kodelja,V., Muller,C., Politz,O., Hakij,N., Orfanos,C.E., and Goerdt,S. (1998) Alternative macrophage activation-associated CC-chemokine-1, a novel structural homologue of macrophage inflammatory protein-1 alpha with a Th2-associated expression pattern. *J Immunol* **160**: 1411-1418.

Kotenko,S.V., Gallagher,G., Baurin,V.V., Lewis-Antes,A., Shen,M., Shah,N.K. *et al.* (2003) IFN-lambdas mediate antiviral protection through a distinct class II cytokine receptor complex. *Nat Immunol* **4**: 69-77.

Kraal,G., and Janse,M. (1986) Marginal metallophilic cells of the mouse spleen identified by a monoclonal antibody. *Immunology* **58**: 665-669.

Kraal,G., Janse,M., and Claassen,E. (1988) Marginal metallophilic macrophages in the mouse spleen: effects of neonatal injections of MOMA-1 antibody on the humoral immune response. *Immunol Lett* **17**: 139-144.

Krappmann,D., Emmerich,F., Kordes,U., Scharschmidt,E., Dorken,B., and Scheidereit,C. (1999) Molecular mechanisms of constitutive NF-kappaB/Rel activation in Hodgkin/Reed-Sternberg cells. *Oncogene* **18**: 943-953.

Kuhn,C., and McDonald,J.A. (1991) The roles of the myofibroblast in idiopathic pulmonary fibrosis. Ultrastructural and immunohistochemical features of sites of active extracellular matrix synthesis. *Am J Pathol* **138**: 1257-1265.

Kulkarni,A.B., Holmes,K.L., Fredrickson,T.N., Hartley,J.W., and Morse,H.C., III (1997) Characteristics of a murine gammaherpesvirus infection immunocompromised mice. *In Vivo* **11**: 281-291.

Kumar,C.S., Muthukumaran,G., Frost,L.J., Noe,M., Ahn,Y.H., Mariano,T.M., and Pestka,S. (1989) Molecular characterization of the murine interferon gamma receptor cDNA. *J Biol Chem* **264**: 17939-17946.

Kurisaki,A., Kose,S., Yoneda,Y., Heldin,C.H., and Moustakas,A. (2001) Transforming growth factor-beta induces nuclear import of Smad3 in an importin-beta1 and Ran-dependent manner. *Mol Biol Cell* **12**: 1079-1091.

Kuwano,K., Nomoto,Y., Kunitake,R., Hagimoto,N., Matsuba,T., Nakanishi,Y., and Hara,N. (1997) Detection of adenovirus E1A DNA in pulmonary fibrosis using nested polymerase chain reaction. *Eur Respir J* **10**: 1445-1449.

Lafaille,J.J. (1998) The Role of Helper T Cell Subsets in Autoimmune Diseases. *Cytokine & Growth Factor Reviews* **9**: 139-151.

Laiho,M., Weis,F.M., Boyd,F.T., Ignotz,R.A., and Massague,J. (1991) Responsiveness to transforming growth factor-beta (TGF-beta) restored by genetic complementation between cells defective in TGF-beta receptors I and II. *J Biol Chem* **266**: 9108-9112.

Lee,B.J., Koszinowski,U.H., Sarawar,S.R., and Adler,H. (2003) A gammaherpesvirus G protein-coupled receptor homologue is required for increased viral replication in response to chemokines and efficient reactivation from latency. *J Immunol* **170**: 243-251.

Lee,B.J., Reiter,S.K., Anderson,M., and Sarawar,S.R. (2002) CD28(-/-) mice show defects in cellular and humoral immunity but are able to control infection with murine gammaherpesvirus 68. *J Virol* **76**: 3049-3053.

Lee,B.J., Santee,S., Von Gesjen,S., Ware,C.F., and Sarawar,S.R. (2000) Lymphotoxin-alpha-deficient mice can clear a productive infection with murine gammaherpesvirus 68 but fail to develop splenomegaly or lymphocytosis. *J Virol* **74**: 2786-2792.

Lee,C.G., Homer,R.J., Zhu,Z., Lanone,S., Wang,X., Koteliansky,V. *et al.* (2001) Interleukin-13 induces tissue fibrosis by selectively stimulating and activating transforming growth factor beta(1). *J Exp Med* **194**: 809-821.

Lee,M.A., Diamond,M.E., and Yates,J.L. (1999) Genetic evidence that EBNA-1 is needed for efficient, stable latent infection by Epstein-Barr virus. *J Virol* **73**: 2974-2982.

Lee,Y.M., and Kaplan,M.M. (1995) Primary Sclerosing Cholangitis. *N Engl J Med* **332**: 924-933.

Leen,A., Meij,P., Redchenko,I., Middeldorp,J., Bloemena,E., Rickinson,A., and Blake,N. (2001) Differential immunogenicity of Epstein-Barr virus latent-cycle proteins for human CD4(+) T-helper 1 responses. *J Virol* **75**: 8649-8659.

Legler,D.F., Loetscher,M., Roos,R.S., Clark-Lewis,I., Baggiolini,M., and Moser,B. (1998) B cell-attracting chemokine 1, a human CXC chemokine expressed in lymphoid tissues, selectively attracts B lymphocytes via BLR1/CXCR5. *J Exp Med* **187**: 655-660.

Letterio,J.J., and Roberts,A.B. (1998) Regulation of immune responses by TGF-beta. *Annu Rev Immunol* **16:137-61.**: 137-161.

Li,H., O'Toole,D., Kim,O., Oaks,J.L., and Crawford,T.B. (2005) Malignant catarrhal fever-like disease in sheep after intranasal inoculation with ovine herpesvirus-2. *J Vet Diagn Invest* **17**: 171-175.

Li,X., Ponten,A., Aase,K., Karlsson,L., Abramsson,A., Uutela,M. *et al.* (2000) PDGF-C is a new protease-activated ligand for the PDGF alpha-receptor. *Nat Cell Biol* **2**: 302-309.

Liang,X., Shin,Y.C., Means,R.E., and Jung,J.U. (2004) Inhibition of interferon-mediated antiviral activity by murine gammaherpesvirus 68 latency-associated M2 protein. *J Virol* **78**: 12416-12427.

Lienhardt,C., Azzurri,A., Amedei,A., Fielding,K., Sillah,J., Sow,O.Y. *et al.* (2002) Active tuberculosis in Africa is associated with reduced Th1 and increased Th2 activity in vivo. *Eur J Immunol* **32**: 1605-1613.

Liggitt,H.D., and DeMartini,J.C. (1980) The pathomorphology of malignant catarrhal fever. I. Generalized lymphoid vasculitis. *Vet Pathol* **17**: 58-72.

Lindahl,T., Adams,A., Andersson-Anvret,M., and Falk,L. (1978) Integration of Epstein-Barr virus DNA. *IARC Sci Publ*: 113-123.

Lindow,M., Nansen,A., Bartholdy,C., Stryhn,A., Hansen,N.J., Boesen,T.P. *et al.* (2003) The virus-encoded chemokine vMIP-II inhibits virus-induced Tc1-driven inflammation. *J Virol* **77**: 7393-7400.

Liu,L., Flano,E., Usherwood,E.J., Surman,S., Blackman,M.A., and Woodland,D.L. (1999) Lytic cycle T cell epitopes are expressed in two distinct phases during MHV-68 infection. *J Immunol* **163**: 868-874.

Liu,T., Dhanasekaran,S.M., Jin,H., Hu,B., Tomlins,S.A., Chinnaiyan,A.M., and Phan,S.H. (2004) FIZZ1 Stimulation of Myofibroblast Differentiation. *Am J Pathol* **164**: 1315-1326.

Lok,S.S., Haider,Y., Howell,D., Stewart,J.P., Hasleton,P.S., and Egan,J.J. (2002) Murine gammaherpes virus as a cofactor in the development of pulmonary fibrosis in bleomycin resistant mice. *Eur Respir J* **20**: 1228-1232.

Lomonte,P., Bublot,M., van,S., V, Keil,G., Pastoret,P.P., and Thiry,E. (1996) Bovine herpesvirus 4: genomic organization and relationship with two other gammaherpesviruses, Epstein-Barr virus and herpesvirus saimiri. *Vet Microbiol* **53**: 79-89.

Lu,B., Ebensperger,C., Dembic,Z., Wang,Y., Kvatyuk,M., Lu,T. *et al.* (1998) Targeted disruption of the interferon-gamma receptor 2 gene results in severe immune defects in mice. *Proc Natl Acad Sci U S A* **95**: 8233-8238.

Mabit,H., Nakano,M.Y., Prank,U., Saam,B., Dohner,K., Sodeik,B., and Greber,U.F. (2002) Intact microtubules support adenovirus and herpes simplex virus infections. *J Virol* **76**: 9962-9971.

Macias,M.P., Fitzpatrick,L.A., Brenneise,I., McGarry,M.P., Lee,J.J., and Lee,N.A. (2001) Expression of IL-5 alters bone metabolism and induces ossification of the spleen in transgenic mice. *J Clin Invest* **107**: 949-959.

Mackey,M.F., Barth,R.J., Jr., and Noelle,R.J. (1998) The role of CD40/CD154 interactions in the priming, differentiation, and effector function of helper and cytotoxic T cells. *J Leukoc Biol* **63**: 418-428.

MacMicking,J., Xie,Q.W., and Nathan,C. (1997) Nitric oxide and macrophage function. *Annu Rev Immunol* **15:323-50.**: 323-350.

Macrae,A.I., Dutia,B.M., Milligan,S., Brownstein,D.G., Allen,D.J., Mistrikova,J. *et al.* (2001) Analysis of a novel strain of murine gammaherpesvirus reveals a genomic locus important for acute pathogenesis. *J Virol* **75**: 5315-5327.

Macrae,A.I., Usherwood,E.J., Husain,S.M., Flano,E., Kim,I.J., Woodland,D.L. *et al.* (2003) Murid herpesvirus 4 strain 68 M2 protein is a B-cell-associated antigen important for latency but not lymphocytosis. *J Virol* **77**: 9700-9709.

Madro,A., Celinski,K., and Slomka,M. (2004) The role of pancreatic stellate cells and cytokines in the development of chronic pancreatitis. *Med Sci Monit* **10**: RA166-RA170.

Mantovani,A., Sica,A., Sozzani,S., Allavena,P., Vecchi,A., and Locati,M. (2004) The chemokine system in diverse forms of macrophage activation and polarization. *Trends Immunol* **25**: 677-686.

Mantovani,A., Sozzani,S., Locati,M., Allavena,P., and Sica,A. (2002) Macrophage polarization: tumor-associated macrophages as a paradigm for polarized M2 mononuclear phagocytes. *Trends Immunol* **23**: 549-555.

Mao,C., Aguet,M., and Merlin,G. (1989) Molecular characterization of the human interferon-gamma receptor: analysis of polymorphism and glycosylation. *J Interferon Res* **9**: 659-669.

Marques,S., Efstathiou,S., Smith,K.G., Haury,M., and Simas,J.P. (2003) Selective gene expression of latent murine gammaherpesvirus 68 in B lymphocytes. *J Virol* **77**: 7308-7318.

Martinet,Y., Bitterman,P.B., Mornex,J.F., Grotendorst,G.R., Martin,G.R., and Crystal,R.G. (1986) Activated human monocytes express the c-sis proto-oncogene and release a mediator showing PDGF-like activity. *Nature* **319**: 158-160.

Martinet,Y., Rom,W.N., Grotendorst,G.R., Martin,G.R., and Crystal,R.G. (1987) Exaggerated spontaneous release of platelet-derived growth factor by alveolar macrophages from patients with idiopathic pulmonary fibrosis. *N Engl J Med* **317**: 202-209.

Massague,J. (1990) The transforming growth factor-beta family. *Annu Rev Cell Biol* **6:597-641.**: 597-641.

McClellan,J.S., Tibbetts,S.A., Gangappa,S., Brett,K.A., and Virgin,H.W. (2004) Critical role of CD4 T cells in an antibody-independent mechanism of vaccination against gammaherpesvirus latency. *J Virol* **78**: 6836-6845.

Mebius,R.E., and Kraal,G. (2005) Structure and function of the spleen. *Nat Rev Immunol* **5**: 606-616.

Meurs,E., Chong,K., Galabru,J., Thomas,N.S., Kerr,I.M., Williams,B.R., and Hovanessian,A.G. (1990) Molecular cloning and characterization of the human double-stranded RNA-activated protein kinase induced by interferon. *Cell* **62**: 379-390.

Meurs,E.F., Watanabe,Y., Kadereit,S., Barber,G.N., Katze,M.G., Chong,K. *et al.* (1992) Constitutive expression of human double-stranded RNA-activated p68 kinase in murine cells mediates phosphorylation of eukaryotic initiation factor 2 and partial resistance to encephalomyocarditis virus growth. *J Virol* **66**: 5805-5814.

Mills,C.D., Kincaid,K., Alt,J.M., Heilman,M.J., and Hill,A.M. (2000) M-1/M-2 macrophages and the Th1/Th2 paradigm. *J Immunol* **164**: 6166-6173.

Mistry,S.K., Zheng,M., Rouse,B.T., and Sidney,M. (2001) Induction of arginases I and II in cornea during herpes simplex virus infection. *Virus Research* **73**: 177-182.

Molesworth,S.J., Lake,C.M., Borza,C.M., Turk,S.M., and Hutt-Fletcher,L.M. (2000) Epstein-Barr virus gH is essential for penetration of B cells but also plays a role in attachment of virus to epithelial cells. *J Virol* **74**: 6324-6332.

Moore,B.B., Kolodsick,J.E., Thannickal,V.J., Cooke,K., Moore,T.A., Hogaboam,C. *et al.* (2005) CCR2-mediated recruitment of fibrocytes to the alveolar space after fibrotic injury. *Am J Pathol* **166**: 675-684.

Moore,K.W., Vieira,P., Fiorentino,D.F., Trounstine,M.L., Khan,T.A., and Mosmann,T.R. (1990) Homology of cytokine synthesis inhibitory factor (IL-10) to the Epstein-Barr virus gene BCRFI. *Science* **248**: 1230-1234.

Moore,P.S., and Chang,Y. (2001) Kaposi's Sarcoma - Associated Herpesvirus. In Feilds Virology. Knipe,D.M., Howely,P.M., Griffin,d.E., Martin,M.A., Lamb,R.A., Roizman,B., and Straus,S.E. (eds). Philadelphia.Baltimore.New York. London. Buenos Aires. Hong Kong. Sydney. Tokyo.: Lippincott Williams & Wilkins, pp. 2803-2834.

Moorman,N.J., Virgin,H.W., and Speck,S.H. (2003a) Disruption of the gene encoding the gammaHV68 v-GPCR leads to decreased efficiency of reactivation from latency. *Virology* **307**: 179-190.

Moorman,N.J., Willer,D.O., and Speck,S.H. (2003b) The gammaherpesvirus 68 latency-associated nuclear antigen homolog is critical for the establishment of splenic latency. *J Virol* **77**: 10295-10303.

Mora,A.L., Woods,C.R., Garcia,A., Xu,J., Rojas,M., Speck,S.H. *et al.* (2005) Lung Infection with Gamma Herpesvirus Induces Progressive Pulmonary Fibrosis in Th2 Biased Mice. *Am J Physiol Lung Cell Mol Physiol.*

Morrison,T.E., Mauser,A., Wong,A., Ting,J.P., and Kenney,S.C. (2001) Inhibition of IFN-gamma signaling by an Epstein-Barr virus immediate-early protein. *Immunity* **15**: 787-799.

Moser,M., and Murphy,K.M. (2000) Dendritic cell regulation of TH1-TH2 development. *Nat Immunol* **1**: 199-205.

Moss,D.J., Wallace,L.E., Rickinson,A.B., and Epstein,M.A. (1981) Cytotoxic T cell recognition of Epstein-Barr virus-infected B cells. I. Specificity and HLA restriction of effector cells reactivated in vitro. *Eur J Immunol* **11**: 686-693.

Mosser,D.M. (2003) The many faces of macrophage activation. *J Leukoc Biol* **73**: 209-212.

Moussad,E.E., and Brigstock,D.R. (2000) Connective tissue growth factor: what's in a name? *Mol Genet Metab* **71**: 276-292.

Munakata,T., Semba,U., Shibuya,Y., Kuwano,K., Akagi,M., and Arai,S. (1985) Induction of interferon-gamma production by human natural killer cells stimulated by hydrogen peroxide. *J Immunol* **134**: 2449-2455.

Munder,M., Eichmann,K., Moran,J.M., Centeno,F., Soler,G., and Modolell,M. (1999) Th1/Th2-regulated expression of arginase isoforms in murine macrophages and dendritic cells. *J Immunol* **163**: 3771-3777.

Munder,M., Eichmann,K., and Modolell,M. (1998) Alternative Metabolic States in Murine Macrophages Reflected by the Nitric Oxide Synthase/Arginase Balance: Competitive Regulation by CD4+ T Cells Correlates with Th1/Th2 Phenotype. *J Immunol* **160**: 5347-5354.

Munro,S., and Maniatis,T. (1989) Expression cloning of the murine interferon gamma receptor cDNA. *Proc Natl Acad Sci U S A* **86**: 9248-9252.

Murata,Y., Shimamura,T., and Hamuro,J. (2002) The polarization of T(h)1/T(h)2 balance is dependent on the intracellular thiol redox status of macrophages due to the distinctive cytokine production. *Int Immunol* **14**: 201-212.

Nair,M.G., Cochrane,D.W., and Allen,J.E. (2003) Macrophages in chronic type 2 inflammation have a novel phenotype characterized by the abundant expression of Ym1 and Fizz1 that can be partly replicated in vitro. *Immunol Lett* **85**: 173-180.

Nakajima,Y., Momotani,E., Ishikawa,Y., Murakami,T., Shimura,N., and Onuma,M. (1992) Phenotyping of lymphocyte subsets in the vascular and epithelial lesions of a cow with malignant catarrhal fever. *Vet Immunol Immunopathol* **33**: 279-284.

Nakao,A., Imamura,T., Souchelnytskyi,S., Kawabata,M., Ishisaki,A., Oeda,E. *et al.* (1997) TGF-beta receptor-mediated signalling through Smad2, Smad3 and Smad4. *EMBO J* **16**: 5353-5362.

Nakase,T., Nomura,S., Yoshikawa,H., Hashimoto,J., Hirota,S., Kitamura,Y. *et al.* (1994) Transient and localized expression of bone morphogenetic protein 4 messenger RNA during fracture healing. *J Bone Miner Res* **9**: 651-659.

Nash,A.A., Dutia,B.M., Stewart,J.P., and Davison,A.J. (2001) Natural history of murine gamma-herpesvirus infection. *Philos Trans R Soc Lond B Biol Sci* **356**: 569-579.

Naylor,S.L., Gray,P.W., and Lalley,P.A. (1984) Mouse immune interferon (IFN-gamma) gene is on chromosome 10. *Somat Cell Mol Genet* **10**: 531-534.

Naylor,S.L., Sakaguchi,A.Y., Shows,T.B., Law,M.L., Goeddel,D.V., and Gray,P.W. (1983) Human immune interferon gene is located on chromosome 12. *J Exp Med* **157**: 1020-1027.

Neidhart,M., Kuchen,S., Distler,O., Bruhlmann,P., Michel,B.A., Gay,R.E., and Gay,S. (1999) Increased serum levels of antibodies against human cytomegalovirus and prevalence of autoantibodies in systemic sclerosis. *Arthritis Rheum* **42**: 389-392.

Neipel,F., Albrecht,J.C., Ensser,A., Huang,Y.Q., Li,J.J., Friedman-Kien,A.E., and Fleckenstein,B. (1997) Human herpesvirus 8 encodes a homolog of interleukin-6. *J Virol* **71**: 839-842.

Nonomura,A., Kono,N., Minato,H., and Nakanuma,Y. (1998) Diffuse biliary tract involvement mimicking primary sclerosing cholangitis in an experimental model of chronic graft-versus-host disease in mice. *Pathol Int* **48**: 421-427.

O'Toole,D., Li,H., Miller,D., Williams,W.R., and Crawford,T.B. (1997) Chronic and recovered cases of sheep-associated malignant catarrhal fever in cattle. *Vet Rec* **140**: 519-524.

Oldroyd,S.D., Thomas,G.L., Gabbiani,G., and El Nahas,A.M. (1999) Interferon-gamma inhibits experimental renal fibrosis. *Kidney Int* **56**: 2116-2127.

Oriente,A., Fedarko,N.S., Pacocha,S.E., Huang,S.K., Lichtenstein,L.M., and Essayan,D.M. (2000) Interleukin-13 modulates collagen homeostasis in human skin and keloid fibroblasts. *J Pharmacol Exp Ther* **292**: 988-994.

Pallesen,G., Sandvej,K., Hamilton-Dutoit,S.J., Rowe,M., and Young,L.S. (1991) Activation of Epstein-Barr virus replication in Hodgkin and Reed-Sternberg cells. *Blood* **78**: 1162-1165.

Panoskaltsis,N., and Abboud,C.N. (1999) Human immunodeficiency virus and the hematopoietic repertoire: implications for gene therapy. *Front Biosci* **4**: D457-D467.

Parker,G.A., Crook,T., Bain,M., Sara,E.A., Farrell,P.J., and Allday,M.J. (1996) Epstein-Barr virus nuclear antigen (EBNA)3C is an immortalizing oncoprotein with similar properties to adenovirus E1A and papillomavirus E7. *Oncogene* **13**: 2541-2549.

Parravicini,C., Chandran,B., Corbellino,M., Berti,E., Paulli,M., Moore,P.S., and Chang,Y. (2000) Differential viral protein expression in Kaposi's sarcoma-associated herpesvirus-infected diseases: Kaposi's sarcoma, primary effusion lymphoma, and multicentric Castleman's disease. *Am J Pathol* **156**: 743-749.

Parry,C.M., Simas,J.P., Smith,V.P., Stewart,C.A., Minson,A.C., Efstathiou,S., and Alcami,A. (2000) A broad spectrum secreted chemokine binding protein encoded by a herpesvirus. *J Exp Med* **191**: 573-578.

Patterson,J.B., Thomis,D.C., Hans,S.L., and Samuel,C.E. (1995) Mechanism of interferon action: double-stranded RNA-specific adenosine deaminase from human cells is inducible by alpha and gamma interferons. *Virology* **210**: 508-511.

Perbal,P.B. (2004) CCN proteins: multifunctional signalling regulators. *The Lancet* **363**: 62-64.

Percy,D.H., and Bartholh,S.W. (2001) Pathology of laboratory Rodents & Rabbits Ames: Iowa state University Press, pp. 19-21.

Pertel,P.E., Spear,P.G., and Longnecker,R. (1998) Human herpesvirus-8 glycoprotein B interacts with Epstein-Barr virus (EBV) glycoprotein 110 but fails to complement the infectivity of EBV mutants. *Virology* **251**: 402-413.

Pfizenmaier,K., Wiegmann,K., Scheurich,P., Kronke,M., Merlin,G., Aguet,M. *et al.* (1988) High affinity human IFN-gamma-binding capacity is encoded by a single receptor gene located in proximity to c-ros on human chromosome region 6q16 to 6q22. *J Immunol* **141**: 856-860.

Phillips,R.J., Burdick,M.D., Hong,K., Lutz,M.A., Murray,L.A., Xue,Y.Y. *et al.* (2004) Circulating fibrocytes traffic to the lungs in response to CXCL12 and mediate fibrosis. *J Clin Invest* **114**: 438-446.

Platanias,L.C. (2005) Mechanisms of type-I- and type-II-interferon-mediated signalling. *Nat Rev Immunol* **5**: 375-386.

Plowright,W., Ferris,D.H., and Scott G.R (1960) Blue wildebeest and the aetiological agent of bovine malignant catarrhal fever. *Nature* **188**: 1167-1169.

Plump,A.S., Azrolan,N., Odaka,H., Wu,L., Jiang,X., Tall,A. *et al.* (1997) ApoA-I knockout mice: characterization of HDL metabolism in homozygotes and identification of a post-RNA mechanism of apoA-I up-regulation in heterozygotes. *J Lipid Res* **38**: 1033-1047.

Prockop,D.J., and Kivirikko,K.I. (1995) Collagens: molecular biology, diseases, and potentials for therapy. *Annu Rev Biochem* **64**: 403-434.

Pyo,R., Jensen,K.K., Wiekowski,M.T., Manfra,D., Alcami,A., Taubman,M.B., and Lira,S.A. (2004) Inhibition of Intimal Hyperplasia in Transgenic Mice Conditionally Expressing the Chemokine-Binding Protein M3. *Am J Pathol* **164**: 2289-2297.

Rabinowitz,S.S., and Gordon,S. (1991) Macrosialin, a macrophage-restricted membrane sialoprotein differentially glycosylated in response to inflammatory stimuli. *J Exp Med* **174**: 827-836.

Raes,G., De Baetselier,P., Noel,W., Beschin,A., Brombacher,F., and Hassanzadeh,G. (2002) Differential expression of FIZZ1 and Ym1 in alternatively versus classically activated macrophages. *J Leukoc Biol* **71**: 597-602.

Rajcani,J., Blaskovic,D., Svobodova,J., Ciampor,F., Huckova,D., and Stanekova,D. (1985) Pathogenesis of acute and persistent murine herpesvirus infection in mice. *Acta Virol* **29**: 51-60.

Ramadori,G., and Saile,B. (2004) Portal tract fibrogenesis in the liver. *Lab Invest* **84**: 153-159.

Ramaiah,K.V., Davies,M.V., Chen,J.J., and Kaufman,R.J. (1994) Expression of mutant eukaryotic initiation factor 2 alpha subunit (eIF-2 alpha) reduces inhibition of guanine nucleotide exchange activity of eIF-2B mediated by eIF-2 alpha phosphorylation. *Mol Cell Biol* **14**: 4546-4553.

Reid,H.W., Buxton,D., Berrie,E., Pow,I., and Finlayson,J. (1984) Malignant catarrhal fever. *Vet Rec* **114**: 581-583.

Reid,H.W., Buxton,D., Pow,I., Finlayson,J., and Berrie,E.L. (1983) A cytotoxic T-lymphocyte line propagated from a rabbit infected with sheep associated malignant catarrhal fever. *Res Vet Sci* **34**: 109-113.

Reiner,S.L., and Locksley,R.M. (1995) The regulation of immunity to Leishmania major. *Annu Rev Immunol* **13**: 151-177.

Renne,R., Blackbourn,D., Whitby,D., Levy,J., and Ganem,D. (1998) Limited transmission of Kaposi's sarcoma-associated herpesvirus in cultured cells. *J Virol* **72**: 5182-5188.

Renne,R., Lagunoff,M., Zhong,W., and Ganem,D. (1996) The size and conformation of Kaposi's sarcoma-associated herpesvirus (human herpesvirus 8) DNA in infected cells and virions. *J Virol* **70**: 8151-8154.

Rickinson,A. (2002) Epstein-Barr virus. *Virus Res* **82**: 109-113.

Rickinson,A.B., and Kieff,E. (2001) Epstein- Barr Virus. In Fields Virology. Knipe,D.M., Howley,P.M., Griffin,d.E., Martin,M.A., Lamb,R.A., Roizman,B., and Straus,S.E. (eds). Philadelphia.Baltimore.New York. London. Buenos Aires. Hong Kong. Sydney. Tokyo.: Lippincott Williams & Wilkins, pp. 2575-2628.

Rochford,R., Lutzke,M.L., Alfinito,R.S., Clavo,A., and Cardin,R.D. (2001) Kinetics of murine gammaherpesvirus 68 gene expression following infection of murine cells in culture and in mice. *J Virol* **75**: 4955-4963.

Rodriguez,P.C., Zea,A.H., DeSalvo,J., Culotta,K.S., Zabaleta,J., Quiceno,D.G. *et al.* (2003) L-arginine consumption by macrophages modulates the expression of CD3 zeta chain in T lymphocytes. *J Immunol* **171**: 1232-1239.

Roizman,B., Carmichael,L.E., Deinhardt,F., de The,G., Nahmias,A.J., Plowright,W. *et al.* (1981) Herpesviridae. Definition, provisional nomenclature, and taxonomy. The Herpesvirus Study Group, the International Committee on Taxonomy of Viruses. *Intervirology* **16**: 201-217.

Roizman,B., and Knipe,D.M. (2001) Herpes Simplex viruses and their replication. In Fields Virology. Knipe,D.M., Howley,P.M., Griffin,d.E., Martin,M.A., Lamb,R.A., Roizman,B., and Straus,S.E. (eds). Philadelphia. Baltimore. New York . London. Buenes Aires. Hong Kong. Sydney. Tokyo.: Lippincott Williams & Wilkins, pp. 2399-2459.

Roizman,B., and Pellett,P.E. (2001) The Family *Herpesviridae* : A Brief Introduction. In Fields Virology. Knipe,D.M., and Howley,P.M. (eds). Philadelphia, Baltimore, New York, London, Buenos Aires, Hong Kong, Sydney, Tokyo: Lippincott Williams & Wilkins, pp. 2381-2398.

Rosbottom,J. The Molecular Pathogenesis of Ovine Herpesvirus -2. 2003. University of Edinburgh, United Kingdom..
Ref Type: Thesis/Dissertation

Rowe,M., Rowe,D.T., Gregory,C.D., Young,L.S., Farrell,P.J., Rupani,H., and Rickinson,A.B. (1987) Differences in B cell growth phenotype reflect novel patterns of Epstein-Barr virus latent gene expression in Burkitt's lymphoma cells. *EMBO J* **6**: 2743-2751.

Roy,D.J., Ebrahimi,B.C., Dutia,B.M., Nash,A.A., and Stewart,J.P. (2000) Murine gammaherpesvirus M11 gene product inhibits apoptosis and is expressed during virus persistence. *Arch Virol* **145**: 2411-2420.

Russo,J.J., Bohenzky,R.A., Chien,M.C., Chen,J., Yan,M., Maddalena,D. *et al.* (1996) Nucleotide sequence of the Kaposi sarcoma-associated herpesvirus (HHV8). *Proc Natl Acad Sci U S A* **93**: 14862-14867.

Sabin,E.A., Araujo,M.I., Carvalho,E.M., and Pearce,E.J. (1996) Impairment of tetanus toxoid-specific Th1-like immune responses in humans infected with Schistosoma mansoni. *J Infect Dis* **173**: 269-272.

Sakatsume,M., Igarashi,K., Winestock,K.D., Garotta,G., Larner,A.C., and Finbloom,D.S. (1995) The Jak kinases differentially associate with the alpha and beta (accessory factor) chains of the interferon gamma receptor to form a functional receptor unit capable of activating STAT transcription factors. *J Biol Chem* **270**: 17528-17534.

Sambrook,J., Russell,D.W., Irwin,N., and Janssen,K.A. (2001) Molecular Cloning A laboratory manual New York: Cold Spring Harbor Laboratory Press, p. A8.19-A8.21.

Sandler,N.G., Mentink-Kane,M.M., Cheever,A.W., and Wynn,T.A. (2003) Global Gene Expression Profiles During Acute Pathogen-Induced Pulmonary Inflammation Reveal Divergent Roles for Th1 and Th2 Responses in Tissue Repair. *J Immunol* **171**: 3655-3667.

Sangster,M.Y., Topham,D.J., D'Costa,S., Cardin,R.D., Marion,T.N., Myers,L.K., and Doherty,P.C. (2000) Analysis of the Virus-Specific and Nonspecific B Cell Response to a Persistent B-Lymphotropic Gammaherpesvirus. *J Immunol* **164**: 1820-1828.

Sarawar,S.R., Cardin,R.D., Brooks,J.W., Mehrpooya,M., HamiltonEaston,A.M., Mo,X.Y., and Doherty,P.C. (1997) Gamma interferon is not essential for recovery from acute infection with murine gammaherpesvirus 68. *Journal of Virology* **71**: 3916-3921.

Sarawar,S.R., Cardin,R.D., Brooks,J.W., Mehrpooya,M., Tripp,R.A., and Doherty,P.C. (1996) Cytokine production in the immune response to murine gammaherpesvirus 68. *Journal of Virology* **70**: 3264-3268.

Sarawar,S.R., Lee,B.J., Reiter,S.K., and Schoenberger,S.P. (2001) Stimulation via CD40 can substitute for CD4 T cell function in preventing reactivation of a latent herpesvirus. *Proc Natl Acad Sci U S A* **98**: 6325-6329.

Sarid,R., Flore,O., Bohenzky,R.A., Chang,Y., and Moore,P.S. (1998) Transcription mapping of the Kaposi's sarcoma-associated herpesvirus (human herpesvirus 8) genome in a body cavity-based lymphoma cell line (BC-1). *J Virol* **72**: 1005-1012.

Sarid,R., Wiezorek,J.S., Moore,P.S., and Chang,Y. (1999) Characterization and cell cycle regulation of the major Kaposi's sarcoma-associated herpesvirus (human herpesvirus 8) latent genes and their promoter. *J Virol* **73**: 1438-1446.

Sato,M., Muragaki,Y., Saika,S., Roberts,A.B., and Ooshima,A. (2003) Targeted disruption of TGF-beta1/Smad3 signaling protects against renal

tubulointerstitial fibrosis induced by unilateral ureteral obstruction. *J Clin Invest* **112**: 1486-1494.

Savage,C., Das,P., Finelli,A.L., Townsend,S.R., Sun,C.Y., Baird,S.E., and Padgett,R.W. (1996) Caenorhabditis elegans genes sma-2, sma-3, and sma-4 define a conserved family of transforming growth factor beta pathway components. *Proc Natl Acad Sci U S A* **93**: 790-794.

Savill,J., and Fadok,V. (2000) Corpse clearance defines the meaning of cell death. *Nature* **407**: 784-788.

Schall,T.J., Lewis,M., Koller,K.J., Lee,A., Rice,G.C., Wong,G.H. *et al.* (1990) Molecular cloning and expression of a receptor for human tumor necrosis factor. *Cell* **61**: 361-370.

Schebesch,C., Kodelja,V., Muller,C., Hakij,N., Bisson,S., Orfanos,C.E., and Goerdt,S. (1997) Alternatively activated macrophages actively inhibit proliferation of peripheral blood lymphocytes and CD4+ T cells in vitro. *Immunology* **92**: 478-486.

Schroder,K., Hertzog,P.J., Ravasi,T., and Hume,D.A. (2004) Interferon-gamma: an overview of signals, mechanisms and functions. *J Leukoc Biol* **75**: 163-189.

Seifert,R.A., Coats,S.A., Raines,E.W., Ross,R., and Bowen-Pope,D.F. (1994) Platelet-derived growth factor (PDGF) receptor alpha-subunit mutant and reconstituted cell lines demonstrate that transforming growth factor-beta can be mitogenic through PDGF A-chain-dependent and -independent pathways. *J Biol Chem* **269**: 13951-13955.

Sekelsky,J.J., Newfeld,S.J., Raftery,L.A., Chartoff,E.H., and Gelbart,W.M. (1995) Genetic characterization and cloning of mothers against dpp, a gene required for decapentaplegic function in Drosophila melanogaster. *Genetics* **139**: 1347-1358.

Sempowski,G.D., Beckmann,M.P., Derdak,S., and Phipps,R.P. (1994) Subsets of murine lung fibroblasts express membrane-bound and soluble IL-4 receptors. Role of IL-4 in enhancing fibroblast proliferation and collagen synthesis. *J Immunol* **152**: 3606-3614.

Sharma,S.K., Maclean,J.A., Pinto,C., and Kradin,R.L. (1996) The effect of an anti-CD3 monoclonal antibody on bleomycin- induced lymphokine production and lung injury. *Am J Respir Crit Care Med* **154**: 193-200.

Shen,X., Hu,P.P., Liberati,N.T., Datto,M.B., Frederick,J.P., and Wang,X.F. (1998) TGF-beta-induced phosphorylation of Smad3 regulates its interaction with coactivator p300/CREB-binding protein. *Mol Biol Cell* **9**: 3309-3319.

Sheppard,P., Kindsvogel,W., Xu,W., Henderson,K., Schlutsmeyer,S., Whitmore,T.E. *et al.* (2003) IL-28, IL-29 and their class II cytokine receptor IL-28R. *Nat Immunol* **4**: 63-68.

Sher,A., Coffman,R.L., Hieny,S., Scott,P., and Cheever,A.W. (1990) Interleukin 5 is required for the blood and tissue eosinophilia but not granuloma formation induced by infection with Schistosoma mansoni. *Proc Natl Acad Sci U S A* **87**: 61-65.

Shi-wen,X., Pennington,D., Holmes,A., Leask,A., Bradham,D., Beauchamp,J.R. *et al.* (2000) Autocrine overexpression of CTGF maintains fibrosis: RDA analysis of fibrosis genes in systemic sclerosis. *Exp Cell Res* **259**: 213-224.

Shimizu,Y.K., Feinstone,S.M., Kohara,M., Purcell,R.H., and Yoshikura,H. (1996) Hepatitis C virus: detection of intracellular virus particles by electron microscopy. *Hepatology* **23**: 205-209.

Shimokado,K., Raines,E.W., Madtes,D.K., Barrett,T.B., Benditt,E.P., and Ross,R. (1985) A significant part of macrophage-derived growth factor consists of at least two forms of PDGF. *Cell* **43**: 277-286.

Simas,J.P., Bowden,R.J., Paige,V., and Efstathiou,S. (1998) Four tRNA-like sequences and a serpin homologue encoded by murine gammaherpesvirus 68 are dispensable for lytic replication in vitro and latency in vivo. *J Gen Virol* **79**: 149-153.

Simas,J.P., and Efstathiou,S. (1998) Murine gammaherpesvirus 68: a model for the study of gammaherpesvirus pathogenesis. *Trends in Microbiology* **6**: 276-282.

Simas,J.P., Marques,S., Bridgeman,A., Efstathiou,S., and Adler,H. (2004) The M2 gene product of murine gammaherpesvirus 68 is required for efficient colonization of splenic follicles but is not necessary for expansion of latently infected germinal centre B cells. *J Gen Virol* **85**: 2789-2797.

Simas,J.P., Swann,D., Bowden,R., and Efstathiou,S. (1999) Analysis of murine gammaherpesvirus-68 transcription during lytic and latent infection. *J Gen Virol* **80**: 75-82.

Simon,S., Li,H., O'Toole,D., Crawford,T.B., and Oaks,J.L. (2003) The vascular lesions of a cow and bison with sheep-associated malignant catarrhal fever contain ovine herpesvirus 2-infected CD8(+) T lymphocytes. *J Gen Virol* **84**: 2009-2013.

Singh,U.P., Singh,S., Ravichandran,P., Taub,D.D., and Lillard,J.W., Jr. (2004) Viral macrophage-inflammatory protein-II: a viral chemokine that differentially affects adaptive mucosal immunity compared with its mammalian counterparts. *J Immunol* **173**: 5509-5516.

Skalli,O., Ropraz,P., Trzeciak,A., Benzonana,G., Gillessen,D., and Gabbiani,G. (1986) A monoclonal antibody against alpha-smooth muscle actin: a new probe for smooth muscle differentiation. *J Cell Biol* **103**: 2787-2796.

Smith,P.G., Coletta,P.L., Markham,A.F., and Whitehouse,A. (2001) In vivo episomal maintenance of a herpesvirus saimiri-based gene delivery vector. *Gene Ther* **8**: 1762-1769.

Smith,P.L., Lombardi,G., and Foster,G.R. (2005) Type I interferons and the innate immune response--more than just antiviral cytokines. *Mol Immunol* **42**: 869-877.

Snapper,C.M., and Paul,W.E. (1987) Interferon-gamma and B cell stimulatory factor-1 reciprocally regulate Ig isotype production. *Science* **236**: 944-947.

Soh,J., Donnelly,R.J., Kotenko,S., Mariano,T.M., Cook,J.R., Wang,N. *et al.* (1994) Identification and sequence of an accessory factor required for activation of the human interferon gamma receptor. *Cell* **76**: 793-802.

Song,E., Ouyang,N., Horbelt,M., Antus,B., Wang,M., and Exton,M.S. (2000) Influence of alternatively and classically activated macrophages on fibrogenic activities of human fibroblasts. *Cell Immunol* **204**: 19-28.

Sonoki,T., Nagasaki,A., Gotoh,T., Takiguchi,M., Takeya,M., Matsuzaki,H., and Mori,M. (1997) Coinduction of nitric-oxide synthase and arginase I in cultured rat peritoneal macrophages and rat tissues in vivo by lipopolysaccharide. *J Biol Chem* **272**: 3689-3693.

Sozzani,S., Luini,W., Bianchi,G., Allavena,P., Wells,T.N., Napolitano,M. *et al.* (1998) The viral chemokine macrophage inflammatory protein-II is a selective Th2 chemoattractant. *Blood* **92**: 4036-4039.

Sparks-Thissen,R.L., Braaten,D.C., Hildner,K., Murphy,T.L., Murphy,K.M., and Virgin,H.W. (2005) CD4 T cell control of acute and latent murine gammaherpesvirus infection requires IFNgamma. *Virology* **338**: 201-208.

Sparks-Thissen,R.L., Braaten,D.C., Kreher,S., Speck,S.H., and Virgin,H.W. (2004) An optimized CD4 T-cell response can control productive and latent gammaherpesvirus infection. *J Virol* **78**: 6827-6835.

Spear,P.G., and Longnecker,R. (2003) Herpesvirus entry: an update. *J Virol* **77**: 10179-10185.

Staeheli,P., and Haller,O. (1987) Interferon-induced Mx protein: a mediator of cellular resistance to influenza virus. *Interferon* **8**: 1-23.

Stein,M., Keshav,S., Harris,N., and Gordon,S. (1992) Interleukin 4 potently enhances murine macrophage mannose receptor activity: a marker of alternative immunologic macrophage activation. *J Exp Med* **176**: 287-292.

Stevenson,P.G., Belz,G.T., Altman,J.D., and Doherty,P.C. (1999) Changing patterns of dominance in the CD8+ T cell response during acute and persistent murine gamma-herpesvirus infection. *Eur J Immunol* **29**: 1059-1067.

Stevenson,P.G., Belz,G.T., Altman,J.D., and Doherty,P.C. (1998) Virus-specific CD8(+) T cell numbers are maintained during gamma-herpesvirus reactivation in CD4-deficient mice. *Proc Natl Acad Sci U S A* **95**: 15565-15570.

Stevenson,P.G., and Doherty,P.C. (1998) Kinetic analysis of the specific host response to a murine gammaherpesvirus. *J Virol* **72**: 943-949.

Stevenson,P.G., Efstathiou,S., Doherty,P.C., and Lehner,P.J. (2000) Inhibition of MHC class I-restricted antigen presentation by gamma 2-herpesviruses. *Proc Natl Acad Sci U S A* **97**: 8455-8460.

Stevenson,P.G., May,J.S., Smith,X.G., Marques,S., Adler,H., Koszinowski,U.H. *et al.* (2002) K3-mediated evasion of CD8(+) T cells aids amplification of a latent gamma-herpesvirus. *Nat Immunol* **3**: 733-740.

Stewart,J.P., Egan,J.J., Ross,A.J., Kelly,B.G., Lok,S.S., Hasleton,P.S., and Woodcock,A.A. (1999) The detection of Epstein-Barr virus DNA in lung tissue from patients with idiopathic pulmonary fibrosis. *Am J Respir Crit Care Med* **159**: 1336-1341.

Stewart,J.P., Usherwood,E.J., Dutia,B.M., and Nash,A.A. (1998a) Immunobiology of Murine Gamma Herpesvirus -68. In Herpesviruses and Immunity. Medveczky,A. (ed). New York: Plenum Press, pp. 149-163.

Stewart,J.P., Usherwood,E.J., Ross,A., Dyson,H., and Nash,T. (1998b) Lung epithelial cells are a major site of murine gammaherpesvirus persistence. *J Exp Med* **187**: 1941-1951.

Stine,J.T., Wood,C., Hill,M., Epp,A., Raport,C.J., Schweickart,V.L. *et al.* (2000) KSHV-encoded CC chemokine vMIP-III is a CCR4 agonist, stimulates angiogenesis, and selectively chemoattracts TH2 cells. *Blood* **95**: 1151-1157.

Sunil-Chandra,N.P., Efstathiou,S., Arno,J., and Nash,A.A. (1992a) Virological and Pathological Features of Mice Infected with Murine Gammaherpesvirus-68. *J Gen Virol* **73**: 2347-2356.

Sunil-Chandra,N.P., Efstathiou,S., and Nash,A.A. (1993) Interactions of murine gammaherpesvirus 68 with B and T cell lines. *Virology* **193**: 825-833.

Sunil-Chandra,N.P., Efstathiou,S., and Nash,A.A. (1992b) Murine Gammaherpesvirus 68 Establishes A Latent Infection in Mouse B Lymphocytes Invivo. *J Gen Virol* **73**: 3275-3279.

Sutterwala,F.S., Noel,G.J., Clynes,R., and Mosser,D.M. (1997) Selective suppression of interleukin-12 induction after macrophage receptor ligation. *J Exp Med* **185**: 1977-1985.

Svobodova,J., Blaskovic,D., and Mistrikova,J. (1982) Growth characteristics of herpesviruses isolated from free living small rodents. *Acta Virol* **26**: 256-263.

Tailleux,L., Schwartz,O., Herrmann,J.L., Pivert,E., Jackson,M., Amara,A. *et al.* (2003) DC-SIGN is the major Mycobacterium tuberculosis receptor on human dendritic cells. *J Exp Med* **197**: 121-127.

Takada,K., and Ono,Y. (1989) Synchronous and sequential activation of latently infected Epstein-Barr virus genomes. *J Virol* **63**: 445-449.

Takahashi,F., Takahashi,K., Okazaki,T., Maeda,K., Ienaga,H., Maeda,M. *et al.* (2001) Role of osteopontin in the pathogenesis of bleomycin-induced pulmonary fibrosis. *Am J Respir Cell Mol Biol* **24**: 264-271.

Talbot,S.J., Weiss,R.A., Kellam,P., and Boshoff,C. (1999) Transcriptional analysis of human herpesvirus-8 open reading frames 71, 72, 73, K14, and 74 in a primary effusion lymphoma cell line. *Virology* **257**: 84-94.

Tan,S.L., and Katze,M.G. (1999) The emerging role of the interferon-induced PKR protein kinase as an apoptotic effector: a new face of death? *J Interferon Cytokine Res* **19**: 543-554.

Tang,Y.W., Johnson,J.E., Browning,P.J., Cruz-Gervis,R.A., Davis,A., Graham,B.S. *et al.* (2003) Herpesvirus DNA is consistently detected in lungs of patients with idiopathic pulmonary fibrosis. *J Clin Microbiol* **41**: 2633-2640.

Taniguchi,T., Mantei,N., Schwarzstein,M., Nagata,S., Muramatsu,M., and Weissmann,C. (1980) Human leukocyte and fibroblast interferons are structurally related. *Nature* **285**: 547-549.

Tanner,J.E., and Alfieri,C. (2001) The Epstein-Barr virus and post-transplant lymphoproliferative disease: interplay of immunosuppression, EBV, and the immune system in disease pathogenesis. *Transpl Infect Dis* **3**: 60-69.

Tau,G., and Rothman,P. (1999) Biologic functions of the IFN-gamma receptors. *Allergy* **54**: 1233-1251.

Taus,N.S., Traul,D.L., Oaks,J.L., Crawford,T.B., Lewis,G.S., and Li,H. (2005) Experimental infection of sheep with ovine herpesvirus 2 via aerosolization of nasal secretions. *J Gen Virol* **86**: 575-579.

Taylor,P.R., Martinez-Pomares,L., Stacey,M., Lin,H.H., Brown,G.D., and Gordon,S. (2005) Macrophage receptors and immune recognition. *Annu Rev Immunol* **23**: 901-944.

Telford,E.A., Watson,M.S., Aird,H.C., Perry,J., and Davison,A.J. (1995) The DNA sequence of equine herpesvirus 2. *J Mol Biol* **249**: 520-528.

Tellides,G., Tereb,D.A., Kirkiles-Smith,N.C., Kim,R.W., Wilson,J.H., Schechner,J.S. *et al.* (2000) Interferon-gamma elicits arteriosclerosis in the absence of leukocytes. *Nature* **403**: 207-211.

Thome,M., Schneider,P., Hofmann,K., Fickenscher,H., Meinl,E., Neipel,F. *et al.* (1997) Viral FLICE-inhibitory proteins (FLIPs) prevent apoptosis induced by death receptors. *Nature* **386**: 517-521.

Thorley-Lawson,D.A. (2001) Epstein-Barr virus: exploiting the immune system. *Nat Rev Immunol* **1**: 75-82.

Tibbetts,S.A., van Dyk,L.F., Speck,S.H., and Virgin,H.W. (2002) Immune control of the number and reactivation phenotype of cells latently infected with a gammaherpesvirus. *J Virol* **76**: 7125-7132.

Townsley,A.C., Dutia,B.M., and Nash,A.A. (2004) The m4 gene of murine gammaherpesvirus modulates productive and latent infection in vivo. *J Virol* **78**: 758-767.

Tripp,R.A., Hamilton-Easton,A.M., Cardin,R.D., Nguyen,P., Behm,F.G., Woodland,D.L. *et al.* (1997) Pathogenesis of an Infectious Mononucleosis-like Disease Induced by a Murine gamma -Herpesvirus: Role for a Viral Superantigen? *J Exp Med* **185**: 1641-1650.

Tsukazaki,T., Chiang,T.A., Davison,A.F., Attisano,L., and Wrana,J.L. (1998) SARA, a FYVE domain protein that recruits Smad2 to the TGFbeta receptor. *Cell* **95**: 779-791.

Ueda,T., Ohta,K., Suzuki,N., Yamaguchi,M., Hirai,K., Horiuchi,T. *et al.* (1992) Idiopathic pulmonary fibrosis and high prevalence of serum antibodies to hepatitis C virus. *Am Rev Respir Dis* **146**: 266-268.

Ulloa,L., Doody,J., and Massague,J. (1999) Inhibition of transforming growth factor-beta/SMAD signalling by the interferon-gamma/STAT pathway. *Nature* **397**: 710-713.

Urban,J.F., Jr., Madden,K.B., Svetic,A., Cheever,A., Trotta,P.P., Gause,W.C. *et al.* (1992) The importance of Th2 cytokines in protective immunity to nematodes. *Immunol Rev* **127**: 205-220.

Usherwood,E.J., Brooks,J.W., Sarawar,S.R., Cardin,R.D., Young,W.D., Allen,D.J. *et al.* (1997) Immunological control of murine gammaherpesvirus infection is independent of perforin. *J Gen Virol* **78 (Pt 8)**: 2025-2030.

Usherwood,E.J., Ross,A.J., Allen,D.J., and Nash,A.A. (1996a) Murine gammaherpesvirus-induced splenomegaly: A critical role for CD4 T cells. *J Gen Virol* **77**: 627-630.

Usherwood,E.J., Stewart,J.P., and Nash,A.A. (1996b) Characterization of tumor cell lines derived from murine gammaherpesvirus-68-infected mice. *J Virol* **70**: 6516-6518.

Usherwood,E.J., Stewart,J.P., Robertson,K., Allen,D.J., and Nash,A.A. (1996c) Absence of splenic latency in murine gammaherpesvirus 68- infected B cell-deficient mice. *J Gen Virol* **77**: 2819-2825.

Utsumi,J., Yamazaki,S., Kawaguchi,K., Kimura,S., and Shimizu,H. (1989) Stability of human interferon-beta 1: oligomeric human interferon-beta 1 is inactive but is reactivated by monomerization. *Biochim Biophys Acta* **998**: 167-172.

Van Berkel,V., Barrett,J., Tiffany,H.L., Fremont,D.H., Murphy,P.M., McFadden,G. *et al.* (2000) Identification of a gammaherpesvirus selective chemokine binding protein that inhibits chemokine action. *J Virol* **74**: 6741-6747.

Van Berkel,V., Levine,B., Kapadia,S.B., Goldman,J.E., Speck,S.H., and Virgin,H.W. (2002) Critical role for a high-affinity chemokine-binding protein in gamma-herpesvirus-induced lethal meningitis. *J Clin Invest* **109**: 905-914.

Van Berkel,V., Preiter,K., Virgin,H.W., and Speck,S.H. (1999) Identification and initial characterization of the murine gammaherpesvirus 68 gene M3, encoding an abundantly secreted protein. *J Virol* **73**: 4524-4529.

van Dyk,L.F., Hess,J.L., Katz,J.D., Jacoby,M., Speck,S.H., and Virgin,H.W., IV (1999) The murine gammaherpesvirus 68 v-cyclin gene is an oncogene that promotes cell cycle progression in primary lymphocytes. *J Virol* **73**: 5110-5122.

van Dyk,L.F., Virgin,H.W., and Speck,S.H. (2000) The murine gammaherpesvirus 68 v-cyclin is a critical regulator of reactivation from latency. *J Virol* **74**: 7451-7461.

van Dyk,L.F., Virgin,H.W., IV, and Speck,S.H. (2003) Maintenance of Gammaherpesvirus Latency Requires Viral Cyclin in the Absence of B Lymphocytes. *J Virol* **77**: 5118-5126.

Van,V.E., Melis,M., and van,E.W. (1985) Marginal zone macrophages in the mouse spleen identified by a monoclonal antibody. Anatomical correlation with a B cell subpopulation. *J Histochem Cytochem* **33**: 40-44.

Varga,J., Olsen,A., Herhal,J., Constantine,G., Rosenbloom,J., and Jimenez,S.A. (1990) Interferon-gamma reverses the stimulation of collagen but not fibronectin gene expression by transforming growth factor-beta in normal human fibroblasts. *Eur J Clin Invest* **20**: 487-493.

Vergnon,J.M., Vincent,M., de,T.G., Mornex,J.F., Weynants,P., and Brune,J. (1984) Cryptogenic fibrosing alveolitis and Epstein-Barr virus: an association? *Lancet* **2**: 768-771.

Verma,S.C., and Robertson,E.S. (2003) Molecular biology and pathogenesis of Kaposi sarcoma-associated herpesvirus. *FEMS Microbiol Lett* **222**: 155-163.

Verrecchia,F., Tacheau,C., Wagner,E.F., and Mauviel,A. (2003) A central role for the JNK pathway in mediating the antagonistic activity of pro-inflammatory cytokines against transforming growth factor-beta-driven SMAD3/4-specific gene expression. *J Biol Chem* **278**: 1585-1593.

Verzijl,D., Fitzsimons,C.P., van Dijk,M., Stewart,J.P., Timmerman,H., Smit,M.J., and Leurs,R. (2004) Differential Activation of Murine Herpesvirus 68- and Kaposi's Sarcoma-Associated Herpesvirus-Encoded ORF74 G Protein-Coupled Receptors by Human and Murine Chemokines. *J Virol* **78**: 3343-3351.

Vilcek,J. (2003) Novel interferons. *Nat Immunol* **4**: 8-9.

Vilcek,J., Henriksen-Destefano,D., Siegel,D., Klion,A., Robb,R.J., and Le,J. (1985) Regulation of IFN-gamma induction in human peripheral blood cells by exogenous and endogenously produced interleukin 2. *J Immunol* **135**: 1851-1856.

Vincendeau,P., Gobert,A.P., Daulouede,S., Moynet,D., and Mossalayi,M.D. (2003) Arginases in parasitic diseases. *Trends Parasitol* **19**: 9-12.

Virdi,A.S., Shore,E.M., Oreffo,R.O., Li,M., Connor,J.M., Smith,R. *et al.* (1999) Phenotypic and molecular heterogeneity in fibrodysplasia ossificans progressiva. *Calcif Tissue Int* **65**: 250-255.

Virgin,H.W., Latreille,P., Wamsley,P., Hallsworth,K., Weck,K.E., Dal Canto,A.J., and Speck,S.H. (1997) Complete sequence and genomic analysis of murine gammaherpesvirus 68. *J Virol* **71**: 5894-5904.

Virgin,H.W., Presti,R.M., Li,X.Y., Liu,C., and Speck,S.H. (1999) Three distinct regions of the murine gammaherpesvirus 68 genome are transcriptionally active in latently infected mice. *J Virol* **73**: 2321-2332.

Virgin,H.W., and Speck,S.H. (1999) Unraveling immunity to gamma-herpesviruses: a new model for understanding the role of immunity in chronic virus infection. *Curr Opin Immunol* **11**: 371-379.

Wagner,E.K., and Bloom,D.C. (1997) Experimental investigation of herpes simplex virus latency. *Clin Microbiol Rev* **10**: 419-443.

Wahl,S.M., Hunt,D.A., Wakefield,L.M., Cartney-Francis,N., Wahl,L.M., Roberts,A.B., and Sporn,M.B. (1987) Transforming growth factor type beta induces monocyte chemotaxis and growth factor production. *Proc Natl Acad Sci U S A* **84**: 5788-5792.

Wajant,H., and Scheurich,P. (2001) Tumor necrosis factor receptor-associated factor (TRAF) 2 and its role in TNF signaling. *Int J Biochem Cell Biol* **33**: 19-32.

Wakeling,M.N., Roy,D.J., Nash,A.A., and Stewart,J.P. (2001) Characterization of the murine gammaherpesvirus 68 ORF74 product: a novel oncogenic G protein-coupled receptor. *J Gen Virol* **82**: 1187-1197.

Wallace,W.A., Ramage,E.A., Lamb,D., and Howie,S.E. (1995) A type 2 (Th2-like) pattern of immune response predominates in the pulmonary interstitium of patients with cryptogenic fibrosing alveolitis (CFA). *Clin Exp Immunol* **101**: 436-441.

Wang,G.H., Garvey,T.L., and Cohen,J.I. (1999) The murine gammaherpesvirus-68 M11 protein inhibits Fas- and TNF-induced apoptosis. *J Gen Virol* **80**: 2737-2740.

Wang,H.C., Kao,Y.C., Chang,T.J., and Wong,M.L. (2005) Inhibition of lytic infection of pseudorabies virus by arginine depletion. *Biochem Biophys Res Commun* **334**: 631-637.

Weck,K.E., Barkon,M.L., Yoo,L.I., Speck,S.H., and Virgin,H.W., IV (1996) Mature B cells are required for acute splenic infection, but not for establishment of latency, by murine gammaherpesvirus 68. *J Virol* **70**: 6775-6780.

Weck,K.E., Dal Canto,A.J., Gould,J.D., O'Guin,A.K., Roth,K.A., Saffitz,J.E. *et al.* (1997) Murine gamma-herpesvirus 68 causes severe large-vessel arteritis in mice lacking interferon-gamma responsiveness: a new model for virus-induced vascular disease. *Nat Med* **3**: 1346-1353.

Weck,K.E., Kim,S.S., Virgin,H.W., IV, and Speck,S.H. (1999b) B cells regulate murine gammaherpesvirus 68 latency. *J Virol* **73**: 4651-4661.

Weck,K.E., Kim,S.S., Virgin,H.W., IV, and Speck,S.H. (1999a) Macrophages are the major reservoir of latent murine gammaherpesvirus 68 in peritoneal cells. *J Virol* **73**: 3273-3283.

Wen,Z., Zhong,Z., and Darnell,J.E., Jr. (1995) Maximal activation of transcription by Stat1 and Stat3 requires both tyrosine and serine phosphorylation. *Cell* **82**: 241-250.

Wiesner,R.H., Porayko,M.K., Dickson,E.R., Gores,G.J., LaRusso,N.F., Hay,J.E. *et al.* (1992) Selection and timing of liver transplantation in primary biliary cirrhosis and primary sclerosing cholangitis. *Hepatology* **16**: 1290-1299.

Willer,D.O., and Speck,S.H. (2005) Establishment and maintenance of long-term murine gammaherpesvirus 68 latency in B cells in the absence of CD40. *J Virol* **79**: 2891-2899.

Willer,D.O., and Speck,S.H. (2003) Long-term latent murine Gammaherpesvirus 68 infection is preferentially found within the surface immunoglobulin D-negative subset of splenic B cells in vivo. *J Virol* **77**: 8310-8321.

Wilson,M.E., Jeronimo,S.M.B., and Pearson,R.D. (2005) Immunopathogenesis of infection with the visceralizing Leishmania species. *Microbial Pathogenesis* **38**: 147-160.

Witte,M.B., Barbul,A., Schick,M.A., Vogt,N., and Becker,H.D. (2002) Upregulation of arginase expression in wound-derived fibroblasts. *J Surg Res* **105**: 35-42.

Wolf,H., zur,H.H., and Becker,V. (1973) EB viral genomes in epithelial nasopharyngeal carcinoma cells. *Nat New Biol* **244**: 245-247.

Wozney,J.M. (2002) Overview of bone morphogenetic proteins. *Spine* **27**: S2-S8.

Wrana,J.L., Attisano,L., Wieser,R., Ventura,F., and Massague,J. (1994) Mechanism of activation of the TGF-beta receptor. *Nature* **370**: 341-347.

Wreschner,D.H., James,T.C., Silverman,R.H., and Kerr,I.M. (1981) Ribosomal RNA cleavage, nuclease activation and 2-5A(ppp(A2'p)nA) in interferon-treated cells. *Nucleic Acids Res* **9**: 1571-1581.

Wright,V., Peng,H., Usas,A., Young,B., Gearhart,B., Cummins,J., and Huard,J. (2002) BMP4-expressing muscle-derived stem cells differentiate into osteogenic lineage and improve bone healing in immunocompetent mice. *Mol Ther* **6**: 169-178.

Wynn,T.A. (2004) Fibrotic disease and the T(H)1/T(H)2 paradigm. *Nat Rev Immunol* **4**: 583-594.

Wynn,T.A., Cheever,A.W., Jankovic,D., Poindexter,R.W., Caspar,P., Lewis,F.A., and Sher,A. (1995) An IL-12-based vaccination method for preventing fibrosis induced by schistosome infection. *Nature* **376**: 594-596.

Wynn,T.A., Eltoum,I., Cheever,A.W., Lewis,F.A., Gause,W.C., and Sher,A. (1993) Analysis of cytokine mRNA expression during primary granuloma formation induced by eggs of Schistosoma mansoni. *J Immunol* **151**: 1430-1440.

Xiao,Z., Liu,X., and Lodish,H.F. (2000) Importin beta mediates nuclear translocation of Smad 3. *J Biol Chem* **275**: 23425-23428.

Yamakage,A., Kikuchi,K., Smith,E.A., LeRoy,E.C., and Trojanowska,M. (1992) Selective upregulation of platelet-derived growth factor alpha receptors by transforming growth factor beta in scleroderma fibroblasts. *J Exp Med* **175**: 1227-1234.

Yang,Y.L., Reis,L.F., Pavlovic,J., Aguzzi,A., Schafer,R., Kumar,A. *et al.* (1995) Deficient signaling in mice devoid of double-stranded RNA-dependent protein kinase. *EMBO J* **14**: 6095-6106.

Yao,Q.Y., Ogan,P., Rowe,M., Wood,M., and Rickinson,A.B. (1989) The Epstein-Barr virus:host balance in acute infectious mononucleosis patients receiving acyclovir anti-viral therapy. *Int J Cancer* **43**: 61-66.

Yates,J.L., Warren,N., and Sugden,B. (1985) Stable replication of plasmids derived from Epstein-Barr virus in various mammalian cells. *Nature* **313**: 812-815.

Yi,E.S., Lee,H., Yin,S., Piguet,P., Sarosi,I., Kaufmann,S. *et al.* (1996) Platelet-derived growth factor causes pulmonary cell proliferation and collagen deposition in vivo. *Am J Pathol* **149**: 539-548.

Yoshida,M., Sakuma,J., Hayashi,S., Abe,K., Saito,I., Harada,S. *et al.* (1995) A histologically distinctive interstitial pneumonia induced by overexpression of the interleukin 6, transforming growth factor beta 1, or platelet-derived growth factor B gene. *Proc Natl Acad Sci U S A* **92**: 9570-9574.

Young,L.S., and Rickinson,A.B. (2004) Epstein-Barr virus: 40 years on. *Nat Rev Cancer* **4**: 757-768.

Yu,Y.Y., Harris,M.R., Lybarger,L., Kimpler,L.A., Myers,N.B., Virgin,H.W., and Hansen,T.H. (2002) Physical association of the K3 protein of gamma-2 herpesvirus 68 with major histocompatibility complex class I molecules with impaired peptide and beta(2)-microglobulin assembly. *J Virol* **76**: 2796-2803.

Yufit,T., Vining,V., Wang,L., Brown,R.R., and Varga,J. (1995) Inhibition of type I collagen mRNA expression independent of tryptophan depletion in interferon-gamma-treated human dermal fibroblasts. *J Invest Dermatol* **105**: 388-393.

Zeisberg,M., and Kalluri,R. (2004) The role of epithelial-to-mesenchymal transition in renal fibrosis. *J Mol Med* **82**: 175-181.

Zhang,K., Rekhter,M.D., Gordon,D., and Phan,S.H. (1994) Myofibroblasts and their role in lung collagen gene expression during pulmonary fibrosis. A combined immunohistochemical and in situ hybridization study. *Am J Pathol* **145**: 114-125.

Zhu,J., Cohen,D.A., Goud,S.N., and Kaplan,A.M. (1996) Contribution of T lymphocytes to the development of bleomycin- induced pulmonary fibrosis. *Cytokines and Adhesion Molecules in Lung Inflammation* **796**: 194-202.

Zhu,Z., Homer,R.J., Wang,Z., Chen,Q., Geba,G.P., Wang,J. *et al.* (1999) Pulmonary expression of interleukin-13 causes inflammation, mucus hypersecretion, subepithelial fibrosis, physiologic abnormalities, and eotaxin production. *J Clin Invest* **103**: 779-788.

Ziegler,J.L., AnderssonM, Klein,G., and Henle,W. (1976) Detection of Epstein-Barr virus DNA in American Burkitt's lymphoma. *Int J Cancer* **17**: 701-706.

Ziesche,R., Hofbauer,E., Wittmann,K., Petkov,V., and Block,L.H. (1999) A preliminary study of long-term treatment with interferon gamma-1b and low-dose prednisolone in patients with idiopathic pulmonary fibrosis. *N Engl J Med* **341**: 1264-1269.

Zurawski,S.M., Vega,F., Jr., Huyghe,B., and Zurawski,G. (1993) Receptors for interleukin-13 and interleukin-4 are complex and share a novel component that functions in signal transduction. *EMBO J* **12**: 2663-2670.

APPENDIX THREE: PUBLICATIONS

Journal of General Virology (2004), 85, 1393–1400 DOI 10.1099/vir.0.79908-0

Identification of a region of the virus genome involved in murine gammaherpesvirus 68-induced splenic pathology

Bernadette M. Dutia,[1] Douglas J. Roy,[1] Bahram Ebrahimi,[1]† Babunilayam Gangadharan,[1] Stacey Efstathiou,[2] James P. Stewart[1]† and Anthony A. Nash[1]

Correspondence
Bernadette M. Dutia
B.M.Dutia@ed.ac.uk

[1]Laboratory for Clinical and Molecular Virology, Division of Veterinary Biomedical Sciences, University of Edinburgh, Summerhall, Edinburgh EH9 1QH, UK

[2]Department of Pathology, University of Cambridge, Cambridge CB2 1QP, UK

Received 16 December 2003
Accepted 1 March 2004

Infection with the murine gammaherpesvirus MHV-68 has profound effects on splenic and mediastinal lymph node pathology in mice which lack the interferon-γ receptor (IFN-γ $R^{-/-}$). In these mice MHV-68 infection causes fibrosis and loss of lymphocytes in the spleen and the mediastinal lymph node as well as interstitial pulmonary fibrosis and fibrotic changes in the liver. The changes are associated with transient elevated latent virus loads in the spleen. Four independent virus mutants with insertions and/or deletions in the left end of the genome fail to induce the pathological changes and establish latency at normal levels in the spleen. The data indicate that the pathology does not correlate with any of the known genes encoded within this region of the genome, genes M1–M4 and the eight vtRNAs. Northern analysis of mRNAs transcribed by wild-type and mutant viruses shows that at least two uncharacterized transcripts are encoded within this region. These transcripts are absent in the mutant viruses and are candidates for the virus genes responsible for the aberrant pathology in IFN-γ $R^{-/-}$ mice.

INTRODUCTION

In immunocompetent mice, the murine gammaherpesvirus MHV-68 causes an acute lung infection which is rapidly cleared, followed by a longer lymphoproliferative phase including lymphadenopathy of the mediastinal lymph nodes, splenomegaly and an infectious mononucleosis like phase involving proliferation of $CD8^+$ T cells (Sarawar *et al.*, 1996; Sunil-Chandra *et al.*, 1992a; Tripp *et al.*, 1997). $CD8^+$ T cells play a major role in clearance of the lung infection and $CD4^+$ T cells are crucial for long-term control of infection, probably via interferon-γ (IFN-γ) (Christensen *et al.*, 1999). The virus establishes a latent infection in lung epithelial cells, B lymphocytes, macrophages and dendritic cells which persists for the lifetime of the animal (Flano *et al.*, 2000; Stewart *et al.*, 1998; Sunil-Chandra *et al.*, 1992b; Weck *et al.*, 1999).

In mice which lack the interferon-γ receptor (IFN-γ $R^{-/-}$ mice), the lymphoproliferative phase is associated with severe pathological changes (Dutia *et al.*, 1997; Ebrahimi *et al.*, 2001; Weck *et al.*, 1997). Following intranasal infection of these mice, the mediastinal lymph nodes draining the lung and the spleen exhibit a drastic drop in cell numbers and become fibrotic (Dutia *et al.*, 1997). These changes are associated with an acute latent load 10–100 times higher than that seen in wild-type mice. After intraperitoneal infection, severe arteritis associated with high mortality occurs (Weck *et al.*, 1997). In this instance splenic pathology is found in 60% of mice (Clambey *et al.*, 2000). The induction of splenic pathology is dependent on $CD8^+$ and $CD4^+$ T cells and the drop in spleen cell numbers is accompanied by lymphocytosis and the exclusion of circulating T and B cells from the spleen and mediastinal lymph node (Ebrahimi *et al.*, 2001).

The left end of the unique region of the MHV-68 genome is important for virus pathogenesis (Macrae *et al.*, 2001). This region contains the four unique protein-coding genes, M1–M4, as well as genes for eight tRNA-like molecules (vtRNAs) (Bowden *et al.*, 1997; Virgin *et al.*, 1997). In a previous study, Clambey *et al.* (2000) constructed two M1 deletion mutants: M1.LacZ, in which the *lacZ* gene replaced nt 1893–2402; and M1Δ511, which lacks nt 1893–2402. These viruses also lack the first 100 nt of the unique region of the genome. M1.LacZ did not cause splenic pathology or mortality in IFN-γ $R^{-/-}$ mice although it did cause severe vasculitis of the great arteries. The outcome of infection of IFN-γ $R^{-/-}$ mice with M1Δ511 or the marker rescue virus was not determined (Clambey *et al.*, 2000). Thus, mutations in the viral genome

†Present address: Department of Medical Microbiology, University of Liverpool, Duncan Building, Daulby Street, Liverpool L69 3GA, UK.

in the region of M1 appeared to have an effect on splenic pathology in the IFN-γ $R^{-/-}$ system.

This study aimed to extend the observations of Clambey *et al.* utilizing mutants of MHV-68 in order to clarify the potential role of the M1 gene product in splenic pathology in IFN-γ $R^{-/-}$ mice. Wild-type 129/Sv/Ev (WT) and IFN-γ $R^{-/-}$ mice were infected with wild-type MHV-68, with V2 virus (Simas *et al.*, 1998) or LHΔgfp virus both of which lack M1 and 4 or 5 of the vtRNA molecules respectively, with V1 virus which has an insertion in vtRNA3, or with MHV-76 which lacks M1–M4 and the tRNAs (Macrae *et al.*, 2001) and the consequences of infection on the spleen virus latency and/or pathology were examined. The data indicate that the M1 gene product is not involved in the pathological changes which occur in IFN-γ $R^{-/-}$ mice following MHV-68 infection. Northern analysis of transcripts in wild-type and mutant infected cells has identified two candidate transcripts present in wild-type infected cells but not in cells infected with mutant virus.

METHODS

Mice. Wild-type 129/Sv/Ev mice and IFN-γ $R^{-/-}$ 129/Sv/Ev (Huang *et al.*, 1993) were purchased from B & K Universal (Hull, UK) and bred in-house.

Virus and cells. Virus working stocks were prepared by infection of BHK-21 cells as described previously (Sunil-Chandra *et al.*, 1992a).

The viruses used are as follows: MHV-68 clone g2.4 (Efstathiou *et al.*, 1990) V1 and V2 (Simas *et al.*, 1998) and MHV-76 (Macrae *et al.*, 2001). LHΔgfp was constructed by co-transfection of viral DNA with DNA containing a human cytomegalovirus (HCMV) immediate-early promoter-driven green fluorescent protein cassette (CMV-GFP) into BHK cells. Resulting recombinant plaques were isolated and purified on the basis of fluorescence under UV illumination. Detailed mapping of the viral genome was performed using Southern analysis, PCR amplification and sequencing. This determined that the viral genome was intact except that the CMV-GFP cassette had inserted by illegitimate recombination at the left end of the unique portion of the genome resulting in the deletion of nt 1–3223 (Fig. 1).

Infection and sampling. Age- and sex-matched mice were anaesthetized with Halothane (Rhone Merieux) and inoculated intranasally with 4×10^5 p.f.u. virus in 40 μl sterile PBS. At various times after infection mice were killed by cervical dislocation and tissues harvested for virus assays or histology.

Latent virus assays. Numbers of latently infected cells were determined by the infective centre assay as described previously (Dutia *et al.*, 1997).

Molecular cloning and sequencing. V1 virus stock was digested with Proteinase K and, after heat inactivation of the protease, the M1 gene coding region (nt 2023–3282, Virgin *et al.*, 1997) was amplified by PCR using the following primers: M1coding for 5′-GCATCATTGAGCGGCGA-3′ (nt 1999–2020); M1coding rev 5′-CAGGCTTAGGACTGCTGCCCA-3′ (nt 3290–3270). PCRs contained 1·5 U recombinant *Taq* DNA polymerase (Invitrogen), manufacturer's buffer, 100 mM dNTPs, 2·0 mM $MgCl_2$ and 50 pmol primer in a total reaction volume of 50 μl. The cycling parameters were as

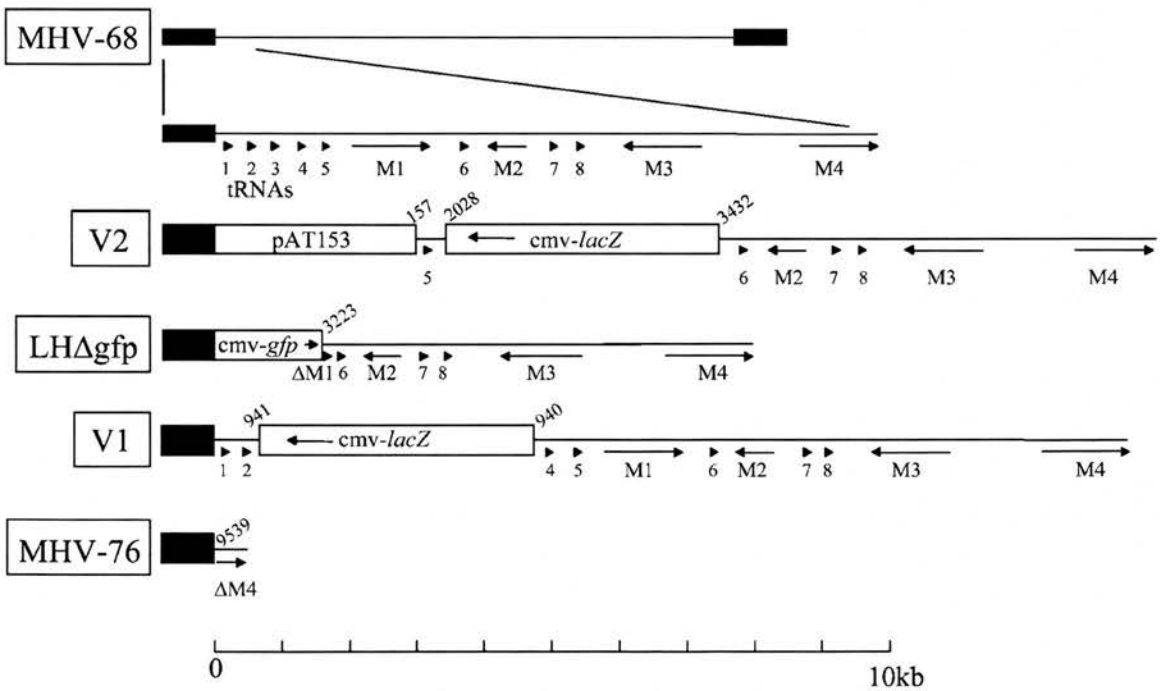

Fig. 1. Genome structures of MHV-68 and the four mutant viruses, V1 and V2 (Simas *et al.*, 1998), LHΔgfp and MHV-76 (Macrae *et al.*, 2001). Solid line represents unique sequence, filled boxes represent repeats. Genome coordinates taken from Virgin *et al.* (1997) given above the line. Approximate positions of genes M1–M4 and vtRNAs given below line.

follows: 94 °C 45 s, 55 °C 45 s, 72 °C 120 s, 35 cycles with a final extension time of 7 min at 72 °C. The PCR product was cloned into pCRII using a TA Cloning Kit (Invitrogen) and three clones were sequenced on a Licor 4000L automated sequencer.

Preparation of RNA from infected cells and RT-PCR analysis. BHK-21 cells were infected with 5 p.f.u. per cell virus, incubated at 37 °C for 20 h and harvested by addition of RNAzolB (Biogenesis). Total cell RNA was prepared from the RNAzolB lysates according to the manufacturer's instructions and the integrity of the RNA was determined by agarose gel electrophoresis. cDNA was prepared as described previously (Roy *et al.*, 2000). PCRs contained cDNA transcribed from approximately 0·1 μg RNA, 1·5 U recombinant *Taq* DNA polymerase (Invitrogen), manufacturer's buffer, 100 mM dNTPs, 2·0 mM $MgCl_2$ and 50 pmol primer in a total reaction volume of 50 μl. Cycling parameters were as for PCR of the M1 coding region. Primers were as follows: M1for 5′-CAGAACCTTACCAGTCATGTG-3′ (nt 2686–2708), M1rev 5′-GTTACTAGGACATACAGTGG-3′ (nt 2947–2966), product 278 bp; M2for 5′-TAATAGGAAGACGTATCTCAGG-3′ (nt 4077–4098), M2rev 5′-CTGCTTCCTTAGCCAGTCTC-3′ (nt 5856–5875), product 589 bp; M3for 5′-TGGCACTCAAACTTGGTTGTGG-3′ (nt 6566–6587), M3rev 5′-TAACAGGCAGATTGCCATTCCC-3′ (nt 6904–6925), product 359 bp; M4for 5′-CCTGGAGAAGATGATGATATTC-3′ (nt 8616–8637), M4rev 5′-AAAGTCATAAATCTCAATACC-3′ (nt 9739–9759), product 1143 bp; murine β-actin for 5′-TGTGATGGTGGGGAATGGGTCA-3′, murine β-actin rev 5′-TTTGATGTCACGCACGATTTC-3′, product 514 bp. Control reactions included PCR on samples from cDNA synthesis reactions carried out without addition of reverse transcriptase and PCRs without addition of template. PCR products were separated on a 1% (w/v) agarose gel and visualized by ethidium bromide staining. In the case of the M2, the PCR product was transferred to charged nylon membrane (Hybond-N; Amersham) and probed with an M2-specific probe as described previously (Usherwood *et al.*, 2000).

Northern analysis. RNA was prepared from BHK cells infected or mock-infected for 20 h at a m.o.i. of 5 p.f.u. per cell as described above. Poly(A)-enriched RNA was prepared from total RNA by Oligotex (Qiagen) and 10 μg of each sample was run on a MOPS/formaldehyde gel (Sambrook, 2001). RNA was transferred to Nylon membrane and probed with ^{32}P-labelled gel-purified PCR product or restriction fragment in Ultrahyb (Ambion) according to the manufacturer's instructions. Size determinations were made with an RNA ladder (Invitrogen). Membranes were exposed to X-ray film at −70 °C.

Histopathology. Spleens were fixed in neutral buffered formaldehyde, processed routinely to 5 μm paraffin wax-embedded sections, stained with haematoxylin and eosin or Masson's trichrome and examined by light microscopy.

RESULTS

Pathological changes in spleens of IFN-γ R$^{-/-}$ mice infected with mutant viruses

In order to assess the role of individual MHV-68 genes in the pathological changes which occur in the spleens of IFN-γ R$^{-/-}$ mice, we infected wild-type 129/Sv/Ev mice and IFN-γ R$^{-/-}$ mice with wild-type MHV-68 or recombinant viruses and monitored the acute latency load, spleen cell numbers and histopathological changes. Fig. 2 shows the kinetics of latency and spleen cell numbers in wild-type and IFN-γ R$^{-/-}$ mice infected with wild-type virus or V2 virus. V2 virus has

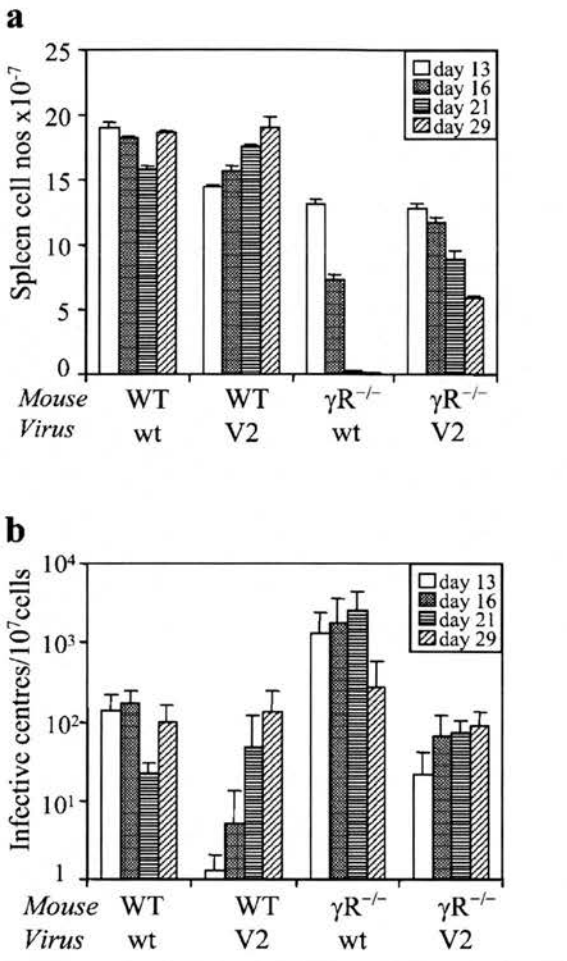

Fig. 2. Spleen cell numbers and latently infected cells (infective centres) in wild-type 129/Sv/Ev (WT) and IFN-γ R$^{-/-}$ 129/Sv/Ev (γR$^{-/-}$) mice infected with 4×10^5 p.f.u. wild-type MHV-68 (wt) or V2 virus (V2) at various times post-infection. Data are representative of three experiments.

a deletion of MHV-68 nt 1–1571 and an insertion of the *lacZ* gene leftwards under control of the HCMV immediate-early promoter replacing MHV-68 nt 2028–3432. It thus retains the viral tRNA gene vtRNA5 and the first 6 nt of the M1 open reading frame but lacks vtRNAs1–4 and the major part of the M1 gene (Fig. 1). On days 13, 16, 21 and 29 post-infection spleens were removed and assessed for pathological changes. As described previously, MHV-68 infection resulted in a significantly higher latent load in IFN-γ R$^{-/-}$ mice than in wild-type mice and caused a drastic drop in spleen cell numbers (Fig. 2a, b). V2, on the other hand, did not cause an increase in latent virus load or a drop in cell numbers. These data indicate that a gene or genes at the left end of MHV-68 is required for the pathological changes which occur in the lymphoid tissue of IFN-γ R$^{-/-}$ mice.

To examine this further, mice were infected with two other recombinant viruses with mutations in the left end of the

genome, V1 and LHΔgfp. V1 has the *lacZ* gene under the control of the HCMV immediate-early promoter inserted leftwards within vtRNA3 (nt 940). LHΔgfp has MHV-68 nt 1–3223 replaced with the green fluorescent protein under the HCMV promoter in the rightwards direction (Fig. 1). Spleens were removed on days 16, 20 and 24 and examined for pathological changes. By day 16 post-infection, wild-type virus infection had produced the expected increase in latent virus load and the decrease in spleen cell numbers in IFN-γ $R^{-/-}$ mice (Fig. 3). However, IFN-γ $R^{-/-}$ mice infected with V1 and LHΔgfp had similar cell numbers and infective centres to wild-type mice.

V1 virus established latency and caused splenomegaly in wild-type mice with kinetics indistinguishable from wild-type MHV-68 (Fig. 3). Both V2 and LHΔgfp consistently showed delayed onset of latent infection in the spleen.

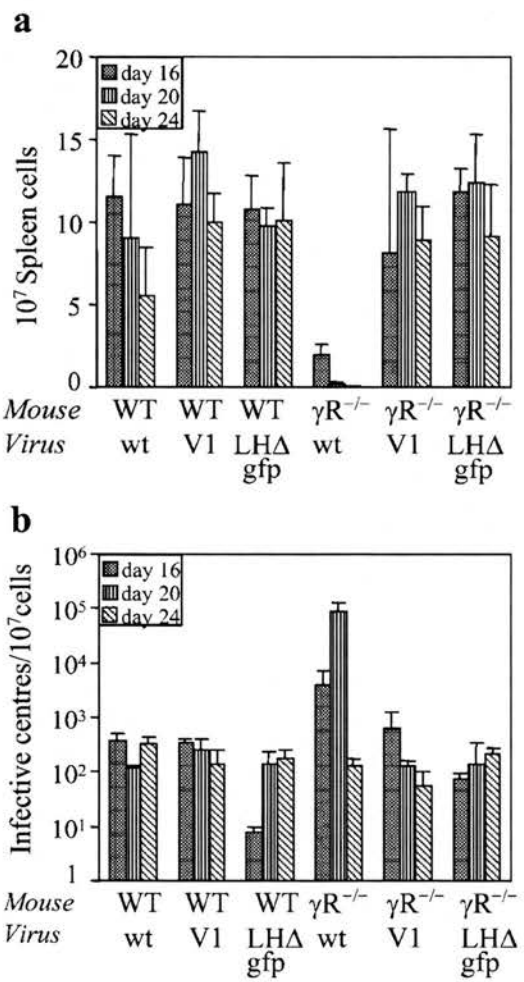

Fig. 3. Spleen cell numbers and latently infected cells (infective centres) in wild-type 129/Sv/Ev (WT) and IFN-γ $R^{-/-}$ 129/Sv/Ev ($\gamma R^{-/-}$) mice infected with 4×10^5 p.f.u. wild-type MHV-68 (wt), V1 virus (V1) or LHΔgfp virus (LHΔgfp) at various times post-infection. Data are representative of three experiments.

However, they both replicate with similar kinetics to wild-type virus in the lung and with identical kinetics of infection to wild-type virus *in vitro* (Simas *et al.*, 1998; S. Selvarajah, personal communication), suggesting that the deleted region plays a role in trafficking of virus to the spleen or in the establishment of latent infection. Interestingly, these changes in kinetics are not evident in IFN-γ $R^{-/-}$ mice.

To address the possibility that there was delayed onset of splenic changes following infection with the mutant viruses infection was monitored up to day 29 for V2 virus and day 24 for V1 and LHΔgfp. No elevated latency load or decrease in cell numbers was observed. It is unlikely therefore that the failure to cause severe splenic pathology is due to delayed kinetics of virus infection.

The lack of splenic pathology following infection of IFN-γ $R^{-/-}$ mice with V1, V2 and LHΔgfp was confirmed by examination of spleen sections stained with Masson's trichrome, which stains collagen. Spleen sections from mice infected with a further mutant virus, MHV-76 (Macrae *et al.*, 2001), which lacks the MHV-68-specific genes M1, M2, M3 and M4 and all eight vtRNAs, were also examined. Fig. 4 shows that while wild-type MHV-68 infection of IFN-γ $R^{-/-}$ produced characteristic changes in the spleen structure, including contraction of the white pulp, destruction of the red pulp and deposition of collagen, these changes did not occur following infection with the three mutant viruses and MHV-76. No evidence of pathological changes was found up to day 35 post-infection.

M1 gene sequence

Because M1 has been implicated in the pathogenesis of splenic atrophy in IFN-γ $R^{-/-}$ mice (Clambey *et al.*, 2000) we considered the possibility that V1 virus had, in addition to the insertion in vtRNA3, a mutation in the M1 gene. Therefore, the coding region of the M1 gene of V1 virus was amplified by PCR, cloned and sequenced. Three independent clones were sequenced, each of which was identical in sequence to the M1 gene of wild-type MHV-68. This established that V1 virus did not have a mutated M1 gene.

Expression of M1 gene in mutant virus infections

We then considered the possibility that, while the coding sequence for M1 was intact, either the insertion into vtRNA3 or a mutation in the promoter meant that the M1 gene was not transcribed. A further possibility was that the insertions/deletions upstream of M1 had altered transcription of other genes in the region. The transcription of M1–4 genes from wild-type, V1, V2 and LHΔgfp viruses was examined in lytically infected BHK cells by RT-PCR as described in Methods. Controls were PCR on cDNA reactions incubated without reverse transcriptase, PCR without cDNA and RT-PCR on mock-infected cell RNA. These were negative in all cases. M1, M3 and M4 RT-PCR products were visible as single bands on ethidium bromide-stained gels. The M2

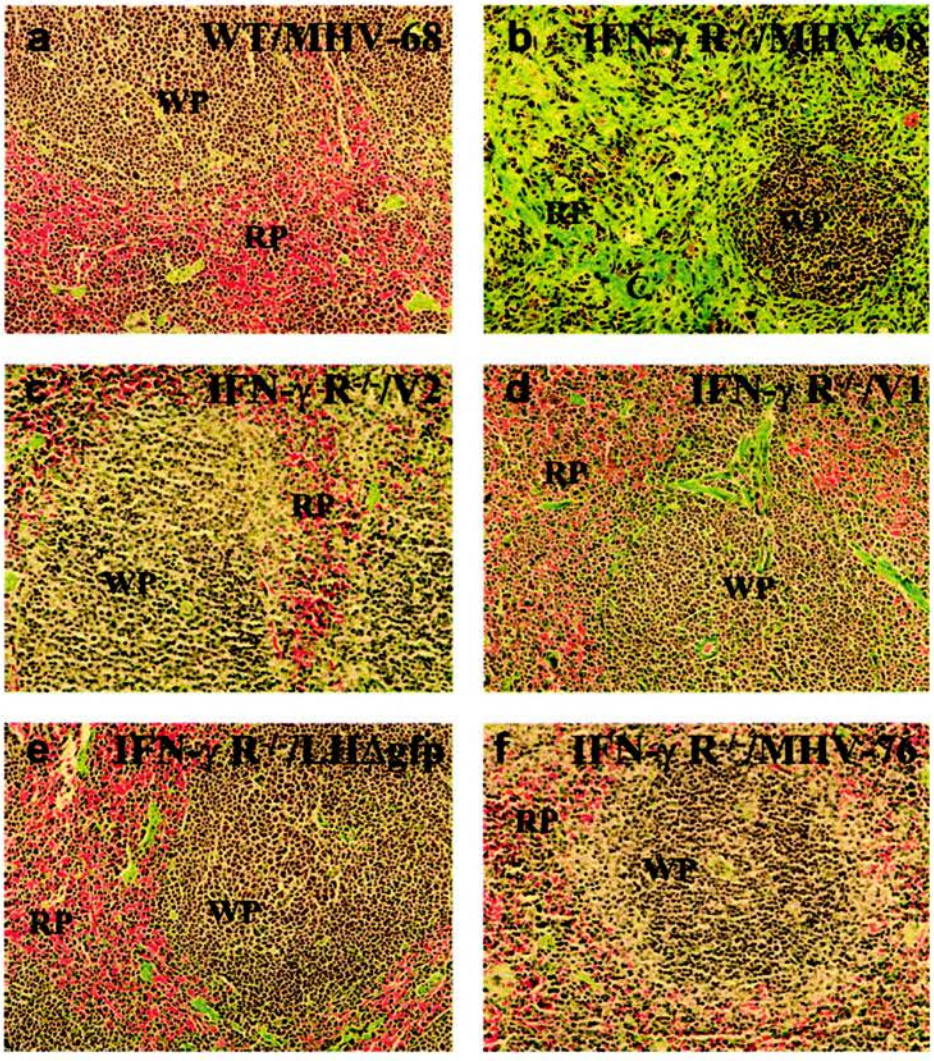

Fig. 4. Histology of wild-type (a) and IFN-γ $R^{-/-}$ (b–f) mice 20 days after infection with wild-type MHV-68 (a, b), V2 (c), V1 (d), LHΔgfp (e) or MHV-76 (f). WP, white pulp; RP, red pulp; C, collagen.

gene is expressed at very low levels in lytically infected cells and hence only a weak signal was detectable on an ethidium bromide-stained gel. The presence of the M2 RT-PCR product was examined by Southern hybridization. Fig. 5(a) shows that the four viruses tested, wild-type, V1, V2 and LHΔgfp, all transcribed M2, M3 and M4. As predicted, V2 and LHΔgfp did not transcribe M1. M1 transcription was readily detected in wild-type virus and V1-infected cells. Thus the insertion in the V1 virus had not resulted in lack of transcription of the M1 gene.

Transcription in BHK cells infected with wild-type virus, V1 virus and LHΔgfp was examined further by Northern blotting. Poly(A) RNA from infected and mock-infected cells was transferred to Nylon membrane and probed with a probe spanning the M1 gene. This showed that transcripts of the expected length were present in V1-infected cells and that the quantity of transcript was similar to that present in wild-type virus (Fig. 5b).

Identification of novel transcripts

In order to investigate the possibility that there are other undefined transcripts encoded within the vtRNA region of the genome, the Northern blot was probed with a probe spanning the vtRNA 1–4 region (nt 106–1517). In wild-type virus-infected cells four major transcripts were detected (Fig. 6). These included the vtRNAs, which were seen as small transcripts of $<0{\cdot}24$ kb, a small transcript of 0·5 kb which is detectable on probing of Northern blots of total RNA with this probe (Bowden *et al.*, 1997; unpublished observations) and two transcripts of approximately 4·3 and 3·2 kb. The 4·3 and 3·2 kb transcripts were present in low abundance and were not evident when total RNA rather

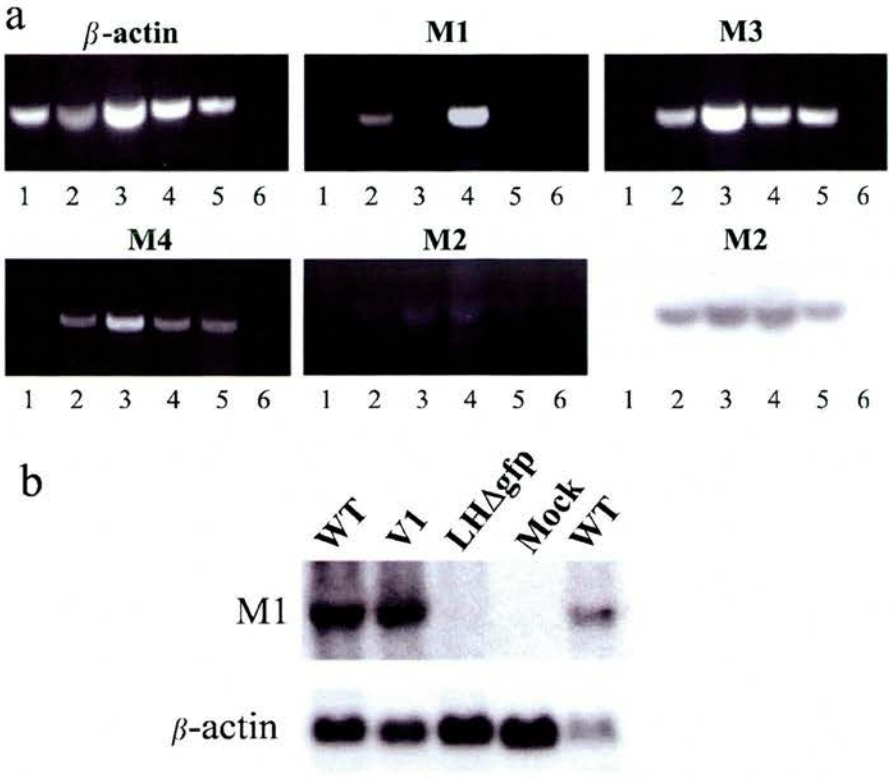

Fig. 5. Transcription of genes M1–M4 of MHV-68 and mutant viruses. (a) RT-PCR analysis of genes M1–M4 and β-actin transcription in BHK cells infected for 20 h with wild-type or mutant MHV-68 viruses. Lane 1, mock-infected; 2, wild-type virus; 3, LHΔgfp; 4, V1; 5, V2; 6, no cDNA. A further control (not shown) in the absence of reverse transcriptase was negative. (b) Northern analysis of M1 and β-actin transcription in BHK cells infected for 20 h with wild-type MHV-68, V1, LHΔgfp or mock-infected.

than mRNA was probed. They were absent in cells infected with V1 virus or LHΔgfp. However, novel transcripts of 10, 6·8, 5·3 and 4·2 kb were detected in cells infected with V1 and a single 5·2 kb transcript was detected in LHΔgfp-infected cells. These transcripts were also found in MHV-68-infected owl monkey kidney cells (data not shown). The vtRNAs were absent from LHΔgfp-infected cells but present in the V1-infected cells. LHΔgfp does not encode vtRNAs 1–5 but the genes for vtRNAs 6–8 are present in the genome. The result indicates that vtRNAs 6–8 are not detected by the vtRNA1–4 probe. V1 lacks vtRNA 3 but expression of vtRNAs 1, 2 and 4 occurs. The 0·5 kb transcript was absent from both V1- and LHΔgfp-infected cells. This transcript may be related to vtRNA 3 or to other changes in the transcription pattern in these mutants.

DISCUSSION

The experiments described here show that the pathological changes that occur in IFN-γ $R^{-/-}$ mice following infection with MHV-68 can be ascribed to genes encoded in the left end of the genome. MHV-76, which lacks nt 1–9538 of MHV-68 encoding genes M1–M4 and the eight vtRNAs does not cause splenic pathology. V2 and LHΔgfp, which also have large deletions in this region of the genome and lack the M1 gene and four or five vtRNAs, do not cause splenic pathology. V1, which has a large insertion at nt 940 disrupting vtRNA3 but encodes the M1–M4 genes, also lacks the ability to cause the pathology. While the data from V2 virus and LHΔgfp, like that described previously for M1 (Clambey *et al.*, 2000), implicate the M1 gene in the process of atrophy, the results from V1 virus suggest that M1 is unlikely to be the primary virus gene involved in the induction of splenic pathology.

V1 virus, like the other mutant viruses investigated here, does not express vtRNA3. The function of the vtRNAs is unknown but as they are not aminoacylated it is unlikely that they function in translation (Bowden *et al.*, 1997). It is more likely that the vtRNAs have a regulatory function during infection. Moreover, a recombinant MHV-76 virus into which we have inserted vtRNAs 1–5 does not cause splenic pathology in IFN-γ $R^{-/-}$ mice (unpublished data). This recombinant virus expresses vtRNA3 (Anna Cliffe, personal communication). It is therefore unlikely that vtRNA3 is involved in induction of splenic pathology. More likely is the possibility that the insertion into vtRNA3 is

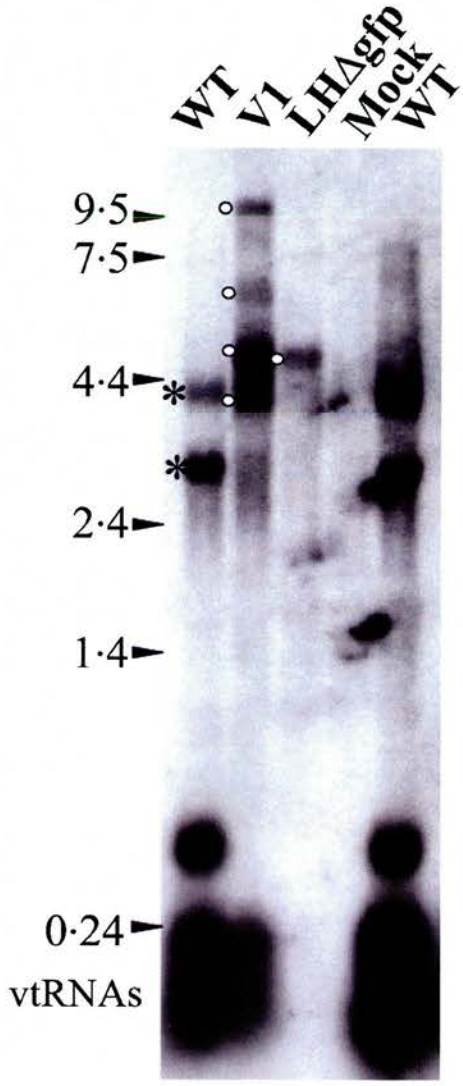

Fig. 6. Northern analysis of transcripts present in BHK cells infected for 20 h with wild-type MHV-68, V1, LHΔgfp or mock-infected. Blot probed with dsDNA probe MHV-68 nt 106–1517. *, Novel transcripts in wild-type virus-infected cells; ○, novel transcripts in V1- and LHΔgfp-infected cells.

disrupting transcription of an unidentified mRNA. Both Epstein–Barr virus and Kaposi's sarcoma-associated herpesvirus encode multi-exon mRNAs which are transcribed across the terminal repeats (Choi *et al.*, 2000; Laux *et al.*, 1988; Sample *et al.*, 1989) and there is evidence for an equivalent transcript in MHV-68 (Husain *et al.*, 1999). We have identified two novel transcripts in wild-type MHV-68-infected BHK cells. These transcripts are expressed at a low level and are not detected when total RNA is probed (Bowden *et al.*, 1997, unpublished data), but can be detected when 10 μg of poly(A) RNA is used for analysis. Although MHV-68 infection of BHK cells is lytic, some transcription of latency-associated genes may occur. The M2 gene, for example, is latency-associated but can be detected at low levels in lytically infected cells. Hence these novel transcripts may be latency-associated genes and are candidates for virus genes involved in the induction of splenic pathology which is associated with latent infection. Cells infected with mutant viruses contain novel transcripts which may be the result of aberrant processing.

A third possibility is that the insertion of the HCMV immediate-early promoter is altering virus gene transcription. There is evidence for both MHV-68 and mouse CMV that insertion of the *lacZ* gene under control of the HCMV promoter-enhancer can alter the ability of the virus to replicate (Clambey *et al.*, 2000; Stoddart *et al.*, 1994). However, the fact that MHV-76 also fails to induce atrophy argues that a gene or genes involved in the induction of atrophy are encoded at least in part within the first 9538 bp of MHV-68.

The replication of V1 and V2 has been characterized previously in BALB/c mice. In these mice no differences between the mutants and wild-type MHV-68 were detected. In contrast, the experiments reported here show a clear difference from wild-type virus phenotype in IFN-γ $R^{-/-}$ mice, highlighting the importance of host phenotype in studies of virus mutants. V2 and LHΔgfp have a distinct phenotype in 129/Sv/Ev mice consistently showing delayed kinetics of latent virus infection in the spleen. The viruses lack four or five vtRNA molecules respectively and the M1 gene product. Studies with an M1 deletion mutant have implicated the M1 gene product in suppression of virus reactivation. These studies are not directly comparable to those described here as virus was inoculated via a different route. No evidence of increased reactivation was found following infection with V2 and LHΔgfp; however, the data are consistent with a role for M1 or a closely related gene in latency.

The data presented here provide evidence for transcripts across the left region of the genome which encodes the vtRNAs. These genes are candidates for novel latency-associated genes and for viral mediators of splenic pathology. Studies to characterize these genes are under way and will clarify these issues further.

ACKNOWLEDGEMENTS

This work was supported by the Biotechnology and Biological Sciences Research Council and the Cancer Research Campaign (UK). J. P. S. is a Royal Society University Research Fellow.

REFERENCES

Bowden, R. J., Simas, J. P., Davis, A. J. & Efstathiou, S. (1997). Murine gammaherpesvirus 68 encodes tRNA-like sequences which are expressed during latency. *J Gen Virol* **78**, 1675–1687.

Choi, J. K., Lee, B. S., Shim, S. N., Li, M. & Jung, J. U. (2000). Identification of the novel K15 gene at the rightmost end of the Kaposi's sarcoma-associated herpesvirus genome. *J Virol* **74**, 436–446.

Christensen, J. P., Cardin, R. D., Branum, K. C. & Doherty, P. C. (1999). CD4(+) T cell-mediated control of a gamma-herpesvirus in B cell-deficient mice is mediated by IFN-gamma. *Proc Natl Acad Sci U S A* **96**, 5135–5140.

Clambey, E. T., Virgin, H. W., IV & Speck, S. H. (2000). Disruption of the murine gammaherpesvirus 68 M1 open reading frame leads to enhanced reactivation from latency. *J Virol* **74**, 1973–1984.

Dutia, B. M., Clarke, C. J., Allen, D. J. & Nash, A. A. (1997). Pathological changes in the spleens of gamma interferon receptor-deficient mice infected with murine gammaherpesvirus: a role for CD8 T cells. *J Virol* **71**, 4278–4283.

Ebrahimi, B., Dutia, B. M., Brownstein, D. G. & Nash, A. A. (2001). Murine gammaherpesvirus-68 infection causes multi-organ fibrosis and alters leukocyte trafficking in interferon-gamma receptor knockout mice. *Am J Pathol* **158**, 2117–2125.

Efstathiou, S., Ho, Y. M., Hall, S., Styles, C. J., Scott, S. D. & Gompels, U. A. (1990). Murine herpesvirus 68 is genetically related to the gammaherpesviruses Epstein–Barr virus and herpesvirus saimiri. *J Gen Virol* **71**, 1365–1372.

Flano, E., Husain, S. M., Sample, J. T., Woodland, D. L. & Blackman, M. A. (2000). Latent murine gamma-herpesvirus infection is established in activated B cells, dendritic cells, and macrophages. *J Immunol* **165**, 1074–1081.

Huang, S., Hendriks, W., Althage, A., Hemmi, S., Bluethmann, H., Kamijo, R., Vilcek, J., Zinkernagel, R. M. & Aguet, M. (1993). Immune response in mice that lack the interferon-γ receptor. *Science* **259**, 1742–1745.

Husain, S. M., Usherwood, E. J., Dyson, H., Coleclough, C., Coppola, M. A., Woodland, D. L., Blackman, M. A., Stewart, J. P. & Sample, J. T. (1999). Murine gammaherpesvirus M2 gene is latency-associated and its protein a target for $CD8^+$ T lymphocytes. *Proc Natl Acad Sci U S A* **96**, 7508–7513.

Laux, G., Perricaudet, M. & Farrell, P. J. (1988). A spliced Epstein–Barr virus gene expressed in immortalized lymphocytes is created by circularization of the linear viral genome. *EMBO J* **7**, 769–774.

Macrae, A. I., Dutia, B. M., Milligan, S., Brownstein, D. G., Allen, D. J., Mistrikova, J., Davison, A. J., Nash, A. A. & Stewart, J. P. (2001). Analysis of a novel strain of murine gammaherpesvirus reveals a genomic locus important for acute pathogenesis. *J Virol* **75**, 5315–5327.

Roy, D. J., Ebrahimi, B. C., Dutia, B. M., Nash, A. A. & Stewart, J. P. (2000). Murine gammaherpesvirus M11 gene product inhibits apoptosis and is expressed during virus persistence. *Arch Virol* **145**, 2411–2420.

Sambrook, J. & Russell, D. W. (2001). *Molecular Cloning. a Laboratory Manual*, 3rd edn. Cold Spring Harbor, NY: Cold Spring Harbor Laboratory.

Sample, J., Liebowitz, D. & Kieff, E. (1989). Two related Epstein–Barr virus membrane proteins are encoded by separate genes. *J Virol* **63**, 933–937.

Sarawar, S. R., Cardin, R. D., Brooks, J. W., Mehrpooya, M., Tripp, R. A. & Doherty, P. C. (1996). Cytokine production in the immune response to murine gammaherpesvirus 68. *J Virol* **70**, 3264–3268.

Simas, J. P., Bowden, R. J., Paige, V. & Efstathiou, S. (1998). Four tRNA-like sequences and a serpin homologue encoded by murine gammaherpesvirus 68 are dispensable for lytic replication *in vitro* and latency *in vivo*. *J Gen Virol* **79**, 149–153.

Stewart, J. P., Usherwood, E. J., Ross, A., Dyson, H. & Nash, T. (1998). Lung epithelial cells are a major site of murine gammaherpesvirus persistence. *J Exp Med* **187**, 1941–1951.

Stoddart, C. A., Cardin, R. D., Boname, J. M., Manning, W. C., Abenes, G. B. & Mocarski, E. S. (1994). Peripheral blood mononuclear phagocytes mediate dissemination of murine cytomegalovirus. *J Virol* **68**, 6243–6253.

Sunil-Chandra, N. P., Efstathiou, S., Arno, J. & Nash, A. A. (1992a). Virological and pathological features of mice infected with murine gamma-herpesvirus 68. *J Gen Virol* **73**, 2347–2356.

Sunil-Chandra, N. P., Efstathiou, S. & Nash, A. A. (1992b). Murine gammaherpesvirus 68 establishes a latent infection in mouse B lymphocytes in vivo. *J Gen Virol* **73**, 3275–3279.

Tripp, R. A., Hamilton-Easton, A. M., Cardin, R. D., Nguyen, P., Behm, F. G., Woodland, D. L., Doherty, P. C. & Blackman, M. A. (1997). Pathogenesis of an infectious mononucleosis-like disease induced by a murine gamma-herpesvirus: role for a viral superantigen? *J Exp Med* **185**, 1641–1650.

Usherwood, E. J., Roy, D. J., Ward, K., Surman, S. L., Dutia, B. M., Blackman, M. A., Stewart, J. P. & Woodland, D. L. (2000). Control of gammaherpesvirus latency by latent antigen-specific $CD8^+$ T cells. *J Exp Med* **192**, 943–952.

Virgin, H. W., Latreille, P., Wamsley, P., Hallsworth, K., Weck, K. E., Dal Canto, A. J. & Speck, S. H. (1997). Complete sequence and genomic analysis of murine gammaherpesvirus 68. *J Virol* **71**, 5894–5904.

Weck, K. E., Dal Canto, A. J., Gould, J. D., O'Guin, A. K., Roth, K. A., Saffitz, J. E., Speck, S. H. & Virgin, H. W. (1997). Murine gammaherpesvirus 68 causes severe large-vessel arteritis in mice lacking interferon-gamma responsiveness: a new model for virus-induced vascular disease. *Nat Med* **3**, 1346–1353.

Weck, K. E., Kim, S. S., Virgin, H. I. & Speck, S. H. (1999). Macrophages are the major reservoir of latent murine gammaherpesvirus 68 in peritoneal cells. *J Virol* **73**, 3273–3283.